Fall and Rise of the Tarentaise Zone, Western Alps

Thesis

UNRESTRICTED

Fall and Rise of the Tarentaise Zone, Western Alps

Simon Lomas, BSc (London)

a thesis submitted for the degree of

Doctor of Philosophy

February 1993

Department of
Earth Sciences

The Open
University

Date of submission : 24th February 1993

Date of award : 26th May 1993

ABSTRACT

The Tarentaise Zone is an intensely deformed thrust–bounded meta-sedimentary package which represents a poorly understood belt of late Cretaceous subsidence on the northern passive continental margin of the Tethyan ocean. This contribution presents new field data which place tighter constraints on models of basin evolution.

Structurally, the Tarentaise units have been stripped from their basement and imbricated to form a WNW-verging fold-thrust stack with complex internal strains. Demonstration that tectonic displacements were uniquely foreland-directed allows a preliminary qualitative reconstruction of basin architecture and hence provides a framework for stratigraphic analysis. The major sequence boundary recording the onset of late Cretaceous subsidence of the Tarentaise Basin is a subaerial erosion surface which truncates Jurassic rift structures of the precursory continental margin. This unconformity is directly overlain by sub– wave-base clastic sediments without any intervening shallow marine facies, indicating that subsidence occurred rapidly relative to sedimentation. The early basin-fill sediments are dominated by coarse, immature mass-flow conglomerates, deposited on a deep water fan-delta adjacent to a rapidly eroding area of high relief. Syn-extensional tholeiitic magmatism (the so-called Versoyen 'ophiolite') is consistent with intense localised crustal stretching: geochemical analyses of these metabasites revealing evidence of hydrothermal alteration but preservation of MORB-like trace element ratios. The implication of active subsidence contradicts those models for the development of the north Tethyan continental margin which predict strong attenuation and deep submergence by the end of the initial subsidence episode: the Tarentaise segment of the passive margin must have been capable both of being elevated above sea level and of being subsequently rifted a second time.

Mont Blanc, Combe de la Neuva and Pierra Menta

CONTENTS

LIST OF ILLUSTRATIONS

TABLES

ACKNOWLEDGEMENTS

Thanks are first of all due to Rob Butler for setting up and supervising the project and for maintaining a strong inverse student–supervisor Tarentaise enthusiasm correlation throughout. Joe Cann and Rob Knipe are thanked for access to facilities at the University of Leeds. The project was funded partly by a NERC studentship grant, partly by the Department of Social Security but largely through the protracted goodwill of the TSB bank and the Visa and Mastercard credit companies.

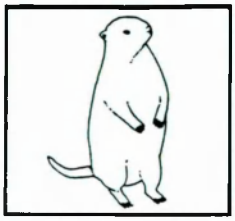

For help and companionship in the field, I am particularly grateful to Clare Stephens, Peter Connolly, Matthew Harvey, Sam Jones and Ned Porter. And to the many marmots, too numerous to mention, who helped me through those long, lonely months in the Alps. For arranging loan of the luxury OU field vehicle, I am extremely obliged to John Holbrook. I would also like to thank those warm-hearted, generous, gullible people from whom I scrounged most of my field gear, without which my Alpine field seasons would have been substantially colder, wetter and less accurately recorded: Peter Connolly, Eddie McAllister, Sue Bowler, Rob Butler, 'Brud' Barton, Matthew Harvey, Charlie Gowing, Chris Melton, Phil Gravestock and Jon Dougherty-Page.

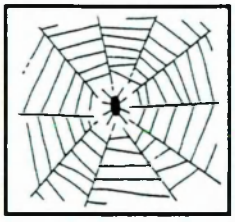

My hesitant, stumbling foray into the occult world of black-box geochemistry witnessed the involvement of almost as many helpers as samples: John Watson, Peter Webb, Tim Bradshaw and Ditta Neumann (Milton Keynes), Tim Brewer (Nottingham), and especially Alan Gray (Leeds) helped me to transform some rather unwieldy lumps of greenish rock into a few scraps of computer printout; Janet Hergt and Tim Bradshaw were polite enough not to snigger too much when they saw the numbers. Ian Chaplin, Kate Chambers, Brian Ellis, Keith Reid and Keith Cowling are thanked for their cheerful surgery on (unanaesthetised) grubby grey rock samples.

The final text of this thesis owes a great deal to perceptive (if scarcely legible) scribbles in the margins of first drafts by Rob Butler. Chapter three was formally reviewed for Sedimentary Geology by Rudolf Trümpy and an anonymous sedimentologist. For entertaining discussions and fraternal kinematic head-scratching, I am grateful to the Leeds Alpine Crap Beard Club of Andy Barnicoat, Sophie Bowtell (honorary crap beard), Rob Butler, Bob Cliff, Ned Porter and Will Ramsbotham. Sue Bowler is thanked for easy-going cynicism and for endeavouring to keep Rob under control. Other personnel at Leeds who deserve an appreciative note are Rob Knipe and Andy Barnicoat, for distracting me with field trips at crucial moments, John Mott for good humoured efficiency, and Geoff Lloyd for daily early morning access to the grapevine.

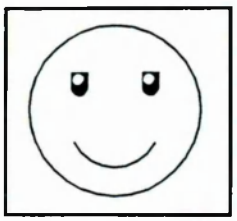

For my time at the OU, I would like to extend an extendible thing of gratitude to Dave Peate for showing me the ropes and to the waiters & waitresses of Café 209 (Charlie Gowing, Ned Porter, Simon Inger, Mark George and Ditta Neumann-Rose) for helping to loosen a few of the knots. Phil Gravestock, Tim Bradshaw, Janet Hergt, John Shaggerty-Page, Paul(a) Yates,

Mabs Kunka and Fiona McGibbon were good company in their isotopically dilute moments. Geoff Brown is remembered with considerable respect.

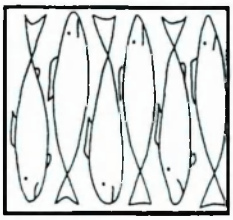

Most of this thesis was written in a cold, noisy, dusty, windowless room in the Structural Research Laboratories at the University of Leeds. I am grateful to the Structure Group (Chopper, Ned, Lochy, sWill, Jock, Napalm, Lardy, Squelch, Yan, Wibbs, Linda-Andy, Ed the Duck) for its obstinate refusal to have any truck with conventional names and for making me feel so welcome that I couldn't bear to leave. I am particularly indebted to the following: Lochlann Magennis for access to his Mac and his coffee jar; Ned Porter for Alpine nostalgia, polite conversation and irrepressible good humour; Andy Farmer for the savanna model of geological research and for licking vital connections; Iain Hendijock McHenderson for cups of tea and for ceasing to sing Proclaimers' songs; and Rich Napalm for square golf balls, green-haired rodents and appalling jokes. Simon 'Troy' Tempest is thanked for advice on cross-section construction and for his inspirational "It's never too late to give up."

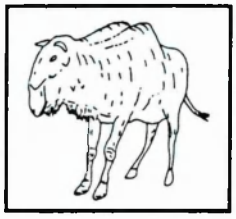

Life outside the Structural Sardine Tin was made bearable by liberal supplies of advice, succour, beer, cola bottles and general *bonhomie* from the following herd of tulip-chomping wildebeest: fAnny Buckley, Purple-Sue Colclough, Roj Griffiths, Randolph Haggerty, Yvette Hague, Greg Jones, James 'Slim' Leddy, Markus Leosson, Eddie McScottish, Bill McCaffrey, Rik Moore, Isaac Njilah, Dave 'chicken tikka' Psaila, Tim 'dorsal fin' Salter, Colin Stark, Pete Talling, Enrico 'pasta belly' Tavernelli, Joshua Tetley, Simon Welsh, Jared West and Liz White.

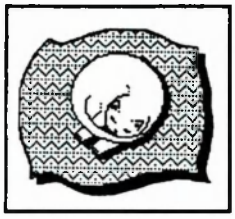

Inevitably, my greatest acknowledgement of gratitude is reserved for Clare Stephens for typing in references, glueing down diagrams, offering shoulders to cry on, supplying pizza in times of crisis, tolerating extreme levels of thesis-induced grumpiness, and for numerous other things. Hope you don't mind too much about p220, Clare. Hartley and Cleo were therapeutically cute and cuddly in times of stress and are now available on short-term loan to other thesis-afflicted geologists.

Finally, I would like to dedicate this thesis to my parents, Ruth and George Lomas, for their unending supply of encouragement and support, both moral and financial, and for not minding too much about my persistent refusal to leave school and get a proper job.

CONVENTIONS

Grid references. Where possible, grid references are quoted relative to the Unified European Grid System (SGEU), which is reproduced on French IGN topographic maps and on some Italian military maps. For that part of the study area covered by the Swiss cartographic survey (*i.e.* Switzerland and Italy close to its Swiss border), grid references are those of the Swiss national system, which utilises the same grid as the SGEU but a different numerical origin.

Structural orientation data. All planar and linear orientations are quoted as plunge/azimuth or dip/azimuth in the form: 34→107, where the two digit number refers to the dip or plunge and the three digit number to the direction of dip. All stereographic projections are lower hemisphere equal-area (Schmidt) plots unless otherwise stated.

'Foliations.' Throughout this thesis, the term 'foliation' is used in a general sense to refer to *any* deformation induced planar rock fabric (*cf.* McClay, 1987 p64). Thus, slaty cleavages, schistosities and transposition fabrics are all regarded as foliations in the following text. This is the standard North American usage rather than the traditional British practice which restricts the term to 'streaky bacon' style metamorphic compositional banding (*cf.* Wilson & Cosgrove, 1982 p35).

CHAPTER 1 INTRODUCTION

Intense orogenic deformation of sedimentary sequences in the internal zones of mountain belts has severely retarded understanding of the basins they represent. In the Alps, clear ideas regarding the subsidence and infilling of various pre-orogenic basins are crucial to the understanding of the collisional saga which produced the Alpine mountain belt. Yet in many instances, the difficulties introduced by a strong tectono-metamorphic overprint have meant that well founded models of basin development are lacking. A case in point is the Tarentaise Zone, a metasedimentary sequence representing a belt of late Cretaceous subsidence which occupied a key palæogeographic position during the early stages of plate convergence. The highly deformed basin-fill of the zone has however been reluctant to yield any credible basin model and thus continues to be a source of perplexity to geologists trying to reconstruct the larger scale evolution of the Western Alps. As a step towards resolving this difficulty, this contribution attempts to establish some primary geological constraints relevant to the evolution of the Tarentaise Basin.

Recent models of Alpine evolution have emphasised first, that most of the structural units exposed in the Alps were derived from the Mesozoic Tethyan ocean and its attendant passive margins, and second, that the development of this extensional system can be explained in terms of simple lithospheric stretching models (Winterer & Bosellini, 1981; Lemoine, 1984; Lemoine *et al.*, 1986; Ménard *et al.*, 1991; Wooler *et al.*, 1992). Thus, it is envisaged that the Tethyan margins experienced active rifting through the early Jurassic followed by mid Jurassic continental break-up and thermal subsidence until the onset of plate convergence in late Cretaceous times. This model appears to accord well with data from the external parts of the Alps but is difficult to test among the intensely deformed nappes of the internal Alps. The Tarentaise Basin is important because it contains a sequence of late Cretaceous sediments deposited on part of the north Tethyan passive margin. The evolution of this basin thus provides information on the subsidence of the margin and, indirectly, the condition of the underlying lithosphere, towards the end of the extension-driven phase of subsidence.

1.1 AIMS AND SCOPE

This thesis describes a deductive geological appraisal of a poorly understood zone of the internal Western Alps. The Alps are perhaps the most intensively studied of all orogenic belts; a long period of descriptive research has built up a wealth of map information and regional geological surveys of unrivalled detail. Out of this descriptive inventory, numerous authors have attempted to distil evolutionary models for the pre-orogenic development of the Alpine region. The diverse scenarios proposed have proved highly contentious. Central to many of the disputes are uncertainties regarding the palæogeographic affinities and subsidence histories of a number of 'difficult' geological zones. The subject of this thesis is one such 'difficult' area which has hitherto largely escaped detailed analysis from sedimentological and stratigraphic viewpoints.

Thus, the aim of this contribution is to help to de-mystify the Tarentaise Basin through an integrated sedimentological, stratigraphic and structural investigation into its palæotectonic significance. The work described in the following chapters is based on eight and a half months of field work in the Tarentaise Zone.

1.1-1 Organisation of this Thesis

The remainder of **chapter 1** provides background information though a regional overview of Western Alpine geology and a discussion of the evolution of the orogen. The basic geological attributes of the Tarentaise Zone, as deduced from this and previous studies, are outlined in the latter part of the chapter.

Chapter 2 describes the Alpine structure of the Tarentaise Zone, focusing particularly on a displacement-parallel traverse through the best exposed and most deeply incised sector of the Zone. Implications for potential reconstructions of Tarentaise Basin architecture are discussed.

Chapter 3 discusses the sedimentology of the least deformed parts of the late Cretaceous sequence. This chapter is a slightly modified version of a paper published recently in Sedimentary Geology (Lomas, S. 1992 Submarine mass flow conglomerates of the Tarentaise Zone, Western Alps: sedimentation processes and depositional setting. *Sediment. Geol.* v81 pp269–287).

Chapter 4 considers a sequence of metabasaltic rocks exposed on the internal margin of the Tarentaise Zone. New stratigraphic and geochemical data are presented which shed some light on the origins and palæogeographic

significance of the metabasites. The implications of this volcanism for the evolution of the Tarentaise Basin are discussed.

Chapter 5 integrates observations from the previous chapters with additional stratigraphic data to place constraints upon models of basin formation. The subsidence of the Tarentaise Basin is considered in the wider context of models for the evolution of the Tethyan passive margins. This chapter also presents a re-evaluation of some of these large scale ideas based on data from the Tarentaise.

Chapter 6 summarises the main conclusions to emerge from this research project and makes a number of recommendations for future work.

1.2 REGIONAL GEOLOGICAL CONTEXT

The Alps form an arcuate mountain belt which is continuous for 1000km between Monte Carlo and Vienna. Classically, the Alps are separated into Eastern (Germany, Austria, Switzerland), Southern (the Italian Dolomites *etc.*) and Western (France, NW Italy, SW Switzerland) segments. This demarcation is partly geological, partly geographic but primarily linguistic, with only limited integration of research between French- Italian- and German-speaking sectors. This thesis is concerned with the evolution of part of the Western Alps.

Tectonically, the Alpine mountain chain marks the zone of late Cretaceous to Tertiary collision between African and Eurasian plates. Thus, the Alps comprise a collage of tectono-stratigraphic packages derived from the continental margins to the consumed oceanic domain and from younger basins related to the mountain building phase (Fig. 1-1). The traditional subdivision of the Alps has therefore been into a number of broad tectonostratigraphic zones, each of presumed palæogeographic significance (Trümpy, 1960, 1982; Ramsay, 1963; Debelmas & Lemoine, 1970; Debelmas & Kerckhove, 1980): mappable lithotectonic **Zones** are thought to equate approximately to Mesozoic palæogeographic **domains**. The larger scale subdivisions (Figs. 1-1 and 1-2) are generally accepted as pragmatically useful and geologically important. Finer scale subdivisions are the source of considerable geological and terminological confusion. The most fundamental division recognises an **internal zone** of complex deformation and pervasive metamorphism, and an **external zone**, where metamorphism is slight and structures are both simpler and younger. The geological units referred to in the following sections are located on Fig. 1-2.

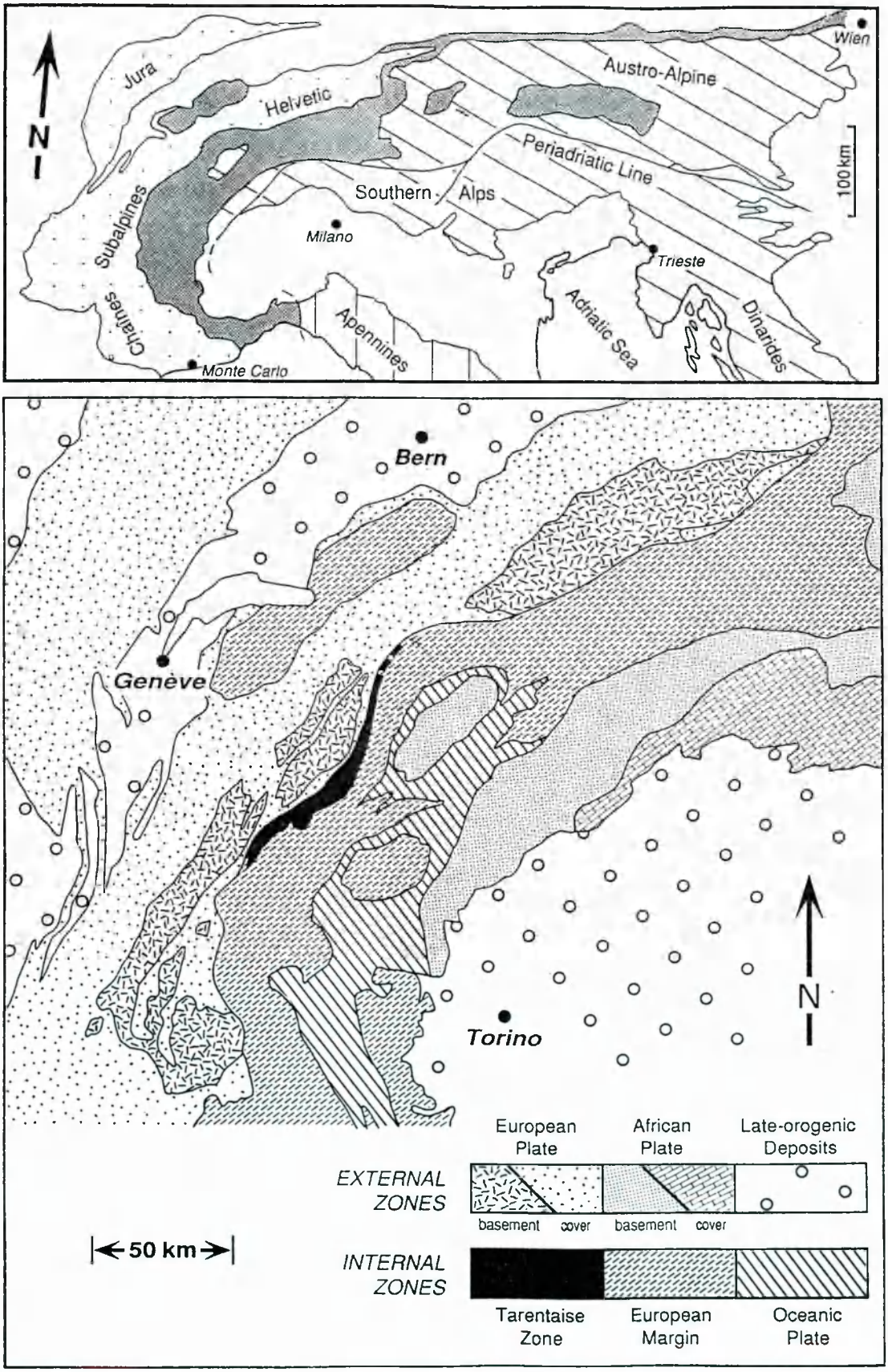

Fig. 1-1 Geology of the Alpine mountain belt. *Upper:* the extent of the Alpine chain, dense shading denotes the Pennine Zone. *Lower:* simplified geological map showing the principal tectono-stratigraphic subdivisions of the Western Alps in terms of their presumed palæotectonic affinities (based partly on Debelmas & Kerckhove, 1980). Note that the Tarentaise Zone may continue much further eastwards than shown (see section 1.4-4).

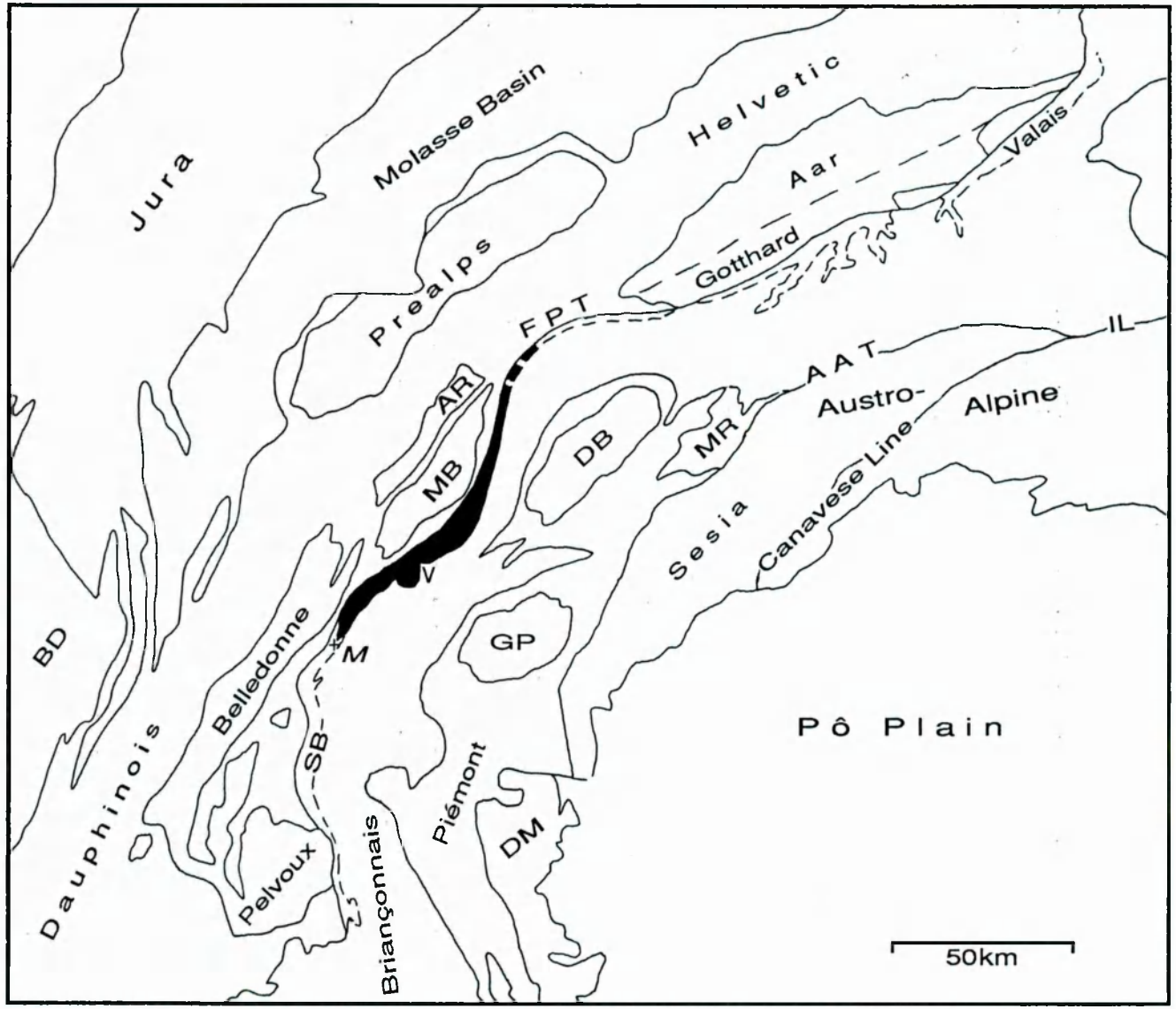

Fig. 1-2 Location map of the Western Alps showing the names of the main geological units referred to in the text. This is an unshaded version of the lower map in Fig. 1-1. Abbreviations: *AAT* = Austro-alpine Thrust; *AR* = Aiguilles Rouges massif; *BD* = Bas Dauphiné; *DB* = Dent Blanche klippe; *DM* = Dora Maira massif; *FPT* = Frontal Pennine Thrust; *GP* = Gran Paradiso massif; *IL* = Insubric Line; M = the town of Moûtiers; *MB* = Mont Blanc massif; *MR* = Monte Rosa 'massif'; *SB* = Sub-Briançonnais Zone; V = Versoyen Zone.

1.2-1 The Internal Western Alps

The internal Alps comprise the so-called **Penninic nappes** (Piémont, Briançonnais, Sub-Briançonnais and Valais Zones) and the overlying Austro-alpine Zone. Palæogeographically, the Austro-alpine Zone is conventionally regarded as part of the southern (African or 'Apulian') plate which overthrusts both the northern (European) continental margin (lower Penninic nappes) and the vestiges of the intervening ocean (Piémont Zone). Parts of the Pennine Zone are now found some 40km north-west of the main Pennine Front as a series of large klippen known collectively as the Prealps .

The **Austro-alpine Zone** is represented in the Western Alps by basement rocks of the Sesia Zone and the Dent Blanche klippe, separated from the underlying Penninic nappes by a major shear zone. In all areas, the basement rocks are dominated by metapelites, metabasites and metagranitoids but three major units can be distinguished on the basis of contrasting metamorphic histories (Compagnoni *et al.*, 1977). Metamorphic facies in the eastern Sesia Zone comprise well preserved high-pressure parageneses (the 'eclogitic mica-schists'), whereas the western Sesia and Dent Blanche areas are dominated by greenschist facies assemblages (the *'Gneiss minuti'* sequence) with only local relics of earlier high-pressure parageneses. A third unit, the *'seconda zona Dioritica-kinzigitica'* (IIDK), structurally overlies the other two. The IIDK lacks high-pressure metamorphic assemblages and shows only limited Alpine deformation. The contrasting tectonothermal histories displayed by these three units may indicate that the Sesia Zone was assembled by tectonic juxtaposition of formerly separate crustal blocks at a relatively late stage (*e.g.* Gosso *et al.*, 1979). The eastern margin of the Sesia Zone is delimited by the Canavese Line, the western segment of a major system of late-collisional fault zones (the Periadriatic Line or Insubric Line) which approximately marks the southern limit of Alpine metamorphism (Ahrendt, 1980; Schmid *et al.*, 1989). The sedimentary cover of the Austro-alpine Zone occurs only as rare slices in the Western Alps but becomes important further east where large thicknesses of Triassic and Jurassic carbonates are exposed.

The **Piémont Zone** is dominated at outcrop by the *schistes lustrés* (equivalent to the *Bündnerschiefer* of German literature and the *Calcescisti* in Italy), a thick composite sequence of calc-micaschists derived from calcareous silts, marls and shales with marine microfossils of mid Jurassic to late Cretaceous age (Pantic & Isler, 1978; Deville *et al.*, 1992). The schistes lustrés are interleaved with

metabasaltic and ultramafic bodies interpreted as ophiolites and thus the Piémont Zone is regarded as the remnants of an oceanic palæogeographic domain. In the more external parts of the Zone, schistes lustrés overlie thin carbonate / psammite formations, perhaps representing onlap of the oceanic sediments onto pre-rift Triassic units of the European passive margin. Metamorphic grade attains eclogite facies in the eastern Piémont zone but blueschist facies at most in the west. The ophiolitic bodies of the Alpine belt are stratigraphically incomplete compared with the classical ophiolite sequences of Oman and Cyprus: pillow lava piles are typically thin compared with associated gabbros and sheeted dyke complexes are largely absent (though small examples are recognised in the Zermatt-Saas ophiolite by Barnicoat & Fry, 1986). Additionally, serpentinite (with basalt+gabbro) breccias are relatively common; sometimes directly overlain by pelagic sediments, suggesting that the ultramafic rocks were exposed at the ocean floor (*e.g.* Tricart & Lemoine, 1983; Weissert & Bernoulli, 1985). These apparently anomalous characteristics have led several authors to propose that Piémont-Ligurian ocean did not open by 'conventional' plate divergence (*e.g.* Lemoine, 1980; Ishiwatari, 1985; Weissert & Bernoulli, 1985; Lemoine *et al.*, 1987). However, studies of the Atlantic passive margins (White, 1992a, b) have indicated that an abnormally thin basaltic layer underlain by partially serpentinised mantle may actually be the norm for ocean crust formed immediately following continental break-up (*i.e.* that ultimately most likely to be obducted). White (1992a, b) has suggested that, since upwelling of hot mantle beneath a nascent rift is necessarily slow, significant heat loss may occur by conduction (as well as adiabatic decompression), suppressing the potential for partial melting and thus initially generating only relatively thin oceanic crust. Geochemically, the Piémont metabasites preserve characteristics typical of mid-ocean ridge basalts (Bearth & Stern, 1979; Beccaluva *et al.*, 1984).

Windows through the Piémont Zone expose a series of polymetamorphic basement 'blocks' (Monte Rosa, Gran Paradiso, Dora Maira) known collectively as the **internal crystalline massifs**. In detail, these 'blocks' appear to be structural composites built of stacked thrust sheets (*e.g.* Ellis *et al.*, 1989). They comprise diverse Hercynian crystalline basement lithologies together with minor Carboniferous clastics. The internal massifs all contain some (retrogressed) eclogite facies rocks of continental affinities, in contrast to the structurally overlying Piémont ophiolites and calc-schists which are regarded as oceanic.

The **Briançonnais Zone** forms a structural belt defined largely by its distinctive Mesozoic stratigraphy. The Briançonnais 'basement' comprises lithologies similar to those of the internal crystalline massifs but with thicker Carboniferous sedimentary sequences (the *Zone Houillère*). Permian clastic sediments and volcanics are present in the Vanoise (Ellenberger, 1958). The Mesozoic sequence commences with a shallow marine quartzite (?Lower Triassic) overlain by several hundreds of metres of platform carbonates with evaporites (Middle/Upper Triassic). Since Jurassic sequences are mostly condensed or absent, the Briançonnais domain is thought to have formed a high-standing area of the south European continental margin at this time (*e.g.* Debelmas & Lemoine, 1970; Trümpy, 1982). This interpretation is supported by the presence of bauxites of presumed mid Jurassic age in the Vanoise (Goffé, 1977). Upper Jurassic deposits however are thin carbonates which include mottled nodular horizons and cherts, possibly representing very low rates of deposition in deep water. The Cretaceous is represented by thin pelagic or hemipelagic calcareous deposits which are unconformably overlain by marine sandstones and marls of Eocene age.

The **Sub-Briançonnais Zone** separates the Briançonnais Zone from the external zones and is stratigraphically transitional between the two, though perhaps with closer affinities to the external domains than the Briançonnais (Debelmas & Kerckhove, 1980; Fry 1989a). The Triassic is represented only by thin dolomites with minor evaporites but a thick heterogeneous Jurassic succession is developed which is shalier in the north and limestone-dominated in the south (Barbier, 1948; Debelmas & Kerckhove, 1980). Cretaceous sediments are thin limestones and calcareous shales, again unconformably overlain by Eocene sandstones. The Sub-Briançonnais Zone narrows north-east of the town of Moûtiers and eventually disappears just north-east of the French-Italian border.

The **Tarentaise Zone** occupies the most external position in the Pennine Zone north-east of Moûtiers but is absent further west. It continues along strike into Switzerland as the **Valais Zone**. In the Franco-Italian sector, the Tarentaise Zone comprises >1km of Cretaceous marine clastics unconformably overlying a Triassic-Jurassic sequence which is lithologically very similar to that of the Briançonnais. The Versoyen Zone on the internal margin of the Tarentaise Zone contains metabasites and serpentinites of uncertain age. The stratigraphy of the Tarentaise Zone is described further in section 1.4.

1.2-2 The External Western Alps

The external zones lie west and north of the Pennine Front, a major tectonic (and, to a certain extent, palæogeographic) boundary which has been interpreted as a strike-slip fault (*e.g.* Ricou & Siddans, 1986) but which is generally regarded as a thrust or a series of thrusts (*e.g.* Ramsay, 1963; Butler *et al.*, 1986). In the French Alps, the external zones are divided into Ultradauphinois, Dauphinois and Jura and the corresponding Mesozoic palæogeographic domains are all thought to belong to the cratonward part of the European continental margin. The Southern Alps, south and east of the Insubric Line, form the opposite external margin to the mountain belt, but are not significantly exposed in the Western Alps.

The **Ultradauphinois Zone** (= the Ultrahelvetic Zone in Switzerland) corresponds to one of the most poorly constrained palæogeographic domains. It forms a narrow strip in the immediate footwall to the Frontal Pennine Thrust and consists of a shaly Lower Jurassic succession directly overlain by Eocene sandstones (Eltchanioff-Lancelot *et al.*, 1982). The latest Cretaceous and Palæocene appears to have been a period of non-deposition across most of the Western Alpine domains.

The **Dauphinois Zone** (=Helvetic Zone ≈Chaînes Subalpines) contains a relatively condensed Triassic succession but a very thick Jurassic sequence. The Triassic in most areas consists of thin shallow marine and supratidal sediments (sandstones + dolomites + shales ± evaporites) with extrusive alkali basalts in the Pelvoux region. Jurassic rocks are marine shales and marls with pelagic or hemipelagic limestones, forming a total thickness of 3-4km (Debelmas & Lemoine, 1970). The Cretaceous sequence is lithologically similar but shows marked lateral variations; a belt of deep-water marls south of the Pelvoux (the Vocontian trough) being flanked by extensive platform carbonates (the Urgonian limestones). Deposition in the Dauphinois domain appears to have been more or less continuous from early Jurassic to late Cretaceous times, in contrast to the situation in the internal zones (Debelmas & Kerckhove, 1980). The basement rocks of the Dauphinois Zone crop out as the **external crystalline massifs** of Argentera, Pelvoux, Belledonne, Mont Blanc, Aiguilles Rouges, Gotthard and Aar. These are a diverse collection of schists and gneisses showing metamorphism (up to upper amphibolite facies) of Hercynian age, together with late Hercynian granitic intrusives (*e.g.* the Mont Blanc granite).

The **Jurassien Zone** of the Jura, the outlying arm of the Alpine system, is dominated by thick (~2km) Jurassic platform carbonates, which contrast with the finer-grained Dauphinois succession of the same age (Collet, 1927). Cretaceous rocks are thin or absent across most of the Jura but syn-orogenic Miocene sediments are preserved locally in synclines.

The **Molasse basins** (Pô Plain, Bas Dauphiné and Swiss Molasse Basin) which fringe the Alpine uplands contain clastic detritus of early Oligocene and younger ages. These basins are regarded as load induced flexural downwarps acting as receptacles for material eroded from the rising Alpine chain (*e.g.* Laubscher, 1978; Karner & Watts, 1983; Sinclair *et al.*, 1991). The fill of the Swiss molasse basin preserves two superimposed regressive sequences: the lower sequence ranging from turbidites through wave-dominated shoreline sands to alluvial and lacustrine deposits; the upper from fan-delta sands and intertidal deposits to alluvial sediments (Homewood *et al.*, 1986).

1.3 EVOLUTION OF THE ALPINE BELT

The Alpine mountain belt marks the zone of crustal thickening generated by collision between Eurasian and African plates (Suess, 1893; Argand, 1922). A century and a half of research into Alpine orogenesis have produced a wealth of data, certain degrees of consensus and a smattering of deeply entrenched dogma. Review papers proliferate; among the most important of which are syntheses by Trümpy (1960, 1982), Dewey *et al.* (1973), Laubscher & Bernoulli (1982), Tricart (1984), Lemoine *et al.* (1986) and Coward & Dietrich (1989). The following overview of Alpine evolution draws heavily on these reviews, to which the reader is directed for further discussion.

1.3-1 Mesozoic Extension

The existence of a Mesozoic seaway between Eurasia and Africa was postulated by Neumayr (1883) and since Suess (1893) this ocean has been referred to as 'Tethys' after an unremarkable character in Greek mythology (Tozer, 1989). The segment of Tethys directly involved in the evolution of the western and central Alps is generally known as the Piémont or Ligurian ocean and remnants of Piémont-Ligurian ocean crust are preserved as ophiolites in the Piémont Zone of the Western Alps, in Corsica and in the Northern Apennines. Formation of the

Mesozoic Tethys is attributed to rifting of the Pangæa supercontinent in the late Triassic to early Jurassic, roughly contemporaneous with the opening of the central Atlantic. Evidence for an earlier (early Permian) rifting phase has been documented by Hunziker (1970) and Dietrich (1976) but this is regarded as a late Hercynian event, unrelated to the regional extension which calved the Piémont ocean (Trümpy, 1982; Lemoine *et al.*, 1986). Possible mid-Triassic extension is evidenced by rift structures and shoshonitic volcanism in the Dolomites (Castellarin *et al.*, 1980; Sloman, 1989) and by a recent attempt to quantify Tethyan extension (Wooler *et al.*, 1992). However, deposition of shallow marine sands, platform carbonates and evaporites across all the palæogeographic domains through the late Triassic (Bernoulli & Jenkyns, 1974) argues against widespread disruption of palæogeography and bathymetry prior to the end of this period.

The onset of Tethyan rifting, and thus the beginning of the Alpine story, is registered by the collapse of the late Triassic platform system and its replacement by a deeper water, horst–graben arrangement. Early Jurassic extensional faults are preserved throughout the Western Alps, associated with breccias, olistoliths and locally derived turbidites (*e.g.* Günzler-Seiffert, 1942; Barfety *et al.*, 1979; Lemoine *et al.*, 1981; Grand *et al.*, 1987; Dumont, 1988; Welbon, 1989; Coward *et al.*, 1991). In most areas, Liassic successions are dominated by bedded limestones, marls and shales with minor coarse siliciclastic interbeds. Condensed bioclastic carbonate sequences are interpreted as shoals developed on the footwall apices of tilted fault blocks (*e.g.* Lemoine *et al.*, 1986).

Geochronological studies have so far failed to produced reliable magmatic crystallisation dates for the Piémont ophiolites to constrain the ages of ocean crust formation (*cf.* Bertrand & Delaloye, 1976): opening of the Piémont-Ligurian ocean is constrained mostly by stratigraphic evidence. However, Corsican and Apennine ophiolites, which presumably derived from essentially the same oceanic segment, have yielded magmatic ages of 160-180Ma (Ohnenstetter *et al.*, 1981). Radiolarian cherts associated with the oldest Apennine ophiolites are also mostly of late mid-Jurassic age (Decandia & Elter, 1972). This is in broad agreement with regional stratigraphic evidence, which places the onset of oceanic spreading within the mid-Jurassic (*ca.* 140-170Ma) from the position of the break-up unconformity in Western Alpine successions (Lemoine *et al.*, 1986).

By the end of the mid-Jurassic, therefore, the region of the future Alps had divided into at least two rifted continental margins bordering a spreading ocean (Fig. 1-3). The late Jurassic to Cretaceous evolution of these passive margins witnessed a general decrease in coarse detrital sedimentation and a preponderance of hemipelagic or pelagic deposits. A dearth of palæontological information from the strongly deformed internal zones makes the bathymetry of the continental margins difficult to assess. Figure 1-4 shows one palinspastic reconstruction which illustrates the inferred positions of the main palæogeographic elements present in the Western Alps. However, the palæogeography of the Piémont-Ligurian Tethys remains controversial in detail (*cf.* Biju-Duval *et al.*, 1977; Dercourt *et al.*, 1986; Lemoine & Trümpy, 1987; Coward & Dietrich, 1989; Hsü, 1989).

1.3-2 Eoalpine Compression

Trümpy (1973) recognised three main compressional pulses in the orogenic evolution of the Alps. These he termed, perhaps somewhat unimaginatively, the '(Pal-)eo-Alpine', 'Meso-Alpine' and 'Neo-Alpine' events. With improved geochronological data and refined ideas of mountain building processes, this simple threefold division has largely fallen out of favour, but the term 'Eoalpine' is still widely used to denote the earliest phases of Alpine compression. Evidence for an Eoalpine 'event' takes the form of high pressure metamorphism recorded by eclogitic and blueschist facies rocks which occur between the Insubric Line and the Pennine Front. Rb-Sr mineral isochrons bracket the Eoalpine temperature peak between 110 and 85 Ma (*e.g.* Hunziker, 1974; Oberhänsli *et al.*, 1985; Chopin & Monié, 1984; Hunziker *et al.*, 1989; Hurford *et al.*, 1989). These findings indicate that subduction of oceanic crust had begun by the early to mid Cretaceous, whilst accumulation of fine-grained sediment continued across the northern continental margin (Fig. 1-5). The width of the ocean (*i.e.* the distance between the European passive margin and the subduction complex) is unconstrained at this time. Very high pressure parageneses in the continental basement massif of Dora-Maira (pyrope + kyanite + talc + phengite + quartz + coesite) suggest temperatures of 700-750°C and pressures of ~28kb (Chopin, 1984) which virtually proves that continental crust was also subducted during the Eoalpine. How these very high pressure rocks were exhumed without retrogression is currently the focus of considerable research interest (Rubie, 1984;

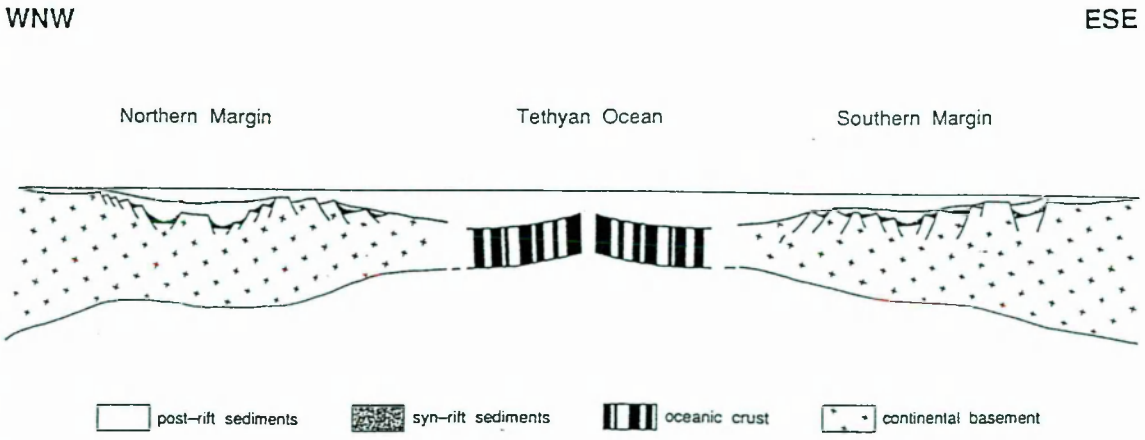

Fig. 1-3 The passive margin concept applied in its simplest form to the Ligurian-Piémont Tethys (late Jurassic situation). Adapted from Laubscher & Bernoulli (1977).

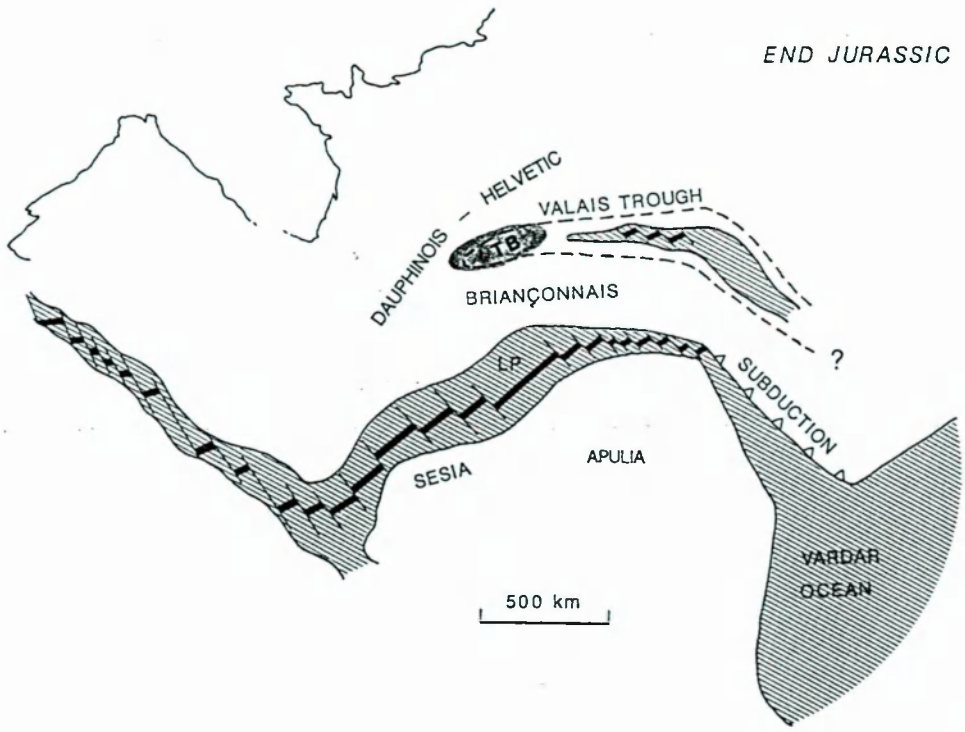

Fig. 1-4 Very simple end-Jurassic palæogeographic reconstruction of the western Tethyan realm showing the presumed relative positions of some of the major Alpine domains. Based on Debelmas (1989). *LP* = Ligurian–Piémont Ocean, *TB* = future Tarentaise Basin.

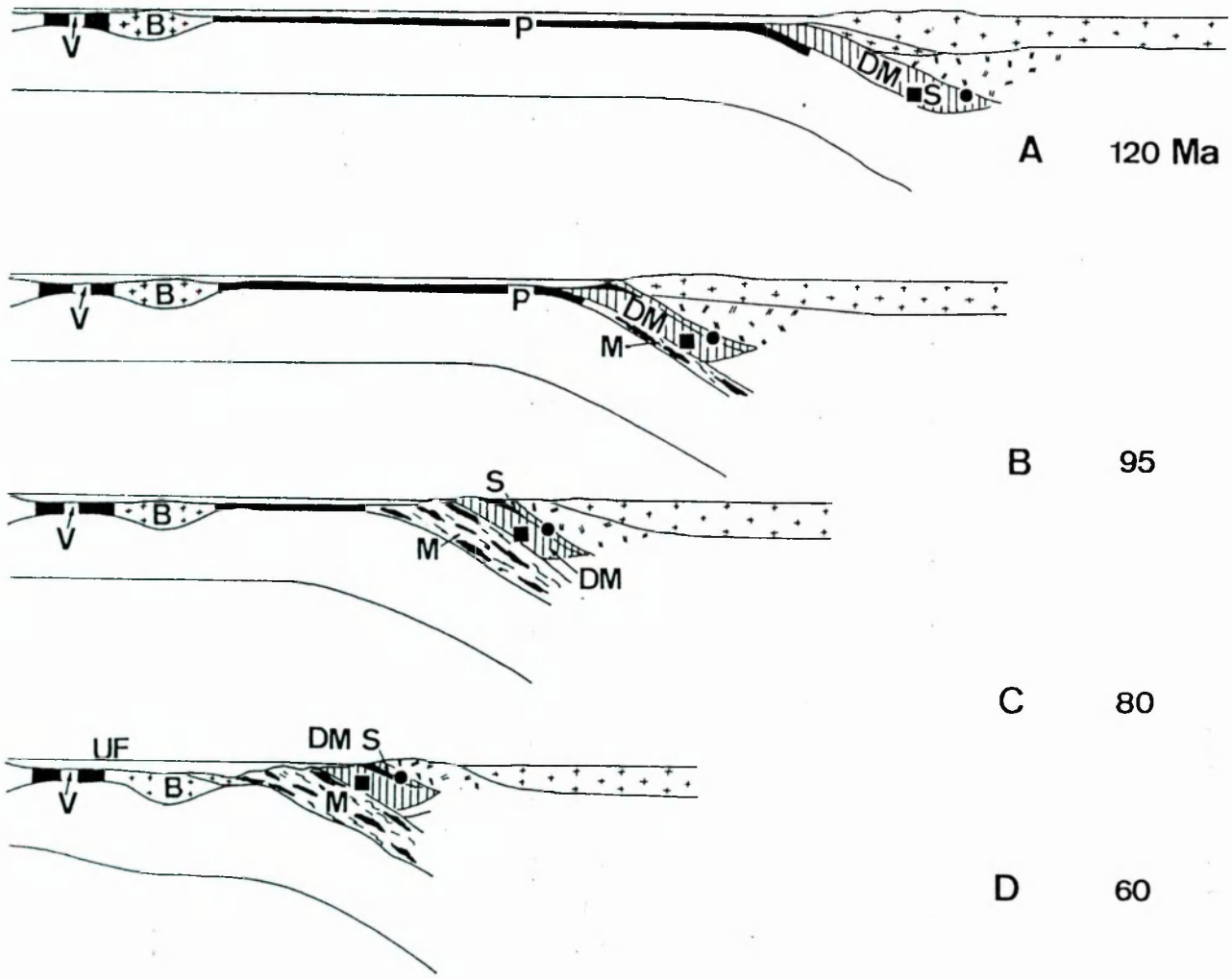

Fig. 1-5 The Eoalpine high–pressure metamorphic episode as envisaged by Hsü (1991). South-dipping subduction of the Ligurian–Piémont ocean beneath Adria is thought to have also involved slivers of continental crust (*e.g.* Dora Maira, Sesia). Hsü proposes that exhumation of these slivers was facilitated by an oceanward shift of the subduction zone, resulting in the accretion of the high pressure slab to the overriding Apulian plate. Note the dynamic evolution of the Valais Trough during the Cretaceous. Abbreviations: *B* = Briançonnais; *DM* = Dora Maira; *M* = mélange; *P* = Piémont ocean; *S* = Sesia; *UF* = 'ultra-' Penninic 'flysch'; *V* = Valais Trough. (Slightly modified after Hsü, 1991).

Platt, 1986, 1987; Chopin, 1987; England & Molnar, 1990; Hsü, 1991; Platt & Hsü, 1992).

From stratigraphic evidence, it is apparent that the late Cretaceous witnessed a major palæogeographic upheaval and the resumption of coarse detrital sedimentation across all of the Western Alpine domains (Trümpy, 1982). This is also presumed to reflect the onset of plate convergence and oceanic closure (*e.g.* Tricart, 1984). The earliest 'flysch' basins, particularly in the north Penninic and Ultrahelvetic domains, came into existence at this time. The term 'flysch' refers to lithostratigraphically distinct sequences of shales, marls, sandstones, conglomerates and clastic limestones, deposited primarily by sediment gravity flows (Homewood & Caron, 1982). Some of the earliest flysch deposits in the Eastern Alps contain clasts of high-pressure/low-temperature metamorphic minerals (lawsonite, glaucophane, crossite), suggesting rapid erosive exhumation of part of the Eoalpine subduction complex (Winkler & Bernoulli, 1986). The flysch concept envisages sediment accumulation in passive deep-water repositories (*i.e.* inherited bathymetry rather than active subsidence) fed by actively uplifting source areas during the earliest phases of orogenesis (Homewood & Lateltin, 1988). Thus, an embryonic foredeep setting is implied, with overall sediment transport from orogen to craton, in the opposite sense to that during the extensional phase. Parts of the *schistes lustrés* (Piémont Zone) have recently been reinterpreted as early Alpine flysch (Deville *et al.*, 1992). The late Cretaceous detrital fill of the Tarentaise Basin has been regarded by some as a 'flysch' sequence (*e.g.* Homewood & Caron, 1982), though this is probably an inappropriate designation (see chapter 5).

1.3-3 Main Alpine Deformation

The main Alpine phase of nappe emplacement and metamorphism is attributed to continent-continent collision in the Eocene or Oligocene. Destruction of the Ligurian-Piémont ocean appears to have been accomplished without significant subduction related volcanism. The only prominent relics of such volcanism at the present erosion level are abundant andesite clasts in the Upper Eocene to Lower Oligocene Taveyannaz 'flysch' of the Helvetics (Stalder, 1979). Collision itself resulted in emplacement of modest volumes of calc-alkaline acid magma in the immediate vicinity of the Insubric Line (the Biella, Traversella, Bergell and Adamello granitoids), which have been dated at 32-30 Ma (Hunziker *et al.*, 1989).

The general scarcity of syn-orogenic or subduction-related magmatism has been attributed to a small ocean size and a low angle of subduction (Smith & Woodcock, 1982). Deep water 'flysch' sedimentation continued to be widespread until the late Eocene. Active subsidence in the Alpine foreland basins appears to date from the early Oligocene (Homewood *et al.*, 1986).

Reconstructions of the relative motions of Africa and Europe using magnetic anomalies place the onset of plate convergence at ~92 Ma (Dewey *et al.*, 1989). Since this time (early late Cretaceous), Africa has apparently moved northwards with respect to Europe (Smith, 1971; Dewey *et al.*, 1973; Biju-Duval *et al.*, 1977; Livermore & Smith, 1985; Savostin *et al.*, 1986). In the early Tertiary, the Apulian promontary of the African plate (*i.e.* the continental underpinnings of North Italy, the Adriatic Sea and parts of Greece and Yugoslavia) began to develop a mind of its own, rotating anticlockwise relative to Africa about a pole near Malta (Vandenberg, 1979a, b). The independent motion of this microplate is widely blamed for the WNW– or NW– directed shortening evident in the Western Alps, which would otherwise be difficult to reconcile with north-south plate convergence (Platt *et al.*, 1989a).

The main phase of collision comprised thrusting of Apulian crust (Austro-alpine and South-alpine domains) onto the European continent, together with foreland-directed thrusting of slices of European (Penninic) crust. In all areas apart from the internal Sesia Zone, Eoalpine assemblages are pervasively overprinted by later regional metamorphism, which also affected the more external domains. Metamorphic grade was predominantly greenschist facies, ranging up to amphibolite facies in the Ossola-Lepontine region and down to prehnite-pumpellyite facies on the internal edge of the Helvetic Zone. Radiometric data from these later Alpine metamorphic parageneses mostly span the range 45 Ma to 8 Ma (*e.g.* Hunziker, 1974; Hunziker *et al.*, 1989), although in detail the timing of metamorphism appears to be spatially rather variable. Peak metamorphism is dated (by a variety of methods) at 45-35 Ma in the Pennine Zone (*e.g.* Hunziker, 1974; Monié, 1985; Hurford *et al.*, 1989); this is essentially the 'Mesoalpine' stage of Trümpy (1973). Younger radiometric ages reflect cooling from peak temperatures during uplift (≈ Trümpy's 'Neoalpine' phase). Plate convergence appears to have been accommodated dominantly by thrusting in the Western Alps whereas additional components of strike-slip and normal faulting are important in the Eastern Alps (*e.g.* Lacassin, 1989; Ratsbacher *et al.*, 1991).

Convergence between Europe and Africa continues today, although the main compressional phase has ceased and the Alps are now uplifting isostatically (at rates of up to ~1.7mm a^{-1}) with little horizontal shortening (Mueller, 1982, 1989). Thrusting in the internal Western Alps occurred under greenschist facies conditions. To a first approximation, deformation appears to have propagated outwards with time from the most internal zones (Coward & Dietrich, 1989). Thus, deformation of the Briançonnais predates folding in the Ultradauphinois and Dauphinois domains, and one of the latest events was the early Pliocene deformation of the Jura. Complexity of deformation diminishes concomitantly towards the foreland. In the external zones, inversion of Mesozoic half-graben and the expulsion of their ductile sedimentary fill appears to have been an important aspect of deformation (Tricart & Lemoine, 1986; Dardeau, 1987; Gillcrist *et al.*, 1987; Graciansky *et al.*, 1988; Butler, 1989a; Coward *et al.*, 1991). In contrast, the more extreme orogenic shortening evident in the internal zones was accomplished largely through pervasive ductile deformation. Figure 1-6 shows the cross-sectional geometry of some high-level structures in the NW Alps. Interpretation of Alpine cross sections have been controversial; in particular, the deep structure of orogen is currently a matter of debate. Seismic reflection and refraction profiles through the Alps (Bayer *et al.*, 1987; Ye & Ansorge, 1990; Holliger, 1990) support the conclusion that a substantial slice of European continental crust has been subducted beneath the Pô basin (Fig. 1-7), as anticipated from mass balance considerations (Smith & Woodcock, 1982; Butler, 1986, 1989a, b; Laubscher, 1988; Mugnier *et al.*, 1990).

1.4 THE TARENTAISE ZONE

The Tarentaise Zone crops out as the external portion of the internal Alps around the north-west segment of the Alpine arc (Fig. 1-1). It comprises a thrust-bounded package of highly deformed marine sediments and basement slices metamorphosed to lower greenschist facies. The physiographic expression of this zone is a rugged chain of alpine peaks which is continuous from the French Tarentaise region (headwaters of the Isère river in Savoie) through the Valle d'Aosta of Italy and into canton Valais in south-west Switzerland. An outcrop passing through three different countries has endowed the Tarentaise Zone with a variety of aliases, including: Zone des Bréches de Tarentaise, Sion–Courmayeur

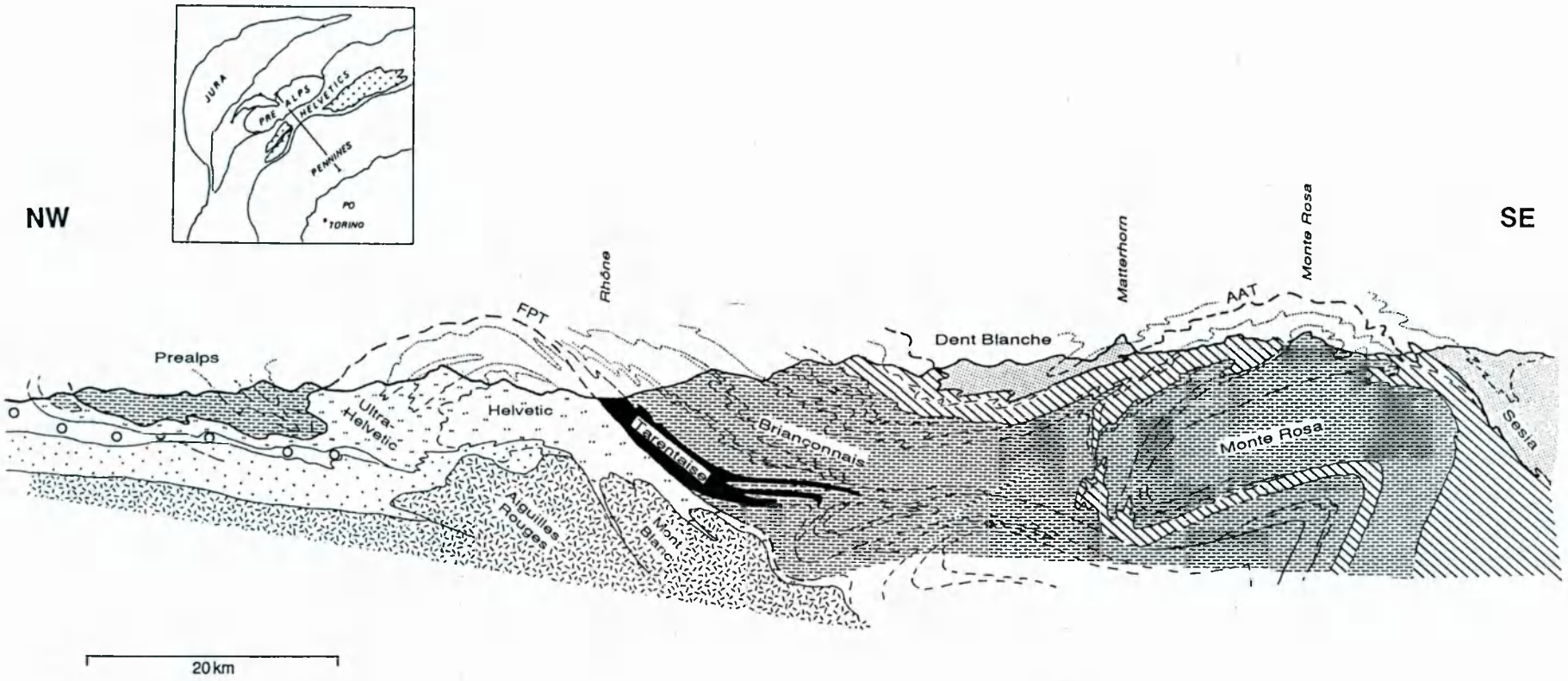

Fig. 1-6. Cross section through the Western Alps showing the complex internal structure of the Penninic nappes and the overall heterogeneity of deformation. Key as for Fig. 1-1 (lower), inset shows line of section. *AAT* = Austro-Alpine Thrust, *FPT* = Frontal Pennine Thrust. Simplified after Homewood *et al.* (1980).

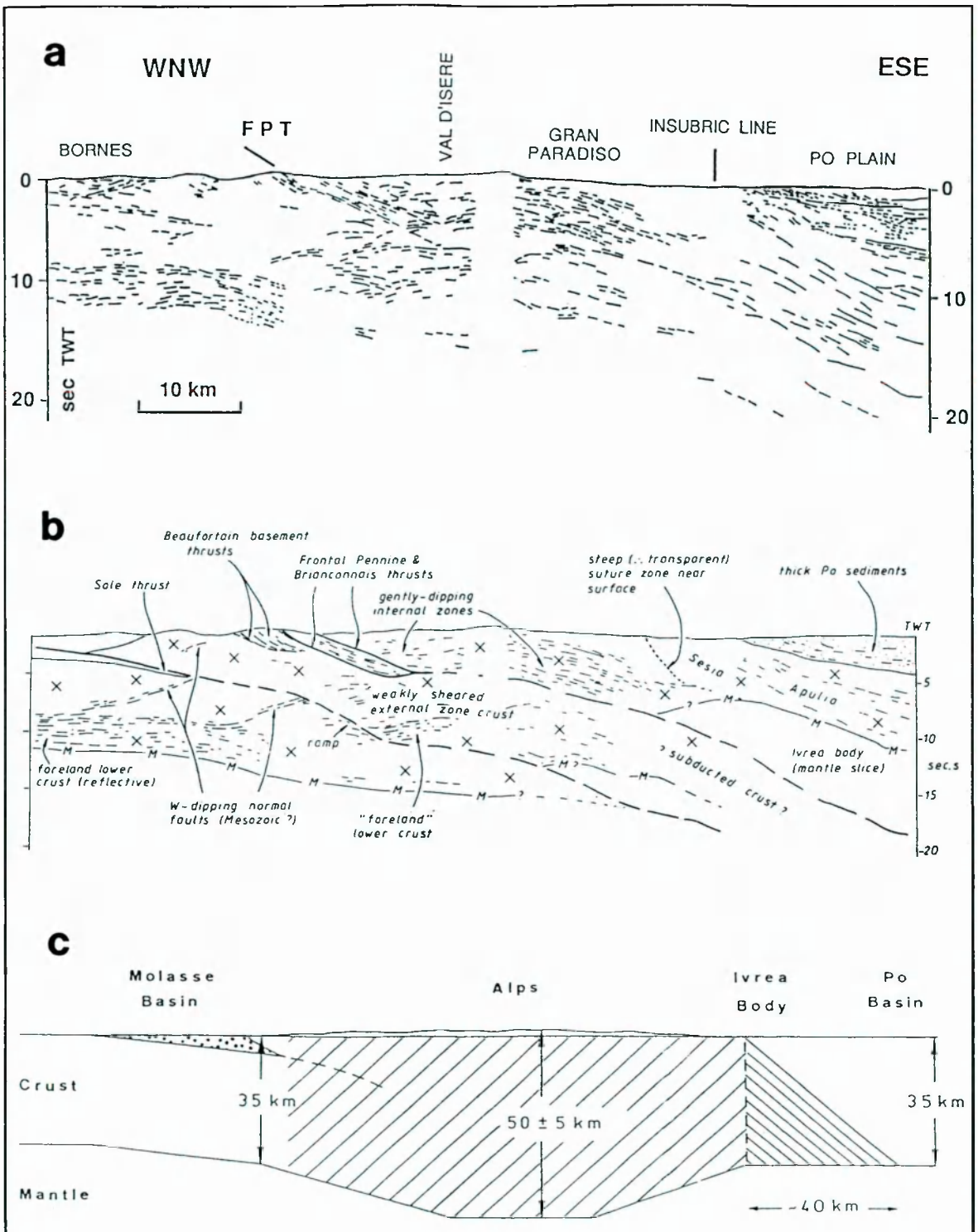

Fig. 1-7. The deep structure of the Western Alps as deduced from seismic data.
a) The ECORS–CROP deep seismic reflection profile (redrawn after Bayer *et al.*, 1987).
b) Butler's (1989a) interpretation of the ECORS–CROP line showing apparent underthrusting of European crust beneath the Pô Plain.
c) Schematic interpretation of Alpine crustal thicknesses (again based essentially on seismic data) from Ménard *et al.* (1991), showing no large scale subduction of continental crust.

Zone and Zone Valaisanne. The general equivalence of the Swiss, Italian and French outcrop segments was demonstrated by Zülauf (1964). A borderline case is the **Versoyen Zone**, a metabasite-pelite complex exposed across the Franco-Italian frontier in the Petit St.-Bernard area. The Versoyen rocks were considered to be part of the Tarentaise Zone by Antoine (1968, 1971) but their structural and palæogeographic affinities await clarification (see chapter 4). The earliest geological descriptions of the Tarentaise Zone appear to be those of Kilian & Revel (1893, 1916). A stratigraphic column for the Zone has subsequently been established through the work of Schoeller (1929), Barbier (1948), Trümpy (1954) and Antoine (1971). It is convenient to distinguish two distinct components: a Cretaceous basin-fill sequence, which constitutes the principal focus of this thesis, and a pre-Cretaceous 'substratum' forming the floor to the later basin (Fig. 1-8).

1.4-1 The Basin Floor

The sedimentary fill of the Late Cretaceous Tarentaise Basin unconformably overlies an eroded succession of Carboniferous to Jurassic terrestrial and shallow marine sediments (Fig. 1-8). The stratigraphy of this pre-Cretaceous succession has been described in detail by Antoine (1971, 1972), Collart (1973) and Fudral (1973) and only a brief summary is presented here.

Crystalline basement crops out only at Hautecour near Moûtiers (307 5040) and at Punta Rossa within the Versoyen Complex. The latter occurrence is described separately in section 4.1 alongside the rest of the Versoyen sequence. The Hautecour exposures comprise quartz-muscovite-chlorite schists with a strong SE-dipping foliation. The general absence of basement involvement in the thrust sheets of the Tarentaise Zone implies regional detachment (*décollement*) at the basement–cover interface.

Dark grey pelites and phyllites containing thin impure psammites form a 50-70m thick succession lithologically identical to the 'Houiller' (Carboniferous) of the Briançonnais Zone. Thin seams (5–10cm) of anthracite are present locally (*e.g.* at 3199 50594 in the Combe de la Neuva). Biostratigraphic evidence is non-existent and these rocks are ascribed to the Carboniferous purely by lithological analogy.

A thick (up to ~150m) heterogeneous succession of **psammites** overlies the Houiller. The basal units have been ascribed to the Upper Permian (Fabre, 1961),

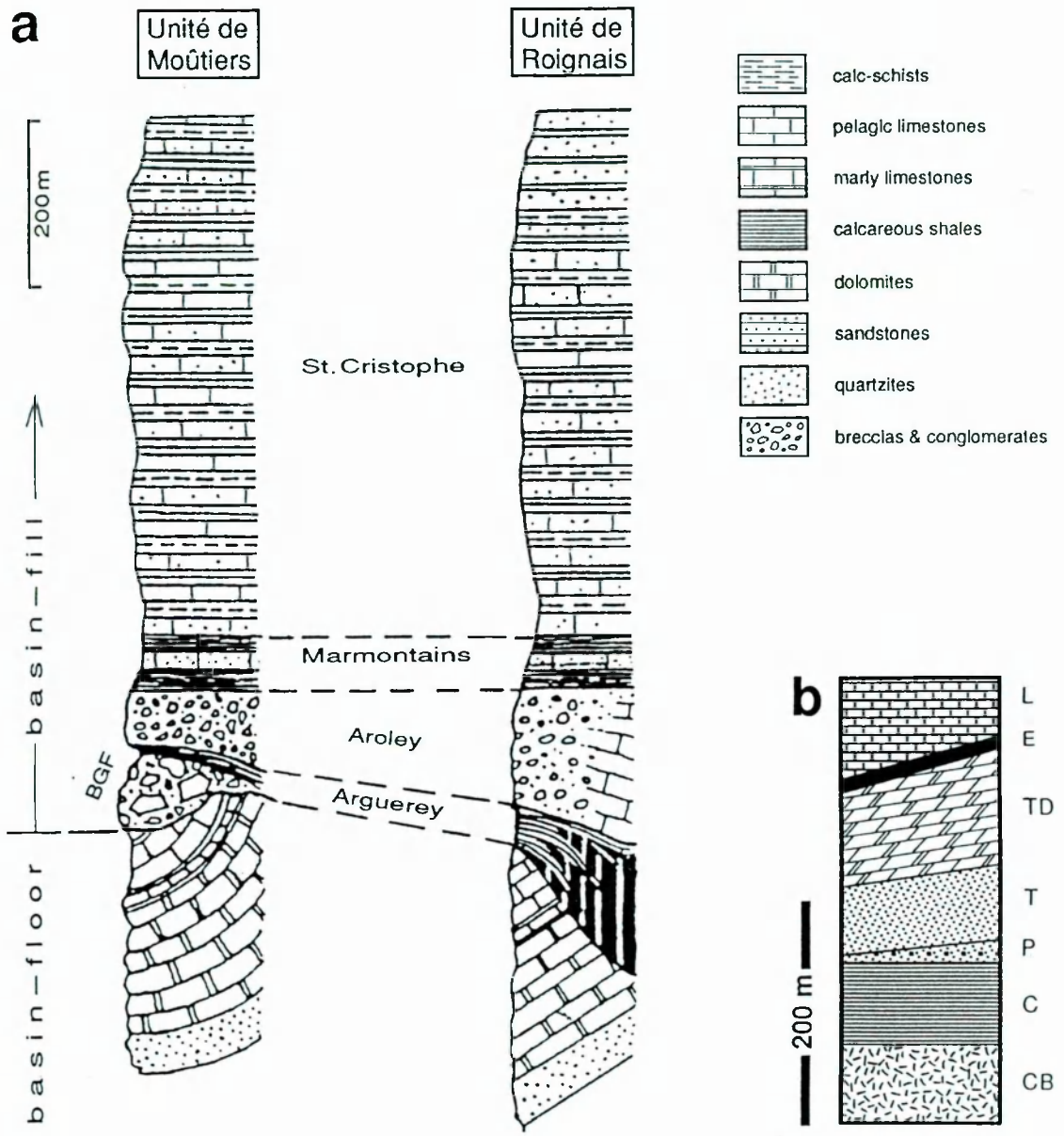

Fig. 1-8 Stratigraphy of the Tarentaise Zone, showing the distinction between basin-fill and basin-floor from the point of view of the Cretaceous Tarentaise Basin.

a) Overall stratigraphy of the Cretaceous basin-fill showing the formation names employed in this thesis (largely after Trümpy, 1954). The first-order division into Moûtiers and Roignais units (Antoine, 1970, 1971) is made essentially on the presence or absence of the Arguerey Formation. *BGF* = Brèches du Grand Fond. Modified after Debelmas & Kerckhove (1980).

b) Generalised stratigraphic column of the pre-Cretaceous rocks forming the floor to the Tarentaise Basin. Abbreviations: *C* = Carboniferous 'houiller'; *CB* = crystalline basement; *E* = evaporites; *L* = Lower Jurassic limestones; *P* = ?Permian psammites; *T* = Triassic psammites; *TD* = Triassic dolomites.

though most of the succession is thought to be Triassic in age (Antoine, 1971; Fudral, 1973). The distinction between Permian and Triassic parts of the sequence is not clear-cut since both comprise unfossiliferous micaceous quartz sandstones. In the area north of le Quermoz (311 5051), the basal part of the psammite sequence includes the 'schistes de la Bagnaz', a 120m thick interval of blue-green chloritic pelites overlying polymict conglomerates which contain clasts of rhyolite, dacite and trachyandesite (Antoine *et al.*, 1972a).

The **dolomites** comprising the greater part of the Triassic succession are crystalline carbonates which pass upwards from the underlying psammites via a transitional zone of black or purplish pelites (*e.g.* Fig. 2-33). The dolomites are predominantly buff coloured towards the base and predominantly grey at higher stratigraphic levels. Again, local age constraint is limited but lithological similarities with the better dated Triassic of the Briançonnais Zone enticed Antoine (1971) to propose an Anisian age (*i.e.* upper Lower Triassic) for the buff dolomites and a Ladinian age (*i.e.* lower Middle Triassic) for the overlying grey units (*cf.* Ellenberger, 1958).

Gypsum and cargneule are thought to belong stratigraphically to the Upper Triassic, though the outcrop of these facies is now confined exclusively to thrust detachments. The term 'cargneule' (for which 'cornieule' and 'rauhwacke' are synonyms) refers to a brecciated carbonate rock with a characteristic porous or cellular appearance (Warrak, 1974). Cargneules are restricted in occurrence to evaporitic sequences and appear to be formed by the repeated tectonic fracturing of a mixed gypsum–dolomite protolith, although the precise details remain controversial (Warrak, 1974; Jeanbourquin, 1985, 1988). The cellular porosity is a late stage feature induced by near surface chemical removal of vein dolomite and gypsum (Warrak, 1974; Amieux & Jeanbourquin, 1989).

The **limestones** which form the youngest component of the Tarentaise 'substratum' have yielded abundant* macrofossils and are therefore of disconcertingly known age. Lithologically, they are massive pale grey recrystallised packstones and wackestones comprising fine sparry (recrystallised) calcite with ghosts of shell debris and abundant post-deformation pyrite. Vertical lithological variations are limited, though the massive packstones appear to pass laterally eastwards into thinly bedded crystalline limestones with argillaceous

* *in the context of Tarentaise palæontology, 'abundant' equates to 'more than three.'*

partings (Antoine, 1971; Collart, 1973). The packstone faunas have been described by Schoeller (1929), Barbier (1951), Elter (1954), Elter & Elter (1965) and Antoine (1971) who all report remnants of stenohaline marine taxa (brachiopods, ammonites, coral fragments, echinoderm plates) along with indeterminate bivalves and gastropods. A Lower Jurassic age for these rocks, originally suspected by Kilian & Revel (1916), has subsequently been demonstrated by the discovery of an *Arietites*–like ammonite (Barbier, 1951).

1.4-2 The Basin Fill

The Cretaceous basin-fill itself may be conveniently split into four main lithostratigraphic units as summarised in Fig. 1-8 (following Trümpy, 1951, 1954; and Antoine, 1971). These four formations constitute a seemingly continuous ~1.5 km thick clastic sequence which has yielded distressingly few fossils other than a small number of benthic foraminifera (notably *Orbitolina* sp.) from the Aroley unit (Trümpy, 1951; Elter, 1954; Sodero, 1968). A fifth unit, the Brèche du Grand Fond, is developed locally at the base of the sequence on the external margin of the Tarentaise Zone. Antoine (1970, 1971) found it useful to divide the Tarentaise Zone into two units, the Unité de Moutiers and the Unité de Roignais, essentially on the presence or absence of the Arguerey Formation (Fig. 1-8).

The **Arguerey Formation** ('Antéflysch' of Antoine (1971)) is a poorly exposed, predominantly argillaceous sequence with intercalations of calcareous litharenites and granule conglomerates. It may be partly equivalent to the 'Couches de la Peula' distinguished by Trümpy (1954) in the Swiss extension of the Tarentaise Zone. Antoine (1971, 1972) regarded the 'Antéflysch' of the Tarentaise Zone *sensu stricto* as being continuous with the thick pelite sequence of the adjacent Versoyen Zone (chapter 4). This interpretation is plausible but unproven. The thickness of the Arguerey Formation varies between zero and 120m; the Versoyen pelites are somewhat thicker.

The **Aroley Formation** (Fig. 1-9a) is a coarse clastic wedge which is thinner and conglomeratic in the west of the Tarentaise Zone and thicker and predominantly arenaceous in the east (Fig. 1-8). It is gradational at its base with the Arguerey Formation, where present, and elsewhere unconformably overlies Liassic and Triassic units. Rare intact foraminifera (Sodero, 1968) indicate a marine environment and sedimentary structures suggest deposition from sediment gravity flows. The Aroley conglomerates contain clasts of limestones, dolomite,

Fig. 1-9 Field photographs of elements of the Tarentaise basin–fill in their natural habitat.
a) The upper, finer-grained, parts of the Aroley Formation near Laval, Vallée de Cormet d'Arêches (31496 505353). View looking north at subvertical beds striking NNW–SSE. Approximately 35m of stratigraphy is visible, younging is from right to left, internal strains are relatively low.
b) The St. Cristophe Formation at 33195 506732 north-east of Bassa Serra. View looking east at inverted beds dipping 55→140. Internal strains are high. Hammer (40cm) for scale.
c) The Brèches du Grand Fond at 3197 50612 WSW of Dent d'Arpire. Relatively very fine-grained part of the Grand Fond unit consisting predominantly of dolomite and limestone clasts. Internal strains are low. Hammer (40cm) for scale.


b

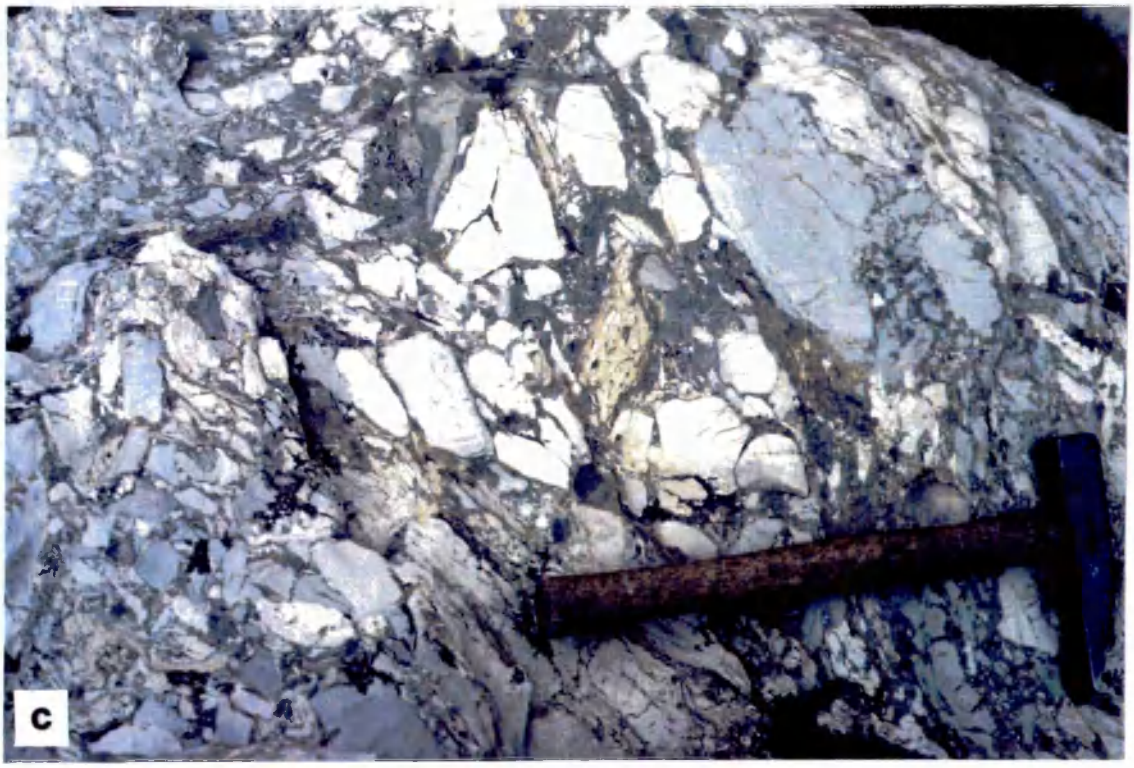
c

sandstone, shale and crystalline basement. Antoine (1971) has noted that the proportion of crystalline basement clasts increases somewhat to the west (towards the Hautecour area, where Cretaceous units directly overly crystalline basement). On these grounds, he proposed that sediment transport was predominantly towards the north-east, sourced from a 'Hautecour Cordillera'* in the south-west (*op. cit.*). Palæocurrent data from the study presented here suggest palæoflow from WNW to ESE. A discussion of Aroley Formation sedimentology forms the subject of chapter 3.

The Aroley Formation passes transitionally upwards into the less calcareous **Marmontains Formation**, which consists of chloritic quartz sandstones and dark grey shales. This relatively thin unit (typically ~30-60m) is present across the entire outcrop length of the Tarentaise Zone and shows somewhat less lateral variation than the underlying formation (Antoine, 1971; Collart, 1973). Its lateral persistence and lithological distinctiveness make the Marmontains Formation a useful stratigraphic marker in the more intensely deformed areas. In most areas, the Marmontains Formation is comprised of relatively thinly bedded (5-30cm) alternations of quartzose litharenites and weakly calcareous mudstones, deformed and metamorphosed into unfossiliferous micaceous psammites and pelites. Cross lamination is locally discernible in the psammites. Sedimentological interpretation is difficult beyond the basic inference of episodic deposition from subaqueous currents. Apparent spatial trends in bed-thickness and sand/shale ratio led Antoine (1971) to suggest that the Marmontains was supplied by a different source area to the Aroley, sediment being derived from the north-east. However, the few palæocurrent indicators observed during this study (an impressive N=7) from the Ruisseau de Jerbois (see Table 3-2) and Comba di Planaval (5728 717) are all directed towards the east or ESE (allowing for tectonic rotations), as in the Aroley Formation.

The overlying **St. Cristophe Formation** (Fig. 1-9b) comprises thinly bedded calcareous alternations of arenaceous and argillaceous lithologies which have accommodated high tectonic strains. Bed thicknesses range between 2cm and 30cm. The arenaceous beds are usually about twice as thick as the finer grained interbeds, which implies that the original sandstone/mudstone ratio was close to unity, allowing for differential compaction (*cf.* Perrier & Quiblier, 1974). Petrographically, the psammites comprise detrital quartz+carbonate lithoclasts+

* *in this context, 'cordillera' refers merely to an elongate emergent topographic high (cf. Debelmas, 1957).*

minor albite in a matrix of recrystallised calcite+whitemica+chlorite. The pelitic interbeds are quartz-bearing calcareous phyllosilicate rocks. No fossils or internal sedimentary structures have been reported to date from beds of the St. Cristophe Formation. Stratigraphic continuity with the underlying formations means that it is usually considered to belong to the same basin-filling episode as the Aroley and Marmontains. Structural complexities combined with the general lithological monotony has defeated all attempts to log vertical or lateral facies changes (Zülauf, 1964; Antoine, 1971; Fudral, 1973). Some variations have been noted however. In many areas, the basal part of the sequence is conglomeratic and resembles the upper parts of the Aroley Formation (Antoine, 1971; Collart, 1973; Fudral, 1973). At higher levels, Zülauf (1964) and Antoine (1971) have recognised a thin series of black pelites within the St. Cristophe Formation (the *'série de Malatra'*), although their precise stratigraphic position is unclear (Antoine, 1971). No stratigraphic 'top' to the formation can be defined but a thickness of 600–1100m is typically present between the Marmontains Formation and the base of the overlying thrust sheet. Whether this represents a level of regional thrust detachment or the primary sediment surface at the onset of thrusting is unknown but the former possibility is more likely in view of the absence of any pronounced sedimentological changes which could reflect proximity to growing thrust structures.

The **Brèches du Grand Fond** (Schoeller, 1929; Antoine *et al.*, 1972b) form a localised assemblage of very coarse polymict breccias developed in the frontal (external) part of the Tarentaise Zone. The name is slightly misleading because the summit of the Aiguille du Grand Fond (3187 50598) is actually composed of a substantial thickness of Aroley Formation conglomerates. The breccias themselves are rather poorly exposed on the north-west and south-east flanks of the Grand Fond massif, underlying the Aroley Formation. Their base is a very irregular erosive unconformity onto Triassic dolomites, Permo-Triassic psammites and, locally, Carboniferous pelites (*cf.* Fig. 1-8). A maximum stratigraphic thickness of approximately 250m is attained below the Aiguille du Grand Fond. The breccias comprise large blocks of limestone, dolomite, sandstone and shale set in a sparse granule-grade matrix of the same composition. Figure 9c shows a relatively fine-grained example. All of the 'substratal' stratigraphic units appear to be represented as clasts with the exception of crystalline basement lithologies. Clast sizes range up to 30x20x15m

(-14.5ø). The breccias are structureless on the scale of most exposure surfaces (*i.e.* a few tens of metres) but Antoine *et al.* (1972b) and Fudral (1973) are able to recognise a large scale internal stratigraphic organisation involving four principal facies types. From base to top these are: structureless breccias dominated by limestone clasts (~25m); finer polymict breccias with crude bedding and discontinuous pelite layers (6–30m); structureless matrix-poor coarse polymict breccias (up to 150m); structureless matrix-rich coarse polymict conglomerates (≥50m). Boundaries between these facies are not sharply defined. The interpretation of the Brèches du Grand Fond is discussed in chapter 5.

1.4-3 Age Constraint

A Cretaceous age for the Aroley Formation is indicated by benthic foraminifera (*Orbitolina* sp.) from the Aroley unit (Trümpy, 1951; Elter, 1954; Sodero, 1968). However, the precise ages of this and the overlying formations are not known. Trümpy (1951, 1955) and Sodero (1968) regarded the *Orbitolinas* as evidence for a mid-Cretaceous age, whereas Elter (1954) felt that the specimens showed *remanié* characteristics and could have been derived from older rocks. The only firm age constraint is afforded by the discovery by Antoine (1965) of rare pyritised specimens of *Globotruncana lapparenti* at the top of the Arguerey formation or the base of the Aroley Formation. *G. lapparenti* is a relatively short age-range planktonic foraminifer indicative of late Santonian to early Maastrichtian age (Caron, 1989).

1.4-4 Lateral Continuity of the Tarentaise Zone

As it passes along strike into Switzerland, the Tarentaise Zone swings from a NE-SW to a north-south orientation and its outcrop width narrows from 5-8km down to less than 1km. Continuity of outcrop is lost at the Rhône Valley near Sion, beyond which levels of metamorphism and exposure becomes unfriendly and study of the Zone becomes heavily fragmented. However, the sequence Aroley–Marmontains–St. Cristophe is apparently recognisable some 50km further east of Sion among the highly deformed nappes on the internal margin of the Aar massif (Jeanbourquin & Burri, 1991; Ackermann *et al.*, 1991).

At its southwestern end in France, the Tarentaise Zone expires abruptly at a lateral thrust termination south of the town of Moûtiers: this termination coinciding with the outcrop of a small enigmatic mélange known as the Niélard

unit, for which an Eocene age can be assigned from a proliferation of *Nummulites* (Barbier, 1948; Martinez-Reyes, 1980). The Frontal Pennine units south of this region (Sub-Briançonnais) are substantially different in terms both of their post-Jurassic stratigraphy and their style of deformation (Spencer, 1992).

1.4-5 Palæogeographic Significance

In palæogeographic terms, the Mesozoic rocks of the Tarentaise Zone are regarded as having been deposited on the northern (European) continental margin of the Piémont-Ligurian ocean. More specifically, the Tarentaise succession has been attributed to the western extremity of a distinct element of the passive margin termed the Valais Trough (*e.g.* Trümpy, 1982). However, the Valais Trough began to open in the east in the early Jurassic (Pantic & Isler, 1978; Dercourt *et al.*, 1986) whereas the main subsidence of the Tarentaise domain did not begin until late Cretaceous times and it is far from clear how this western region of subsidence relates to the Valais Trough proper to the east (*i.e.* sequences exposed in the central and Eastern Alps). For this reason, it is preferable to regard the Cretaceous sequence of the Tarentaise Zone as the fill of a Cretaceous Tarentaise Basin.

The origins and palæotectonic setting of the Tarentaise Basin are poorly understood. It has been regarded variously as an early orogenic 'flysch' basin (*e.g.* Homewood & Caron, 1982), a continental pull-apart (*e.g.* Trümpy, 1988), a back-arc basin (Hsü, 1989), a rift flank 'rim-basin' (Stampfli & Marthaler, 1990) and "...a topographically and structurally complicated not-quite oceanic trough" (Caron *et al.*, 1989). An evaluation of these basin models is presented in chapter 5. It is clear that uncertainty regarding the significance of the Tarentaise Basin derives from a primary lack of robust sedimentological and stratigraphic constraints, hence this thesis.

CHAPTER 2 STRUCTURE

The Tarentaise Zone lies within the most external portion of the belt of ductile fold–thrust deformation known as the Penninic Alps. In order to reconstruct the extensional evolution of the Mesozoic sedimentary basin represented by the Tarentaise Zone, it is necessary to understand how subsequent deformation has modified basin architecture. Accordingly, the chief aim of this chapter is to characterise the Alpine structure of the Tarentaise Zone in terms of geometry and kinematics.

A number of previous attempts have been made to describe and interpret the geometry of various parts of the Tarentaise Zone. Early structural appraisals of the Tarentaise can be found in the pioneering work of Schoeller (1929), although modern interpretations date back only to Antoine (1971, 1972), who painted a picture of large recumbent isoclines reworked by later folds and thrusts. Subsequent interpretations (Fudral, 1973, 1980; Collart, 1973; Antoine *et al.*, 1973a; Butler, 1989b; Spencer, 1990) have all built upon Antoine's work. Some of these efforts have been essentially cursory (*e.g.* Collart, 1973), others have been strongly interpretative (*e.g.* Butler, 1989b) but most are mutually contradictory and none particularly satisfactory (see section 2.4-1). Whilst most authors have acknowledged a high degree of structural complexity, none has applied detailed structural analysis in an attempt to resolve it. This study re-examines some of the problem areas and explores the possible implications for reconstructions of the Tarentaise Basin.

Reconnaissance of the whole of the Tarentaise Zone between Moûtiers and Sion (see section 1.4-4) established that the best exposed section through the Zone is afforded by a traverse between the high Breuil Valley (Italy) and the Mya massif (France), as indicated on Fig. 2-1. This is a region of appreciable topographic relief (>2km total vertical relief – pant, gasp) which provides relatively accessible and relatively continuous exposure between the most internal and most external portions of the Tarentaise Zone. The gory structural details of the Breuil–Mya traverse are elaborated in section 2.3, which forms the core of this chapter.

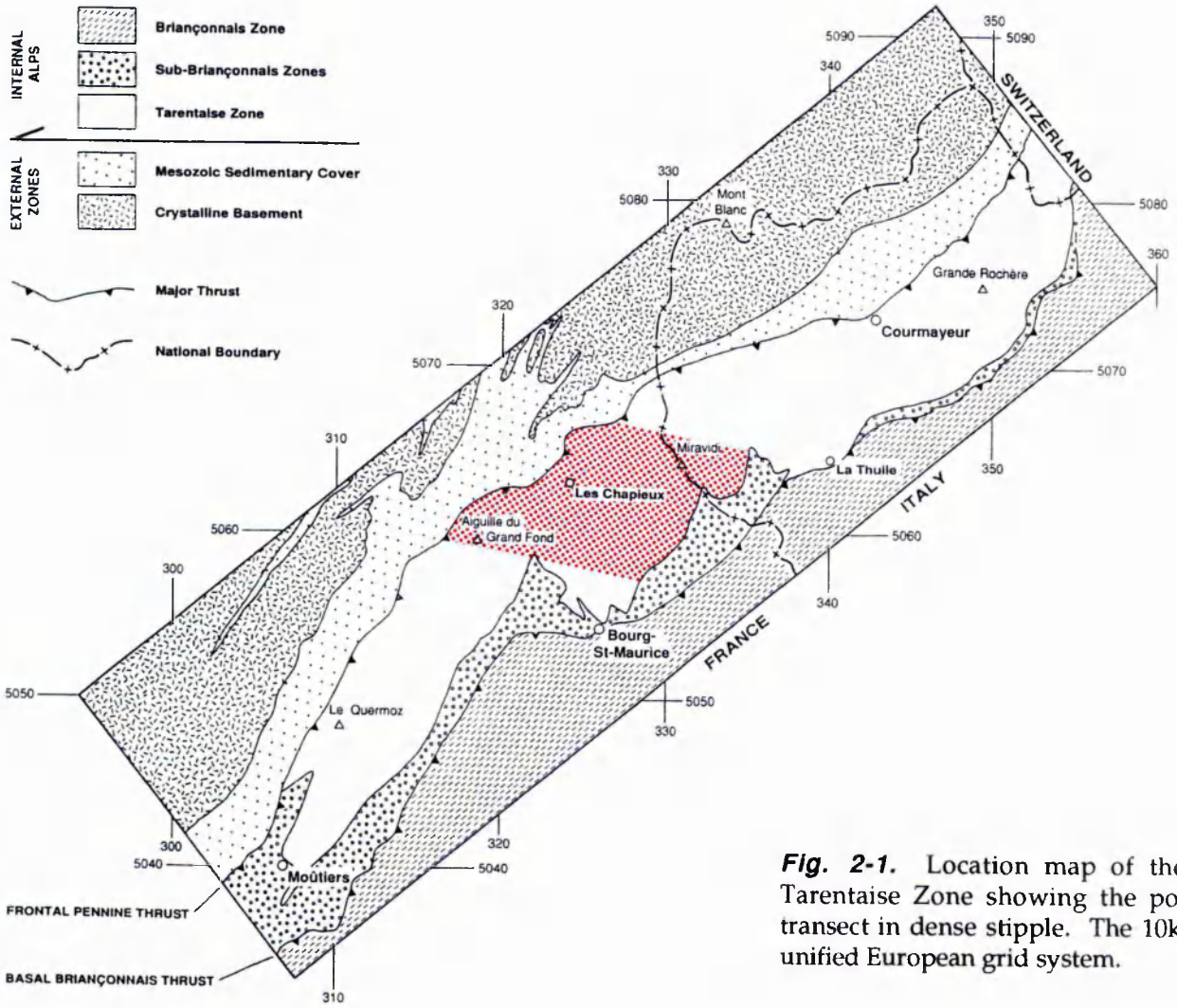

Fig. 2-1. Location map of the Franco-Italian sector of the Tarentaise Zone showing the position of the Breuil–Chapieux transect in dense stipple. The 10km grid lines correspond to the unified European grid system.

2.1 STRUCTURAL STYLE

This short section introduces some of the fundamental characteristics of Alpine deformation which typify the exposed Tarentaise Zone, as background to the map-scale structures described in section 2.3.

2.1-1 Metamorphic Grade and Deformation Mechanisms

Throughout the Tarentaise Zone mineral assemblages are indicative of metamorphism to lower greenschist facies: quartzose pelites being dominated by the association: chlorite + muscovite/phengite ± albite. Evidence for higher grade metamorphism has, however, been reported locally from metabasites of the adjacent Versoyen Complex (Miravidi Thrust Sheet) which is discussed separately in section 4.3-1. For much of the Tarentaise Zone, grain-scale deformation mechanisms appear to be dominated by diffusive mass transfer, though there is also abundant microstructural evidence of crystal plastic flow of both quartz and calcite (Fig. 2-2). Typically, stress–temperature–strain-rate conditions appear to have been such that quartz and calcite were able to deform plastically, whereas feldspar behaved in a brittle fashion (Fig. 2-2).

2.1-2 Relative Competences

It is virtually a truism that structural features of orogenic zones are related to the differing rheological properties of the deforming materials. Competence contrast, the variation in ductility between different lithologies deforming in response to the same imposed stress field, is one expression of these mechanical differences which can be readily deduced from the geometrical properties of deformation structures (Ramsay, 1982; Lister & Williams, 1983). The polymict conglomerates of the Aroley Formation provide a convenient microcosm for assessment of relative competences since they comprise clasts derived from all the underlying stratigraphic units. From the contrasting shapes of different clast species in these deformed conglomerates (Fig. 2-3), it is possible to infer a competence series thus:

dolomite > granite > psammite > limestone > pelite

which is essentially the same as the sequence regarded by Ramsay (1982) as typical of sedimentary sequences deformed under greenschist facies conditions. However, the least competent elements of the Tarentaise stratigraphy are not

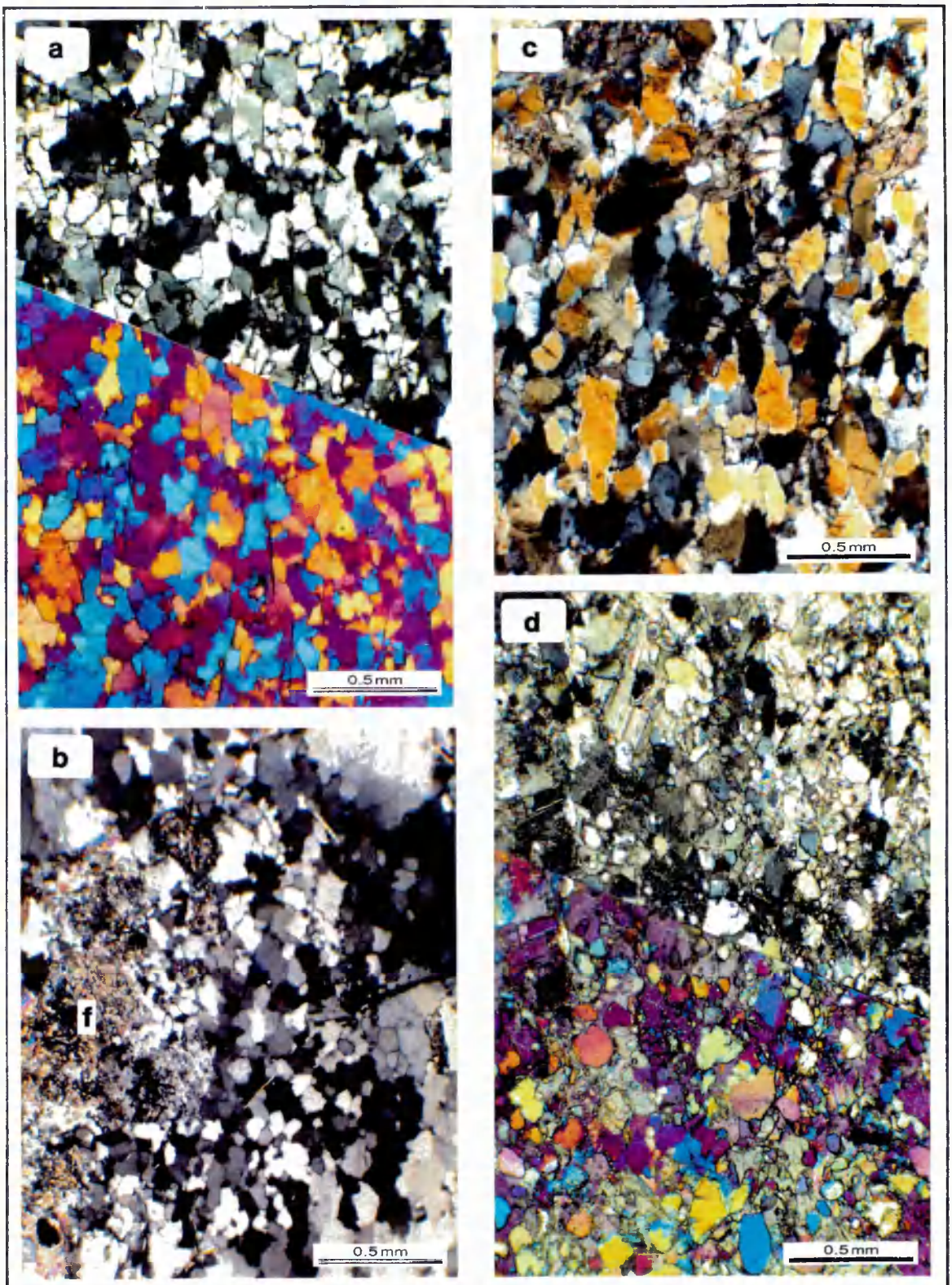

Fig. 2-2. Deformation microstructures. (See appendix 1 for specimen details.) **a)** Section cut normal to the foliation and parallel to the stretching lineation (*i.e.* close to the XZ plane of the finite strain ellipsoid) showing a strong shape fabric but relatively weak crystallographic preferred orientation (shown by sensitive tint image, lower) in quartzose domain of quartz+calcite mylonite. Trace of foliation is picked out by mica flakes. Sample FC LC 3, crossed polars. **b)** Contrasting behaviour of quartz and feldspar in leucocratic schist. Quartz domain has deformed by intracrystalline plasticity (shown by sutured grain boundaries and sub-grain formation) whereas feldspar, **f**, (now somewhat sericitised) appears to have behaved in an essentially brittle fashion. Sample FB WM 1, crossed polars. **c)** Rather thick thin section of quartzose domain in calcareous tectonite with strong stretching lineation. Section cut parallel to foliation and normal to lineation (*i.e.* close to the XY plane of the finite strain ellipsoid). Quartz grains (mostly yellow!) show evidence of deformation by intracrystalline plasticity: strong shape fabric, sutured grain boundaries, undulose extinction and internal deformation lamellae. Sample FC LC 4, crossed polars. **d)** Calcareous domain in same thin section as (c) showing lack of preferred orientation (picked out by range of colours in lower image, tinted by sensitive quartz plate) andvirtualabsence of internal strain in quartz grains, bulk deformation being accommodated by plastic strains in calcite.

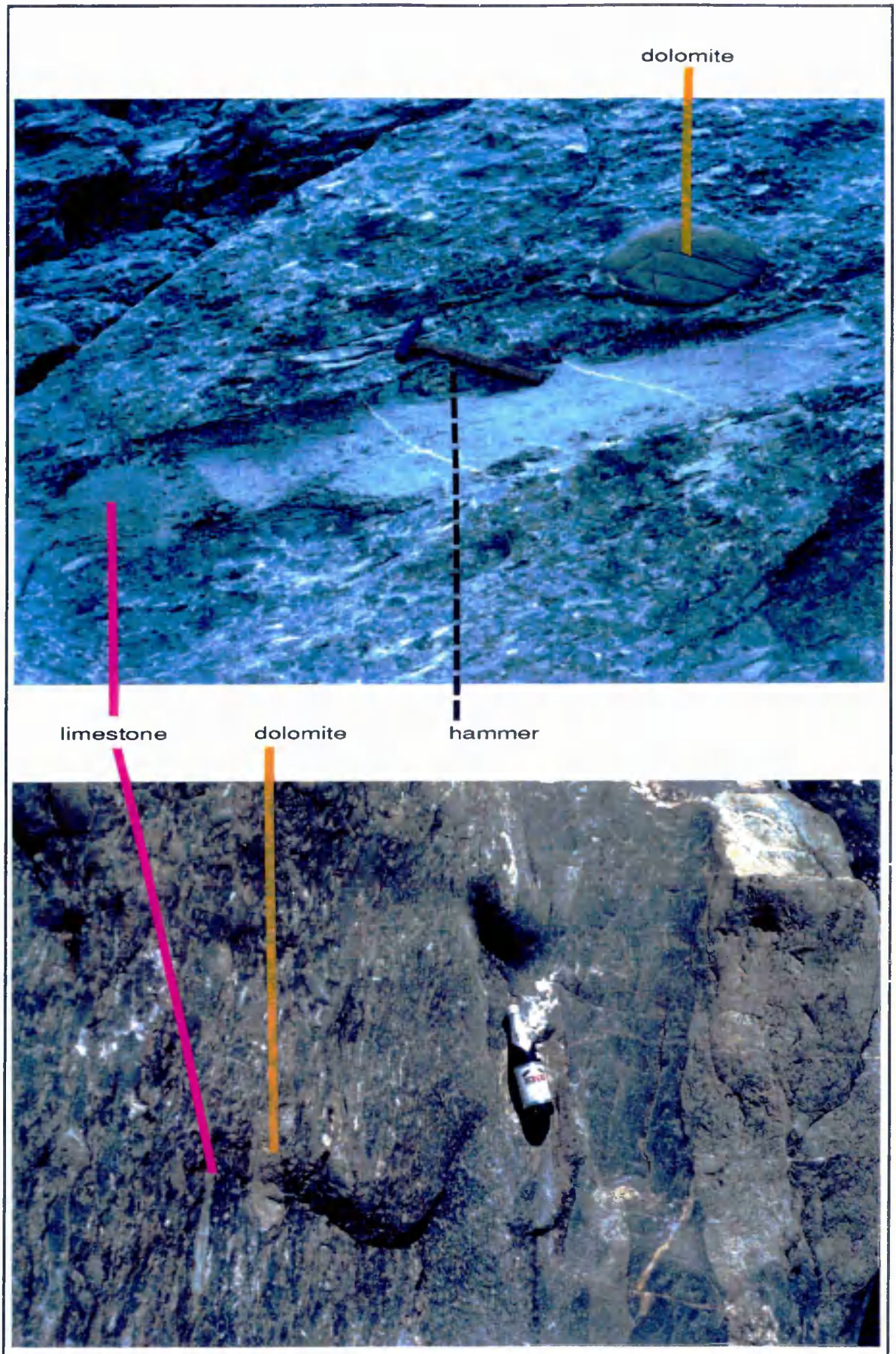

Fig. 2-3. Ductility contrast between different clast types in deformed conglomerates of the Aroley Formation, examples from west of les Glinnettes (3266 50596). Note the low aspect ratios of limestone compared with dolomite clasts.

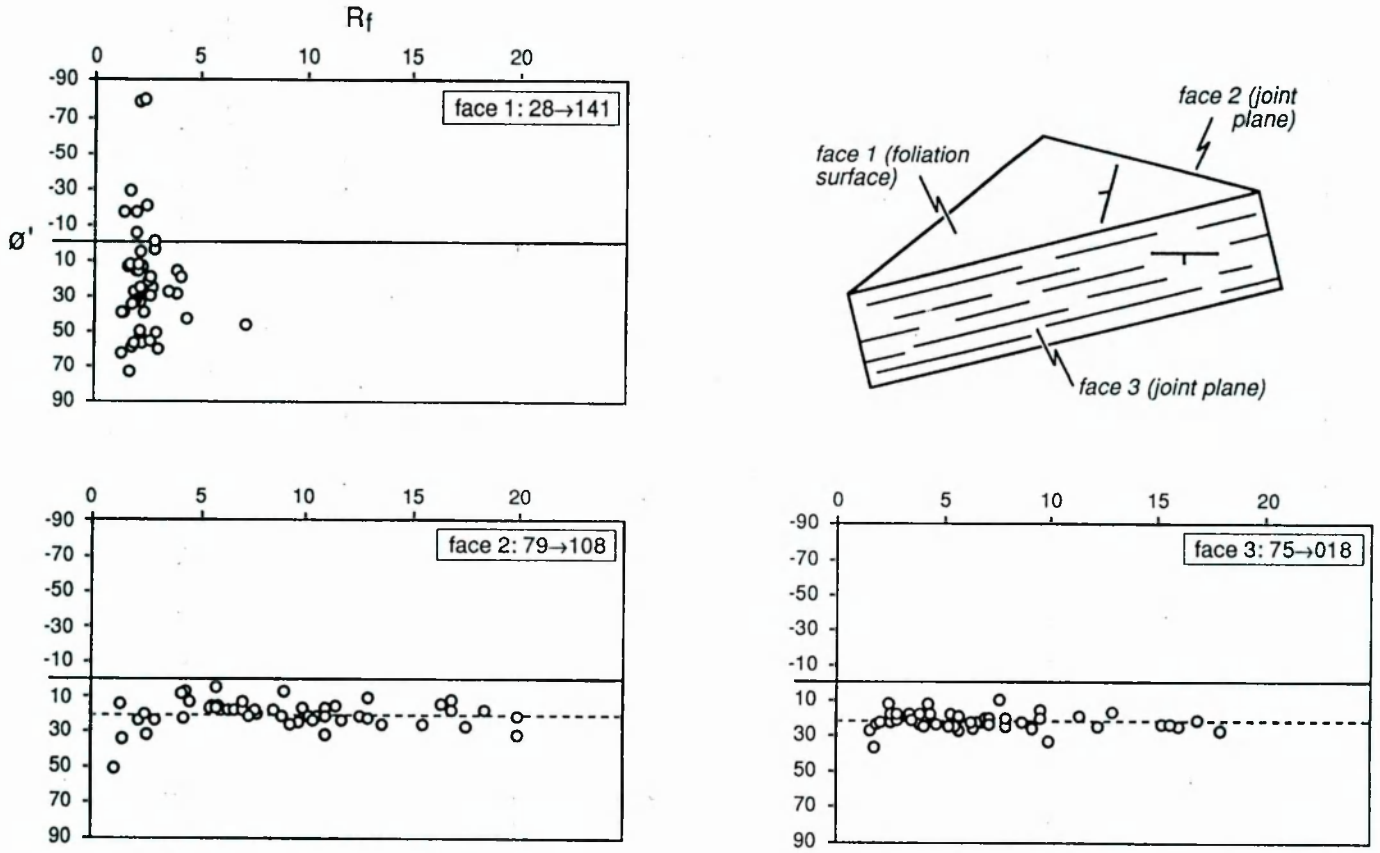

Fig. 2-4. Graphs of R_f (aspect ratio) against ø′ (long axis orientation) for deformed clasts in Aroley Formation conglomerates from the Col de la Seigne (32953 506890). Data from three mutually perpendicular (well, nearly...) exposure surfaces as shown. All data are from dolomite grains, 50 clasts per face. Reference lines (*i.e.* ø′=0°) are the horizontal for faces 2 and 3, and the north-south azimuth (projected orthogonally onto the foliation plane) for face 1. The dashed line on the plots for faces 2 and 3 represents the trace of the foliation on those surfaces. These R_f/ø′ plots demonstrate strong (foliation-parallel) flattening strains with only a weak development of a linear stretching fabric in the foliation plane (slight preferred clast orientation at ø′=20°-40° *i.e.* plunging towards 200°-220°). Since the analysis employs the most competent clast type involved in the deformation, the strains implied by these graphs will underestimate the magnitude of strain enjoyed by the rock as a whole and will also underestimate the oblateness of the bulk strain ellipsoid (Freeman & Lisle, 1987).

observed as clasts in the Aroley Formation. Serpentinite, gypsum and cargneule (see section 1.4-1) all occur as intensely sheared packages localised along structural discontinuities. In terms of the bulk competence of formations as a whole, where bedding–related anisotropy is an important consideration, the least ductile elements of the stratigraphy are the massive Triassic dolomites and Jurassic limestones. Bulk competence diminishes upwards through the Aroley, Marmontains and St. Cristophe Formations as bed thicknesses and psammite / pelite ratios decrease.

2.1-3 Strain and Deformation Fabrics

The orientations of planar and linear tectonic fabrics constitute the basic framework for structural interpretation. In particular, stretching lineations and cleavages are regarded as reliable indicators of total strain directions (respectively the X axis and XY plane of the finite strain ellipsoid). The Tarentaise Zone and adjacent zones are characterised almost everywhere by intense oblate (flattening) finite strains associated with lithology parallel foliations (Fig. 2-4). Strong linear fabrics (generally associated with plane or prolate strains) are only locally important, particularly within shear zones and fold hinge regions.

Cleavages in most of the Tarentaise Zone lithologies are defined by spaced pressure solution seams which may form continuous, planar arrays or discontinuous anastamosing fabrics (Fig. 2-5). Penetrative cleavages are commonly developed in phyllosilicate-rich lithologies and true slaty cleavages are locally evident in the pelites of the Arguerey Formation and the Carboniferous *'Houiller'*. In many parts of the Tarentaise Zone, two cleavages are recognisable: an earlier layer-parallel foliation and an overprinting spaced cleavage which commonly has a north-westerly vergence with respect to bedding and the first cleavage.

Stretching lineations, formed by rotation and elongation of pre-existing grains under intense non-coaxial shear (*e.g.* Escher & Watterson, 1974; Malavieille *et al.*, 1984), are not widely developed in the calcareous lithologies which account for the bulk of the Tarentaise Zone stratigraphy. Convincing stretching lineations are only common in coarse granular lithologies such as Triassic psammites, Aroley Formation conglomerates and the Punta Rossa granitic schists. **Intersection lineations** and **mineral growth lineations** are more abundant and in

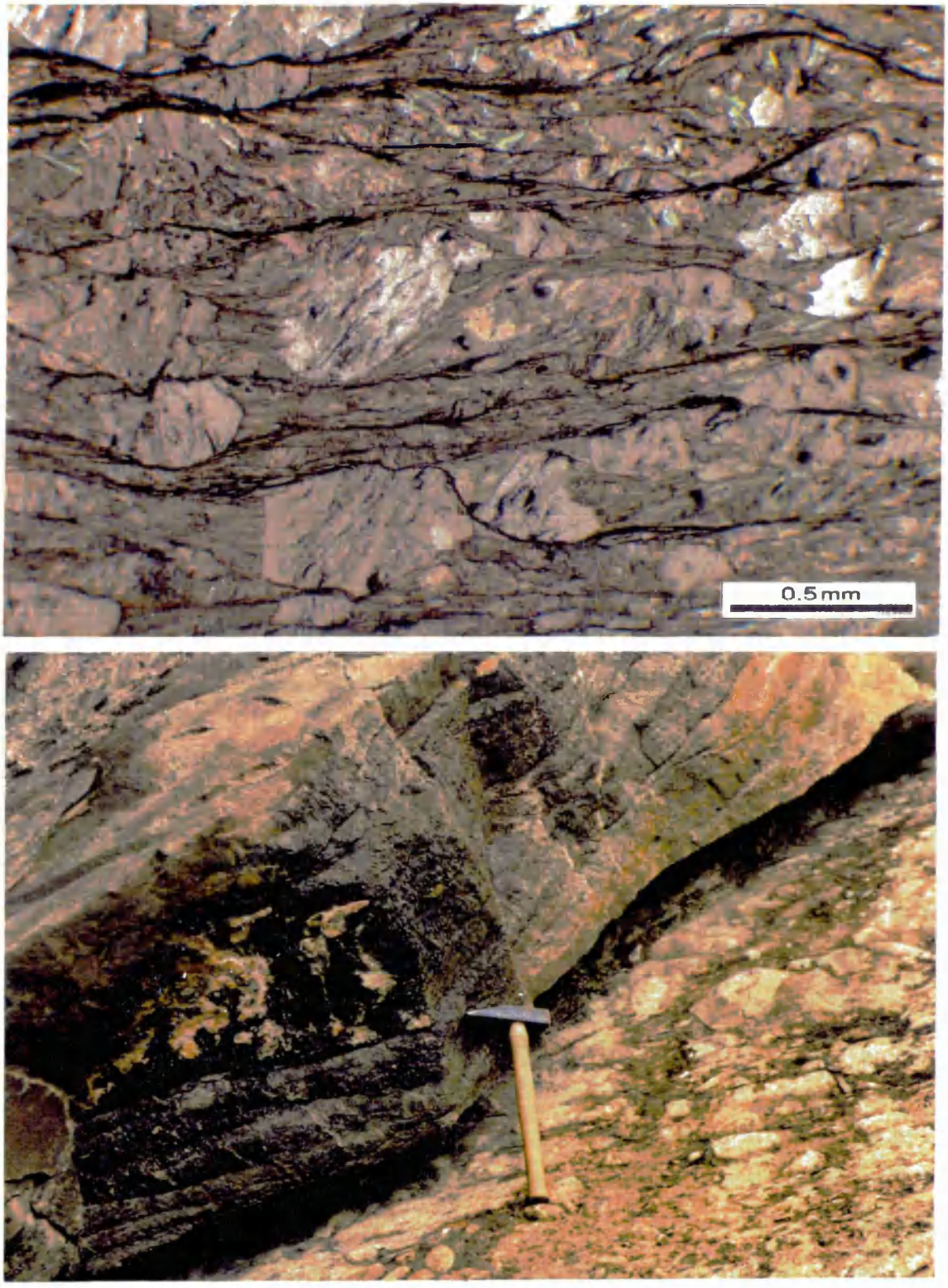

Fig. 2-5. Typical foliation types. ***Upper:*** Photomicrograph in plane polarised light of a planar cleavage defined by pressure solution seams and (to a lesser extent) mica orientations. Lithology is schistose quartz-muscovite-chlorite semi-pelite (Marmontains Formation), sample FB CH 1 (see appendix 1 for details). ***Lower:*** Anastamosing spaced pressure solution cleavage in calcareous litharenite bed (Aroley Formation) at 32466506035 in the Vallée des Chapieux. Note the weak clast long-axis alignment parallel to the bedding–cleavage intersection in the underlying conglomerate unit. Bedding and cleavage dip 34→130 and 65→120 respectively, intersection lineation plunges 22→196. The hammer is 40cm long.

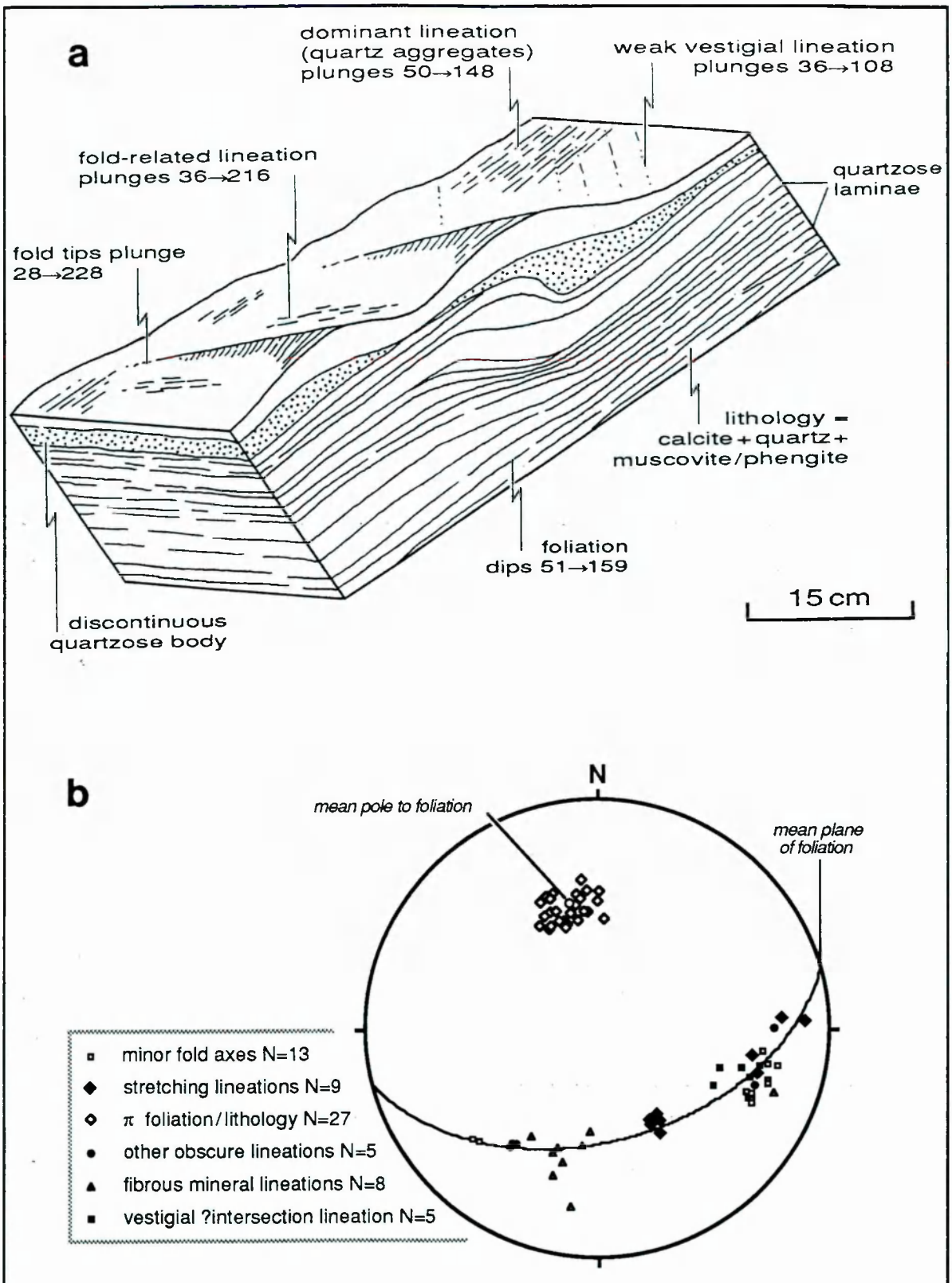

Fig. 2-6. The co-existence of multiple lineation sets. **a)** Field sketch showing the relationship between three lineation sets and laterally impersistent minor folds in calcite-quartz-mica tectonites (Aroley Formation?) at 56656 6656, ENE of Testa d'Arpi. A dominant stretching lineation, defined by streaked out aggregates of polycrystalline quartz, plunges to the south-east. Hinge-parallel, SSW-plunging fibre lineations are developed locally in fold troughs. Weak, sporadically developed, ESE-plunging lineations appears to parallel the intersections between lithological discontinuities and foliation. **b)** Lower hemisphere equal area stereoplot of structural data from the Testa d'Arpi area.

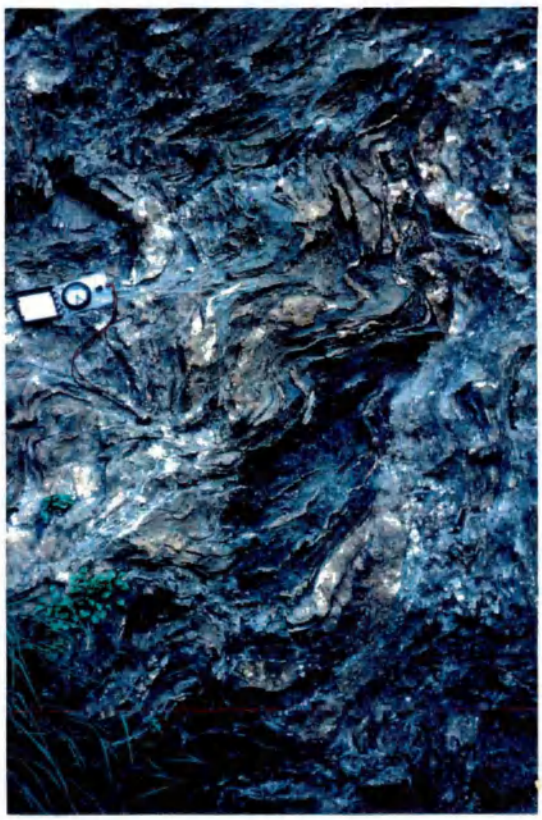

Fig. 2-7. Small scale examples of complex deformation from the Tarentalse Zone.
a) Extreme boudinage and subsequent folding of very competent dolomitic layers in calc-psammites from the Vallone del Breuil, 33385 506440 (*not in situ*).
b) Curvilinear mineral growth (?intersection) lineation from 32418 506057, Ruisseau de Belleface (*not in situ*).
c) Refolded minor fold in manky gunk (pelite and litharenite) lithologies (St. Cristophe Formation) at 32510 505983, looking south, sheet dip towards SSE, F1 hinges plunge 19→179.
d) Folded boudins in litharenites interbedded with calcareous pelites (basal St. Cristophe Formation) at 32385 506105.
e) Folded domainal pressure solution cleavage in calcite-quartz tectonites from 32650 505965 (*not in situ*).

d

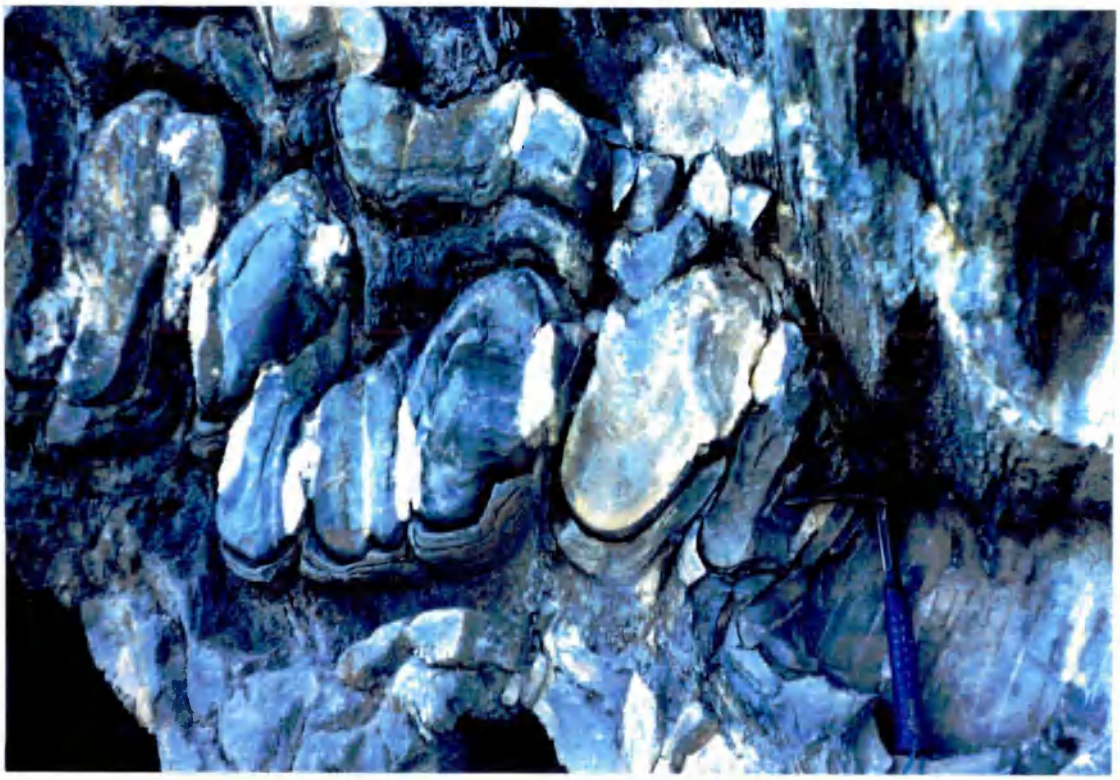

e

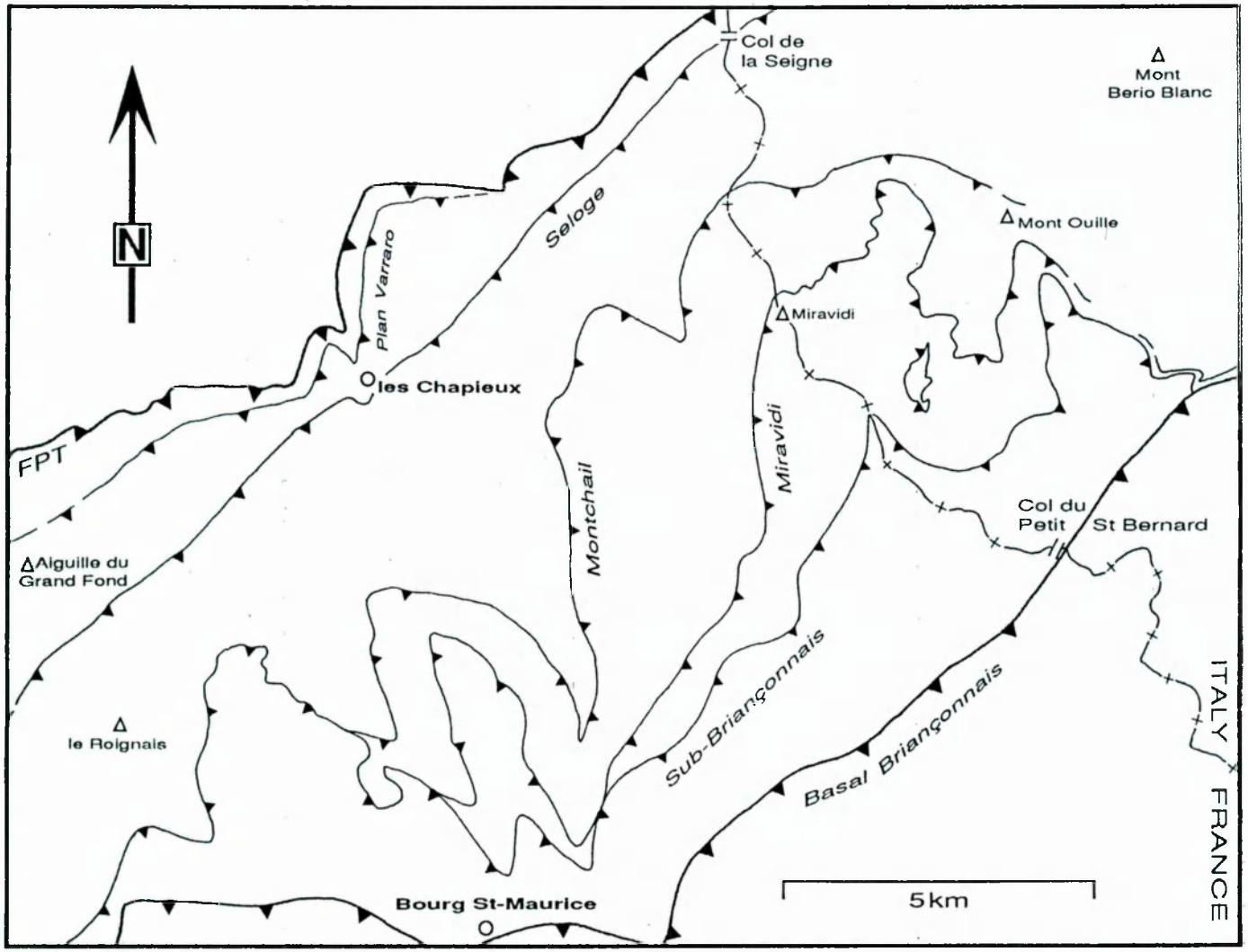

Fig. 2-8. Map of the central Tarentaise Zone showing the outcrop of the most important thrust sheets (named in *italics*). Teeth denote hanging-wall.

some areas several distinct lineation families are discernible in the same exposure (Fig. 2-6).

2.1-4 Evidence for Complex/Multiple Deformation

Few geologists have ever proposed that the structural evolution of the Alps was simple. It is clear from a range of evidence (*e.g.* multiple cleavages, curvilinear lineations, refolded boudins, refolded cleavages) that the Tarentaise Zone has been the lucky recipient of a complex deformation history. Figure 2-7 shows a few small scale examples of this complexity. It is not immediately apparent whether these features are the product of a number of distinct tectonic events or simply a single episode of complex progressive deformation. This question is addressed in section 2.4.

2.2 KINEMATICS

A fundamental first-order field interpretation of the Tarentaise Zone arises from the recognition of a number of laterally persistent structural discontinuities coinciding with zones of intense localised strain; an observation first noted by Schoeller (1929). Figure 2-8 shows the map patterns of some of the important shear zones traced in this study. Though they are mapped as thrusts (since they produce contractional offsets with respect to stratigraphic layering), they are nevertheless *zones* of deformation rather than discrete fault planes. Map relationships do not tightly constrain the movement vectors of these shear zones so it is necessary to examine the associated deformation structures in order to deduce the direction of tectonic transport.

2.2-1 Rationale for Kinematic Analysis

Kinematic analysis is concerned with interpreting the deformational movements responsible for the development of observed structures. Of particular interest in orogenic belts are the movement paths of the shear zones which accommodate much of the crustal shortening. How can the direction of displacement in these shear zones be determined in the field? The problem is relatively straightforward when deflected markers can be traced into a shear zone (Ramsay, 1980; Wheeler, 1987) but in most instances such direct kinematic information is unavailable and

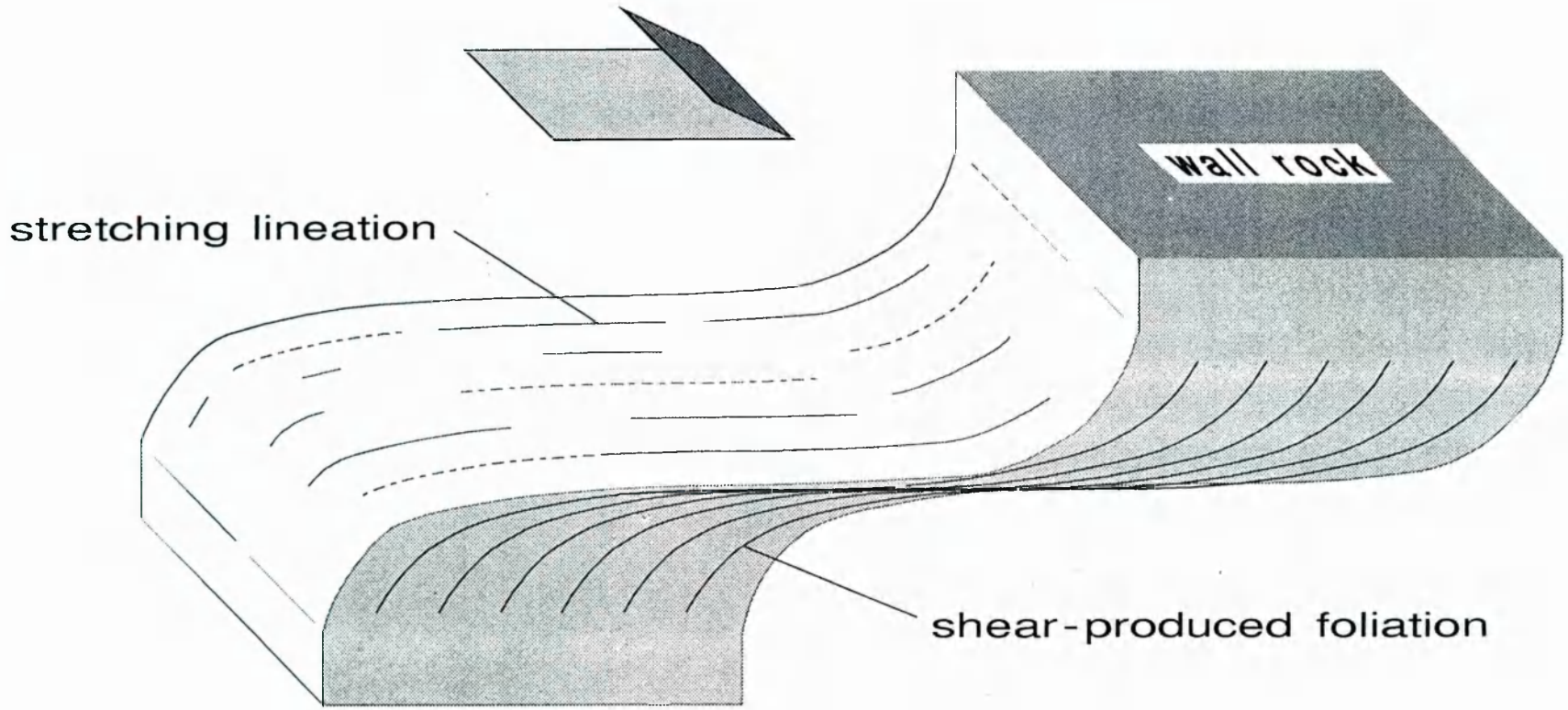

Fig. 2-9. Block diagram of a hypothetical ductile shear zone illustrating the kinematic reference frame. The shear plane can be identified on the basis of the strain gradient, the extension lineation approximates to the displacement axis (X) and the foliation (≈ XY) rotates towards the flow plane with increasing strain. Shear-sense criteria need to be sought in that plane normal to the shear plane which contains the extension direction; that is, in the XZ plane of the finite strain ellipsoid. (Based on Hanmer & Passchier, 1991).

recourse has to be made to subtler clues. It is widely accepted that the finite extension lineation (stretching lineation) may approximate to the shear direction in intensely strained rocks (*e.g.* Escher & Watterson, 1974; Malavieille *et al.*, 1984; Choukroune *et al.*, 1986), but the lineation does not indicate the *sense* of motion. Over the past decade, considerable interest has focused on small scale deformation structures which can be used to infer the sense of shear in shear zones (*e.g.* Simpson & Schmid, 1983; White *et al.*, 1986; Hanmer & Passchier, 1991). The rationale is as follows: ductile shear zones are localised zones of enhanced flow in which strain accumulates incrementally during progressive deformation. In general, the flow is non-coaxial: that is, the imposed shear induces a progressive rotation ('vorticity') of the principal directions of the finite strain ellipsoid with respect to the instantaneous stretching axes (and the shear zone walls). Consequently, any minor structures whose geometries are systematically modified by this progressive non-coaxial flow will reflect the induced vorticity and thus indicate the sense of shear. Hanmer & Passchier (1991) define a shear-sense indicator specifically as: *"a structure, resulting from progressive deformation, whose geometry is indicative of the progressive rotation of the finite strain axes with respect to the instantaneous stretching axes and/or the flow plane, at the scale of observation."* which is another way of saying that shear criteria are structures whose asymmetry is related to the vorticity of the deformation. Such structures include: rotated porphyroclasts (Passchier & Simpson, 1986), S/C fabrics (Berthé *et al.*, 1979; Lister & Snoke, 1984), extensional shear bands (Platt & Vissers, 1980), pressure shadows and fringes (Ramsay & Huber, 1983), crystallographic fabrics (Lister & Williams, 1979) and asymmetric intrafolial fold systems. The use of these deformation structures as shear criteria has recently been comprehensively reviewed by Hanmer & Passchier (1991) who emphasise that potential indicators of movement sense should be interpreted in relation to a well constrained kinematic framework. Figure 2-9 illustrates the point that valid observations of shear-sense criteria need to be made in the plane perpendicular to the shear-produced foliation and parallel to the stretching lineation (*i.e.* in the XZ plane of the finite strain ellipsoid).

2.2-2 Kinematics of the Western Alps

Despite being the focus of much research over the last twenty years, the kinematic evolution of the Western Alps remains controversial. The Alps have

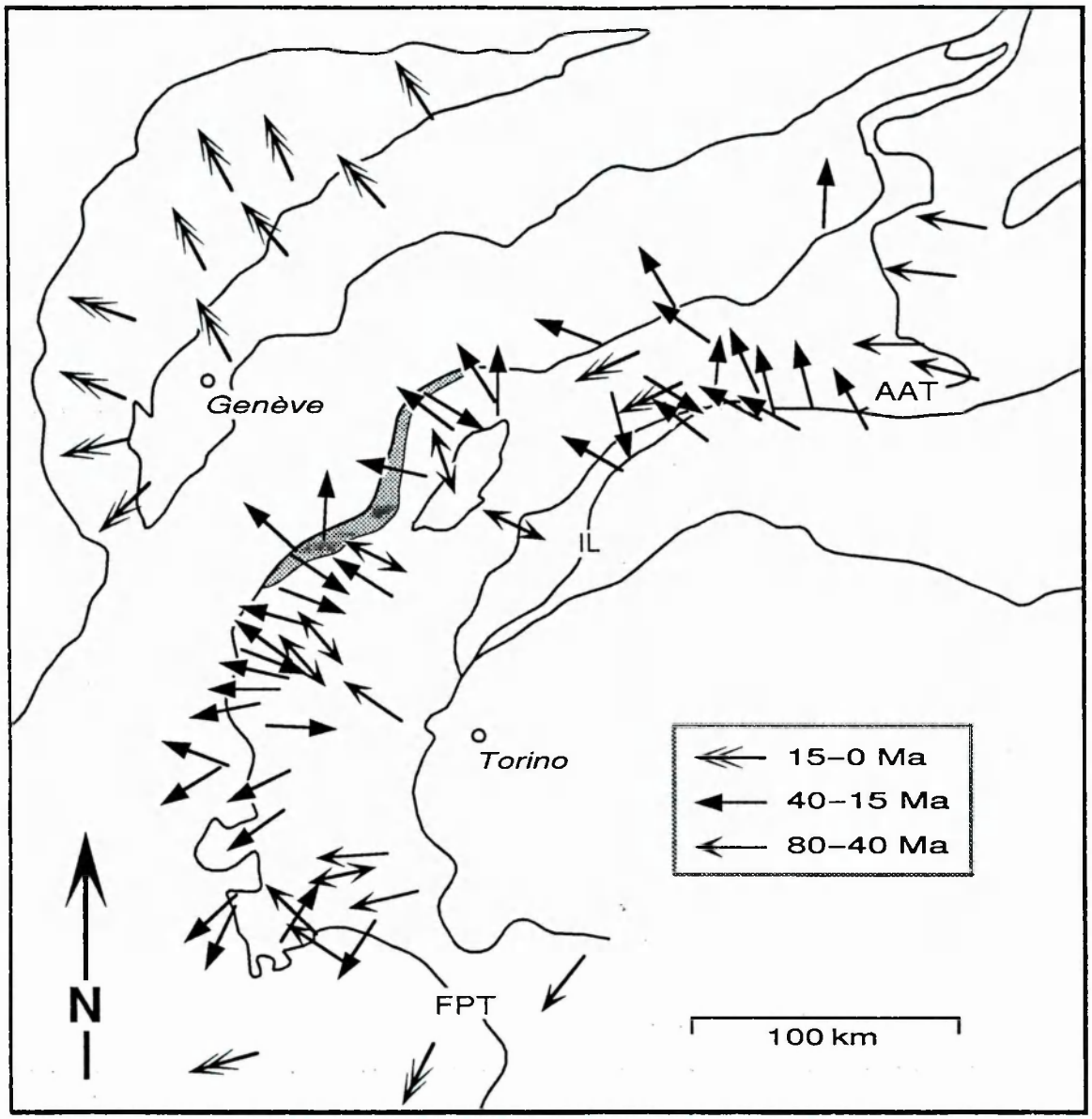

Fig. 2-10. Kinematic data for the Western Alps plotted by age (simplified after Platt *et al.*, 1989a). The Tarentaise Zone is indicated by a grey smudge. Arrows give the direction and sense of shear; double-ended arrows indicate that the shear sense is not known. The data location lies at the arrow tip for single-ended arrows and at centre of the shaft for bi-directional arrows. The large black arrow with 'N' on it is of no kinematic significance. *AAT* = Austro-Alpine Thrust, *FPT* = Frontal Pennine Thrust, *IL* = Insubric Line.

traditionally been interpreted in terms of north-south convergence between Africa and Europe (Argand, 1916) but more recent research has found some difficulties with this interpretation (*e.g.* Goguel, 1963; Ricou, 1984; Butler, 1985; Platt *et al.*, 1989a,b). There are two aspects to the problem. The first concerns the question of thrust transport directions in the Alps, the second is the broader question of the relative motions of the plates which interacted to induce the Alpine collision. Intuitively the two problems must be linked: the transport vectors of orogenic shear zones should be related, albeit indirectly, to the vectors of plate motion responsible for the orogenic contraction. Shackleton & Ries (1984) articulated the belief that regionally consistent stretching lineations are essentially coincident with the relative motions of the converging plates. This view was extended by Platt *et al.* (1989a) who attempted to use kinematic data from Alpine tectonites to constrain plate motions, on the assumption that thrusting directions are the resultant of forces set up by plate convergence and those generated by gravity within the uplifting orogen. Platt *et al.* interpreted the available kinematic data (Fig. 2-10) in terms of apparently simultaneous radial thrusting directions around the Alpine arc (*op. cit.*). In contrast, Fry (1989a, b) has suggested that the relative plate motions were partitioned into a small number of distinct but overlapping thrusting directions, giving the illusion of a radial arc-normal spread of displacement directions. Other workers have emphasised the possible importance of strike-slip displacements as either a primary (*e.g.* Laubscher, 1971; Ricou & Siddans, 1986) or secondary mechanism of accommodating Alpine convergence (*e.g.* Coward & Dietrich, 1989; Hubbard & Mancktelow, 1992).

The Alpine kinematic dataset, though difficult to interpret, is now quite voluminous (Fig. 2-10). Regional syntheses of movement indicators have been compiled by Malavieille *et al.* (1984), Choukroune *et al.* (1986) and Platt *et al.* (1989a). For the external zones, where only late Cenozoic translations are recorded, kinematic data are remarkably coherent and indicate foreland directed motion apparently normal to the Alpine arc since the Eocene (*i.e.* since about 40 Ma) (Choukroune *et al.*, 1986; Platt *et al.*, 1989a). For the internal Alps, this radial pattern is much less apparent and indeed the older kinematic indices (80–40 Ma on Fig. 2-10) define an approximately unimodal NW–SE distribution (Malavieille *et al.*, 1984; Platt *et al.*, 1989a). An added complexity in the internal zones is the presence of east– or SE–directed structures (Fig. 2-10). These have traditionally

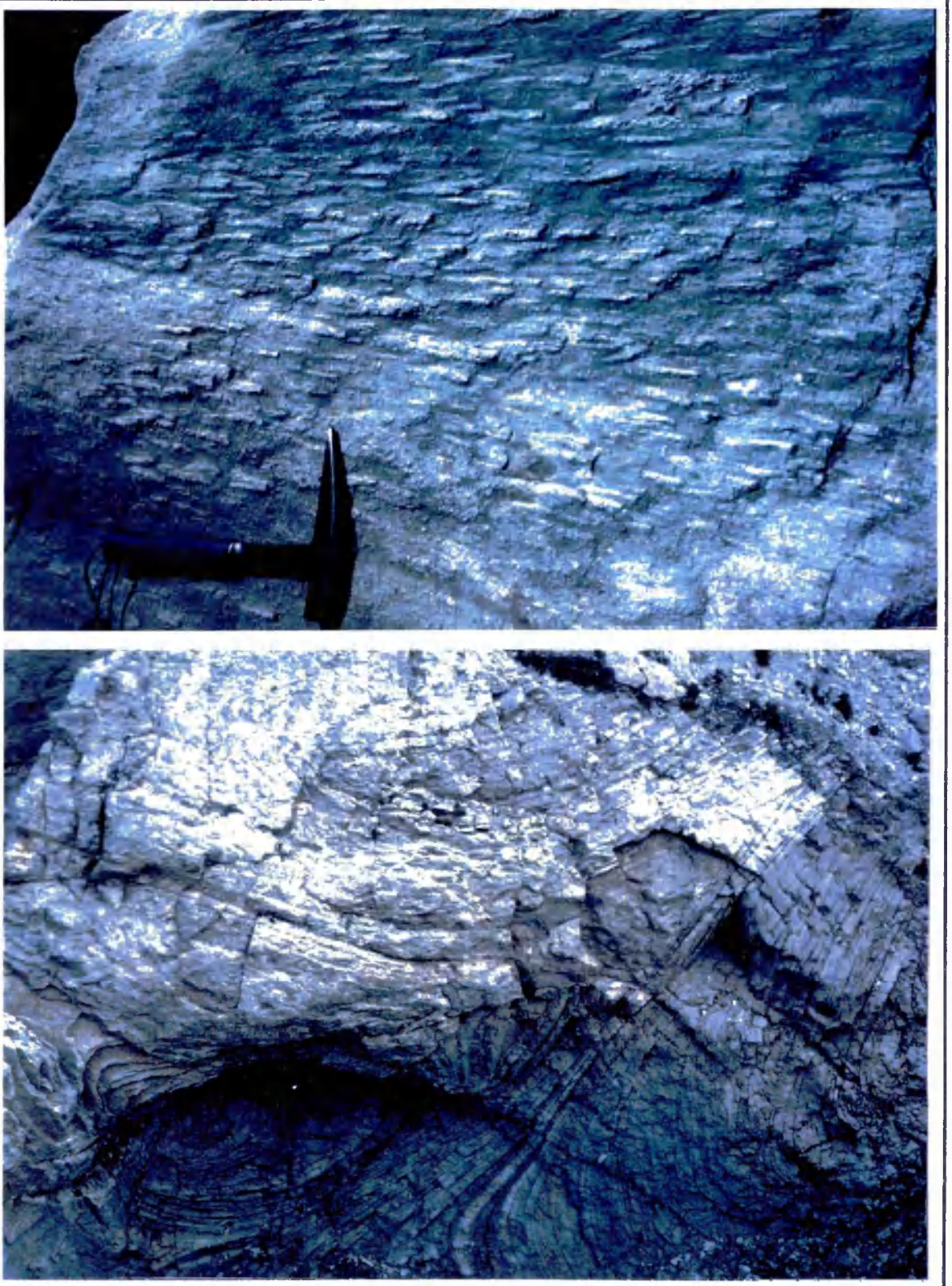

Fig. 2-11. Constraints on the thrust transport axis in the Tarentaise Zone. ***Above:*** stretching lineations: this example from Triassic psammites in the immediate hangingwall to the Seloge Thrust, Combe de Neuva (not *in situ*). Hammer for scale. ***Below:*** sheath folds developed in gypsum along the Seloge Thrust in the Combe de Neuva at 32036 505987. Looking SE, field of view ~10m high. The sheath axes at this locality plunge approximately 29→120 (associated foliation dips 31→106), suggesting transport towards 300°.

been interpreted in terms of *rétrocharriage* (backthrusting) and more recently partly in terms of hinterland–directed extensional shearing (*e.g.* Wheeler, 1991; Avigad, 1992).

The zones both internal and external to the Tarentaise Zone appear to have been dominated by thrust transport on a WNW–ESE to NW–SE axis (Fig. 2-10), though some of this displacement in the Briançonnais Zone was directed towards the hinterland (Debelmas, 1976; Platt *et al.*, 1989b). The dominant motion on the Frontal Pennine Thrust, which forms the external edge of the Tarentaise Zone, is thought to have occurred towards the WNW in this area (Butler, 1985; Butler *et al.*, 1986; Spencer, 1992).

2.2-3 Shear Criteria from the Tarentaise Zone

Constraints on the displacement axes of the shear zones in the study area are provided by stretching lineations (Fig. 2-11a), and by sheath folds in gypsum along a branch of the Seloge Thrust (Fig. 2-11b). As noted in section 2.1-3, stretching lineations are not well developed in the calcareous rocks which dominate the Tarentaise Zone and consequently the transport direction is poorly known in some areas. Throughout most of the zone, finite extension lineations are oriented NNE–SSW (Fig. 2-12), parallel to the regional strike, which is problematic (section 2.4-2). Within the shear zones themselves, however, a movement axis within the range west–east to NW–SE is invariably demonstrable. For this reason the cross-section lines discussed in section 2.3 are oriented WNW–ESE.

Figure 2-13 shows examples of the criteria used to deduce the movement sense in these shear zones. In many instances the available structures are equivocal, but for all unambiguous criteria a consistent shear sense of top-to-the-west or top-to-the-NW is indicated. There is no convincing evidence of hinterland-directed thrusts or shallowly dipping extensional faults within the Tarentaise Zone itself. Antoine (1971) and Spencer (1990) discuss possible backthrust geometries from the 'Salins' area on the internal margin of the Tarentaise Zone, but kinematic data (Fudral, 1980; this study) indicate that this is a gently folded WNW-directed structure.

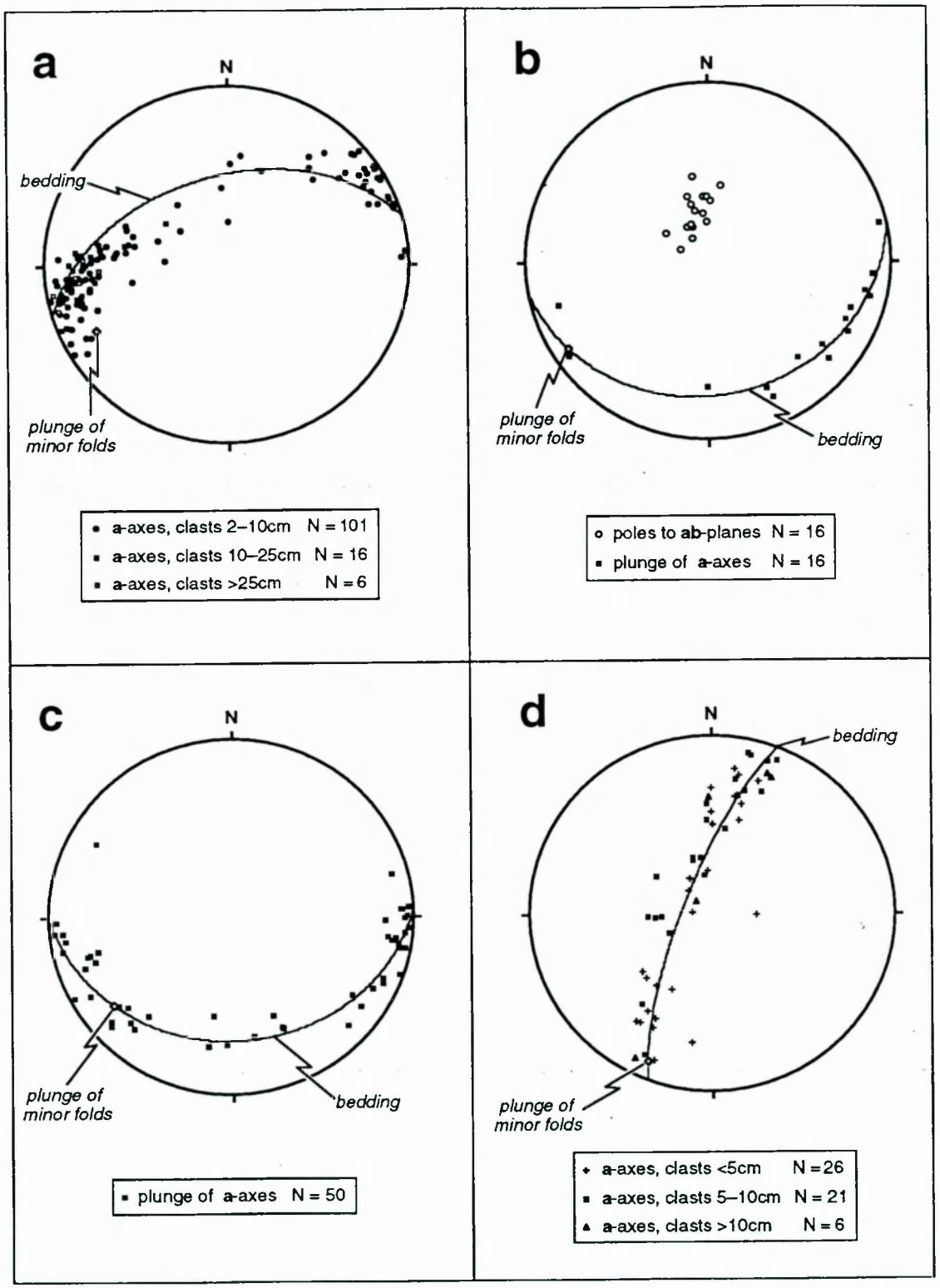

Fig. 2-12. Grain-shape fabrics from Aroley Formation conglomerates in relation to bedding and local fold hinges. **a**) from the high Vallone di Chavannes at 33476 506980. **b**) from the high Vallone di Chavannes at 33482 506980 **c**) from the high Vallone di Chavannes at 33480 505976. **d**) from the Ruisseau de la Jerbois at 31595 505546.

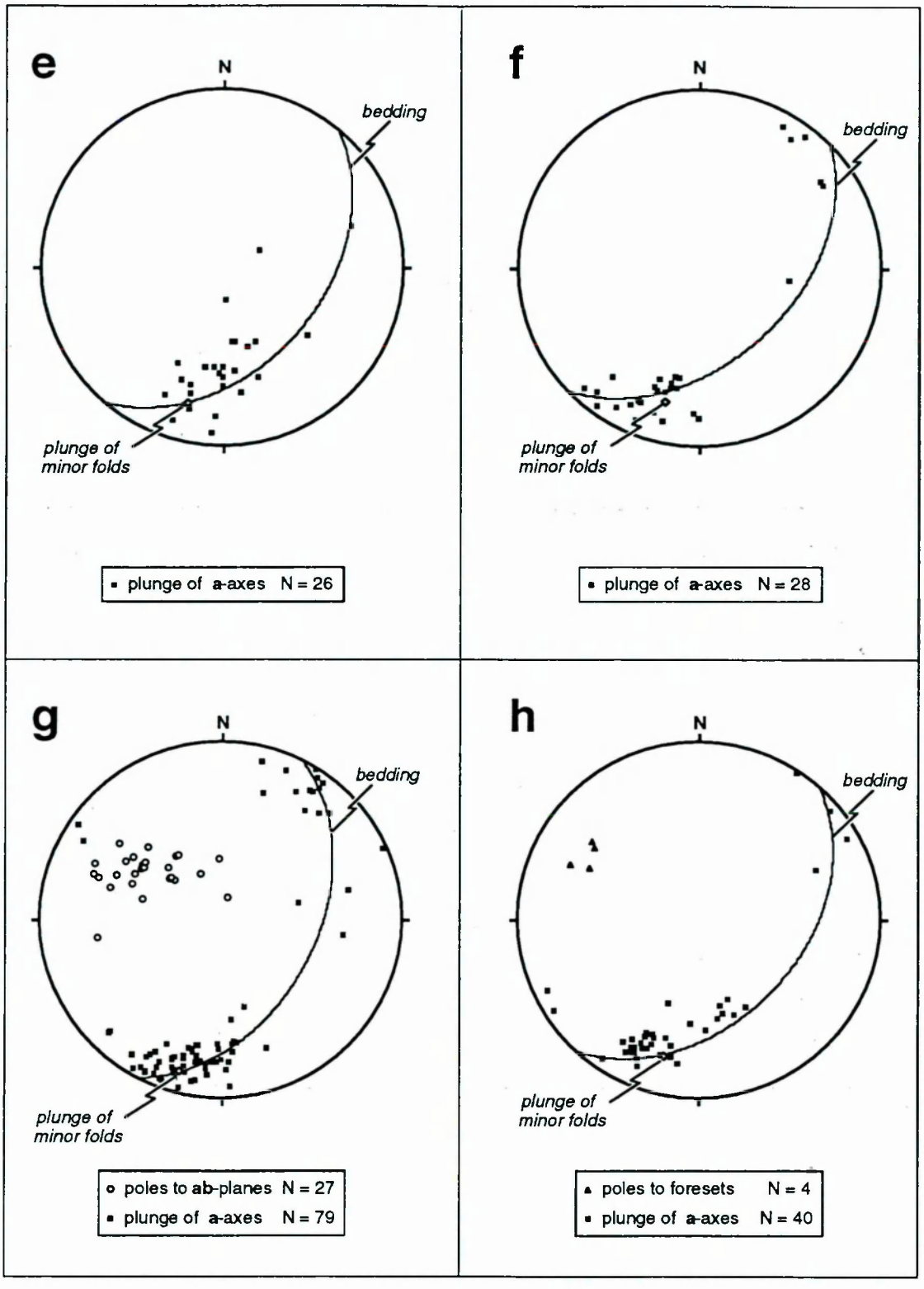

Fig. 2-12 continued.
e) from the Vallée des Chapieux at 32491 506070. **f**) from the Vallée des Chapieux at 32491 506070. **g**) from the Vallée des Chapieux at 32466 506035. **h**) from the Vallée des Chapieux at 32495 506072.

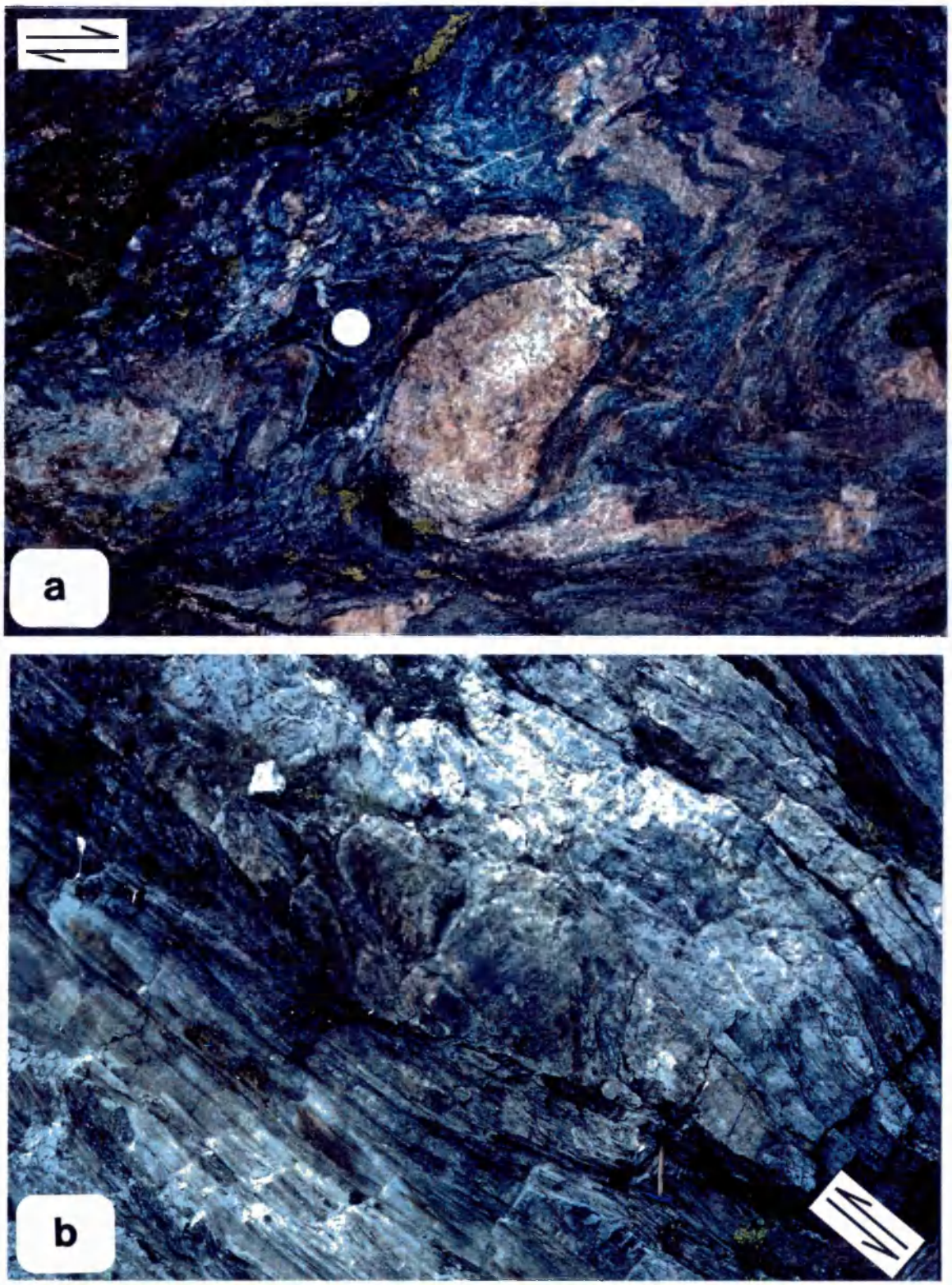

Fig. 2-13. Examples of shear criteria in tectonites from the Tarentaise Zone. Inferred sense of shear is indicated, see appendix 1 for sample details. **a)** Rotational asymmetry of granitic clasts in deformed matrix-supported conglomerate at 33354 506267. Left-hand-side=WSW, right=ENE, coin for scale. Interpretable as 'δ-type' winged porphyroclasts (see Passchier & Simpson, 1986) but other origins are possible: hence shear sense is ambiguous. **b)** Asymmetric sheared pod of dolomite-rich conglomerate enclosed in quartz-chlorite (above) and quartz-calcite (below) tectonites. Plan Vans, Swiss Val Ferret (5766 8142). View looking north at an east–west face, 40cm long hammer for scale. Mylonitic foliation dips 50→098, stretching lineation plunges 45→112. Seems to represent deflected shear around more rigid pod but ambiguous. **c)** Extensional crenulation cleavage in leucocratic basement schists (sample FB LEPT 1), left=ENE, right=WSW, coin is 17mm in diameter. Convincing. **d)** Photomicrograph showing stepped micaceous domains on chlorite porphyroclast (sample FB LT 5), foliation dips 48→173, left=WNW, right=ESE, crossed polars. Appears to be a 'σ-type' winged porphyroclast. Fairly convincing. **e)** Photomicrograph showing rotational asymmetry around polycrystalline quartz porphyroclast in limestone mylonite (sample FA M1), crossed polars, left=NW, right=SE. Very ambiguous.

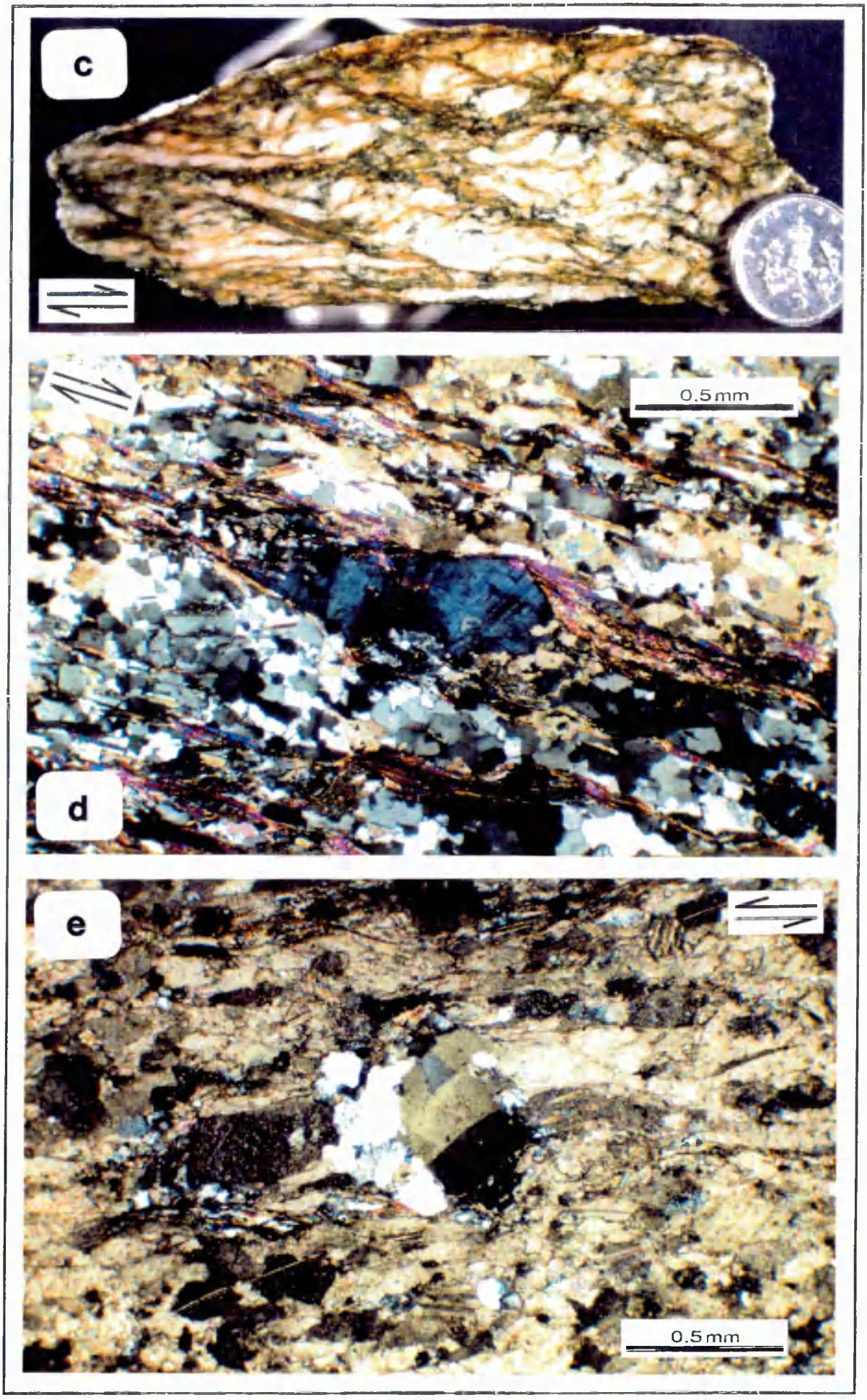
c
0.5 mm
d
e
0.5 mm

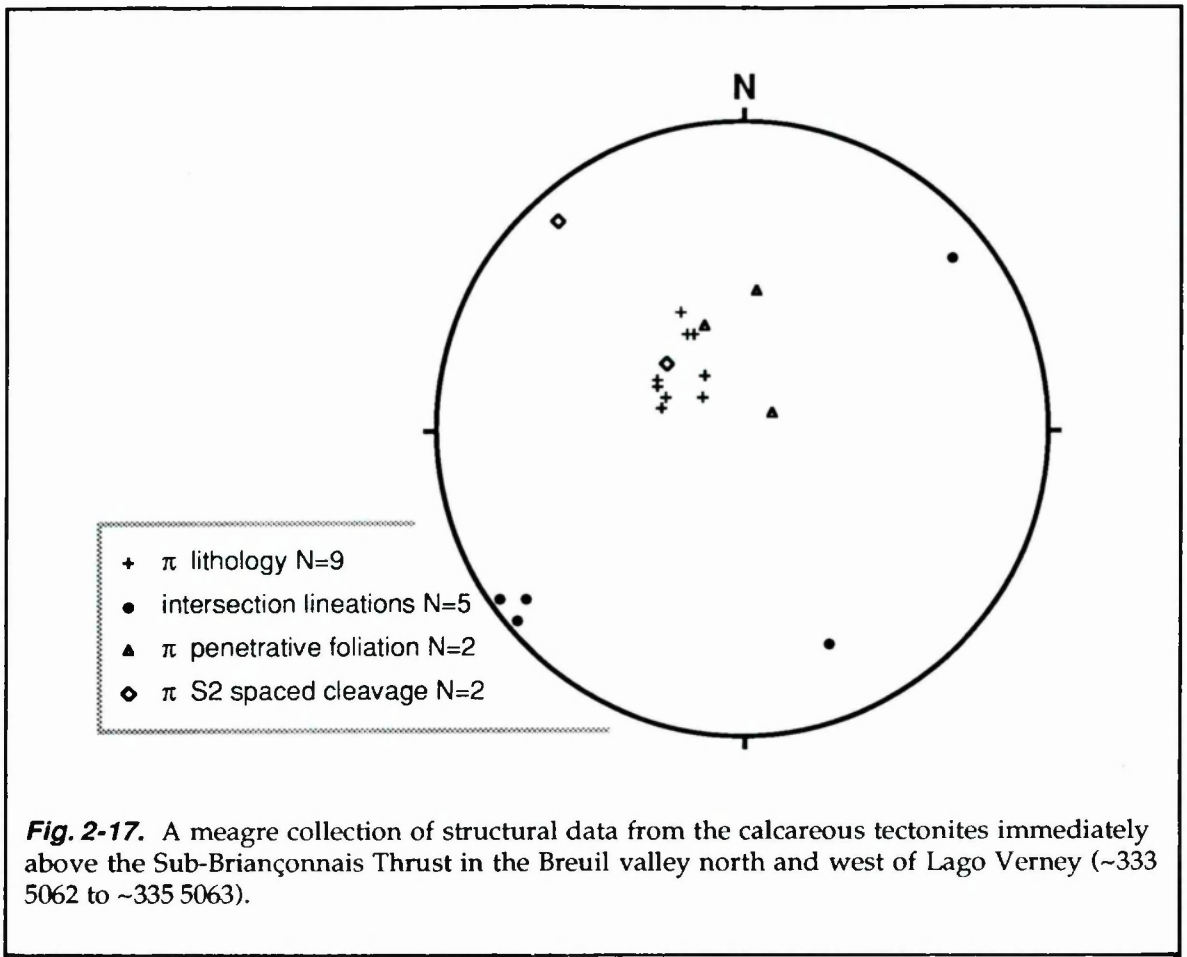

Fig. 2-17. A meagre collection of structural data from the calcareous tectonites immediately above the Sub-Briançonnais Thrust in the Breuil valley north and west of Lago Verney (~333 5062 to ~335 5063).

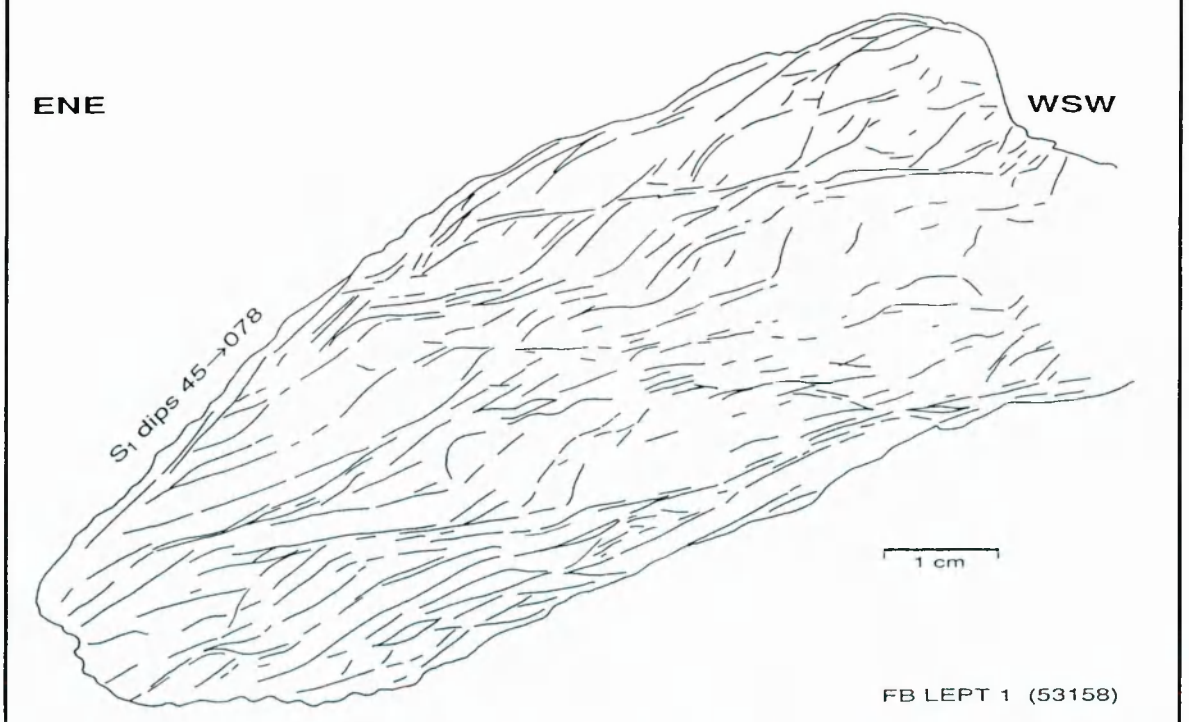

Fig. 2-18. Asymmetric extensional crenulation cleavage in a foliated leucogranitic lithology from 33353 506270, south of Punta Rossa. Tracing of a polished surface of hand specimen FB LEPT 1 (thin section n° 53158) cut perpendicular to the foliation and parallel to the ENE-plunging stretching lineation. Shear sense is top-to-the-WSW.

2.3 THE BREUIL–CHAPIEUX TRANSECT

This section describes the structure of a broad traverse between the high Breuil valley (Italy) and the hills above the hamlet of les Chapieux (France). The transect runs ESE–WNW, perpendicular to the trend of most of the folds and parallel to the inferred tectonic transport direction (see section 2.2-3). The basic data from this traverse are projected onto three parallel cross-sections (Figs. 2-14 to 2-16 as enclosures) and the outcrop segments used to construct these sections are described in turn below. As noted in section 2.2, the Tarentaise Zone is compartmentalised by a number of laterally persistent thrusts (Fig. 2-8). The following description is organised in the context of these tectonic packages, dealing with each thrust sheet sequentially downwards from the structurally highest (most internal) unit.

2.3-1 The Sub-Briançonnais Thrust Sheet

The Sub-Briançonnais Zone in this region is represented by a stratigraphically distinct thrust sheet known as the Petit St-Bernard unit (Elter & Elter, 1957, 1965; Zülauf, 1964). The thrust sheet crops out as a monotonous tract of strongly foliated calcareous and pelitic tectonites whose protolith is thought to be a lower Jurassic limestone–marl sequence (Antoine, 1971). The dominant foliation is a penetrative lithology–parallel cleavage, S1, associated with tight to isoclinal intrafolial closures. This S1 fabric is locally crenulated by a well developed spaced cleavage which is axial planar to tight NW-vergent F2 folds. Figure 2-17 shows some structural data from this thrust sheet close to the Sub-Briançonnais Thrust.

The **Sub-Briançonnais Thrust** itself is marked along much of its outcrop by a persistent horizon of cargneule, approximately 3-12m thick. Where the cargneule is absent (*e.g.* at 33353 506207), the contact between the Sub-Briançonnais and Miravidi sheets comprises an interval of highly strained (but non-mylonitic) calc-tectonites which exhibit an exasperating lack of both stretching lineations and macroscopic shear criteria. In the area WSW of les Balmettes (3346 50628), the Sub-Briançonnais Thrust clearly cross-cuts the structural grain of the Miravidi thrust sheet and on a regional scale the outcrop pattern of the thrust truncates the structurally lower thrusts (Fig. 2-8), suggesting that this is an out-of-sequence thrust which 'breaches' earlier formed structures.

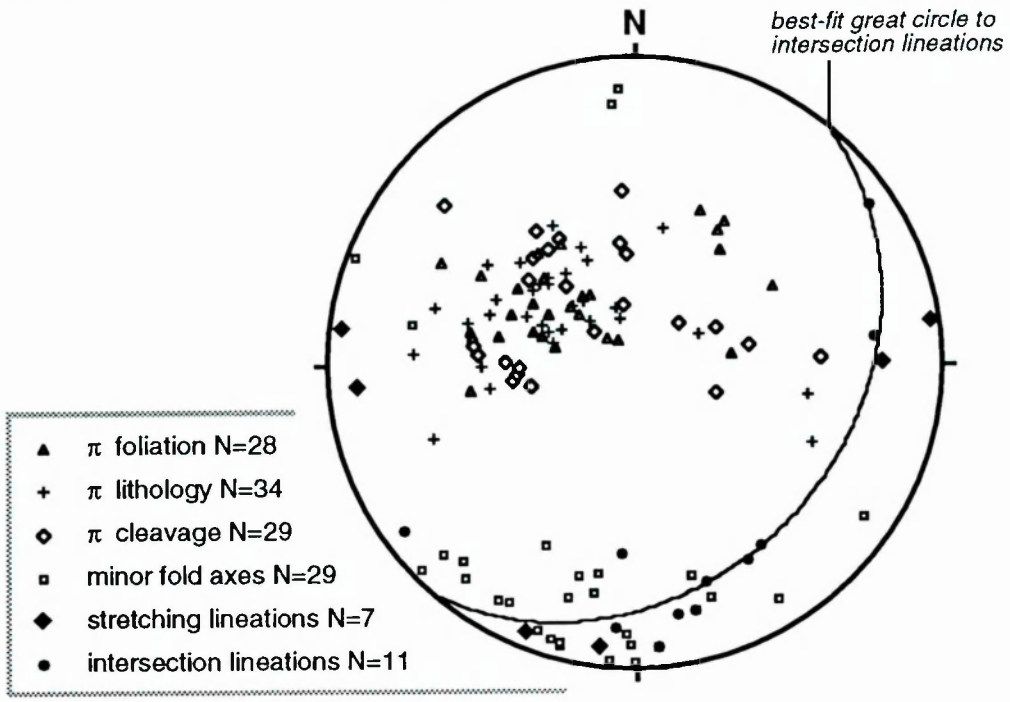

Fig. 2-20. Structural data from the Miravidi thrust sheet in the high Breuil valley showing the general ESE-dip of planar structures and the scatter of linear structures around the mean foliation plane. π indicates 'pole to.'

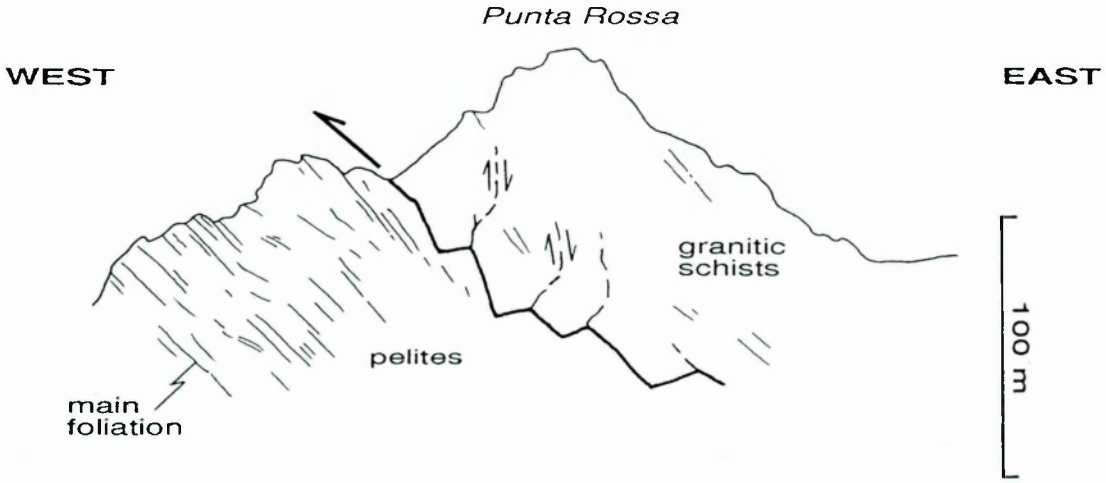

Fig. 2-19. View looking due north towards Punta Rossa (3334 50633), high Breuil valley, showing stepped basal contact of granitic schists onto pelites and local shear-sense as deduced from S/C fabrics. Line drawing from a photograph.

2.3-2 The Miravidi Thrust Sheet

The Miravidi Thrust emplaces distinctive lithologies of the so-called Versoyen Complex onto the Tarentaise Zone proper. The Versoyen Complex is a lithotectonic assemblage of pelites, metabasites, granitic schists and serpentinites which forms the subject of chapter 4. The core of the Miravidi thrust sheet involves a 130m thick basement slice (the Punta Rossa granitic schists and associated serpentinites) interposed between thicker metabasite–pelite panels (Fig. 2-16 encl.). At their upper contact, the granitic schists are adherent to their sedimentary cover (see section 4.1-3), whereas the lower boundary of the basement slice is a tectonic contact onto more intensely schistose pelites. Stretching lineations in the granitic rocks adjacent to this contact are aligned east–west or ENE–WSW and shear criteria define a top-to-the-west movement sense (*e.g.* Fig. 2-18). Local reversals of shear sense are associated with minor high-angle discontinuities (Fig. 2-19). Structures in the enclosing pelites and metabasites are poorly defined on account of a lack of mesoscale anisotropy, although small quartz-rich layers within the pelitic sequences pick out a spread of south–plunging folds. As in the adjacent Sub-Briançonnais Zone, two cleavages are evident: a penetrative lithology-parallel foliation and a SE-dipping spaced S2 cleavage. Figure 2-20 summarises structural data from the Miravidi thrust sheet in the high Breuil valley.

The **Miravidi Thrust** (= Versoyen Thrust of Spencer (1990)) is broad zone of ductile shear associated with strong foliation development and intrafolial folding (Fig. 2-21). The associated strain gradient is picked out by decreasing fabric intensity and decreasing fold tightness with distance into the footwall (Fig. 2-22). Stretching lineations and shear criteria are scarce and fold axis orientations do not exhibit a simple relationship to the strain gradient (Table 2-1). Structure contours on this shear zone reveal a complex pattern of open folds (Fig. 2-23) which also deform the S1 foliation (Fig. 2-24).

2.3-3 The Montchail Thrust Sheet

This is relatively thin (~400m thick in the Versoyen valley) and previously unrecognised thrust sheet which was considered as part of the Seloge sheet by Butler (1989b) and Spencer (1990). It is distinguished here from the underlying Seloge sheet by virtue of a major structural discontinuity and somewhat different internal structural relationships. The dominant component of the Montchail

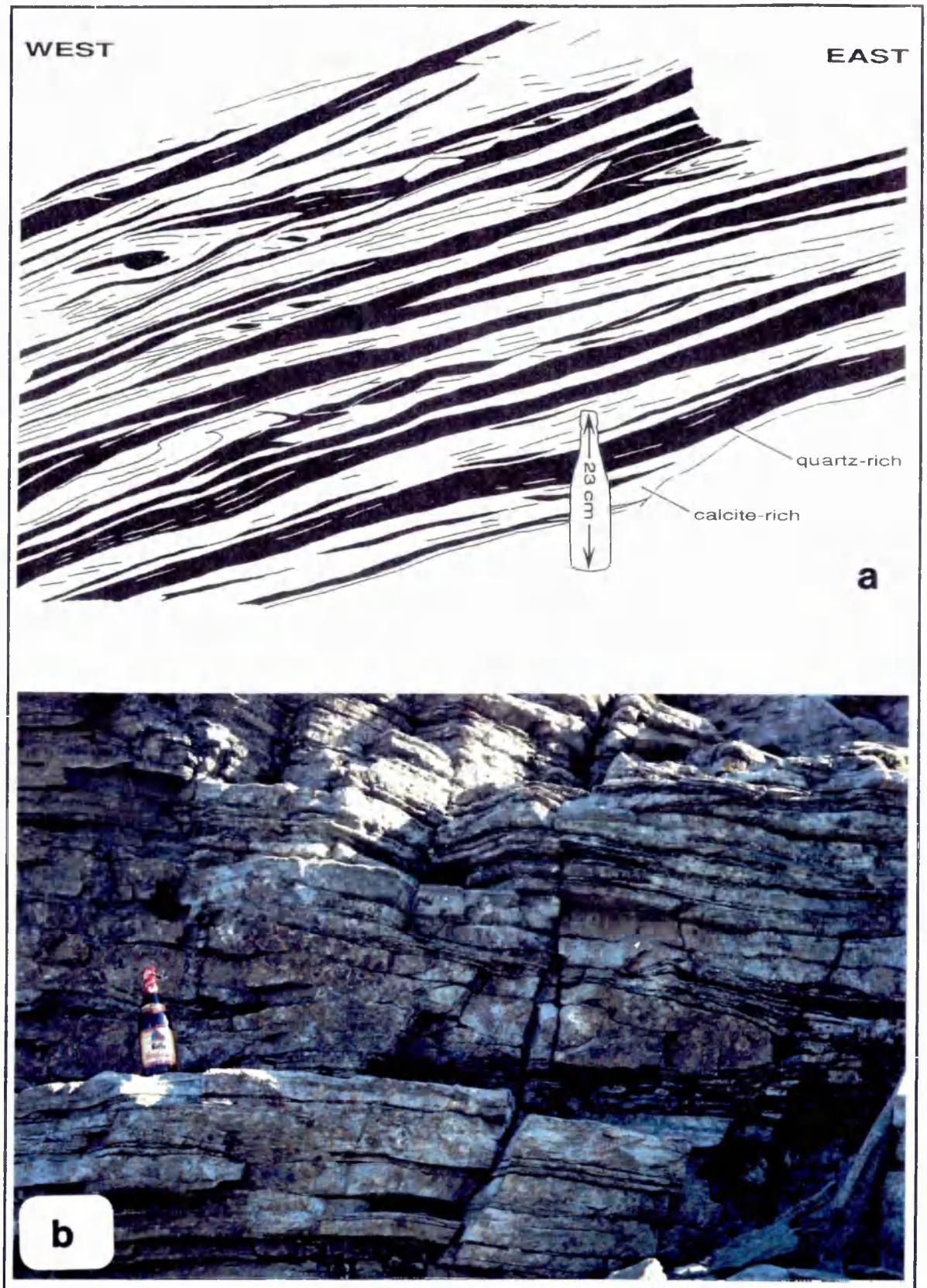

Fig. 2-21. Isoclinal fold closures in calc-psammite tectonites a few metres below the Miravidi Thrust. Protolith = Aroley Formation calc-sandstones and conglomerates. **a)** Line drawing from a photograph from 33274 506515, NNW of Tormotta. The foliation here dips at 24→230 and the fold axes plunge approximately 9→208. **b)** Photograph looking south at an east-west face, 33310 506345. Fold plunge ≈ 4→175, dip of foliation = 14→280. The scale is 22cm high (and 8.2% alc/vol).

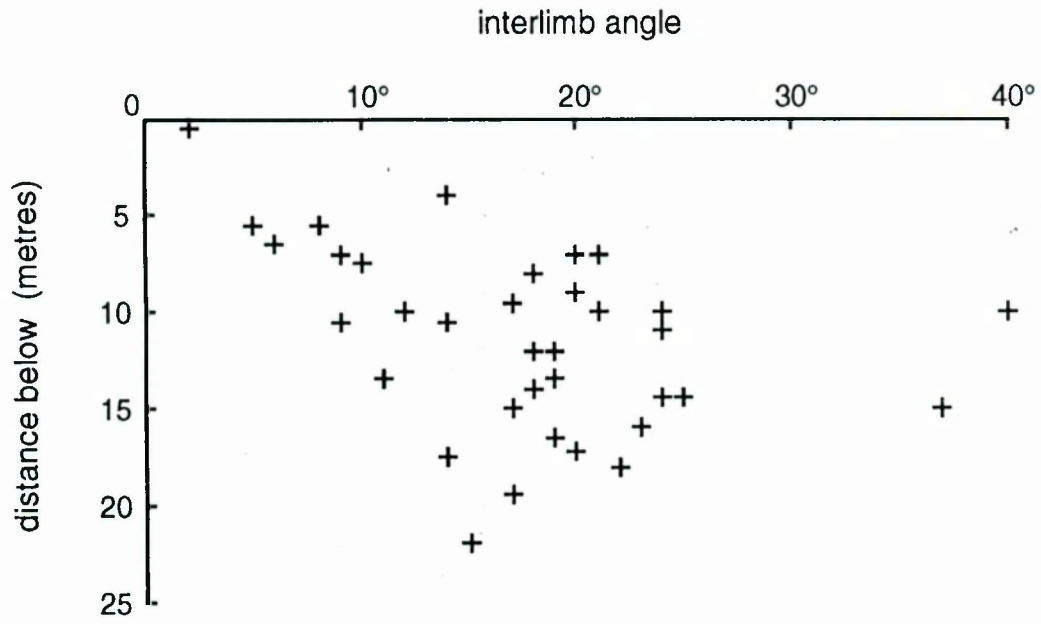

Fig. 2-22. Graph of interlimb angle against distance below the Miravidi Thrust for tight to isoclinal folds of lithology in Aroley Formation tectonites. The raw data are tabulated in Table 2-1.

Table 2-1.

distance below MT	*interlimb angle*	fold axial plunge	*dip of foliation*
0.4m	2°	5→005	42→277
4m	14°	10→175	21→121
5.5m	5°	5→002	12→270
5.5m	8°	–	14→283
6.5m	6°	6→171	11→263
7m	9°	8→013	
7m	20°	24→345	
7m	21°	25→345	42→271
7.5m	10°	9→015	
8m	18°	8→017	
9m	20°	5→181	10→269
9.5m	17°	9→005	
10m	12°	5→343	11→307
10m	21°	11→023	49→296
10m	24°	4→169	14→288
10m	40°	5→178	6→337
10.5m	9°	22→011	
10.5m	14°	9→026	
11m	24°	9→346	15→298
12m	18°	9→350	
12m	19°	9→344	
13.5m	11°	4→167	
13.5m	19°	3→356	
14m	18°	2→337	14→297
14.5m	24°	3→349	9→264
14.5m	25°	3→348	10→293
15m	17°	11→020	24→319
15m	37°	3→172	26→088
16m	7°	9→012	
16m	23°	14→023	34→310
16.5m	19°	14→020	
17.3m	20°	8→020	19→276
17.5m	14°	7→009	37→305
18m	22°	1→338	8→296
19.5m	17°	10→018	
22m	15°	5→023	8→010
~230m	70°	10→211	
~230m	65°	12→201	
~230m	35°	10→201	
~230m	53°	28→232	
~250m	30°	16→183	
~250m	60°	20→188	
~250m	55°	12→189	
~250m	30°	27→180	
~250m	55°	18→186	
~300m	60°	28→201	
~300m	75°	3→221	

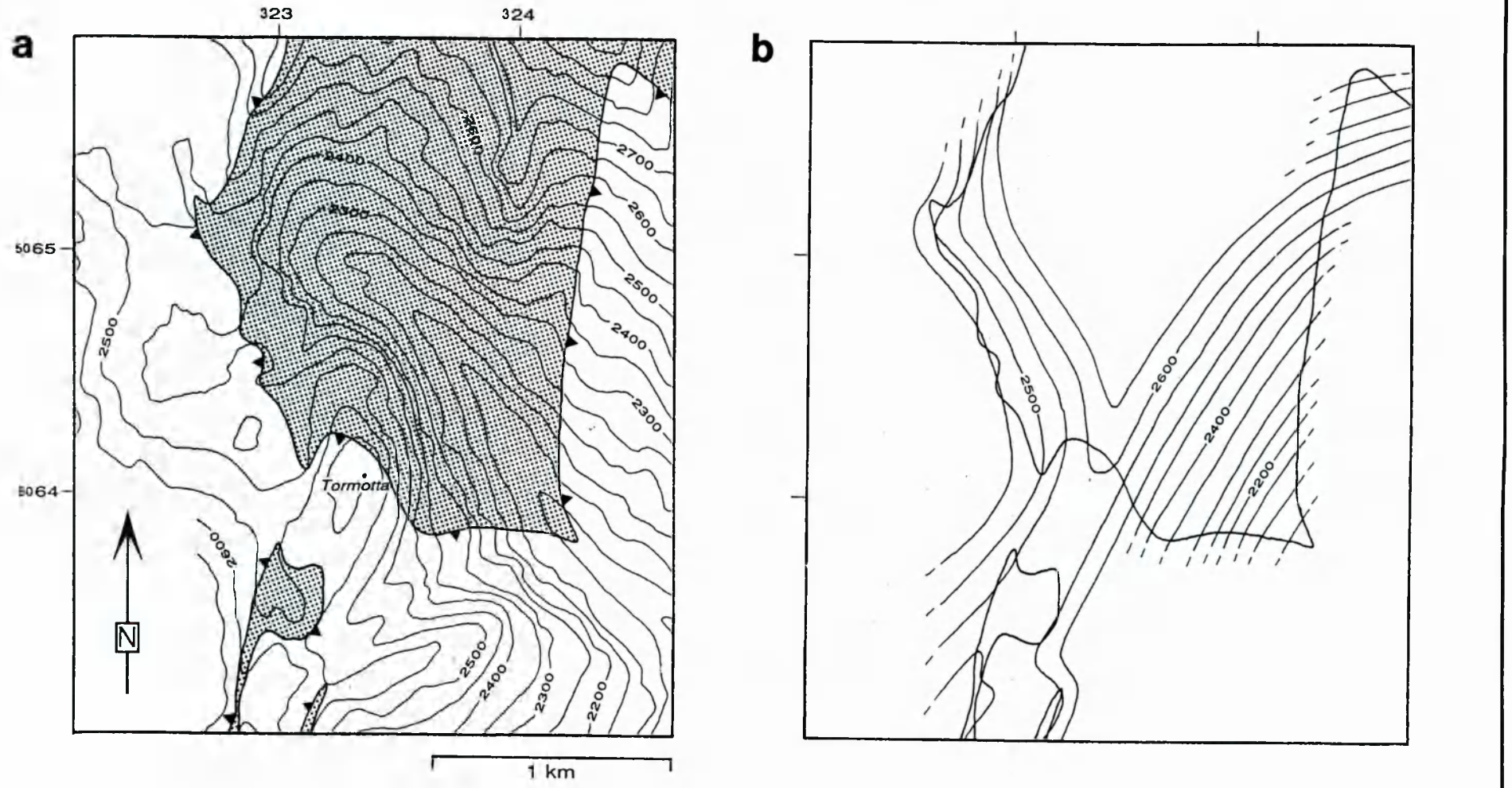

Fig. 2-23. Structure of the Miravidi Thrust in the Breuil valley. **a)** Outcrop of the Miravidi Thrust (triangles denote hanging-wall) and the underlying Montchail thrust sheet (stippled). **b)** Inferred structure contours on the Miravidi Thrust, showing irregular flexure about broadly NNE–SSW trending axes.

Fig. 2-24. ?NNW-vergent folding of protomylonitic foliation in quartz-calcite tectonites (protolith = Aroley Formation) approximately 15-20m below the Miravidi Thrust. View looking west at a north–south face (33285 506460). The scale is 18cm high.

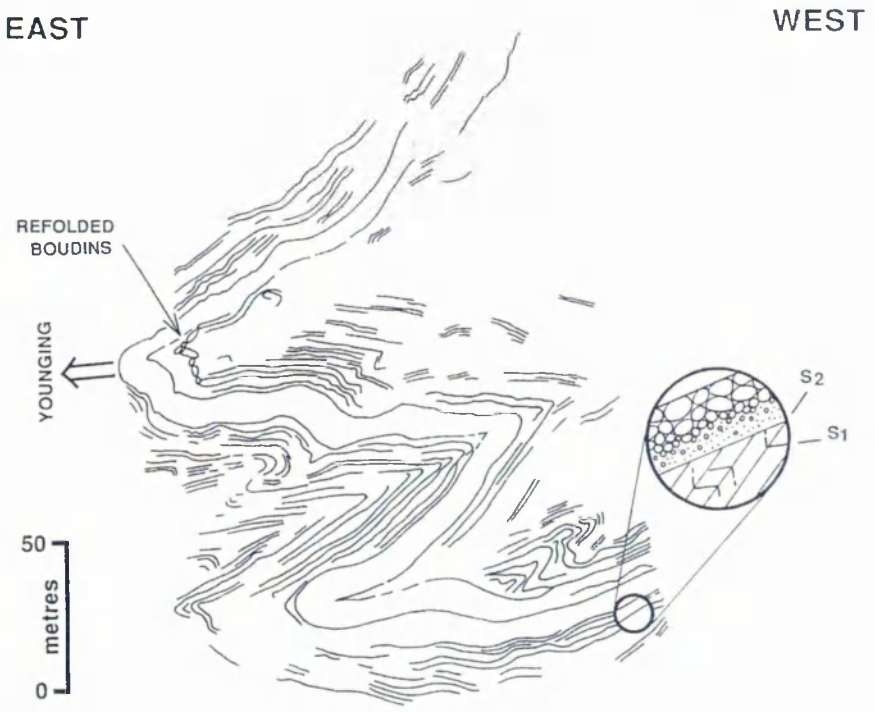

Fig. 2-25. Geometry of the Versoyen Wiggle, a complex tight fold structure in conglomerates interbedded with thin pelites (Aroley Formation). See Fig. 2-26 for structural data. Sedimentary structures in the conglomerates indicate an apparent facing direction *down* to the east, though this is uncorroborated. Line drawing from a photograph, looking south towards 3254 50593.

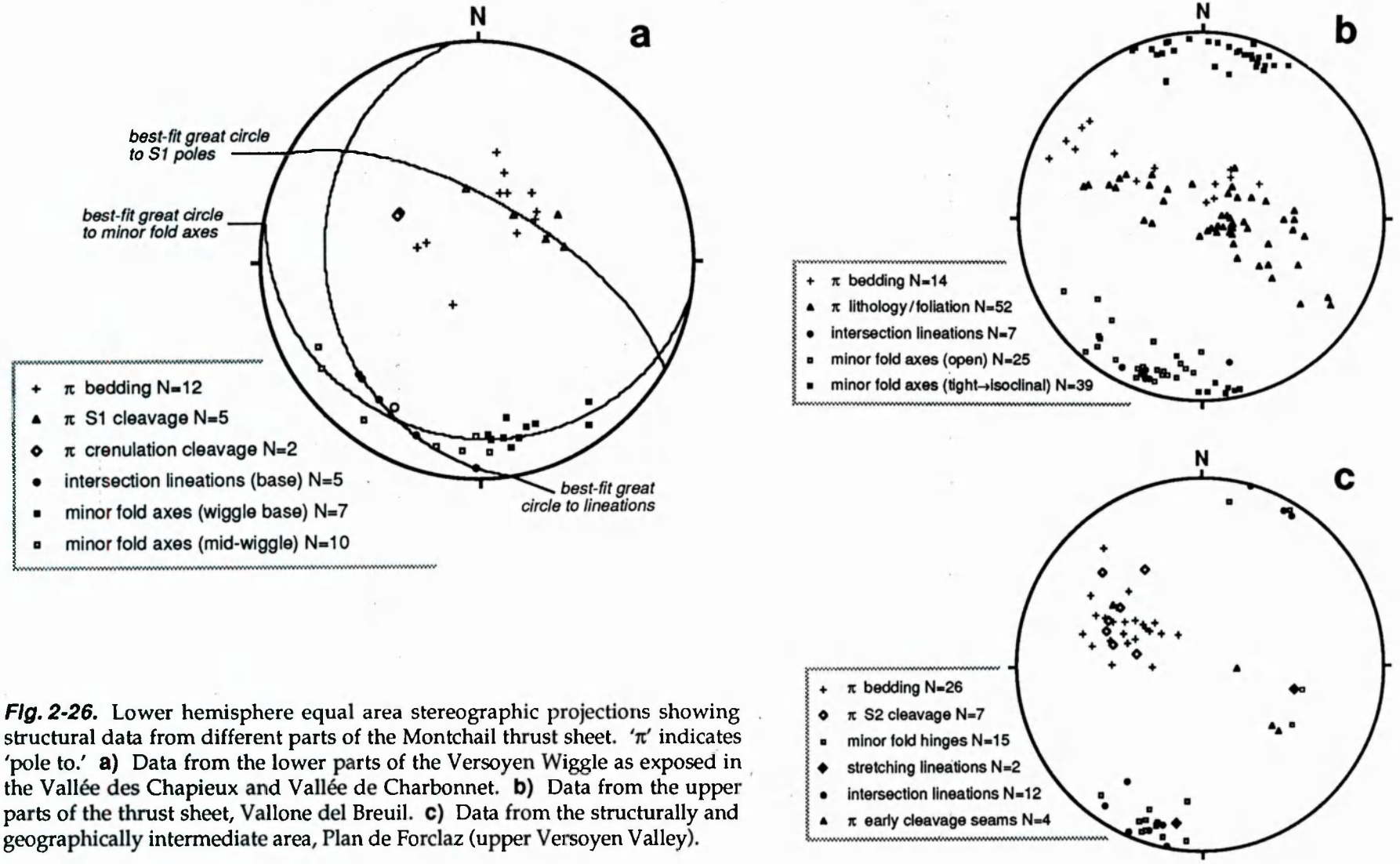

Fig. 2-26. Lower hemisphere equal area stereographic projections showing structural data from different parts of the Montchail thrust sheet. 'π' indicates 'pole to.' **a)** Data from the lower parts of the Versoyen Wiggle as exposed in the Vallée des Chapieux and Vallée de Charbonnet. **b)** Data from the upper parts of the thrust sheet, Vallone del Breuil. **c)** Data from the structurally and geographically intermediate area, Plan de Forclaz (upper Versoyen Valley).

thrust sheet is the 'Versoyen Wiggle,' a laterally persistent but devastatingly unphotogenic complex tight fold structure (Fig. 2-25) exposed at the east end of the Terrasse massif in the Vallée des Chapieux and traceable along the Versoyen valley to the cliffs below Tormotta in the Vallone del Breuil. The facing direction of this structure is problematic: below Tormotta (332 5065 to 333 5064) younging is demonstrably towards the north-west (mappable transition Aroley Fm.→ Marmontains Fm.) whereas on the Terrasse massif (325 5059), well defined sedimentary structures indicate the opposite way-up sense. Figure 2-26 shows structural data from different parts of the Montchail thrust sheet. Poles to lithology and S1 foliation form a broad girdle essentially within the profile plane of the F2 folds and the axes of F1 minor folds occupy a relatively tight arc sub-perpendicular to this plane. Refolded boudins in the fold noses (Fig. 2-27) are oriented such that their long dimensions are parallel to the F2 axes.

The **Montchail Thrust** itself is a broad (tens of metres) zone of intense ductile deformation exposed on the cold, dark, rank, slimy miserable north-facing slopes of the Terrasse massif at 3251 50595. Here the shear zone emplaces Aroley Formation (older) onto St. Cristophe Formation (younger) and consists of calcite–quartz tectonites derived chiefly from the latter formation. These tectonites display a strong sub-horizontal foliation but no stretching lineation. However, sheath-like folds (Fig. 2-28) and asymmetric porphyroclast systems tentatively point towards top-to-the-west displacement.

2.3-4 The Seloge Thrust Sheet

The Seloge thrust sheet crops out over a broad area of poor exposure into which the Vallée des Chapieux provides a convenient vertical section. The thrust sheet is dominated at outcrop by the Cretaceous detrital formations (Aroley, Marmontains and St. Cristophe) with limited exposure of pre-Cretaceous units in the valley bottom. Structural data are summarised in Fig. 2-29. In contrast to the structurally higher thrust sheets, a strong layer-parallel fabric (S1) is only evident in the finer-grained lithologies. Bedding and S1 are folded around tight WNW-verging F2 folds associated with a SE-dipping spaced pressure solution cleavage. These folds mostly plunge at a low angle to the SSW, although some SE-verging minor folds (parasitic to larger WNW-verging folds) have the opposite (→NNE) plunge (Fig. 2-29c). Figure 2-30 shows the geometry of one of the major folds and illustrates some of the associated complexities. The contrasting behaviour of the

Fig. 2-27. Boudins of gritty litharenite in calc-pelites (Aroley Formation) from the base of the Versoyen Wiggle at 32539 505935. The boudin long-axes plunge 13→193, parallel to the local F2 minor fold hinges. View looking SSW at a WSE–ENE face, the hammer is 40cm long.

Fig. 2-28. Sheath folds or type 1 fold interference patterns (*sensu* Ramsay, 1962, 1967) developed in calcareous tectonites of the Montchail Thrust at 3251 50595. View looking north-west at a north–south face. Orientation of sheath long-axis uncertain.

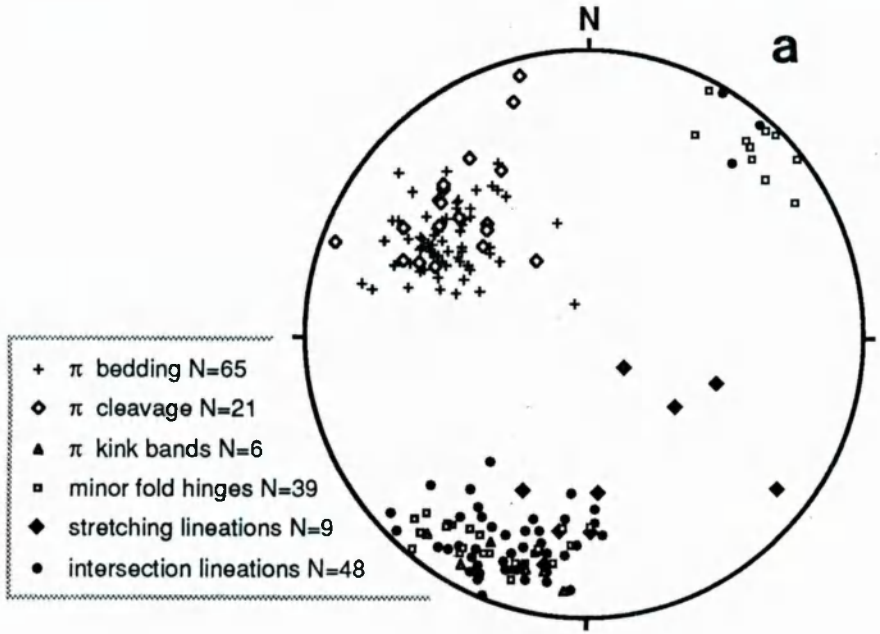

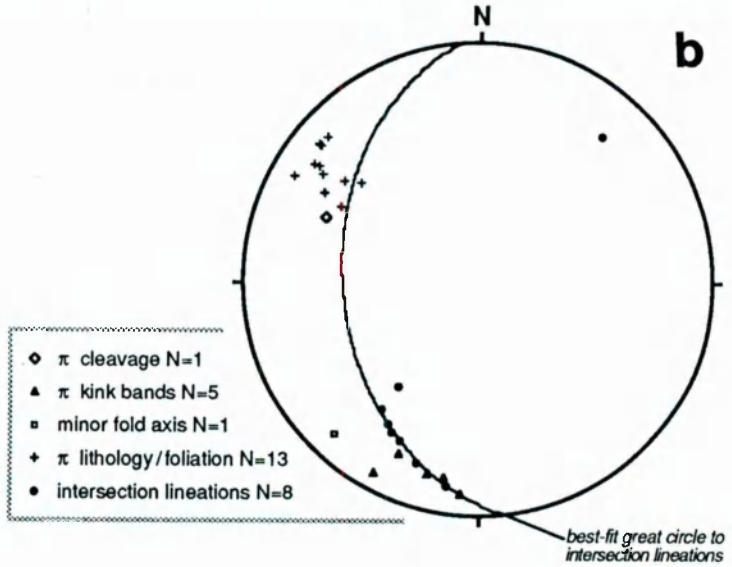

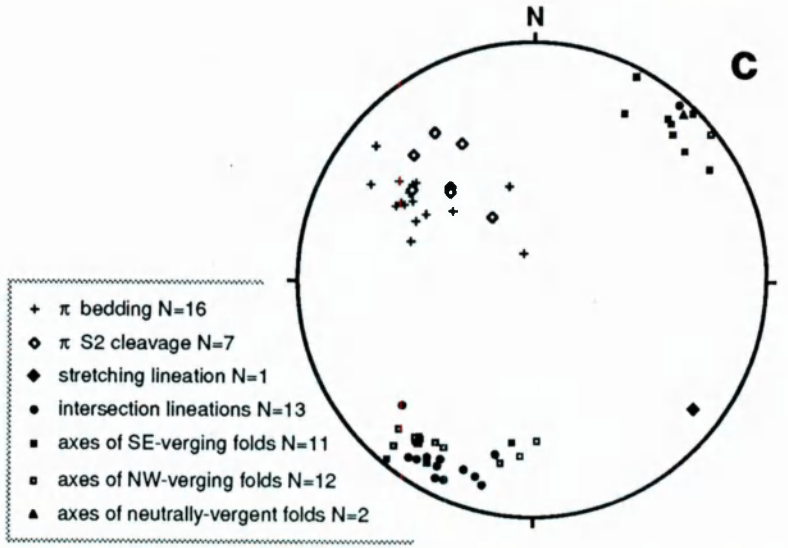

Fig. 2-29. Structural data from the Seloge thrust sheet in the Vallée des Chapieux. **a)** All data from this area. **b)** Data from a sub-area around 3242 50616, north-east of Tête de Gontard showing the disposition of intersection lineations along a partial great circle. **c)** Data from a sub-area around 3235 50613, south of the Ruisseau des Aroulles showing the opposing plunge of parasitic F2 fold sets from the upper and overturned limbs of a larger asymmetric anticline. π indicates 'pole to.'

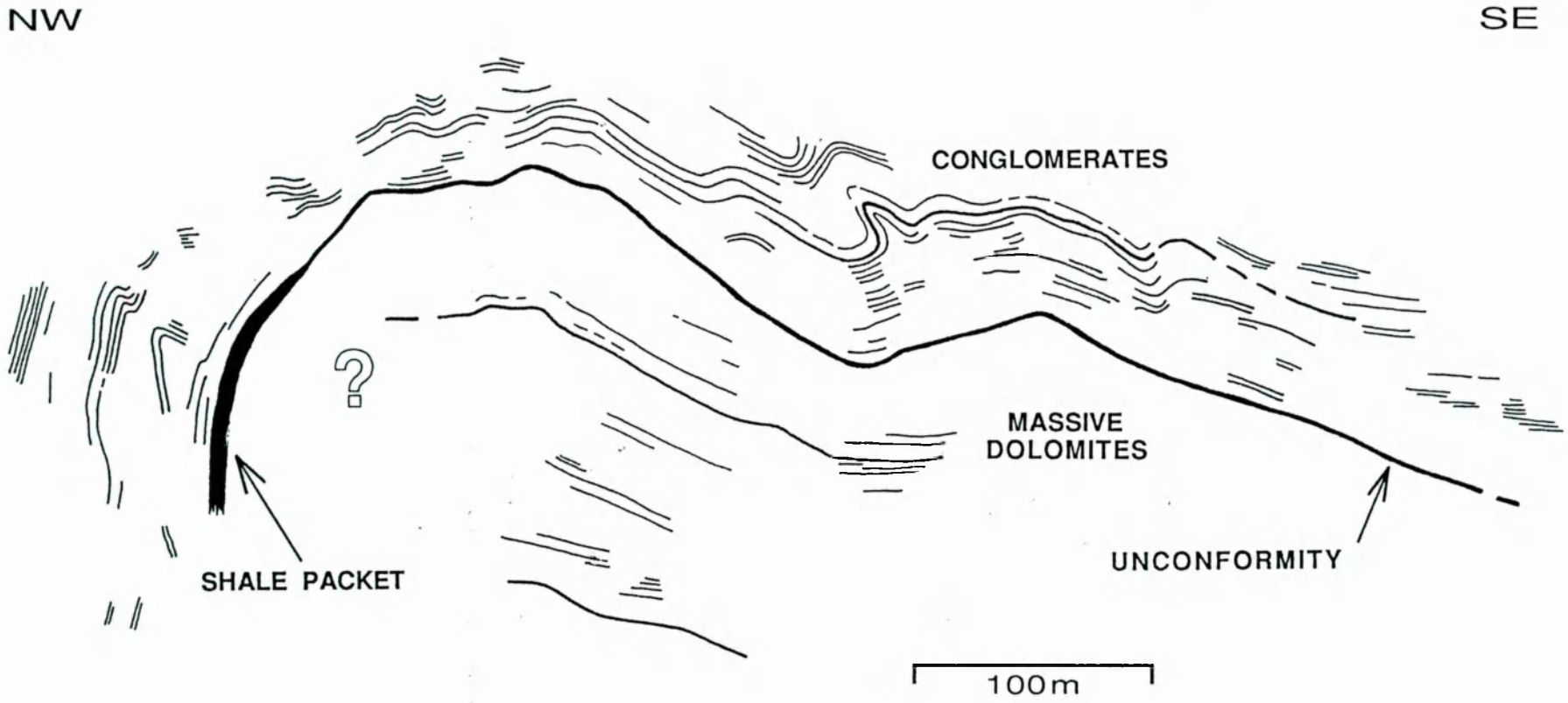

Fig. 2-30. Folding of the unconformity between Aroley Formation conglomerates and underlying Triassic dolomites in the Vallée des Chapieux. Rootless minor folds in the conglomeratic sequence indicate an abrupt strain gradient across the unconformity. Line drawing from a photo-montage, looking north-east towards 3245 50614.

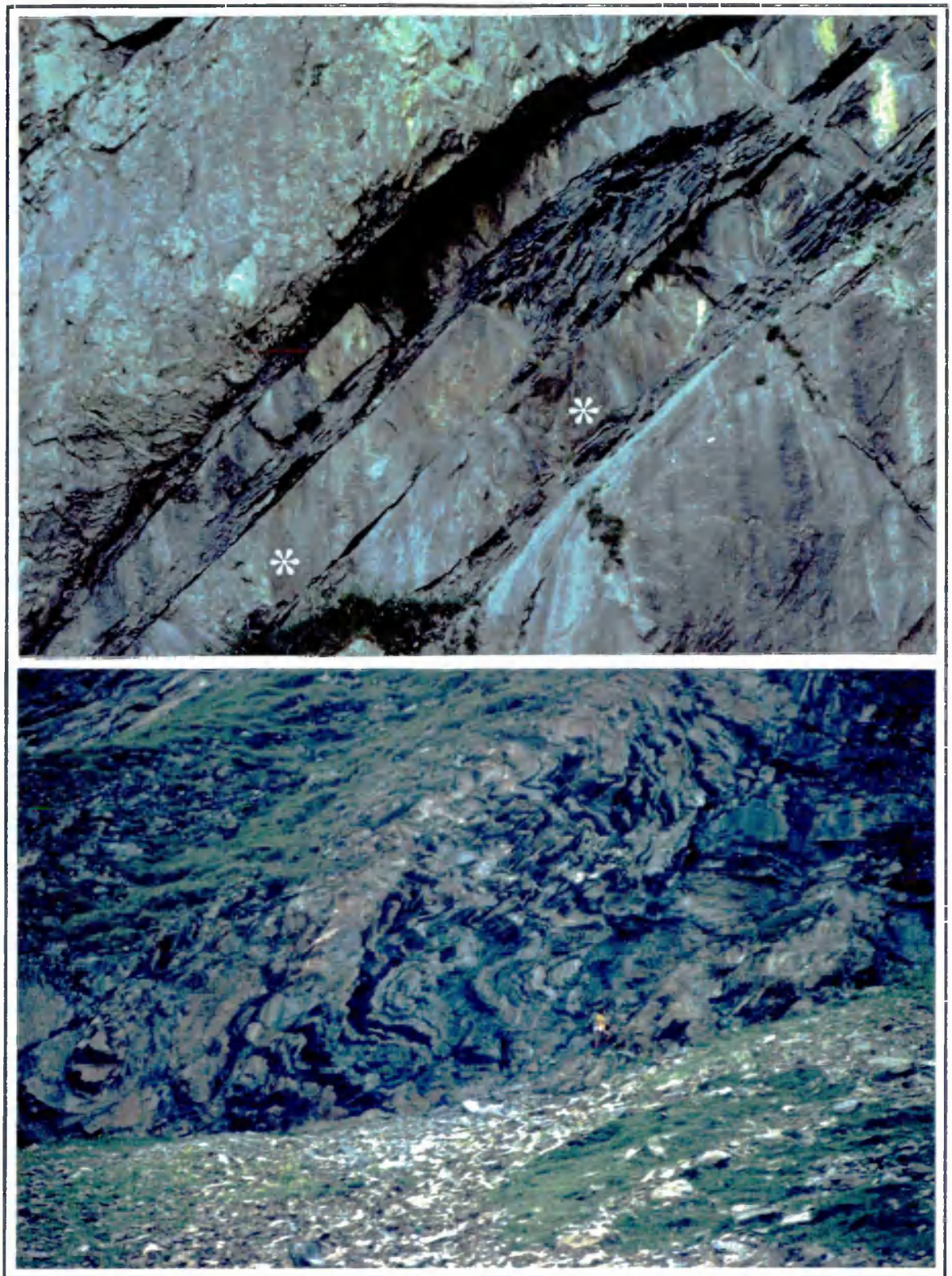

Fig. 2-31. Photographs illustrating the contrasting deformational behaviour of the Aroley and St. Cristophe Formations. *Upper:* Shortening by decoupling and stacking of relatively coherent units in the proximal Aroley Formation at 32466 506035. The two panels labelled * appear to be the same normally graded pebbly litharenite bed. The darker material 'bulldozed' ahead of the upper panel is an argillaceous unit. Sheet bedding dip is 34→130. View looking south at a vertical east-west face; the labelled bed is 1.6m thick. *Lower:* Asymmetric WNW-verging minor folds with strongly attenuated shallow-dipping limbs in the basal St. Cristophe Formation. Note that this is the thickest-bedded, most competent part of the formation. Minor folds plunge 12→010, associated cleavage dips 46→110. View looking south-west towards 32824 506417, medium-sized depressed geologist for scale.

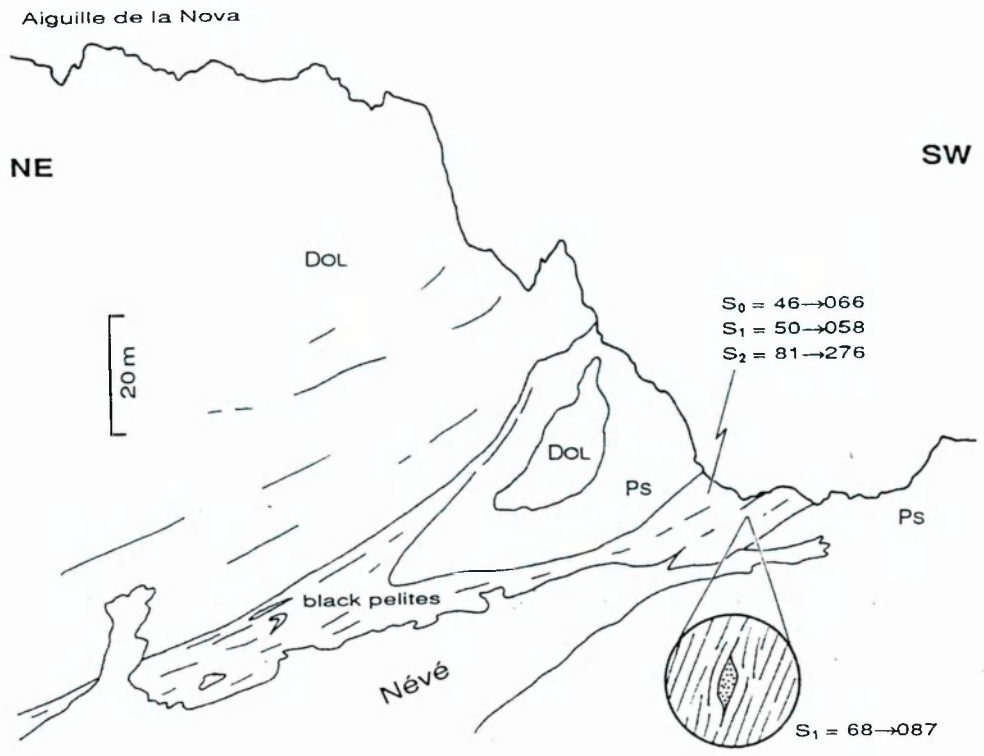

Fig. 2-32. The junction between dolomites and underlying psammites on the north-west flank of the Aiguille de la Nova. Line drawing from a photograph, looking south-east towards 3186 50581.

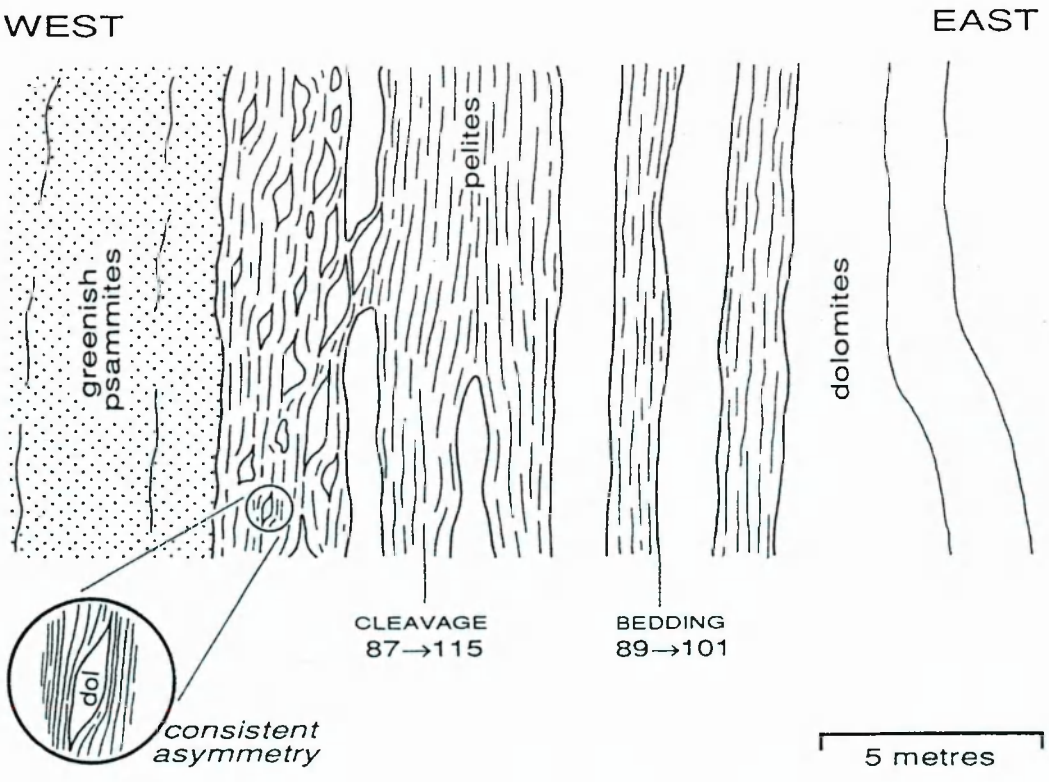

Fig. 2-33. The junction between psammites and dolomites in the Combe de la Neuva, showing consistent asymmetry of sheared dolomite fragments. Field sketch from a precarious hillside 500m ENE of the Dent d'Arpire (32085 506140).

different stratigraphic units under deformation is strikingly illustrated in this area (Fig. 2-31).

The **Seloge Thrust** (Butler, 1989b) is a relatively steep structure (dipping ~50° to the SE where visible north-east of Seloge, below Col de la Seigne) which is associated with compressional structures in its hangingwall but which displays a net extensional offset with respect to the stratigraphy. The fault is traceable westwards towards the Combe de la Neuva where it appears to branch into two separate strands. The Combe de la Neuva is an elongate NE-SW trending valley eroded out along thrust-controlled outcrops of gypsum and Carboniferous pelites. Detailed geological interpretation of the Combe de la Neuva is difficult because all the critical relationships are inconveniently buried by scree and moraine in the valley bottom. Several possible structural correlations are feasible across this area of unexposed outcrop, although much depends on the stratigraphic assignment placed on a 15-20m thick unit of unfossiliferous black pelites interposed between Triassic dolomites and psammites at 3186 50581, 300m WNW of the Aiguille de la Nova (Fig. 2-32). These pelites could belong to the Carboniferous *Houiller* (which would constrain the Seloge Thrust to lie above them) or they could represent a preferentially sheared argillaceous horizon stratigraphically *in situ* between psammites and dolomites (in which case the Seloge Thrust would lie somewhat further to the WNW). The former interpretation is preferred, although a shale-rich transition at this stratigraphic level is well known in the area (Fudral, 1973) and strain localisation along those shales is also a common feature (Fig. 2-33). The alternative correlation would link the Seloge Thrust with a structural discontinuity exposed in the base of the Combe de la Neuva, 600m WNW of the site indicated in Fig. 2-32. This second thrust, which does appear to connect laterally with the Seloge Thrust, emplaces Carboniferous pelites onto Triassic dolomites and is adorned by a layer of gypsum displaying ESE-dipping sheath folds (Fig. 2-11b).

2.3-5 The Frontal Pennine Sheets

The 3km wide strip of outcrop between the Seloge Thrust and the Frontal Pennine Thrust is occupied by a number of small, laterally impersistent thrust sheets. These Frontal Pennine sheets are exposed, albeit rather poorly, in the Combe de la Neuva and Mya regions north and west of les Chapieux (Fig. 2-1). At outcrop, they are dominated by Triassic dolomites and psammites, with only

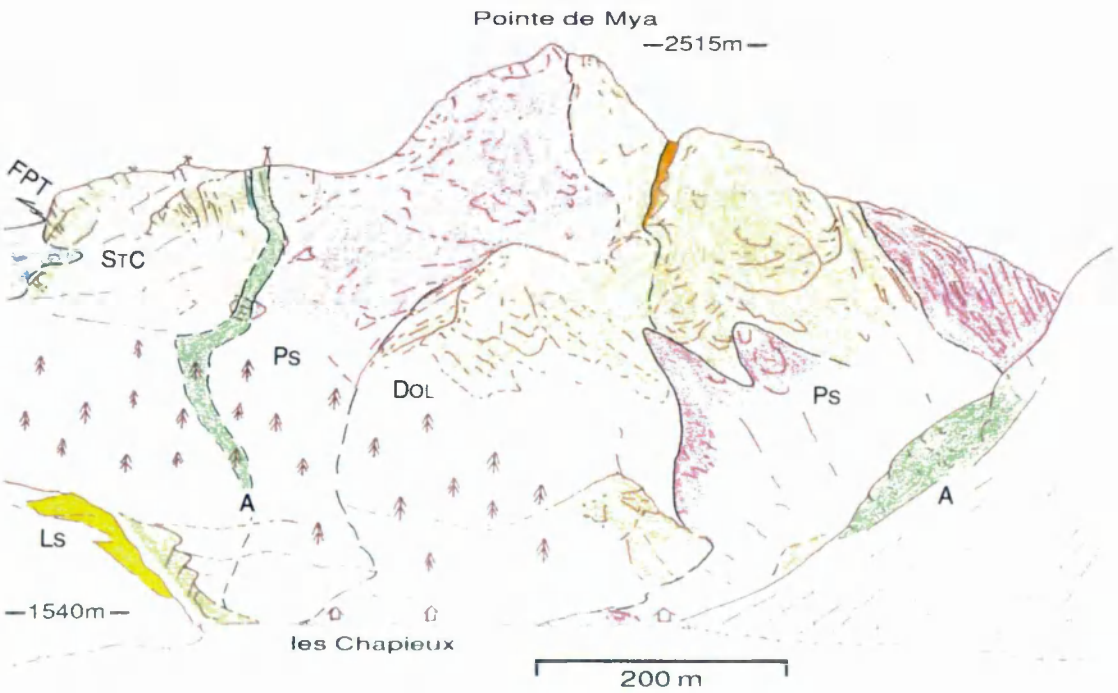

Fig. 2-34. View looking NNE towards the Mya massif from 3237 50621. Tectonic transport direction is to the left and slightly into the page. Abbreviations: *A* = Aroley Formation; *DOL* = Triassic dolomites; *LS* = Liassic limestones; *MPS* = semi-pelitic schists (Ultra-Helvetic); *PS* = Permo-Triassic psammites; STC = St Cristophe Formation.

relatively limited involvement of the younger stratigraphic units (Fig. 2-34). Structures are complex and difficult to resolve in the absence of abundant way-up criteria (Fig. 2-35). The most prominent feature is a large antiformal closure which forms the Grand Fond ridge on the north-west side of the Combe de la Neuva. A strong layer–parallel foliation, characteristic of all the lithologies in this area, is locally carved up by an intense transposition cleavage sub-parallel to the axial surface of this fold (Fig. 2-36). The fold constitutes the hanging-wall to the **Plan Varraro Thrust**, a planar SE-dipping discontinuity marked by limestone mylonites with ESE-plunging stretching lineations. Other steeper discontinuities appear to branch down onto this detachment. In the Combe de la Neuva, the minor thrusts are displaced by an *en echelon* array of NW–SE trending slickensided strike-slip faults which produce sinistral offsets of a few tens of metres.

The **Frontal Pennine Thrust** (FPT) is marked along much of its outcrop by a thick (up to 20m) seam of structureless breccia and cargneule which are utterly bereft of all kinematic information. Structure contours on the FPT outcrop around the Mya massif (Fig. 2-37) indicate a shallow dip to the south-east, parallel to the local stretching lineations, with no indication at this scale of folding of the thrust (*cf.* Fig. 2-23). Figure 2-38 illustrates some of the small-scale deformation features developed in mylonitic rocks in the immediate hangingwall to the thrust and Fig. 2-39 shows structural data from these mylonites.

2.3-6 The Ultrahelvetic Thrust Sheet

The immediate footwall to the Frontal Pennine Thrust comprises a package of lower to middle Jurassic sedimentary units which Butler (1983) has referred to as the Gitte thrust sheet and which has been correlated with the Ultrahelvetic thrust sheet of the Swiss Alps (Antoine *et al.*, 1975). In the area south and east of the Crête des Gittes (5063 320 to 5066 323), these Ultrahelvetic units exhibit structural relationships similar to those characteristic of the Tarentaise Zone: a ubiquitous bedding-parallel S1 is folded around WNW-verging F2 folds associated with a more sporadically developed spaced S2 cleavage (Fig. 2-40). Stretching lineations plunge both to the ESE and to the SSW.

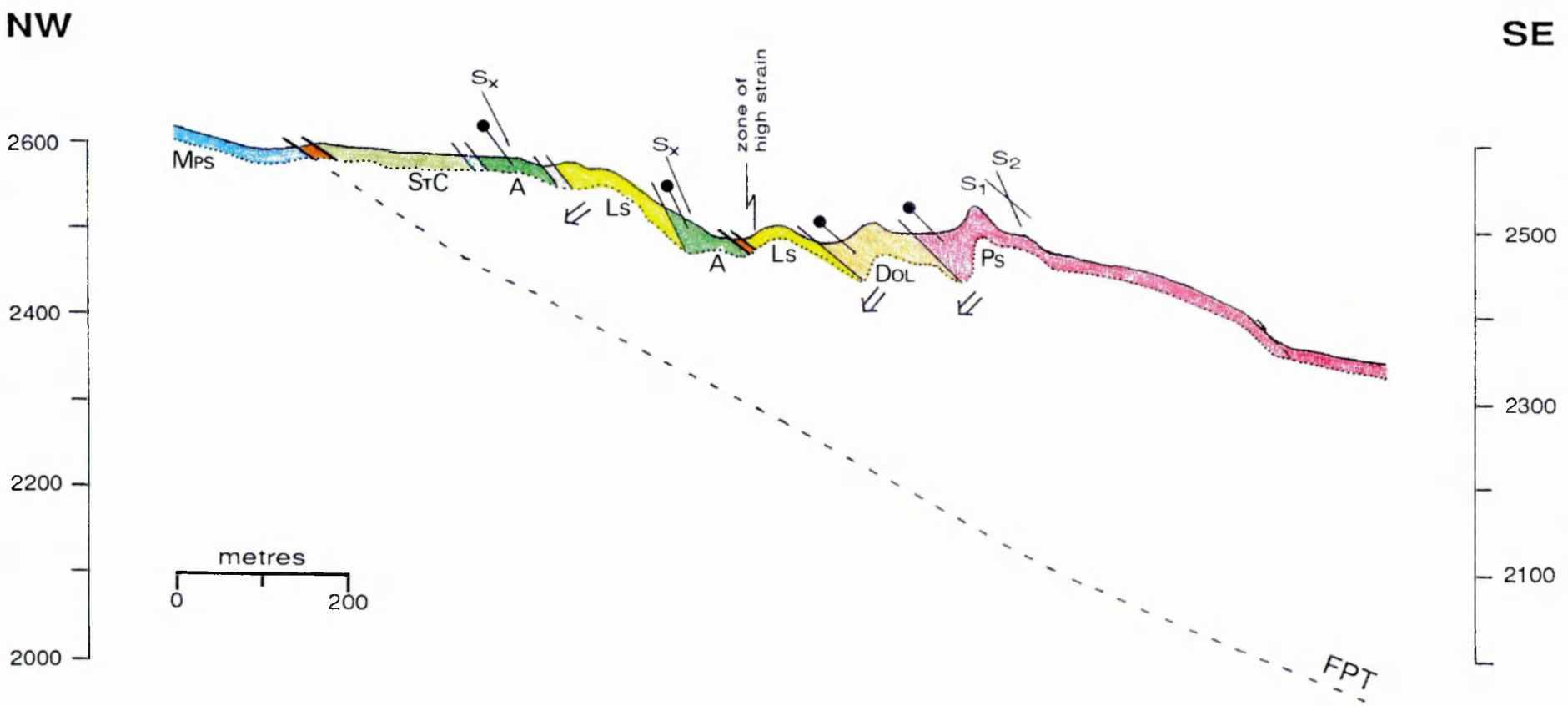

Fig. 2-35. Cross-section through the Mya massif (between 32336 506640 and 32437 506545) showing basic outcrop data. Key as for Figs. 2-14 to 2-16. Obvious tectonic discontinuities shown by bolder lines. Dotted line indicates vertical extent of exposure within 500m (horizontally) of the section line. The subsurface trajectory of the Frontal Pennine Thrust (FPT) is projected onto the section from structure contours (Fig. 2-37).

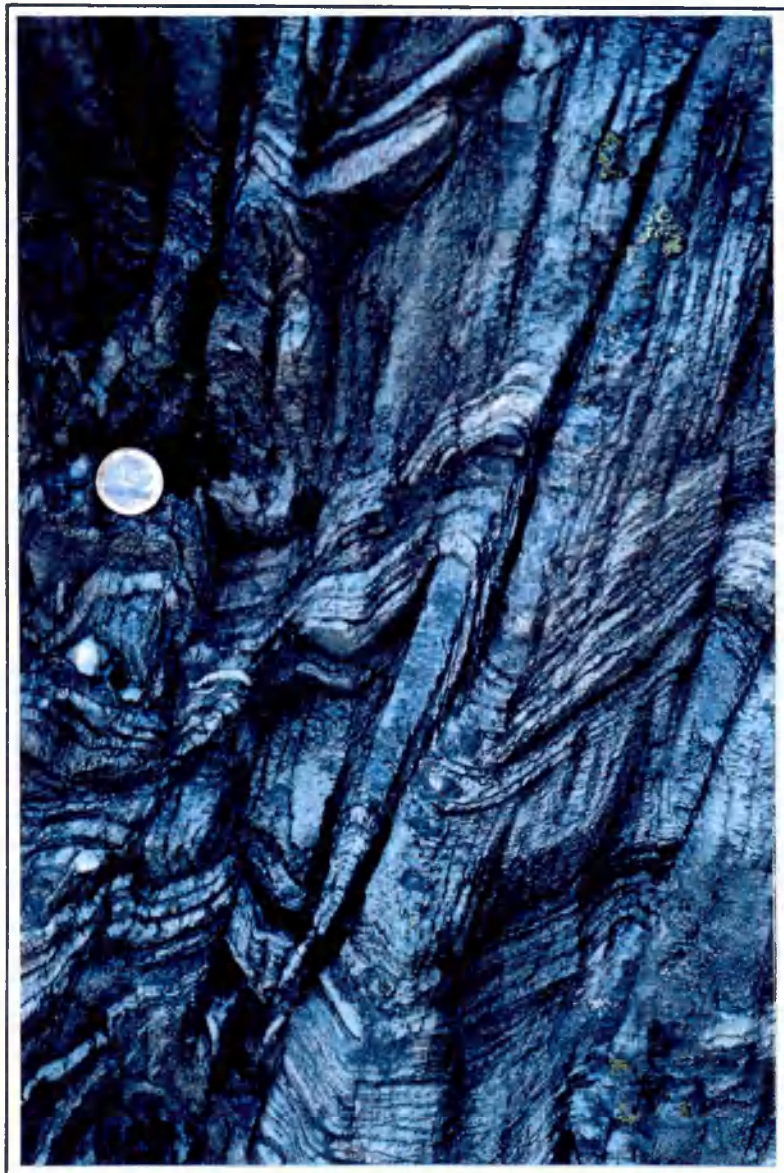

Fig. 2-36. Photographs showing transposition of an earlier pressure solution cleavage (shallower dip) by a later crenulation fabric (steeper dip) of variable intensity in chloritic psammites (presumed Triassic) at 32111 506180, north-east of Dent d'Arpire in the Combe de la Neuva. S1 dips 48→184, S2 dips 74→150. The coin is about 2cm in diameter.

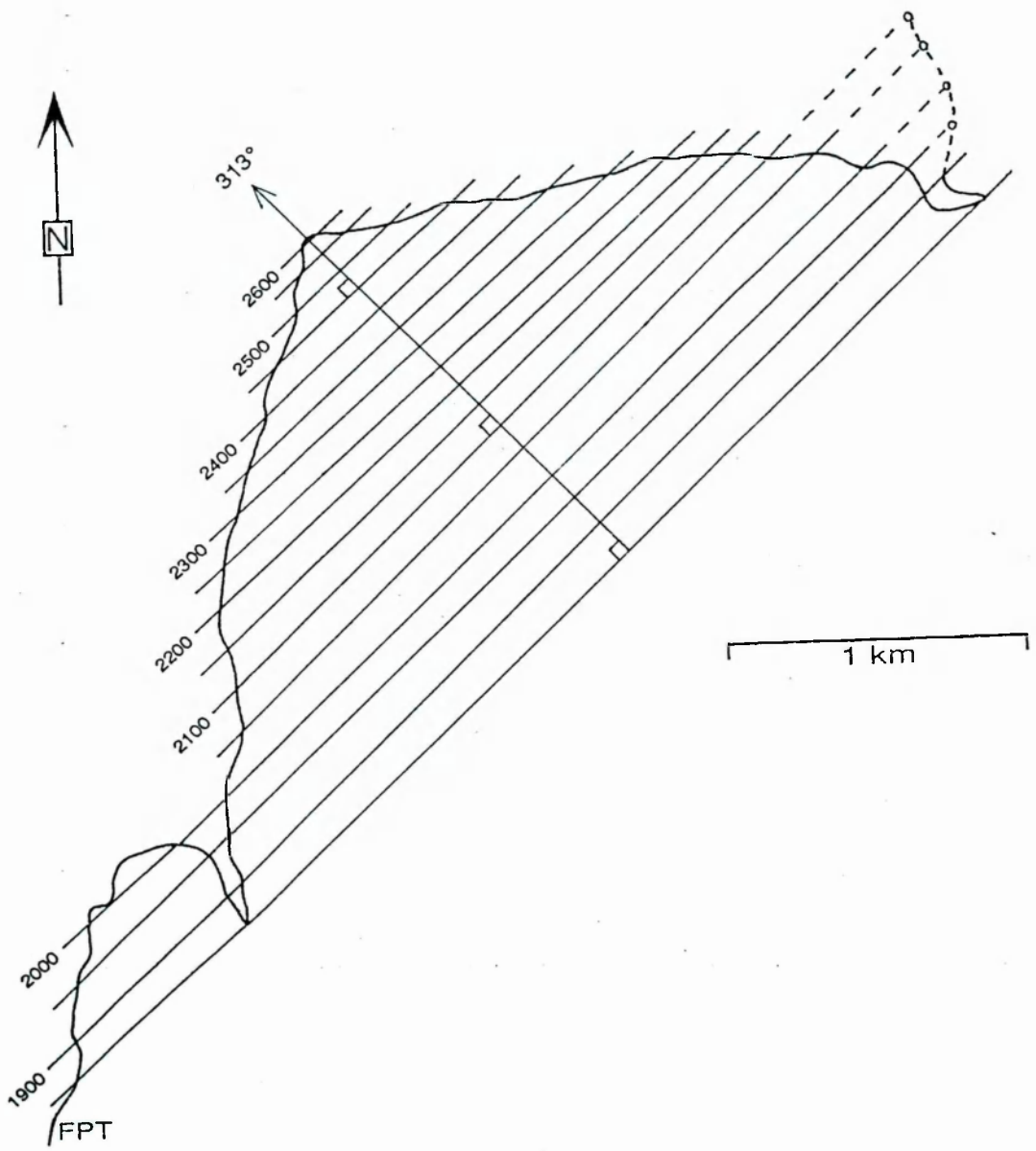

Fig. 2-37. Structure contour map of the Frontal Pennine Thrust across the Mya massif. Contour interval is 50m. The structure contours indicate that the FPT has an overall dip of ~24° towards the south-east in this area (although dips steepen up to ~29° for the NW part of the outcrop).

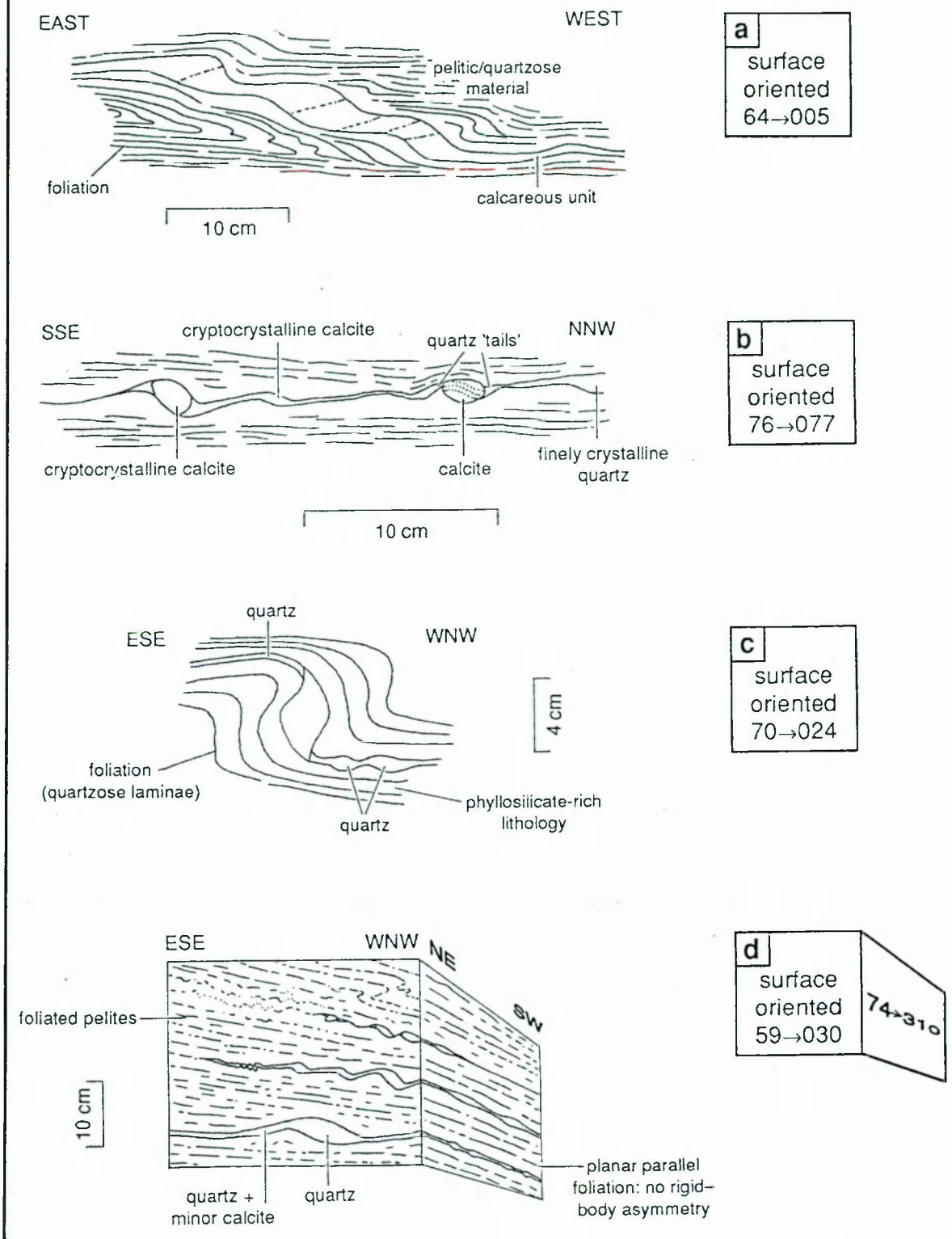
EAST
WEST
pelitic/quartzose material
foliation
calcareous unit
10 cm
a
surface oriented 64→005
SSE
cryptocrystalline calcite
quartz 'tails'
NNW
cryptocrystalline calcite
calcite
finely crystalline quartz
10 cm
b
surface oriented 76→077
quartz
ESE
WNW
4 cm
foliation (quartzose laminae)
quartz
phyllosilicate-rich lithology
c
surface oriented 70→024
ESE
WNW
NE
SW
foliated pelites
10 cm
quartz + minor calcite
quartz
planar parallel foliation: no rigid-body asymmetry
d
surface oriented 59→030
74→310

Fig. 2-38....

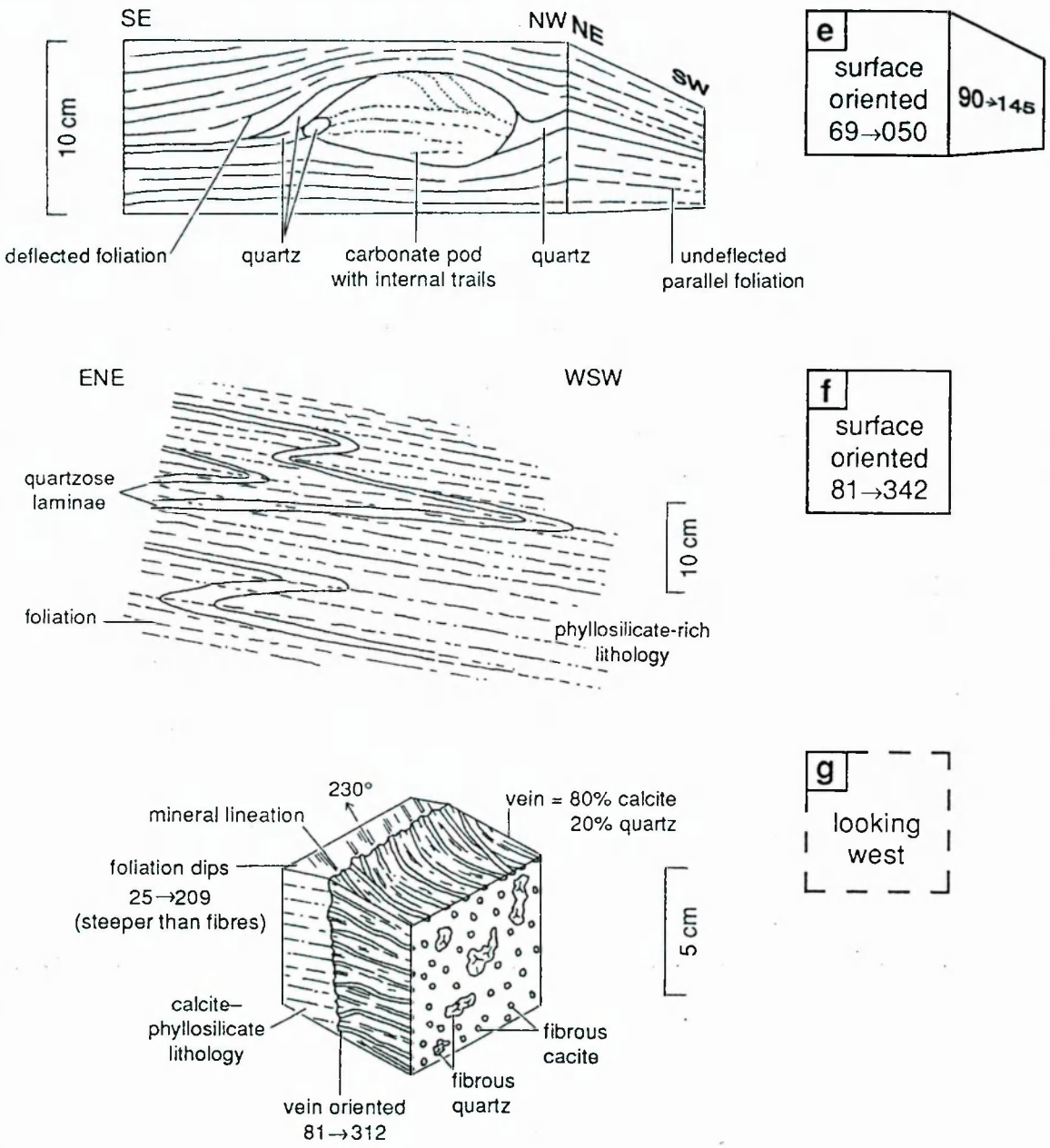

Fig. 2-38. Field sketches of small-scale structures in the high-strain rocks in the hanging wall to the FPT north of Mont Fortin in the Vallon de la Lée Blanche. Square panels indicate the orientation of exposure surfaces. Examples **a**, **b**, **c**, **d**, **e** and **f** are from 33495 507115, **g** is from 33495 507083.

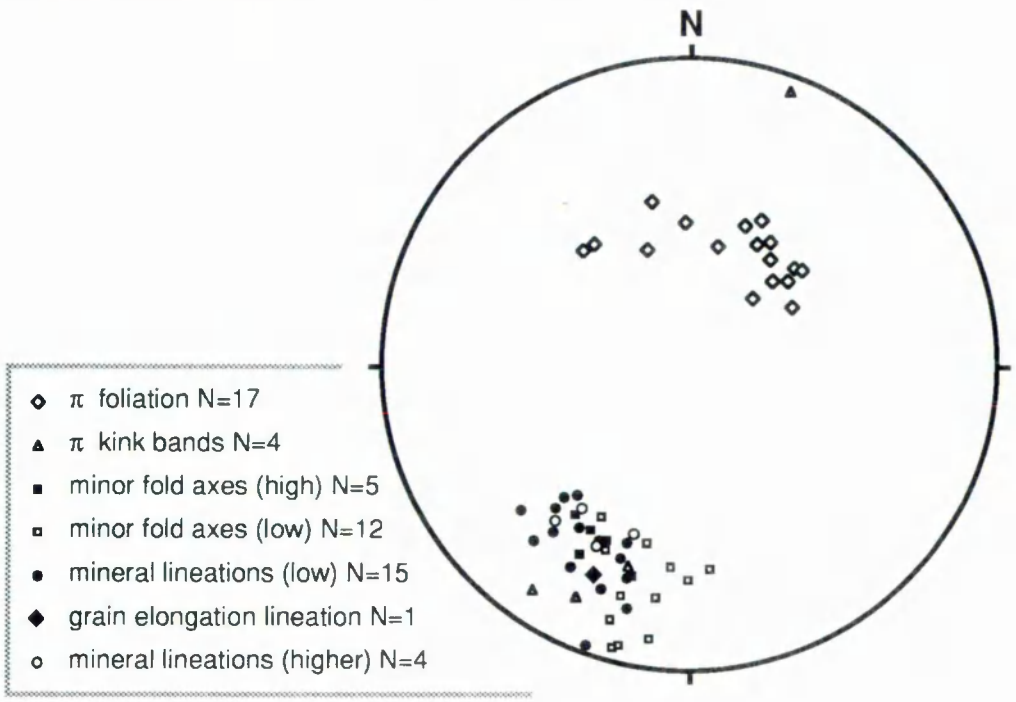

Fig. 2-39. Structural data from the mylonites above the Frontal Pennine thrust, south-east of Lago di Combal, around 334 5071.

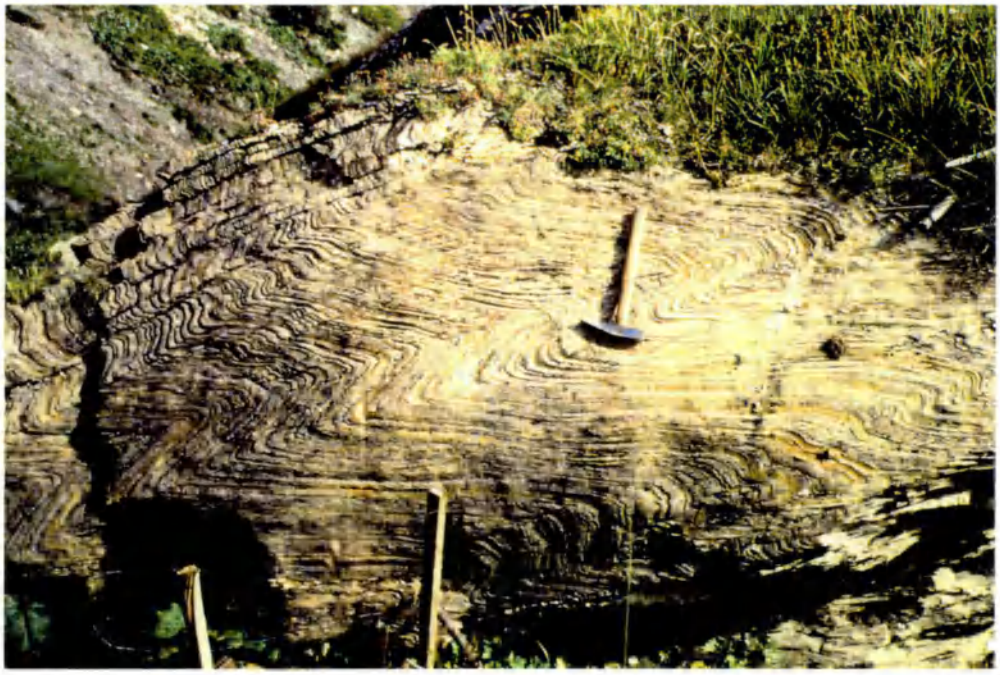

Fig. 2-40. Folding of a strong S1 pressure solution cleavage by (WNW-verging) F2 folds in calcareous pelites of the Ultrahelvetic thrust sheet at 3219 50638 (not *in situ*). The hammer is 40cm long and the fence is electrified.

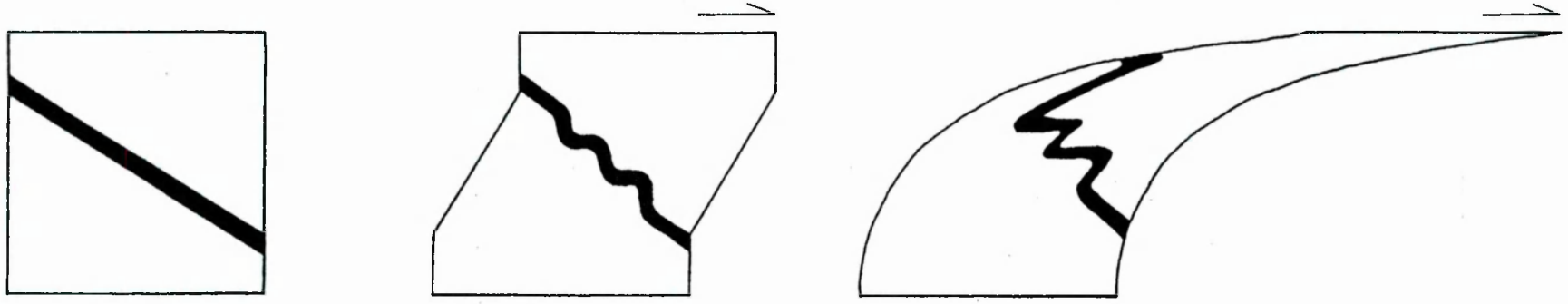

Fig. 2-42. Simple model (left to right in time) for the formation of the recumbent F1s of the Montchail thrust sheet by transmitted shear during emplacement of the Miravidi thrust sheet. Simple shear on a competent layer inclined at a moderate angle to the shear zone boundary results in initial buckling. Continuing heterogeneous shear produces asymmetric fold profiles with simultaneous thinning and thickening of differently oriented limbs. Folds tighten upwards with increasing finite strain.

2.4 INTERPRETATION

The Tarentaise Zone is a belt of ductile greenschist facies deformation delimited by major thrusts and disrupted internally by other minor shear zones. Figure 2-41 (enclosure) shows two interpretative cross-sections through the Zone. Ostensibly, the mesoscale structure of the Seloge thrust sheet is attributable to a single combined phase of WNW-vergent folding and thrusting. Small-scale complexities are suggestive of a rather more involved structural history (Fig. 2-7) but these could potentially be accounted for in terms of local instabilities developed during progressive non-coaxial shear. The observed geometries of the other Tarentaise thrust sheets, however, are not readily explained without recourse to at least two distinct deformation episodes.

It is clear from exposures in the Breuil valley that the Montchail thrust sheet contains both recumbent isoclinal folds and upright or WNW-vergent open folds. From the relationship shown in Fig. 2-22 it seems probable that the tightening of the recumbent folds is attributable to shear on the overriding Miravidi Thrust, which implies that the isoclinal folding either preceded or was coeval with emplacement of the Miravidi thrust sheet. Kinematically, it is feasible that the two structures are the product of the same compressional episode (Fig. 2-42). However, in detail, the structure of the Montchail thrust sheet (Fig. 2-26) cannot be explained by one phase of deformation. Figure 2-43 depicts a scenario of two superimposed fold phases which appears to account for the overall structure: early NNE- or SSW-plunging recumbent isoclines (F1) being partly refolded by later WNW-verging open folds (F2).

Many of the structural features observed in the Tarentaise Zone can be explained in terms of rheological variations between adjacent stratigraphic units. For example, the antithetic minor shears in the Punta Rossa basement slice (Fig. 2-19) are suggestive of brittle failure of a competent inclusion embedded in a ductile matrix (Fig. 2-44), which is a well known small-scale phenomenon in highly strained rocks (*e.g.* Simpson & Schmid, 1983). The competence contrast between massive dolomites and highly anisotropic Cretaceous units which is apparent in Fig. 2-30 may have resulted in independent behaviour under compression (Fig. 2-45). Such partial decoupling of different lithological units during deformation is also suggested by the preferential shearing along a weak interface evident in Fig, 2-33. The extreme manifestation of this phenomenon is the *décollement* (detachment) of thrust slices along weak horizons which occurs on a regional

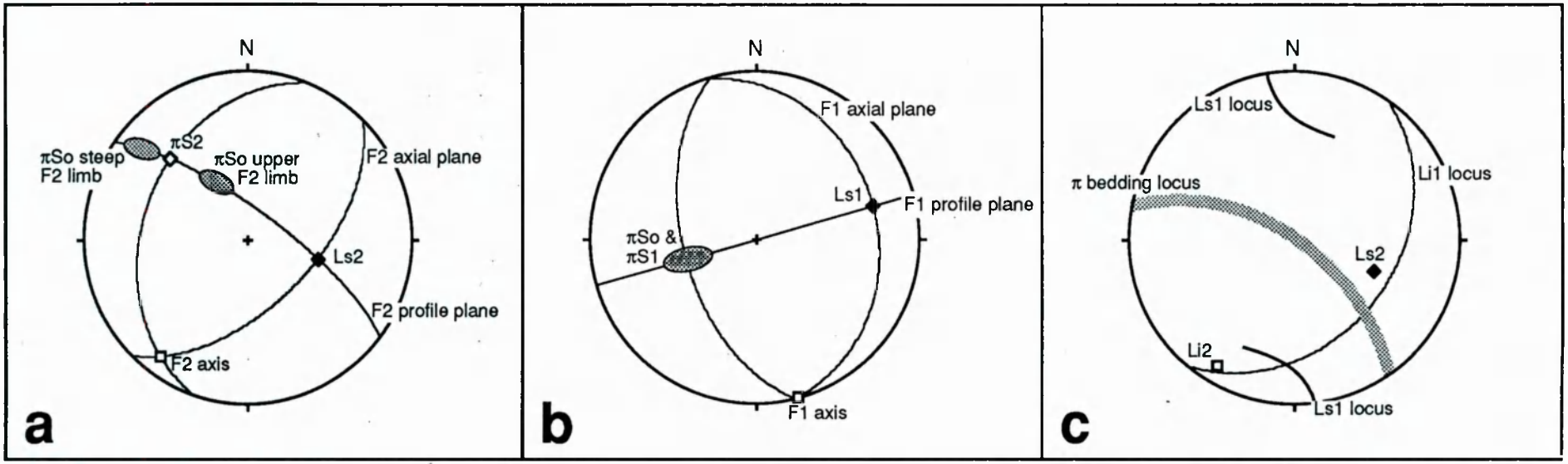

Fig. 2-43. Synthetic stereonets summarising a simplified model to account for the structure of the Montchail thrust sheet via WNW-vergent folding superimposed on south- or SSE-plunging tight/isoclinal F1s: **a)** situation where only F2 folding is recorded (*cf.* Figs. 2-29, 2-26c); **b)** situation where only F1 folding is recorded (entirely hypothetical); **c)** likely result of superimposition of F2 on an area previously deformed into near-isoclinal F1 folds (*cf.* Figs. 2-20, 2-26b). Abbreviations: π = 'pole to'; Li = fold axis lineation (*e.g.* the fold hinge itself or a bedding-cleavage intersection parallel to it); Ls = stretching lineation; S_0, S_1, S_2 = bedding, first cleavage, second cleavage.

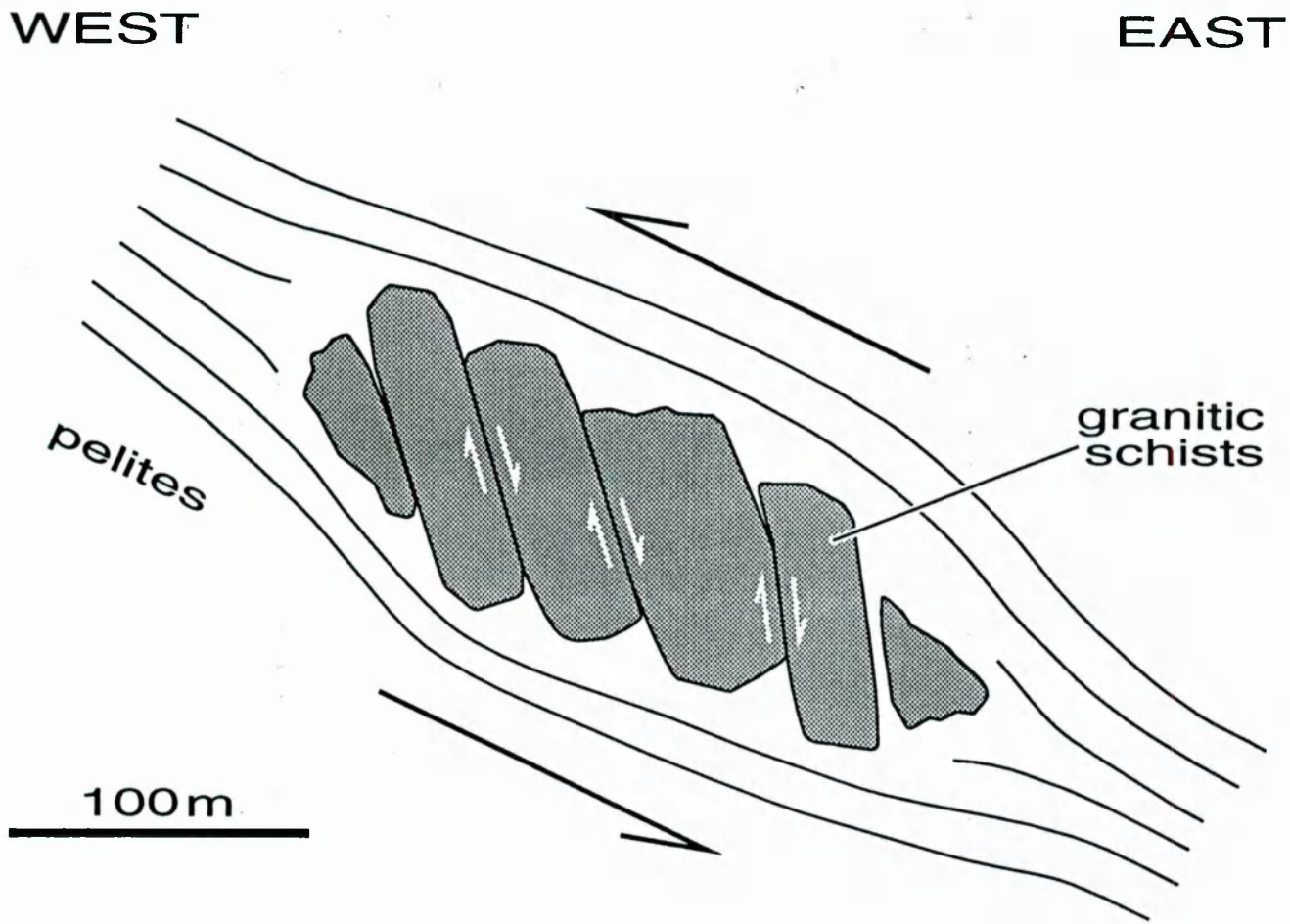

Fig. 2-44. Interpretation of the stepped basal contact of the Punta Rossa granitic schists (onto underlying pelites) in terms of tensile fractures developed antithetically to the main movement sense. Thus, the granitic slice appears to have behaved as a rigid inclusion within an incompetent matrix subjected to non-coaxial shear, akin to the 'tuilage' structure described by Blumenfeld & Bouchez (1988).

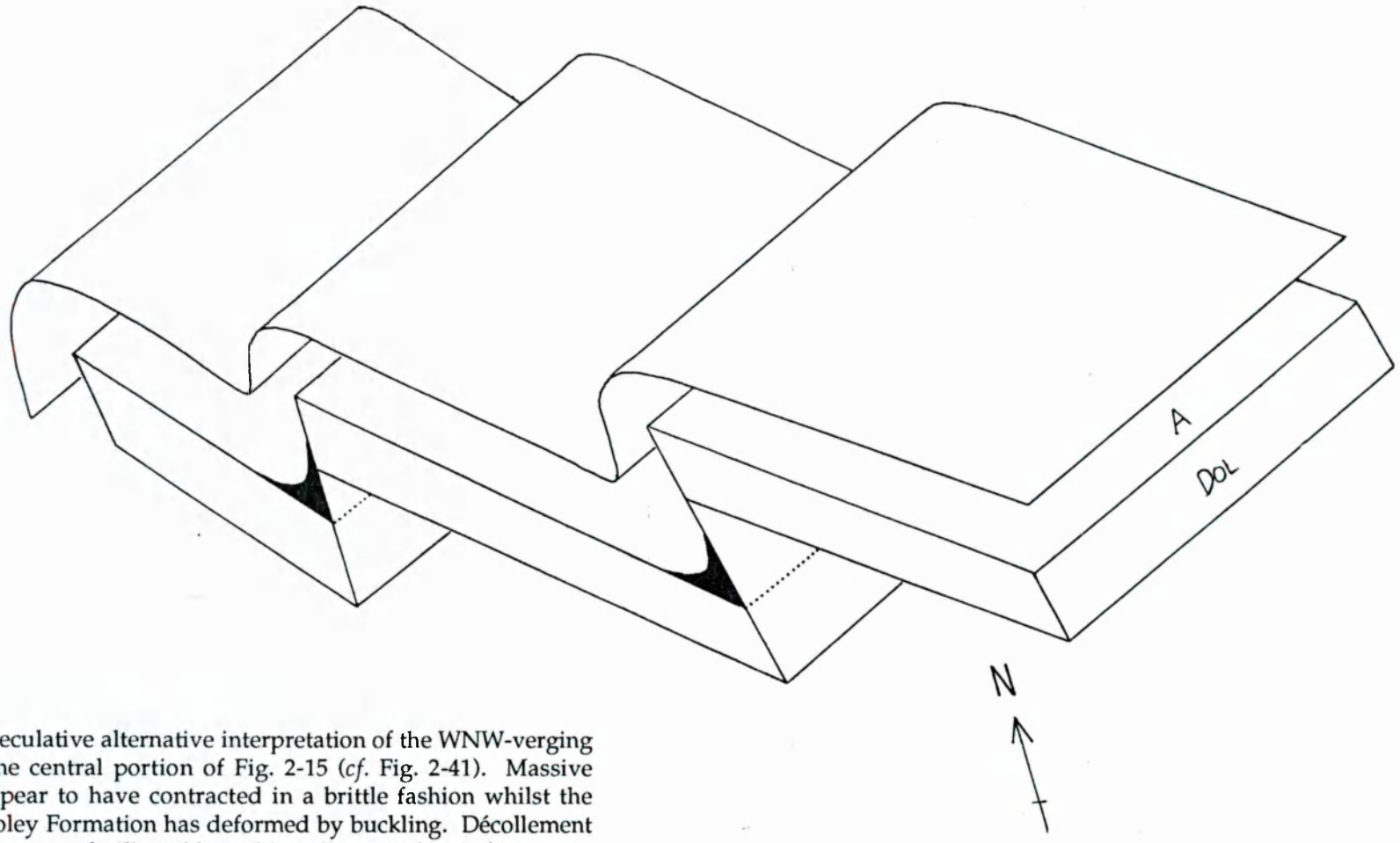

Fig. 2-45. Speculative alternative interpretation of the WNW-verging F2 folds in the central portion of Fig. 2-15 (*cf.* Fig. 2-41). Massive dolomites appear to have contracted in a brittle fashion whilst the overlying Aroley Formation has deformed by buckling. Décollement between the two was facilitated by a thin pelitic unit (Peula/Arguerey Formation). Behaviour of the underlying Triassic psammites is unknown but detachment between psammites and dolomites is evident locally. A = Aroley Formation, DOL = Triassic dolomites.

scale in the Alps (*e.g.* Laubscher, 1988b) and which may have facilitated the propagation of the Miravidi Thrust (along Arguerey Formation pelites) and the Sub-Briançonnais and sub-Seloge Thrusts (along evaporite-rich horizons). The general absence of basement involvement in the Tarentaise thrust sheets implies regional *décollement* at the basement–cover interface, typically utilising the relatively weak Carboniferous pelites. This partial lithological control of thrust trajectories implies an important link between inherited stratigraphic architecture and orogenic structures.

The thrusts or shear zones themselves all have approximately parallel outcrop traces whose orientations between terminations suggest transport towards the NW quadrant according to the 'bow and arrow' rule of Elliott (1976). Where available, kinematic indicators indicate thrusting towards the west or NW (section 2.2-3). On the internal edge of the Tarentaise Zone, the Sub-Briançonnais Thrust clearly breaches structures in the underlying pile (Fig. 2-8), indicating motion on this thrust after emplacement of the structurally lower thrust sheets. The most external Tarentaise thrust, the FPT, is undeformed on the scale of observation (though it is apparently folded on a regional scale by imbrication in its footwall, Butler, 1985) whereas the most internal thrust, the Miravidi Thrust, is affected by later WNW-directed deformation (Fig. 2-23). None of the intermediate thrusts visibly truncate early formed structures in their footwalls, and their geometries are broadly consistent with the propagation of a linked thrust system via sequential foreland directed footwall collapse, which is considered to be the most common *motif* of thrust belt development (Boyer & Elliott, 1982; Butler, 1987). The Seloge Thrust is a slightly anomalous case in that a net extensional offset is evident across it (section 2.3-4). For this reason Spencer (1990) regarded the fault as a Mesozoic extensional fracture reactivated with reverse motion during Alpine compression. This is plausible and, with a bit of imagination, it is possible to tentatively interpret the progressive westerly steepening of F2 axial planes towards the Seloge Thrust (Fig. 2-41) in terms of buttressing against an uplifted basement block (*i.e.* the footwall to a Mesozoic normal fault) with subsequent modification under continuing compression.

2.4-1 Comparison with Earlier Interpretations

The first thorough structural appraisal of the Tarentaise Zone was provided by Antoine (1971, 1972) who interpreted the internal structure of the Zone in terms

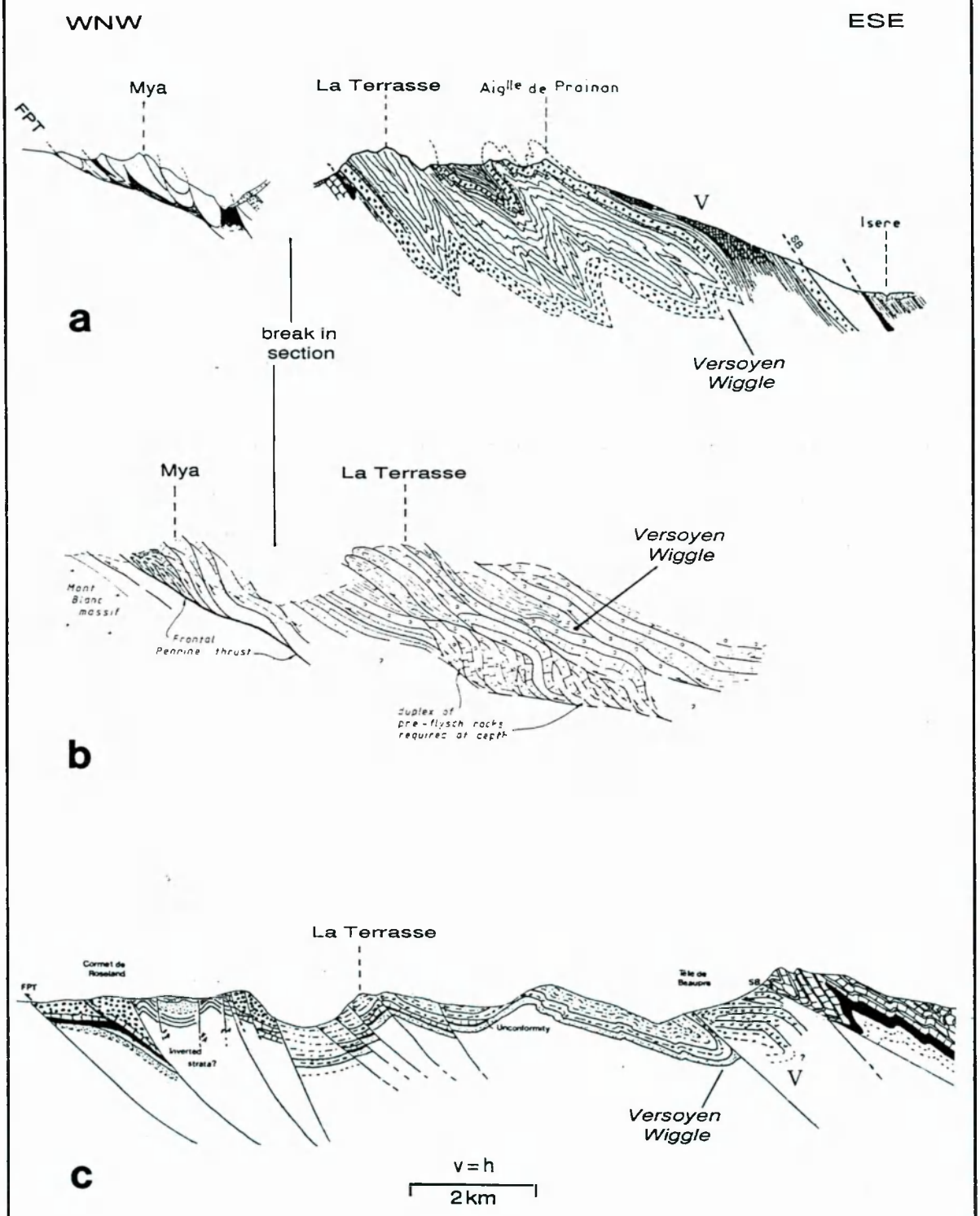

Fig. 2-46. Previous interpretations of the structures exposed in the Vallée des Chapieux: **a)** from Antoine (1971); **b)** from Butler (1989b); **c)** from Spencer (1990). Annotations have been added to the originals. The scale is the same for each section. The Aroley Formation is indicated by assorted pebble-like symbols. Sections lie approximately along the line of Fig. 2-14, the Mya segments in **a** and **b** lie close to the line of Fig. 2-35. Abbreviations: *FPT* = Frontal Pennine Thrust; *SB* = Sub-Briançonnais Thrust; *V* = Versoyen complex (Miravidi thrust sheet).

of large isoclines deformed by later folds and minor thrusts (Fig. 2-46a). A radical reinterpretation was proposed by Butler (1989b) who invoked a much simpler WNW-verging imbricate stack to explain the same geometries (Fig. 2-46b). In contrast, Spencer (1990) envisaged a complex situation in which huge (tens of kilometres) recumbent F1 isoclines were deformed by WNW-verging F2 folds and thrusts, and by extensional and strike-slip faults (Fig. 2-46c). None of these previous interpretations is consistent with the structural data presented in section 2.3. How can a well exposed, accessible area with a well established stratigraphy support such a serious divergence of opinion? Antoine's (1971, 1972) interpretative sections are closely sympathetic to the observed styles of deformation but his failure to recognise important structural discontinuities (*e.g.* the Miravidi Thrust and the Montchail Thrust) led him to construct spurious fold geometries by inferring subsurface connections between stratigraphic units offset by the thrusts. However, the piggy-back thrusting model of Butler (1989b) is less satisfactory because: **a)** it fails to account for the observed reversals in younging directions; **b)** it interprets all folds as thrust related; and **c)** it fails to reflect the local structural style. Spencer's (1990) interpretation is essentially a refined version of that proposed by Antoine (1971). The cross-sectional geometries are similar but Spencer is able to establish a detailed sequence of events with which to explain the development of these geometries (*op. cit.*). Nevertheless, Spencer's (1990) cross-sections, and the deformation chronology implied by them, are in places irreconcilable with the data presented in section 2.3. The regional scale recumbent isoclines envisaged by Spencer (1990) are consistent with, but not demanded by, the available data. It is equally possible that the F1 structures were developed only in the Miravidi, Montchail and Frontal Pennine thrust sheets rather than as regionally continuous features. This is the interpretation favoured here since the impersistence of the Arguerey/Peula Formation in the Seloge thrust sheet (Antoine, 1971) would have inhibited the *décollement* necessary for the development of large recumbent structures in the Cretaceous formations. The weak layer-parallel S1 cleavage in the Seloge sheet, as elsewhere, could be a load induced fabric attributable to emplacement of overlying thrust sheets.

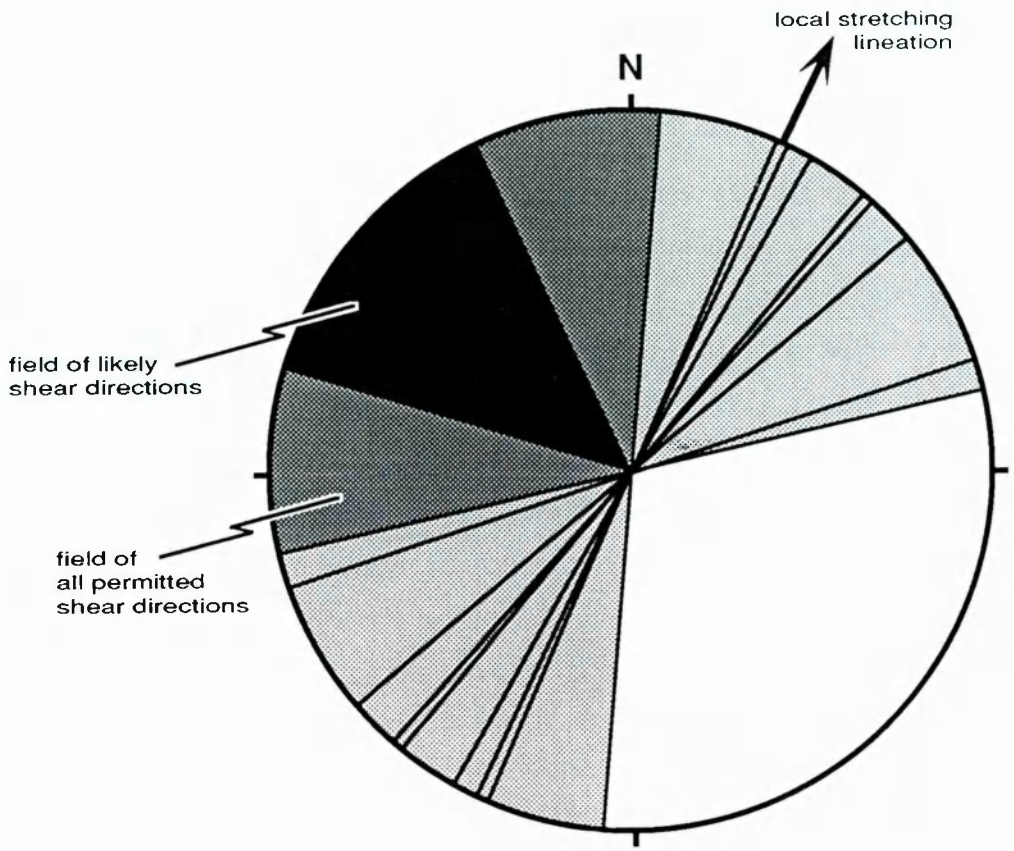

Fig. 2-47. A structural dartboard. Simplified upper hemisphere stereoplot showing the field of feasible overshear directions for mylonites above the Frontal Pennine Thrust in the region SW of Lago di Combal (3349 50711). Constraint on the kinematic framework is provided only by rotated porphyroclast systems and a proto-myonitic foliation. The vertical great circles represent notional planes which lie normal to both the foliation and to exposure surfaces exhibiting unambiguous shear-sense indicators. Assuming that the displacement axis lies within 90° of the strike of these exposure surfaces, then shear criteria indicate that the transport direction must lie on the shaded side of each great circle. Making the further assumption that all observed shear-sense indicators relate directly to a single bulk flow regime, then the displacement direction has to be contained within the overlap of these fields, denoted by denser stippling. The black slice indicates the field of possible overshear directions obtained by assuming that the displacement axis lies within 60° of the strike of the exposure surfaces.

2.4-2 The Lineation Problem

It was noted in section 2.2-3 that the majority of stretching lineations encountered in the Tarentaise Zone are aligned NNE–SSW (Fig. 2-12), parallel to the F2 fold axes and at right-angles to the inferred direction of tectonic transport. Although parallelism between fold axes and extension lineations is commonplace in zones of very high non-coaxial strain (because material lines tend to rotate towards the shear direction with progressive strain increments) this is clearly not the situation in the Tarentaise. Spencer (1990, 1992) regarded the hinge-parallel stretching lineations as evidence for major along-strike extension in the Tarentaise Zone. However, SSW-trending stretching lineations are only common in the vicinity of F2 fold hinges and not on fold limbs or within the shear zones themselves, suggesting that these lineations may reflect only local strains accumulated during fold amplification. An exception is the mylonitic sequence exposed 80–100m above the FPT north of Mont Fortin (Fig. 2-38), where stretching lineations, though sparse, consistently plunge towards the SSW. Does this orientation reflect the local thrust movement direction? As illustrated in Fig. 2-39, these mylonites are relatively rich in small-scale shear-sense indicators. A fundamental observation in this area is that such asymmetric shear-produced structures are exposed only on faces which lie in certain orientations (differently oriented surfaces showing purely symmetric strain features). By plotting these exposure orientations relative to the sense of shear evident upon them, it possible to loosely constrain the field of possible bulk shear directions, assuming a single bulk shear direction (Fig. 2-47). The result is suggestive of top-to-the-NW shear and exiles the local stretching lineations beyond the range of viable shear directions. Thus in at least one high strain zone, stretching lineations do not coincide with the extension direction. Away from the shear zones, strong NNE–SSW stretching lineations are best developed in the hinges of F2 folds, to which they lie parallel. The development of stretching lineations parallel to the associated fold axes implies a situation where strain associated with folding is such that a significant extension occurs along the hinge. This could be envisaged to occur when folds lock up and buckling ceases to be an effective mechanism of shortening (Price & Cosgrove, 1990). This may be a feasible model for the Tarentaise Zone because most of the folds concerned have interlimb angles of ~70° (typical lock-up angle for buckle folds (*op. cit.*)) and are oriented such that their short limbs would have been approximately normal to the principal comp-

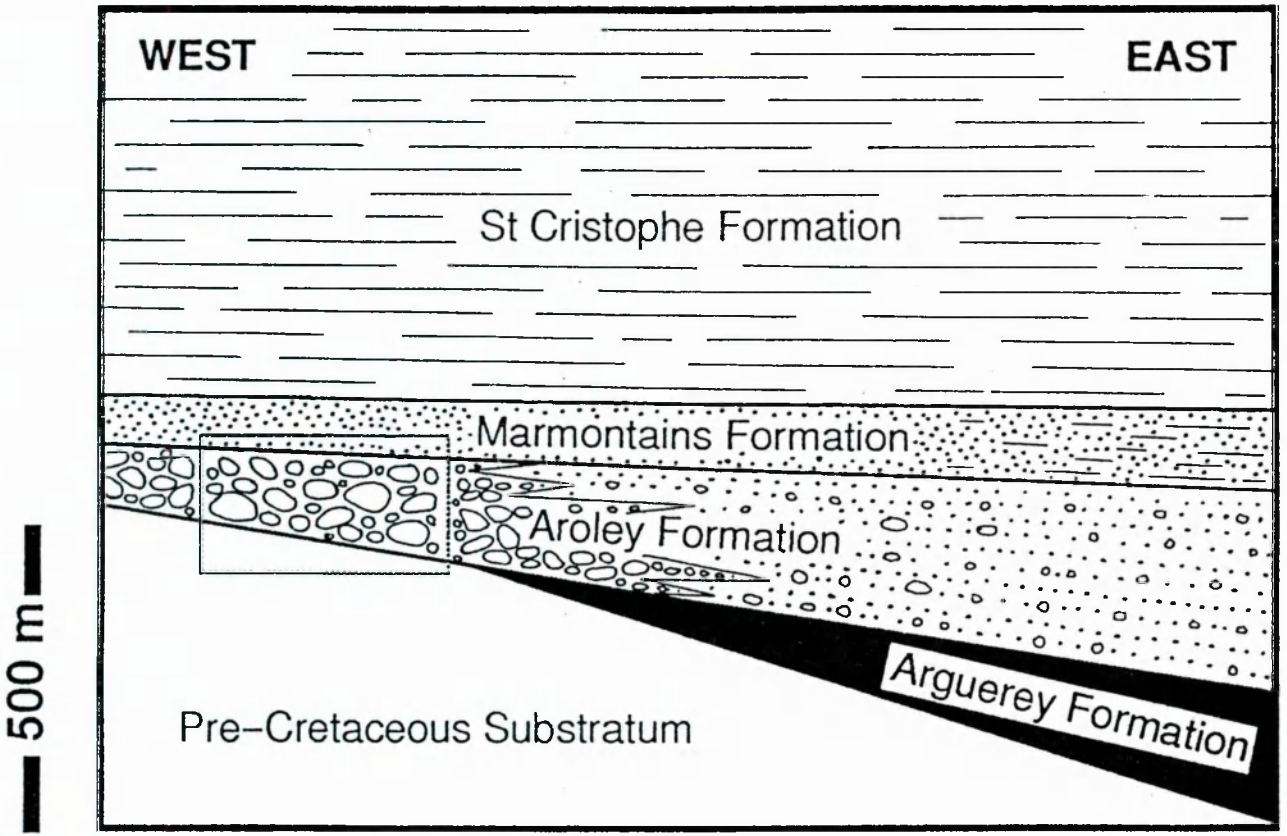

Fig. 2-48. Stratigraphic cartoon to show the schematically restored variations in grain-size and thickness for the late Cretaceous basin-fill of the Tarentaise Zone in the Courmayeur–les Chapieux area. The dotted rectangle indicates the stratigraphic position of the main focus of sedimentological studies discussed in the following chapter.

ressive stress, giving maximum resistance to layer-parallel shear. Alternatively, strike-parallel extension during fold growth would be favoured if the boundary conditions were such that extension normal to the layering is markedly more difficult than extension within the plane of the layering (Watkinson, 1975). Interestingly, Cobbold & Watkinson (1981), have suggested that in some instances, pervasive linear fabrics can force late folds to form with their axes sub-parallel to the lineation because the L-fabric induces a strong bending anisotropy, though this is not regarded as a likely mechanism in the Tarentaise since WNW - vergent folding is a regional phenomenon in the NW Alps whereas NNE–SSW oriented lineations are not.

2.4-3 Implications

The most important result is the establishment that the orogenic re-stacking of the Tarentaise Basin stratigraphy was accomplished by essentially foreland–directed sequential imbrication. Aside from the Sub-Briançonnais Thrust, which unashamedly breaches the underlying thrust sheets, there is no evidence of any form of out-of-sequence thrusting. This deduction allows stratigraphic and sedimentological observations (chapters three, four and five) to be placed in a meaningful palæogeographic context: for example, the structurally lower, more external thrust sheets were derived from the western part of the basin. Figure 48 shows a schematic restoration of the Tarentaise Basin stratigraphy in the Chapieux–Courmayeur region. However, detailed palæogeographic restorations remain difficult and will not be attempted here.

2.4-4 Remaining Problems

Even in the well exposed zones of the internal Alps, outcrop limitations preclude the unequivocal characterisation of regional scale structural geometries. Hence it is necessary to employ small-scale structures to guide the larger scale interpretations between the well constrained segments of a cross section. Thus, the structure of the Tarentaise Zone remains poorly understood because large scale interpretations have not been anchored in detailed smaller scale structural analyses. Ultimately, quantitative restoration of orogenic structures will be essential for a full understanding of budgets of crustal shortening and for accurate reconstructions of basin architecture. However, simplistic two-dimensional balancing techniques of the type employed by Butler (1989b) are of

limited value in areas of complex polyphase deformation and useful three-dimensional restorations will only become possible when detailed geometric and kinematic studies have adequately characterised the structure of the region. Conversely, since the Tarentaise Zone is essentially a telescoped sedimentary basin in which inherited features appear to have influenced the deformation, analysis of its Alpine structure cannot be divorced from analysis of the precursor basin itself.

2.5 SUMMARY

1) The Tarentaise Zone represents a stratigraphically distinct package bounded by major thrusts.

2) The Sub-Briançonnais thrust has a breaching geometry with respect to the underlying Tarentaise Zone. The Miravidi thrust has been folded by subsequent deformation whereas the Frontal Pennine Thrust is apparently unfolded in this area.

3) Emplacement of the Versoyen Complex on the Miravidi Thrust was probably kinematically linked with the formation of tight to isoclinal SSE-plunging F1 folds in its footwall.

4) Internally, the Tarentaise Zone is dissected by other minor (ductile) thrusts with a top-to-the-WNW movement direction.

5) All thrust sheets exhibit regionally consistent WNW-vergent open folding.

6) Strike-parallel (NNE-SSW) stretching lineations are abundant and may be interpreted as localised zones of prolate strain developed in the F2 fold hinges when amplification became mechanically inhibited.

7) Many of the observed deformation structures are explicable in terms of rheological contrasts between adjacent stratigraphic units.

8) Despite good exposure, a clearly recognisable stratigraphy and appreciable vertical relief, field observations permit a broad range of interpretations.

CHAPTER 3 SEDIMENTOLOGY

This chapter attempts to establish some basic sedimentological constraints relevant to the evolution of the Tarentaise Basin. The study focuses on the earliest coarse clastic fill of the basin, the Aroley Formation, and uses detailed information from low-strain exposures to build up a picture of the depositional systems responsible for early basin infilling. As described in chapter 2, the Tarentaise units (Cretaceous basin-fill plus pre-Cretaceous basin-floor) have essentially been detached from their basement and carried WNW towards the Alpine foreland in the hanging-wall of the Frontal Pennine Thrust. The Tarentaise Zone is itself dissected by a number of smaller displacement thrusts and the enclosed thrust-sheets show complex internal deformation related both to thrusting and to pre-thrust folding. It is the distribution of these strains which largely dictates the areas where sedimentological studies are feasible. During Alpine contraction, the sedimentary pile appears to have deformed as a complex multilayer in which different components responded differently to compression: influenced not only by their own rheologies but also by the behaviour of adjacent units (section 2.4). In general, the least deformed elements of the Tarentaise basin-fill are found where the thickest-bedded facies are adherent to a relatively rigid substratum: that is, where the 'proximal' facies association of the Aroley Formation rests directly on Triassic dolomites and massive Lower Jurassic limestones (see Figs. 1-8a and 2-48). Within these low-strain oases, the conglomeratic facies have been the most deformation resilient, and hence the most amenable to sedimentological analysis. Figure 3-1 indicates the most important areas of low-strain exposure discovered and utilised in this study. .

Thus, this study focuses on sections of the 'proximal' Aroley Formation. The formation as a whole formed a coarse clastic wedge which was thinner and conglomeratic in the west of the Tarentaise Basin and thicker and predominantly arenaceous in the east (Fig. 2-48). In the western (structurally lower) part of its present outcrop, which comprises the main area of study, this formation is 100-150m thick and consists of thickly bedded conglomeratic and arenaceous units which exhibit features consistent with deposition from sediment gravity flows.

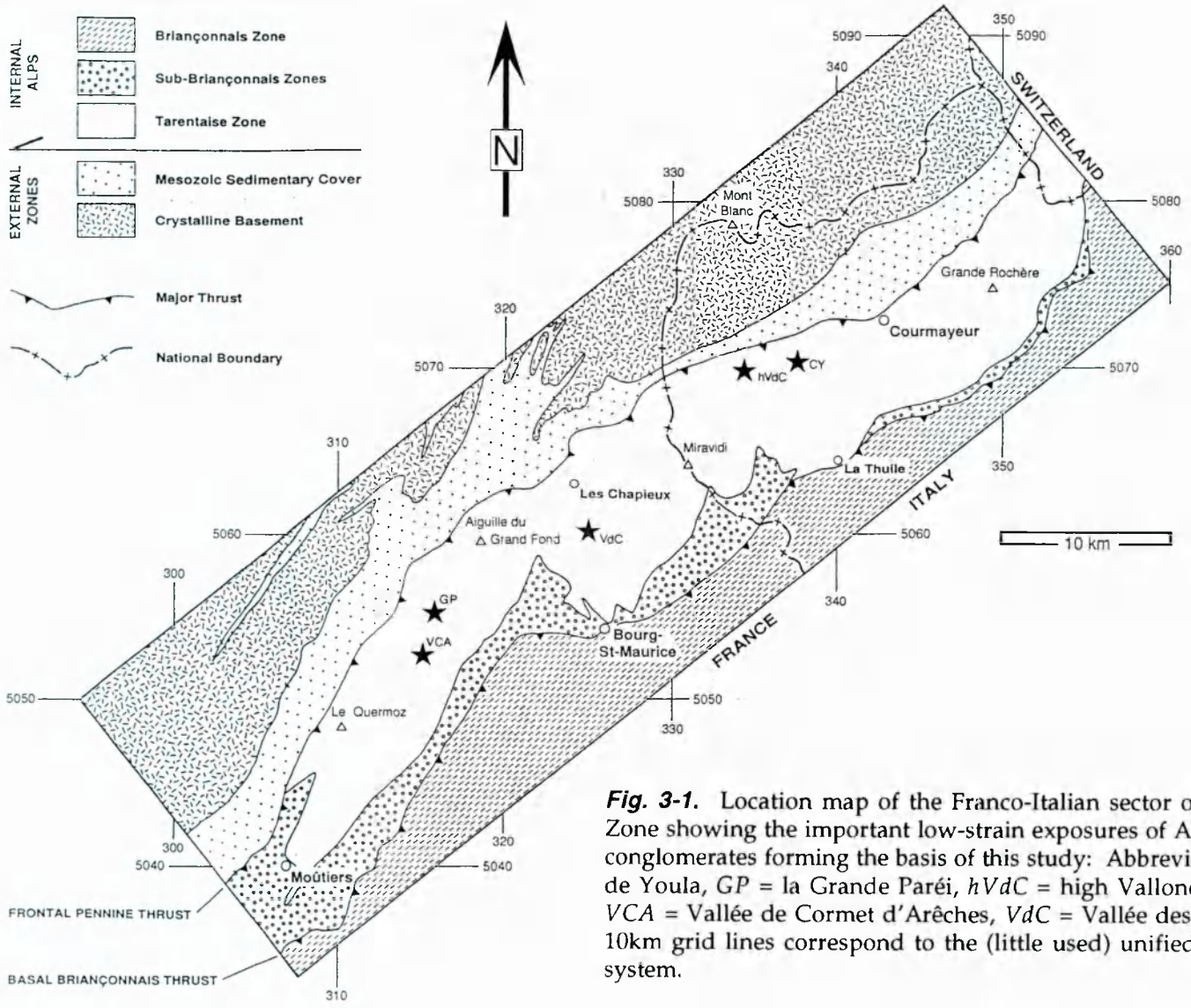

Fig. 3-1. Location map of the Franco-Italian sector of the Tarentaise Zone showing the important low-strain exposures of Aroley Formation conglomerates forming the basis of this study: Abbreviations: *CY* = Col de Youla, *GP* = la Grande Paréi, *hVdC* = high Vallone di Chavannes, *VCA* = Vallée de Cormet d'Arêches, *VdC* = Vallée des Chapieux. The 10km grid lines correspond to the (little used) unified European grid system.

3.1 DESCRIPTION OF THE CONGLOMERATES

3.1-1 Facies

The Aroley conglomerates are a highly variable ensemble of polymictic rocks interbedded with compositionally similar litharenites and calcareous mudrocks (Fig. 3-2). Conglomerate beds are generally sheet-like with planar or weakly undulatory bases: deep basal scours are scarce. Bed thickness for the conglomerates varies between 0.2 and 14m, although most beds are 0.5 to 2m thick. Maximum clast size (MCS, expressed here as the mean of the long axes of the ten largest visible clasts) exceeds 1m in a few matrix-poor beds and many beds contain isolated metre-scale megaclasts. In the field, seven main conglomerate facies were distinguished on the basis of grading, stratification and grain-size properties (Table 3-1). It has not proved feasible to extend the classification to include the associated finer-grained lithologies in consequence of a dearth of low-strain examples. The scheme outlined in Table 3-1 is specific to the Aroley Formation, but shares the same basis as the more general classification of deep-water facies proposed by Pickering *et al.* (1986, 1989). The use of a single, widely applicable facies classification is essential to objective comparisons between sequences, and is therefore important in the development of depositional models for deep-water sedimentation. Unfortunately, the scheme of Pickering *et al.* (1986), though relatively comprehensive, is difficult to apply because complex beds (for example ones which are graded in the lower portion and stratified in the upper portion) cannot be classified unambiguously.

Facies CD is essentially a structureless, matrix-supported deposit comprising large clasts dispersed relatively uniformly through an arenaceous to argillaceous matrix. Beds of this facies can be very thick (in places >10m) but they are usually laterally impersistent. Boulders several metres in diameter are common and in general this facies contains larger clasts than any other facies. Facies CD approximates to both facies A1.2 ('disorganised muddy gravel') and A1.3 ('disorganised gravelly mud') of the Pickering *et al.* (1986) classification.

Facies UG (Fig. 3-3) consists of coarse clast-supported conglomerate beds which lack grading and stratification. Beds are frequently thick (1-8m) and moderately to poorly sorted. Boulders several metres across are common. Figure 3-3b shows a grain-size profile through part of one bed of this facies which illustrates the general absence of internal organisation. In some instances, there may be a weak

FACIES		MAIN FEATURES	IMPLICATIONS
CD: *CHAOTIC MATRIX-RICH DIAMICT* *(A1.2 to A1.3 of Pickering et al., 1986)*		Total lack of internal organisation. Matrix-supported with near uniform dispersion of clasts. Strongly bimodal grain-size distribution. Very thick beds (≥10m) which are laterally impersistent.	Clasts suspended in and supported by a dense, cohesive interstitial matrix. Deposition by 'freezing' of a cohesive debris flow (*sensu* Lowe, 1982).
UG: *VERY COARSE, MATRIX-POOR, DISORGANISED CONGLOMERATE* *(A1.1 of Pickering et al., 1986)*		Lack of vertical grain-size segregation. Lack of preferential clast orientation fabric. Clast-supported. Beds typically 2-8m thick. Very coarse mean and maximum grain-sizes.	Non-operation of size-sorting processes. Clasts not fully suspended in matrix. Matrix may provide buoyant lift and grain lubrication. Frictional 'freezing' of an incohesive debris flow?
GUS: *COARSE, CLAST-SUPPORTED, CRUDELY GRADED CONGLOMERATE* *(A2.2 to A2.3 of Pickering et al., 1986)*		Normally graded, sometimes with a thin basal zone. of inverse grading. No discernible stratification. Imbrication of clast a-axes fairly common.	Sedimentation from highly concentrated grain dispersions ('traction carpets') under intense laminar shear. Rapid fall-out directly from turbulent suspension without an intervening phase of tractional transport.
NG: *NORMALLY GRADED CONGLOMERATE* *(A2.3 of Pickering et al., 1986)*		Grading often progressive rather than abrupt. Crude low-angle stratification occasionally present. Clast-supported, with a marked paucity of arenaceous material.	Strong separation of clast sizes in current, perhaps with surging segregations of coarse & fine material. Direct deposition of suspended sediment. Progressive loss of flow competence.
GS: *CRUDELY STRATIFIED CONGLOMERATE* *(A2.1 & A2.4 of Pickering et al., 1986)*		Normal grading confined to basal portion of bed. Grading typically abrupt rather than gradational. Gently inclined (<20° to bed base) near-planar stratification transitional to multiply graded profile.	The association normal grading→stratification may reflect deposition from turbulent suspension followed by tractional flow conditions at the base of a decelerating high-density turbidity current.
SPS: *CROSS-STRATIFIED PEBBLY SANDSTONE OR F. CONGLOMERATE* *(A2.5 & A2.1 of Pickering et al., 1986)*		Cross-bedding typically of asymptotically- or planar-based tabular morphology, less commonly trough-like. Basal part may show weak normal grading.	Fully turbulent flows with less deposition directly from suspension. Slower depositional rates, allowing bed-load rolling and development of dune-like bedforms.
GPS: *GRADED PEBBLY SANDSTONE* *(A2.7 & A2.8 of Pickering et al., 1986)*		Normally graded through most of the bed. Matrix-supported except in lower portion. Crude low angle stratification common in higher parts.	Deposition directly from turbulent suspensions undergoing oscillatory (surging) decline in flow competence.

Table 3-1. Summary of the lithofacies scheme used in this paper to classify the rudaceous units of the Aroley Formation. Approximate correspondence with elements of the Pickering *et al.* (1986) classification is indicated. The right hand column suggests some possible hydrodynamic inferences.

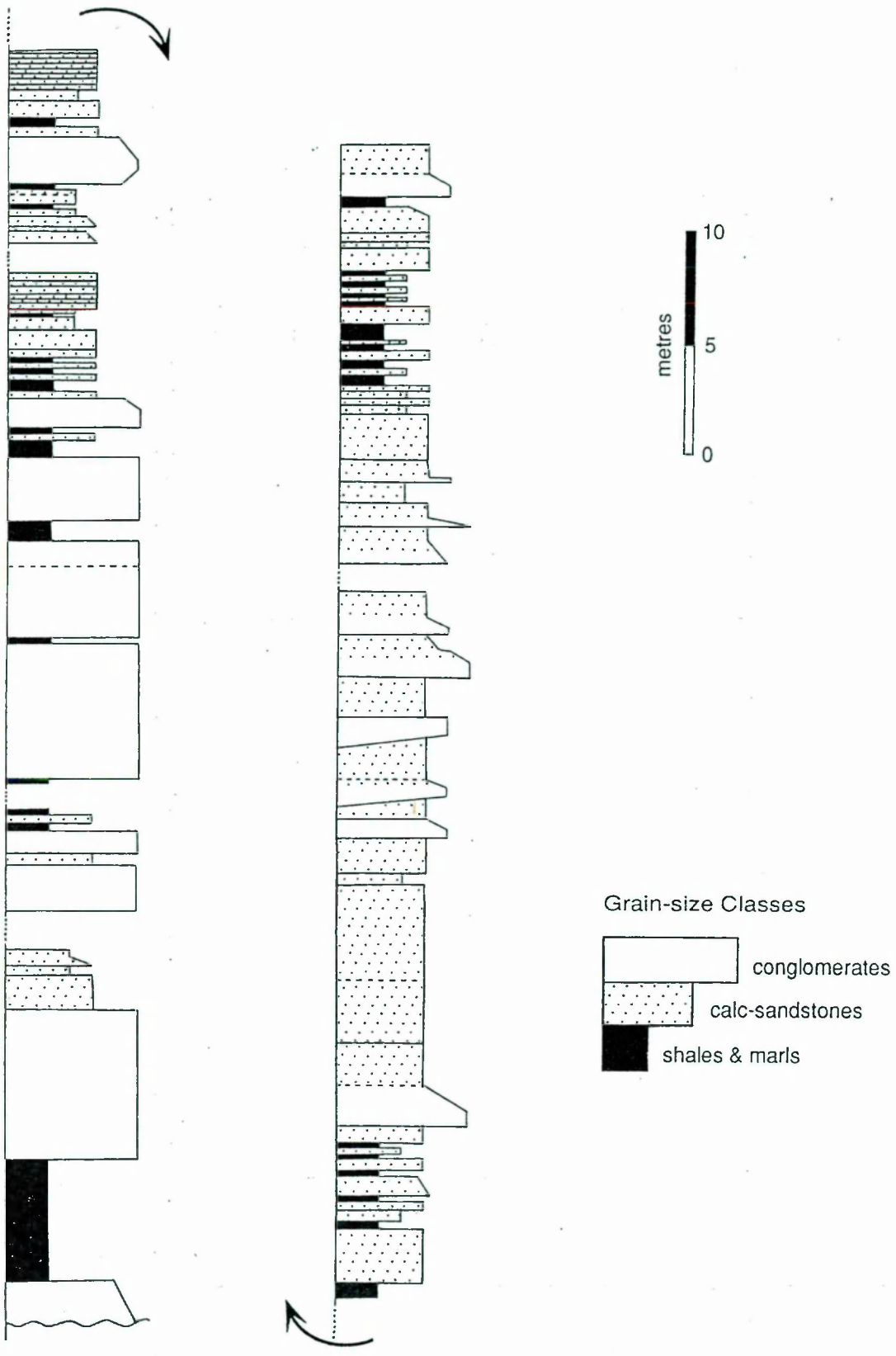

Fig. 3-2. Simplified graphic log of the Aroley Formation between 32490 506070 and 32497 506073 in the Vallée des Chapieux, France (see Fig. 3-1). The base of the log corresponds to the unconformity which separates the Aroley units from underlying massive Triassic dolomites.

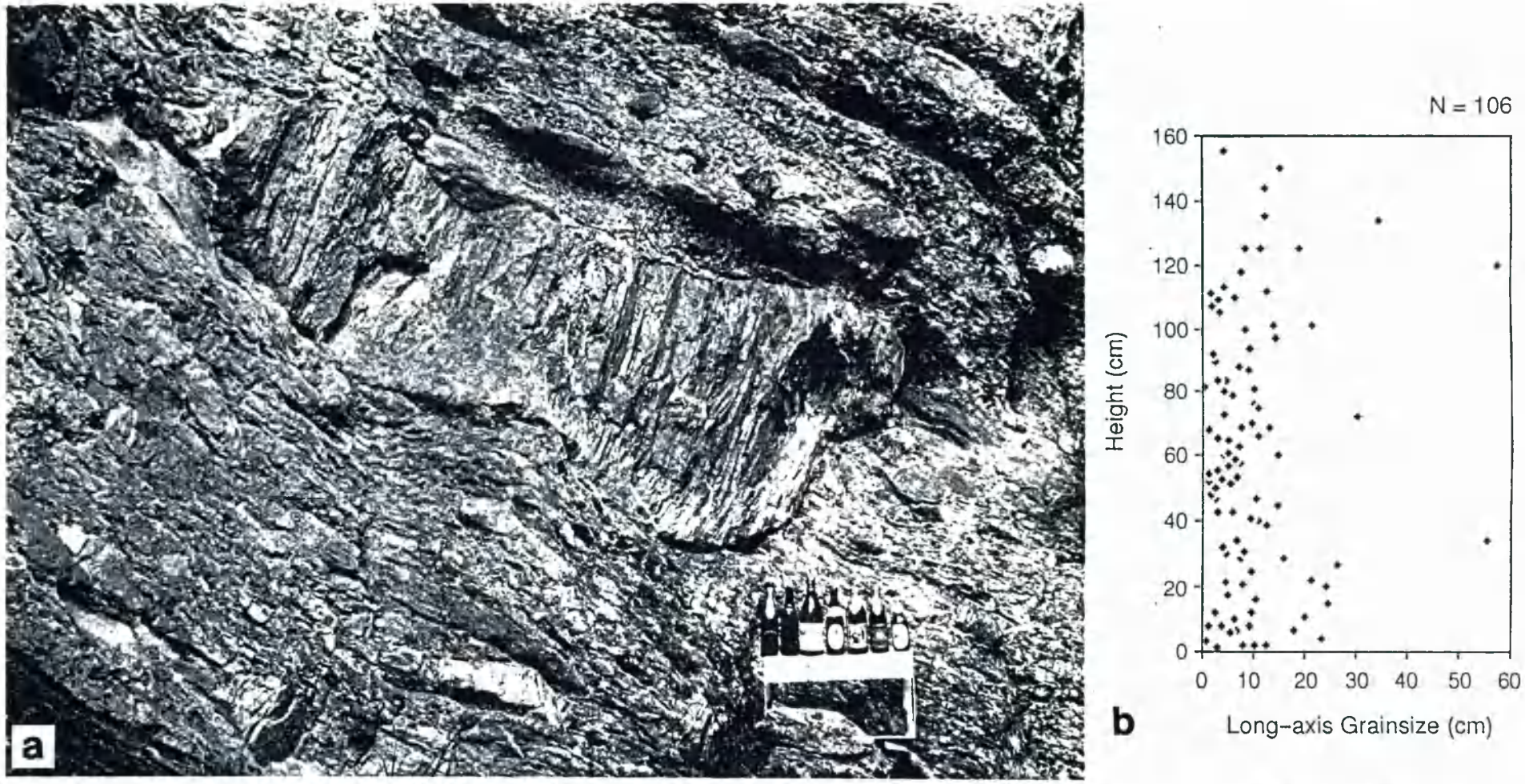

Fig. 3-3. Facies UG. **a)** Photograph of a very coarse (MCS=120.7cm), 3.2m thick, clast-supported, matrix-poor, disorganised conglomerate containing a highly compacted 3m long dolomite megaclast. This is an example of facies UG from 32491 506070, occurring at a height of 33m on the log shown in Fig. 3-2. The scale bar is 50cm long. **b)** Grain-size profile through the lower half of the same bed. The graph shows maximum visible dimensions of framework grains plotted against approximate orthogonal height of grain centres above bed base and was constructed by simply measuring the size and position of each clast larger than 2mm intersected by bedding-normal chalk lines drawn on the exposure face. No significant vertical grain-size variations are apparent.

development of normal grading in the uppermost part of the bed. Facies UG is similar to facies A1.1 ('disorganised gravel') of the Pickering *et al.* (1986) classification.

Facies GUS (Fig. 3-4) is essentially a coarse clast-supported conglomerate akin to facies UG but displaying internal organisation in the form of normal grading. This grading (Fig. 3-4b) is 'coarse-tail' rather than 'distribution grading' in the terminology of Middleton (1967) and in some instances involves a thin basal zone which is inversely graded (Fig. 3-4b). Beds of this facies are usually less than 3m thick. Facies GUS is not directly equivalent to any element of the Pickering *et al.* (1986) scheme, having affinities with both their facies A2.3 ('normally graded gravel') and facies A2.2 ('inversely graded gravel').

Facies NG (Fig. 3-5) differs from facies GUS in that grading usually occurs progressively through most of the thickness of the bed (in contrast to the more abrupt basal coarse-tail grading of Fig. 3-4). Additionally, crude sub-planar stratification is usually present in the uppermost portion of the bed. Beds of this facies are mostly 0.3 to 2m thick and often show scoured bases. Facies NG resembles facies A2.3 ('normally graded gravel') of the Pickering *et al.* (1986) classification.

Facies GS is transitional in many respects between facies NG and facies GUS (*cf.* Fig. 3-4), differing in the style and relative importance of grading and stratification. In facies GS, grading is relatively abrupt (*cf.* Fig. 3-4b) rather than progressive (*cf.* Fig. 3-5b) and is largely confined to the lower part of the bed. In common with facies NG and GUS, a thin, finer-grained basal zone is typical. Much of the higher thickness of the bed exhibits poorly defined, gently inclined stratification. Facies GS equates in part to facies A2.1 ('stratified gravel') and in part to facies A2.4 ('graded-stratified gravel') of the Pickering *et al.* (1986) classification.

Facies SPS is characterised by the presence of well developed cross-bedding which is inclined at a high angle to the bed base (Fig. 3-6). These cross-sets frequently exhibit tabular rather than trough geometries and typically comprise normally graded foresets. Beds are generally 0.4 to 2m thick and in some instances show a thin normally graded basal zone. High angle cross-stratification appears to be absent from conglomerates containing significant amounts of cobble–sized or coarser material. Facies SPS overlaps facies A2.5 ('stratified

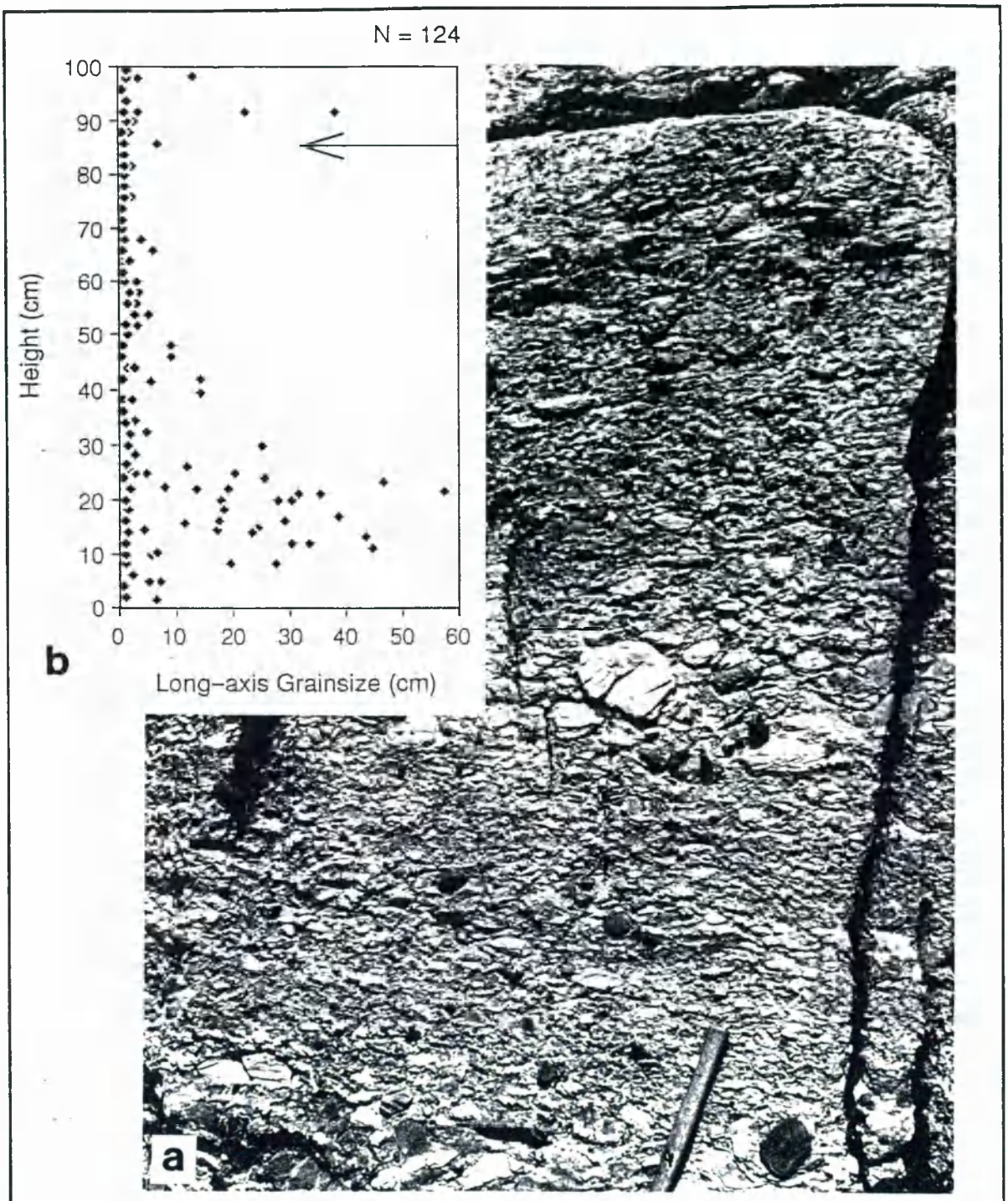

Fig. 3-4. Facies GUS. **a)** Beds of facies GUS overlying a thinner litharenite unit. Looking NNW at an east-west face in the high Vallone di Chavannes (33480 506975). The photograph actually shows at least three separate conglomeratic units, each comprising a basal zone of normal grading overlain by an essentially structureless interval, although the lowest example is vaguely stratified and could be regarded as transitional to facies GS. This lower conglomerate is 87cm thick with MCS=35.0cm whereas the unit occupying the middle of the photograph is approximately 110cm thick and has MCS=52.1cm. The photograph illustrates some of the difficulties of distinguishing individual depositional units in stacked conglomeratic sequences where finer grained interbeds are absent. The hammer is 40cm long. **b)** Grain-size profile through the facies GUS bed which occupies the lower part of the photograph. The graph shows a relatively abrupt fall-off in clast sizes above a 20cm thick coarser interval, which in turn overlies a thin basal zone of inverse grading. The arrow indicates the approximate base of the overlying bed.

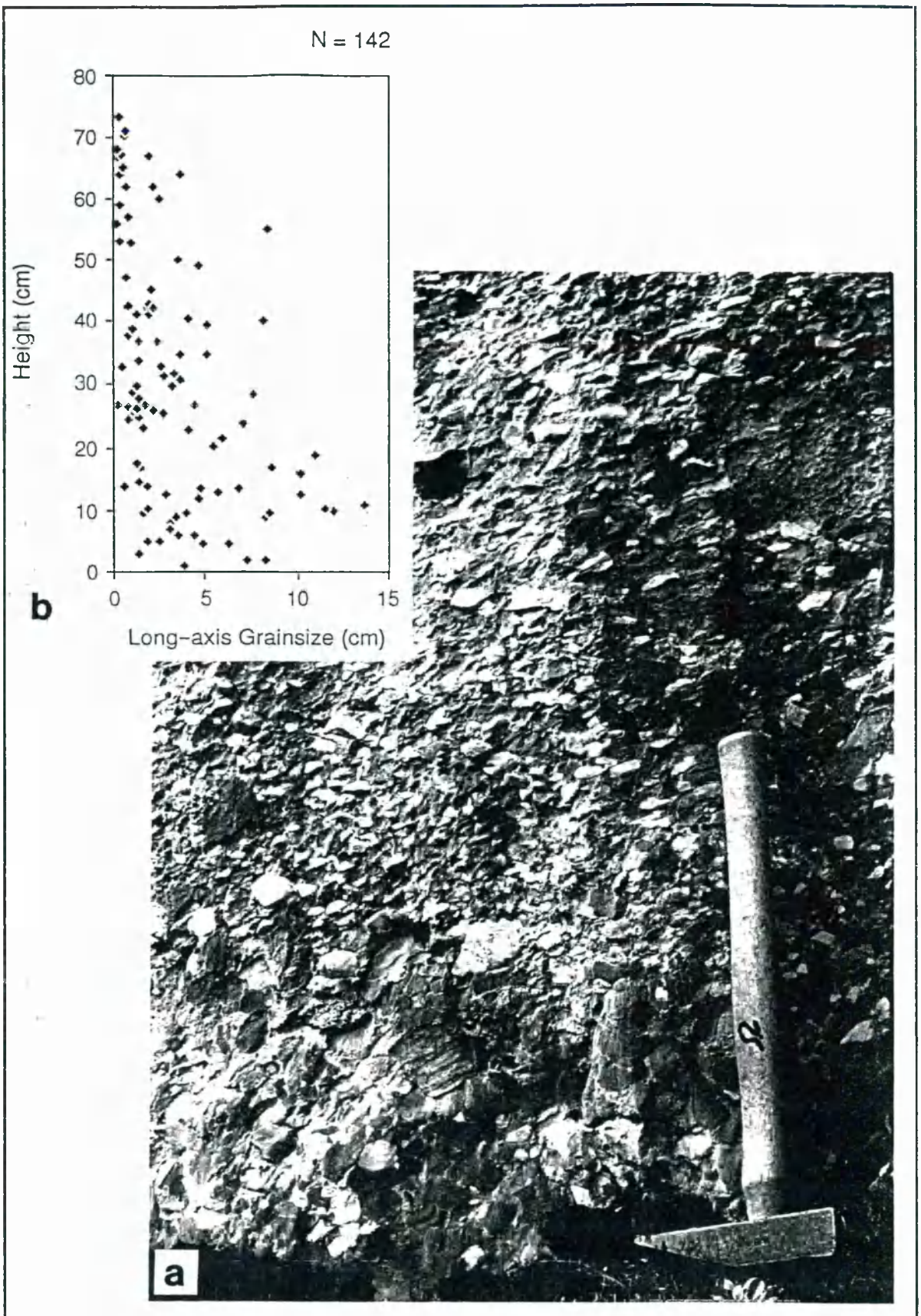

Fig. 3-5. Facies NG. **a**) Clast-supported normally graded conglomerate from the high Vallone di Chavannes (33482 506974). 40cm hammer for scale. **b**) Grain-size profile through the clast-supported part of a facies NG bed from 32467 506035 in the Vallée des Chapieux. The graph displays a relatively gradual decrease in both mean and maximum clast size with elevation (*cf.* Fig. 3-4). (Note that this is not the bed shown in Fig. 3-5a.)

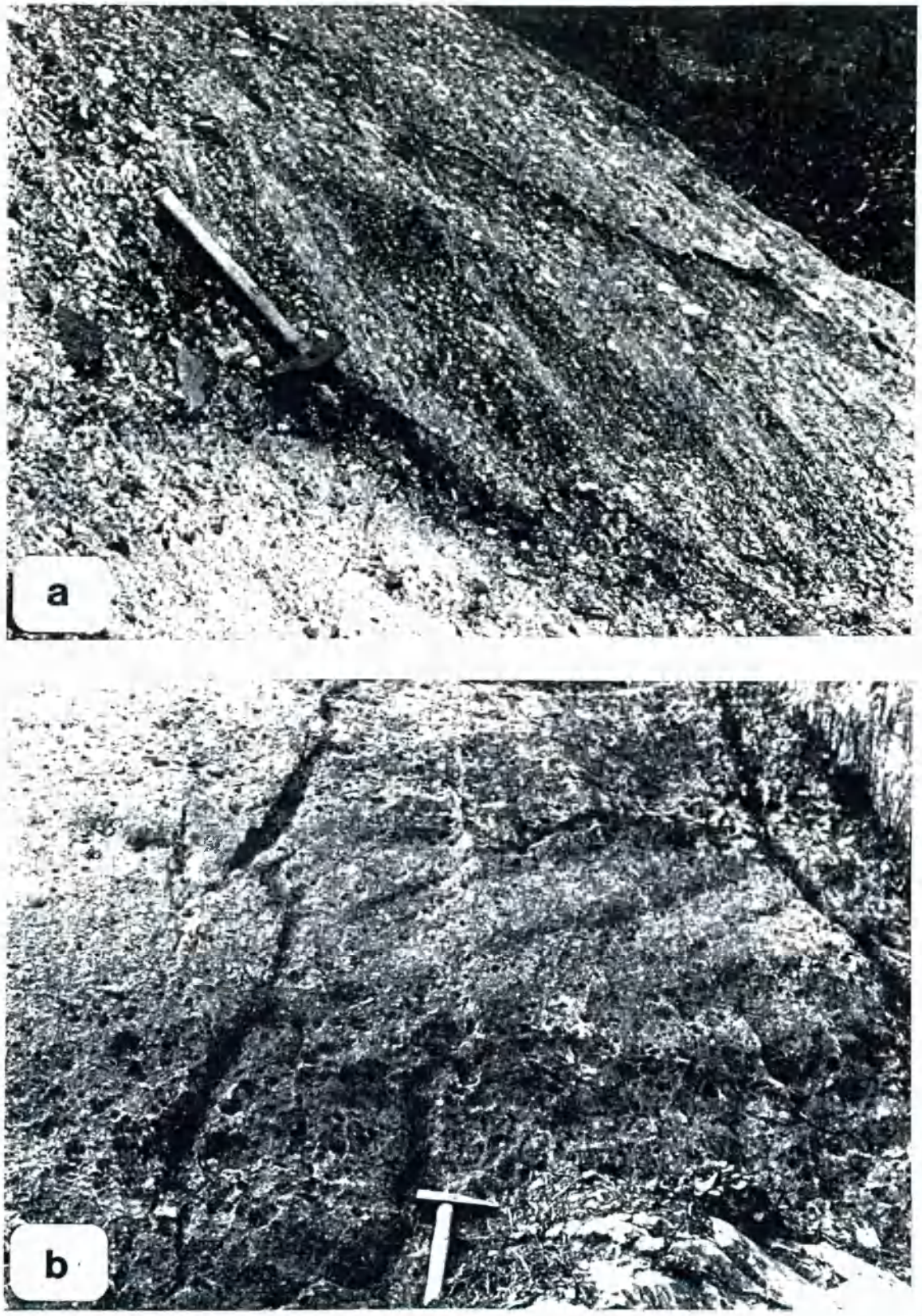

Fig. 3-6. Cross-bedding in facies SPS. **a)** Planar-based tabular cross-bedding from 32495 506072 in the Vallée des Chapieux. The cross-bedded interval is relatively fine (MCS = 17.2cm), approximately 1m thick, and appears to grade down into a much coarser (MCS = 56.5cm) normally graded unit. The restored foreset orientation is 26→107. The hammer is 40cm long. **b)** Asymptotically-based cross-bedding from the Vallée des Chapieux at 32467 506031. Looking south at SE-dipping beds on an east-west face. The hammer is *still* 40cm long.

pebbly sand') and facies A2.1 ('stratified gravel') of the Pickering *et al.* (1986) classification.

Facies GPS (Fig. 3-7) comprises matrix-rich (usually >30% matrix, which is mostly sand-sized material) pebbly sandstone beds with typical thicknesses in the range 0.25 to 1.5m. These beds generally involve a coarser clast-supported zone in the lower part of the bed which grades upward as the proportion of framework clasts decreases into a matrix-supported unit, within which thin clast-rich layers may define an indistinct stratification inclined at a low angle to the bed base. Bed bases are commonly scoured into the underlying sediment and may be overlain by a thin layer of finer material beneath the main normally graded unit. Facies GPS involves essentially the same characteristics as facies A2.7 ('normally graded pebbly sand') and facies A2.8 ('graded-stratified pebbly sand') in the Pickering *et al.* (1986) scheme.

Since the work of Walker & Mutti (1973), most classifications of conglomeratic rocks have recognised a basic distinction between organised and disorganised facies on the basis of the presence or absence of clearly defined sedimentary structures (*e.g.* Kelling & Holroyd, 1978; Walker, 1978; Pickering *et al.*, 1986). For the Aroley Formation, the disorganised facies (facies UG and CD) are the coarsest in terms of maximum clast sizes, and also usually the most thickly bedded. The most abundant manifestation of organisation within the Aroley Formation conglomerates is normal grading, which is evident in 23 of the 35 conglomerate beds shown on the logged sections in Figs. 3-2, and 3-8. Well developed inverse grading is rare, although numerous beds exhibit a thin basal zone of finer grained material beneath an otherwise normally graded interval (*e.g.* Figs. 3-4b and 3-5b). Some form of stratification is apparent in 10 of the 35 logged rudaceous beds (Figs. 3-2 and 3-8). Cross-bedding composed of steeply inclined foresets is confined to the finer grained facies and usually only occupies the upper portions of beds. In contrast, stratification which lies at a low angle relative to the bed base often occurs in coarser grain-sizes and may involve the entire thickness of the bed. Apart from facies CD, the distinctions between adjacent facies in Table 3-1 are subtle and together may form a continuum. No beds transitional between facies CD and any other facies were observed.

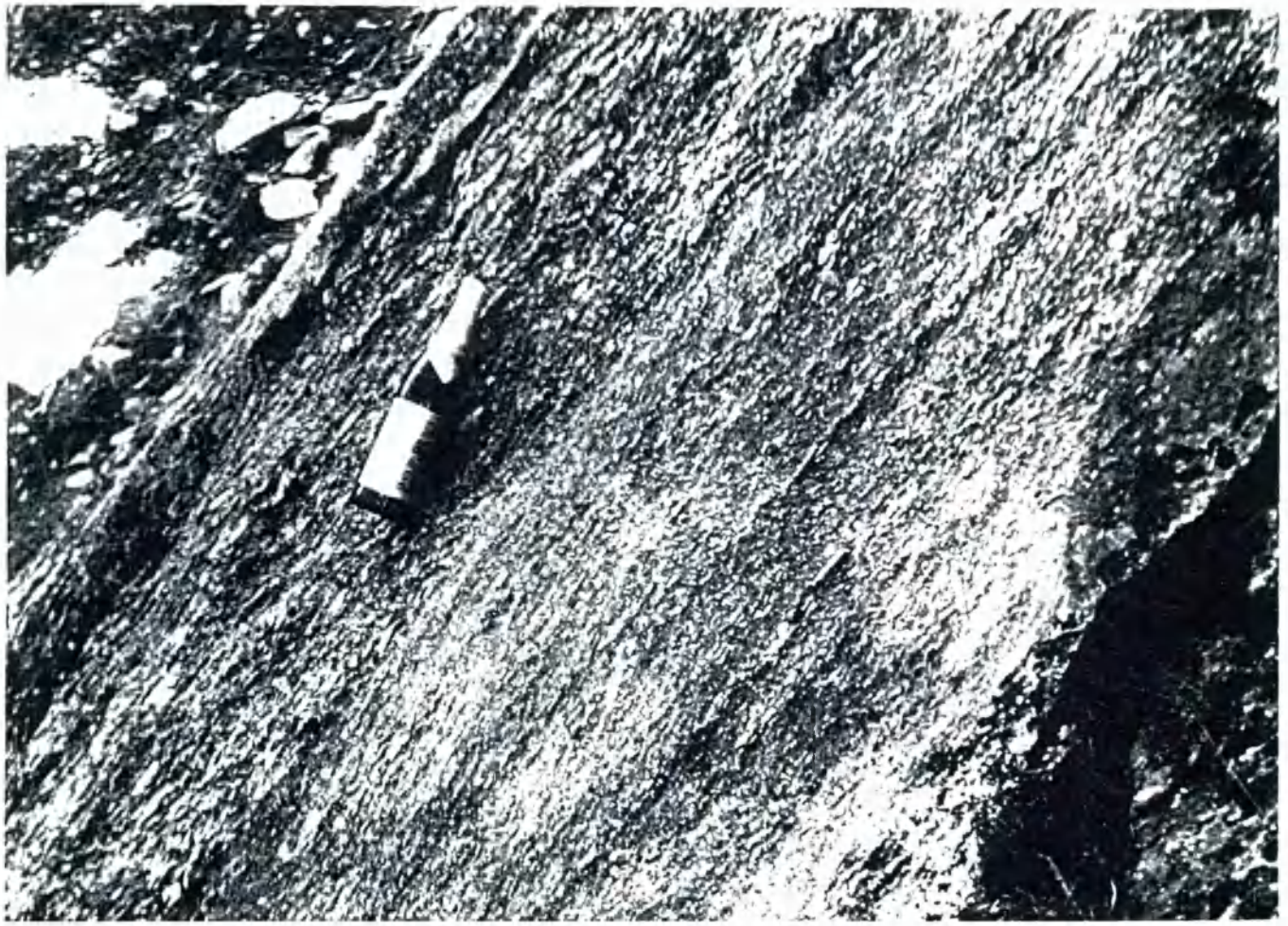

Fig. 3-7. An upside down example of facies GPS which lives at 32320 506180 in the western Vallée des Chapieux. View looking SSW at a 1.2m thick overturned bed dipping at 50° to the SSE. The scale is 232mm high.

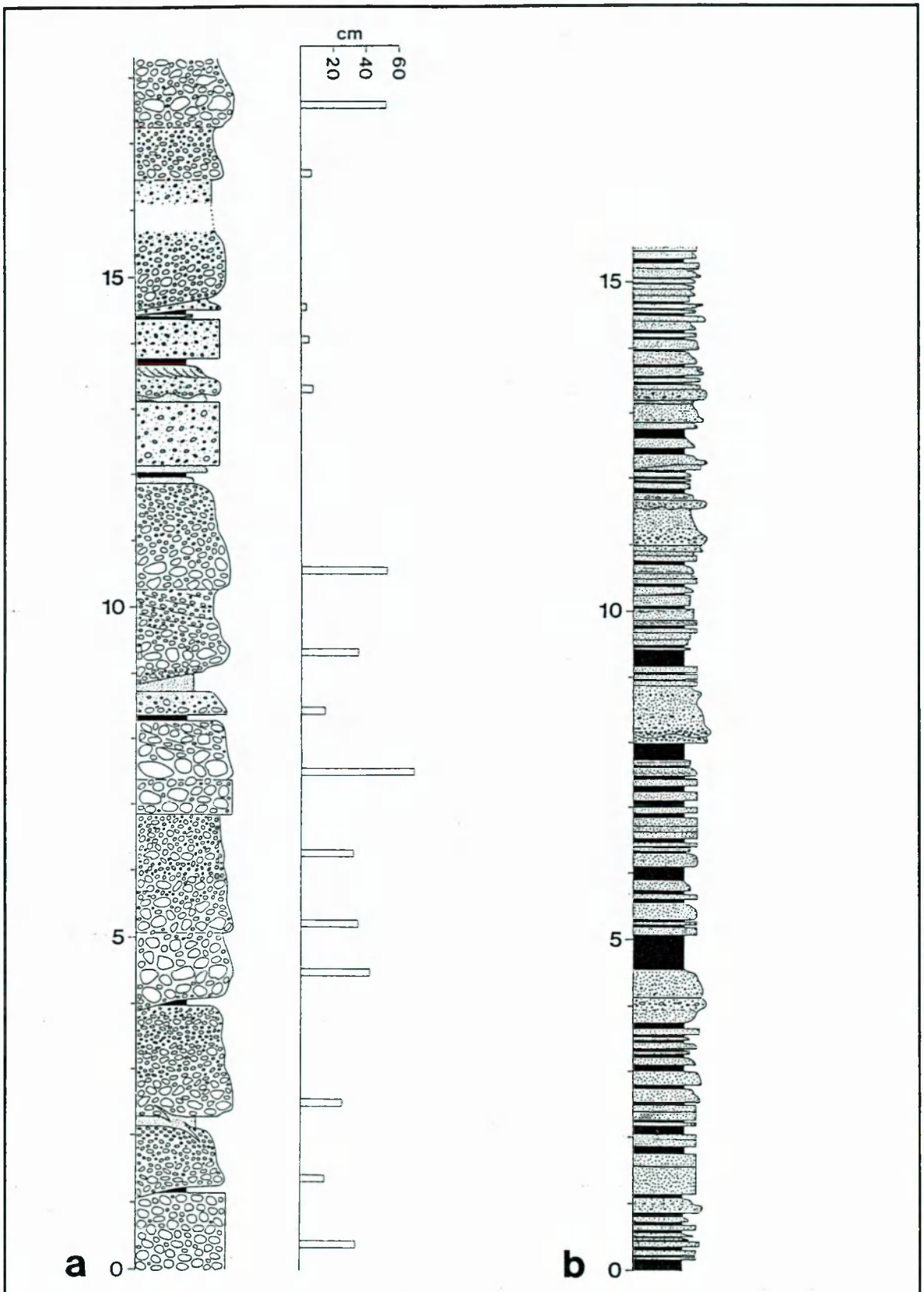

Fig. 3-8. Detailed graphic logs of the 'proximal' Aroley formation, illustrating the contrast between lower and higher parts of the formation. Vertical scales are in metres. **a)** The near-basal Aroley Formation from 33480 506975 in the high Vallone di Chavannes, Italy, showing maximum clast sizes (MCS = mean of ten largest visible clasts) for some of the beds. Note the paucity of fine-grained material. **b)** The upper parts of the Aroley Formation at 31496 505353 in the Vallée de Cormet d'Arêches, France.

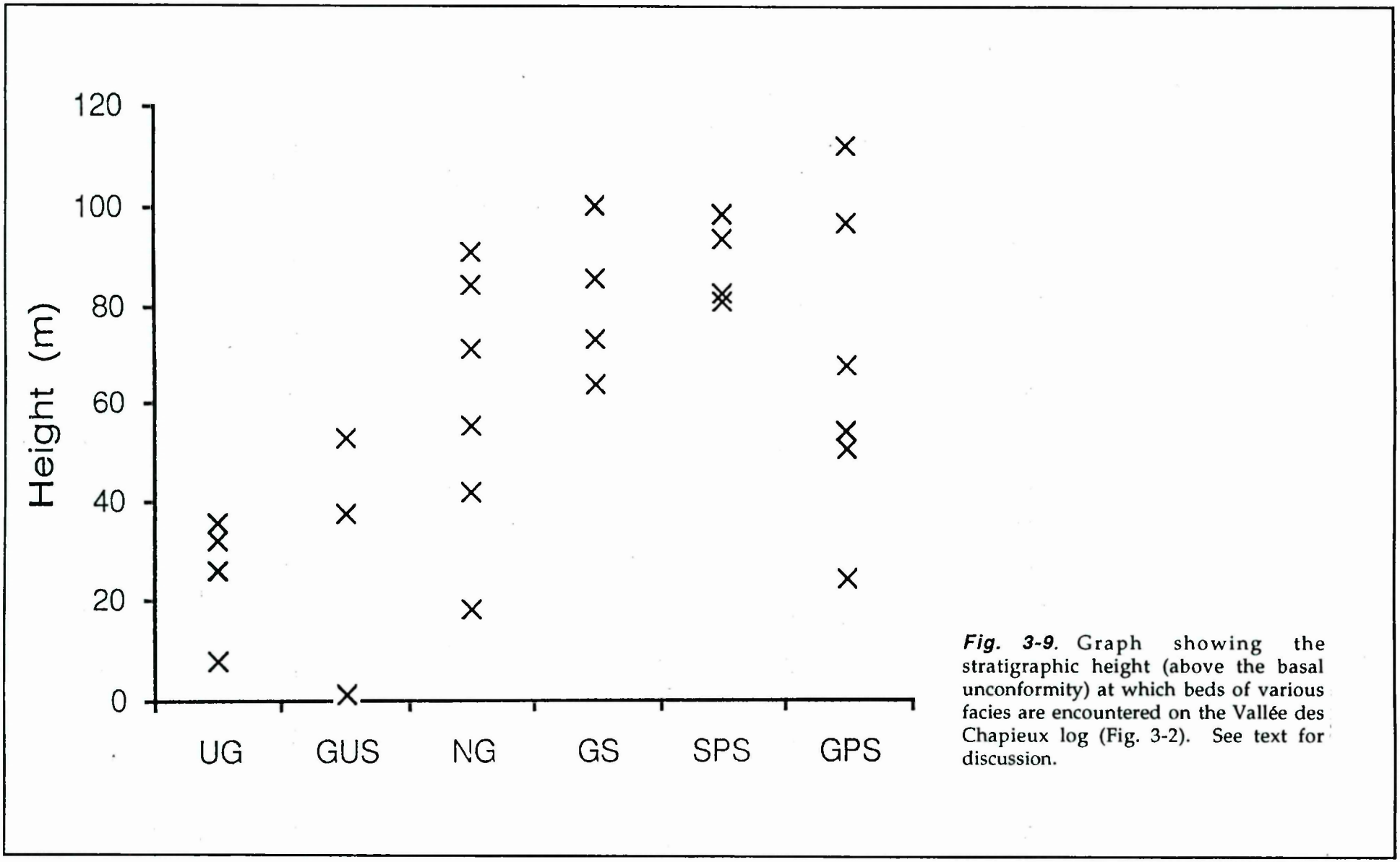

Fig. 3-9. Graph showing the stratigraphic height (above the basal unconformity) at which beds of various facies are encountered on the Vallée des Chapieux log (Fig. 3-2). See text for discussion.

3.1-2 Vertical Sequence

Logs through the coarser Aroley Formation (*e.g.* Fig. 3-2) display an erratic but conspicuous upward decrease both in bed thickness and in the proportion of coarse conglomerate beds (compare Fig. 3-8a from the base of the formation with Fig. 3-8b from near the top). Essentially the same pattern has been documented previously by Fudral (1973) and is implicit in stratigraphic columns drawn by Jeanbourquin & Burri (1991) from the NE extension of the Tarentaise Zone in Switzerland. It is important to emphasise that this upward fining and thinning trend appears to be a fundamental attribute of the Aroley Formation across the entire width of its outcrop. Superimposed on this general trend is a progressive shift in the dominant facies types (Fig. 3-9). Thus, the very coarse disorganised beds of facies UG and GUS are dominant through the lower part of the log, being superseded by facies GS and SPS at higher stratigraphic levels. Facies NG and GPS are present throughout the sequence. No beds of facies CD were intersected by the logs shown in Figs. 3-2 and 3-8 but elsewhere they are invariably restricted to the base of the formation.

3.1-3 Clast Types

The Aroley conglomerates are composed of a relatively restricted suite of clast types, of which dolomites and limestones are the dominant extrabasinal species. Quartz sandstones, schists, granites and rare mudrocks account for a significant subsidiary proportion. All of these clast types are closely comparable to the lithologies forming the floor or 'substratum' to the Tarentaise Basin (see Fig. 1-8b). Probable intrabasinal components include calcareous mudrocks and wackes which sometimes exhibit textures suggestive of deposition in a partially lithified state. All of these intra- and extra-basinal rock types occur as megaclasts but fine-grained extrabasinal limestones are the most common, accounting for 66% of clasts larger than 200mm in 14 sampled beds.

Figure 3-10 shows the compositional make-up of conglomerate beds from various stratigraphic levels on Figs. 3-2 and 3-8a. The survey demonstrates a lack of distinct systematic changes in source geology through the Aroley Formation, other than a slight upward increase in the relative proportion of non-carbonate lithoclasts. In general, compositional differences between adjacent beds are of comparable magnitude to the differences between the highest and lowest beds

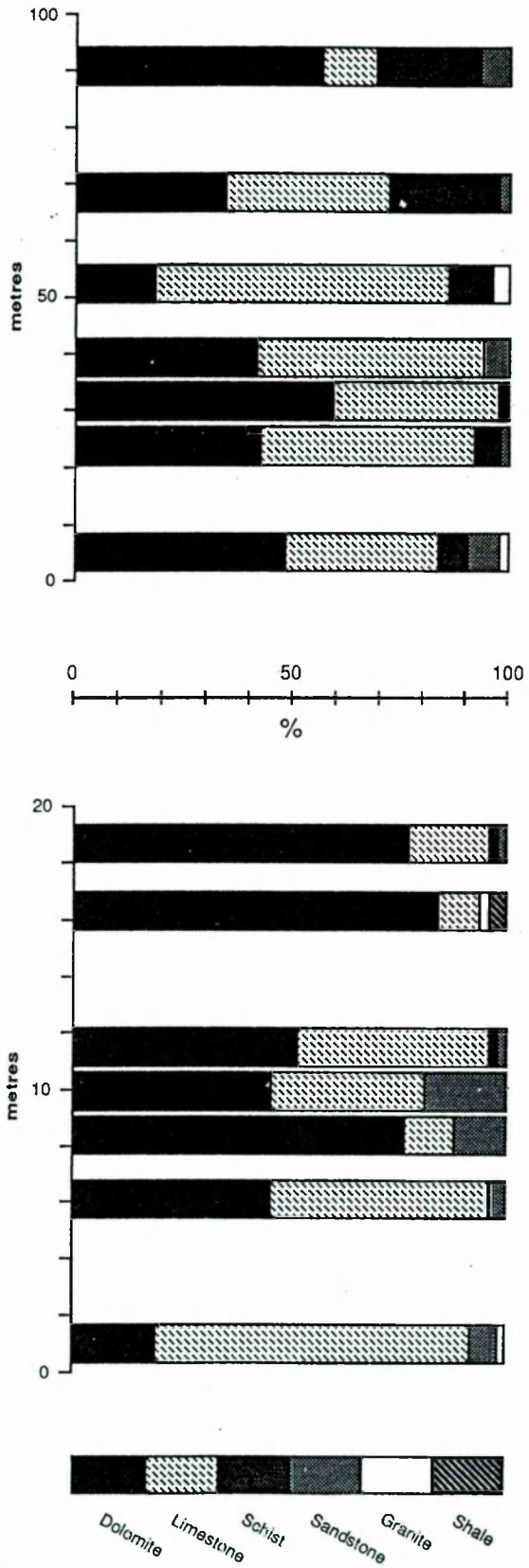

Fig. 3-10. Graphs to show the framework composition of conglomerate beds at different heights in the proximal Aroley Formation, based on systematic (gridded) samples of 60–120 clasts per bed. **a)** A survey covering most of the stratigraphic thickness of the Aroley Formation, Vallée des Chapieux (from the log shown in Fig. 3-2). **b)** The near-basal Aroley Formation, High Vallone di Chavannes (from the log shown in Fig. 3-8a).

sampled (Fig. 3-10). Notably, clasts of 'basement' lithologies (granites and micaschists) are present even in the stratigraphically lowest conglomeratic beds.

In shape, extrabasinal grains are typically of low to moderate sphericity and moderate roundness where tectonic strains are low, though shape varies somewhat with clast composition. Figure 3-11 summarises a semi-quantitative field survey of grain roundness among a sample of dolomite clasts. A preponderance of sub-rounded grains is indicated, with larger clasts being generally more rounded than smaller ones. Roundness analysis was restricted to dolomite clasts because they appear to have behaved most rigidly during Alpine deformation and are therefore likely to have experienced least tectonic modification of grain shape.

3.2 INTERPRETATION

3.2-1 Subaqueous or Subaerial Deposition?

The conglomerates of the Aroley Formation display a range of characteristics (discussed below) suggestive of gravity-driven mass-flow processes. A submarine palæoenvironmental setting is suggested by a few poorly preserved benthic foraminifera reported from various parts of the Aroley Formation by Trümpy (1951), Elter (1954) and Sodero (1968). Additionally, Antoine (1965, and pers. comm., 1992) reports a well preserved planktonic foraminifer from an argillaceous bed which he regards as the top of his 'Antéflysch' unit (Arguerey Formation of this paper) but which could be ascribed to the lower part of the western ('proximal') Aroley Formation on lithostratigraphic grounds. This sparse palæontological information is important because sedimentological evidence alone does not compel a wholesale submarine interpretation for the Aroley Formation. For example, similar transport-depositional processes are envisaged for both gravelly alluvial fans and submarine fan-deltas (*e.g.* Wescott & Ethridge, 1990). Subærial and subaqueous debris flows are thought to produce sediments which may be indistinguishable in many circumstances (Enos, 1977; Pickering *et al.*, 1989), hyperconcentrated stream flood-flow deposits may closely resemble coarse-grained high-density turbidites (Smith, 1986) and braided submarine channel-fills may strikingly resemble braided alluvial deposits (Hein & Walker, 1982). Diagnostic sedimentological criteria for discrimination between

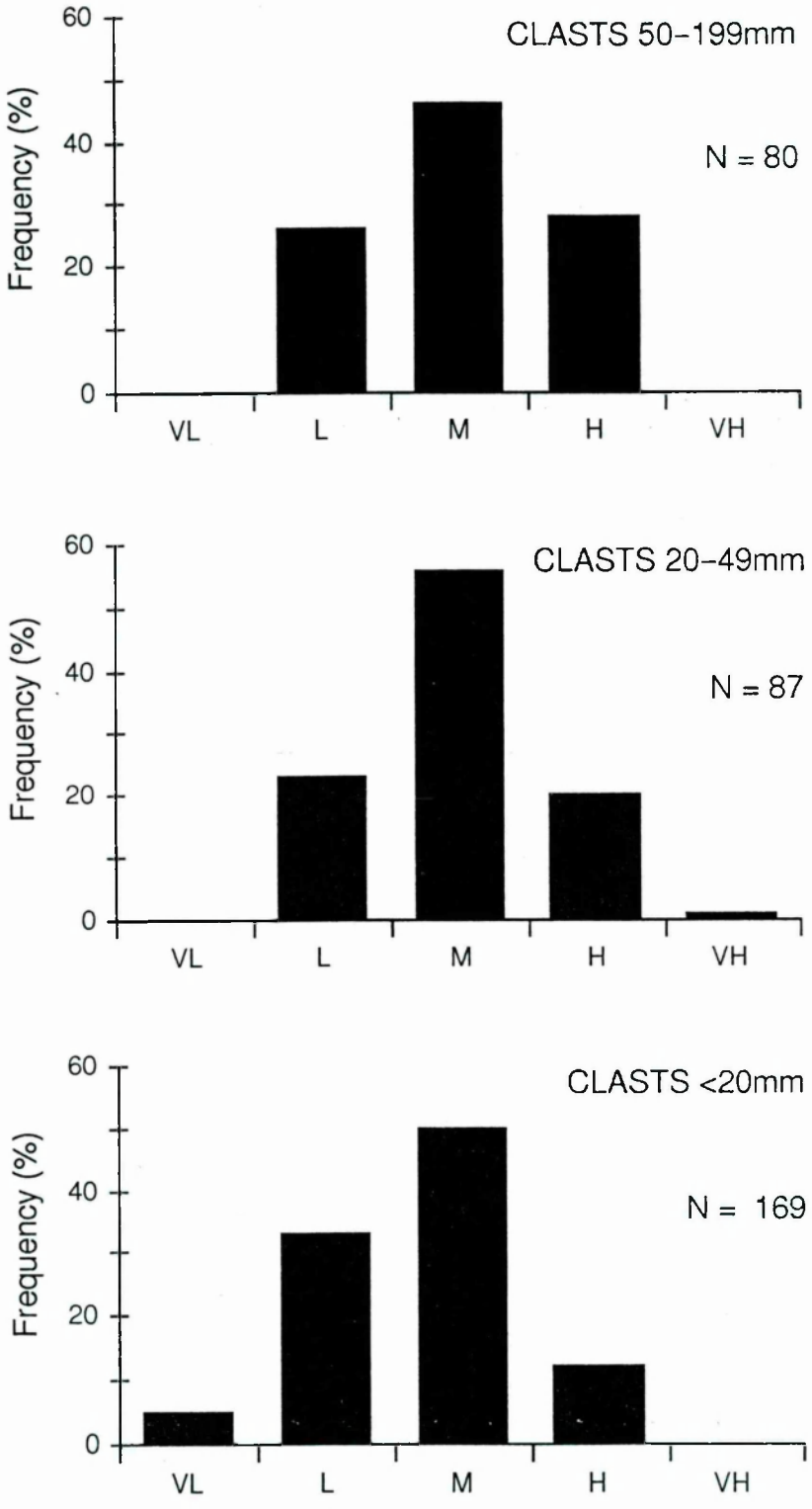

Fig. 3-11. Histograms of dolomite grain roundness sampled over different grain-size ranges in twelve conglomerate beds from the high Vallone di Chavannes and the Vallée des Chapieux. Roundness was assessed by visual comparison with a set of images based on the scheme devised by Powers (1953) but omitting his 'very angular' class (*i.e.* **VL** equates to 'angular,' **M** corresponds to 'sub-rounded' etc.). A modal shape of moderate roundness is indicated. See text for discussion.

the mass-flow deposits of subærial versus subaqueous environments are not yet well established and environmental interpretations must necessarily derive from the collective attributes of the entire sequence. This is not a trivial problem with respect to the Aroley conglomerates where the associated facies are finer-grained, more severely deformed and hence difficult to interpret. Nonetheless, evidence of subærial exposure (desiccation cracks, palæosols, æolian deposits, abundant hematite pigmentation) is entirely absent, preservation of fines is relatively high and the balance of facies (discussed below) is difficult to reconcile with a subærial setting. For example, the Aroley Formation contains very few beds which could be interpreted as the product of normal streamflow processes. Thus, no clear evidence exists to contradict the palæontological indication of marine deposition. Water depth however, remains unknown: it is assumed to be generally greater than storm wave base from the absence of any evidence of wave reworking of arenaceous facies.

3.2-2 Depositional Processes

The Aroley Formation conglomerates exhibit features suggestive of deposition from sediment gravity flows and the associated faunas may indicate that deposition took place in a relatively deep marine setting (see above). Understanding of the emplacement mechanisms of deep-water mass-flow conglomerates is severely handicapped by the understandable lack both of experimental work and of direct observations from modern analogues. Process interpretations are therefore based predominantly on theoretical reasoning applied to the features of ancient deposits (Walker, 1975; Nemec & Steel, 1984) and are inevitably somewhat conjectural. The principal depositional structures forming the basis for process interpretations in conglomerates are graded bedding, stratification and clast fabric (Walker, 1975). These features are discussed in turn below and basic process inferences for each of the seven conglomeratic facies are suggested (summarised in the right hand column of Table 3-1).

Graded bedding implies clast-size sorting in the transporting flow. Normal grading is regarded as a characteristic feature of deposits from fully turbulent sediment gravity flows, reflecting an inherent tendency for the coarsest grains to settle fastest through a turbulent suspension. In a fully turbulent flow, the action of turbulence tends to segregate finer clasts from larger ones (Middleton &

Southard, 1978). On deceleration, progressive loss of flow competence leads to sedimentation of sequentially smaller (*i.e.* less heavy) particles. Facies GUS, NG, GS and GPS all display normal grading profiles which are consistent with rapid suspension sedimentation from turbulent flows. In facies GUS and GS, the grading is coarse-tail (Middleton, 1967) which may indicate that settling occurred as a non-turbulent suspension. Distribution grading is more common in facies NG and GPS, suggesting that deposition of the finer grains may have been delayed by lingering turbulence (Lowe, 1982). The thin finer grained or inversely graded layer observed at the base of many of these normally graded units (*e.g.* Figs. 3-4 and 3-5) could represent a highly concentrated, non-turbulent 'carpet' driven along by high shear stresses at the base of the overriding turbulent suspension (Sanders, 1965; Lowe, 1982; Postma *et al.*, 1988); that is, a 'traction carpet' in the sense of Dzulynski & Sanders (1962) or 'inertia flow layer' (*sensu* Carter, 1975). Since the maintenance of a dense concentration of dispersed clasts requires a high applied shear stress, Walker (1975) has suggested that inverse grading may be related to steeper slopes and hence, in general, to more proximal environments. Poorly sorted, ungraded conglomerates may represent flows in which turbulence and grain interaction were inhibited by high shear strengths or high viscosities.

Stratification is another expression of clast-size segregation; most commonly developed in the finer, higher portions of conglomerate beds. Crudely planar, parallel, low-angle stratification defined by alternating pebblier and sandier bands is characteristic of facies GS, GPS and NG. This style of stratification is thought to reflect alternate deposition of bedload and suspended load (Walker, 1975; Hein, 1982). The boundaries between the layers involved are typically gradational, suggesting a fluctuating but continuous process rather than a sequence of discrete events (Walker, 1975). As pointed out by Lowe (1982), many sediment gravity flows may decelerate in an oscillatory rather than a continuous fashion. The velocity fluctuations in such surging flows might account for the repetitive graded divisions making up these stratified units.

In contrast to this gently inclined stratification, facies SPS exhibits well defined high-angle cross-bedding. Cross-bedding in mass-flow conglomerates is widely assumed to reflect slip-face accretion of large migrating dune-like bedforms akin to those seen to be developed in arenaceous sediments under more accessible circumstances (Hendry, 1972; Rocheleau & Lajoie, 1974; Sadler, 1982; Hein, 1982).

Since the foresets involved would have been inclined to the bed base at angles close to the angle of repose (allowing for compaction effects), these faces may have been surfaces of sediment emplacement by grain-flow avalanching. However, most examples of this facies in the Aroley Formation appear to comprise foresets which are normally graded, rather than inversely graded as would be expected for grain-flow deposits. It has been suggested (*e.g.* by Winn & Dott, 1977; Hein, 1982) that much cross-bedding in mass-flow gravels may be produced by tractional reworking of material previously emplaced by debris flow or modified debris flow processes.

Clast fabric studies have furnished a great deal of useful information about the processes responsible for ultimate grain deposition in conglomerates (e.g. Walker, 1975; Hein, 1982). Unfortunately, clast fabrics in the Aroley Formation are difficult to interpret in view of the ubiquitous tectonic modification: grain orientation distributions even in the least strained beds having undergone partial reorientation towards parallelism with local fold axes (Fig. 2-12).

Grading, stratification and preferred grain orientations all have in common an underlying implication of some degree of independent clast motion within the depositing gravity flow and hence are all features of relatively fluidal (cohesionless) flows: the deposits of more concentrated and more cohesive sediment gravity flows are presumably characterised mainly by the absence of such internal organisation. Facies CD lacks any indication of sedimentary organisation, which is suggestive of deposition from a flow in which freedom of clast motion was inhibited. The high matrix content could point to particle support primarily by the strength of the enclosing matrix and hence it seems reasonable to interpret beds of this facies in terms of deposition from cohesive debris flows. Facies UG also displays a lack of grading and stratification, which indicates that size sorting was suppressed within the depositing flow. Hence, fluid turbulence was probably not an important contributor to particle support. The low matrix content suggests that dispersive pressures arising from strong grain interaction could have been the dominant clast-support mechanism, although buoyant lift conferred by the interstitial matrix-water mixture may also have played a significant role. Facies UG therefore seems to represent sedimentation as a result of the 'freezing' of a non-cohesive debris flow (or 'density-modified grain flow' in the sense of Lowe, 1976). Poorly developed normal grading at the top of some UG beds may reflect interaction between the

debris flow top and an overlying water mass (Johnson, 1970; Hampton, 1975; Naylor, 1980). Flow dilution due to water ingress would diminish bulk viscosity and thereby allow the limited downward migration of larger clasts. In an extreme case, the incorporation of water could lead to the formation of an entrained layer of fully turbulent flow (Nemec *et al.*, 1984; Broster & Hicock, 1985), direct suspension sedimentation from which might produce an interval of well developed normal grading.

Thus, facies CD and UG seem to represent cohesive and cohesionless debris flows respectively. The features of facies GUS, NG, GS, SPS and GPS (and possibly various other Neanderthal utterances) are all consistent with deposition from high-concentration turbidity currents, according to a sequence involving freezing of a basal inertia-flow carpet followed by grain-by-grain suspension sedimentation and finally tractional bedload sedimentation (Lowe, 1982; Massari, 1984). Differences between the various facies are largely determined by the relative importance of each of these three phases.

3.2-3 Vertical Sequence Development

The recognition and analysis of asymmetric vertical trends on a range of scales has become an important contributor to the understanding of controls on sedimentation in deep-water successions (*e.g.* Ricci Lucchi, 1975; Shanmugam, 1980). The 100-200m thick thinning- and fining-upward *motif* evident through the Aroley Formation (Fig. 3-2) is a second-order sequence in these terms (see Ricci Lucchi, 1975) and its basin-wide extent argues for extrabasinal forcing of its development. Upward fining and thinning are indicative of decreasing availability of coarse sediment and decreasing magnitudes of depositional events with time. Ostensibly, it is possible to account for these trends in several ways, including: retreat of the entire depositional system in response to eustatic sea level rise coupled with drowning of the sediment source; overall subsidence of the basin and its hinterland; gradual peneplanation of the source area; major fault displacements at the flanks of the basin. However, the bed thickness and grain-size changes are accompanied by upwardly declining evidence for debris flow deposits (facies UG and CD) and well developed inertia-carpets (especially in facies GUS), and increasing importance of tractional sedimentation (*e.g.* cross-stratification in facies SPS). This shift in dominant depositional processes is strongly suggestive of decreasing dip of the depositional slopes over time. If the

initial basin margin relief was tectonically generated, as seems likely in view of the nature of the deposits, then successive sedimentation events would have served to decrease these slopes regardless of the influence of eustatic changes. Thus, it is possible to explain the observed vertical trends simply in terms of the response of sedimentary processes to an initial tectonic relief-forming episode, without having to appeal to other controls: hence, as aggradation and basin filling progressively reduced bottom slopes and overall relief, available potential energy diminished, leading to lower energy transport-deposition events. Simultaneously, subaerial denudation operated to subdue topography of the source area, resulting in decreased production of coarse grained detritus.

3.2-4 Sediment Derivation

The clast composition of the conglomerates (Fig. 3-10) indicates a source in the same pre-Cretaceous rock types which form the floor to the Tarentaise Basin (Fig. 1-8b). The bulk of the material appears to have been derived from Triassic and Liassic sedimentary units; clasts of granitic and schistose lithologies are entirely comparable with the pre-Triassic crystalline basement of the Tarentaise Zone. Grain shape characteristics are also consistent with derivation from a relatively local source. A sizeable number of field and experimental studies has indicated that transported clastic particles coarser than a few millimetres (*i.e.* pebble-sized or larger) are almost inevitably rounded (Sneed & Folk, 1958; Mills, 1979). Thus, angular to sub-rounded pebbles of a near-isotropic carbonate lithology are highly suggestive of extreme proximity to their source. In view of this, the predominantly sub-rounded to sub-angular Aroley Formation clasts (Fig. 3-11) are texturally relatively immature and are unlikely to have experienced an extended transport history prior to their redeposition via sediment gravity flows.

It is clear from the large-scale eastward fining (Fig. 2-48) that the main source of coarse sediment input during deposition of the Aroley Formation lay somewhere to the west of the basin. Most direct information concerning palæocurrent directions comes from high-angle cross-bedding in finer-grained conglomerates and associated litharenites. The dataset is small but adequate to define a low variance unimodal pattern of transport from WNW to ESE when tectonic rotations are removed (Table 3-2 and Fig. 3-12). Thus, the general eastward reduction in grain-size and bed thickness noted by Antoine (1971) and Lomas (in prep.) represents a pronounced proximal to distal facies variation. In contrast,

Locality	Grid Ref.	Altitude	Formation	Facies	Current Index	Crude Vector	Dip of Bed Base	Plunge of Minor Folds	Restored Vector
South-east of Cormet d'Arêches	31496 505353	~1760m	top Aroley	c litharenite	foreset	80/080	84/094 o/t	28/183	13/166
			top Aroley	c litharenite	foreset	80/260	84/094 o/t	28/183	12/102
			top Aroley	c litharenite	foreset	70/251	84/094 o/t	28/183	24/104
			top Aroley	litharenite	flute	40/160	84/084 o/t	28/183	14/196
			top Aroley	vc litharenite	trough XB	10/185	84/084 o/t	28/183	3/190
Ruisseau de Jerbois	31565 505533	~2380m	Marmontains	qz arenite	foreset	66/271	75/275	7/205	9/108
			Marmontains	qz arenite	foreset	67/279	75/275	7/205	9/062
	31582 505538	~2450m	Marmontians	vc qz arenite	foreset	60/117	41/123	8/206	20/112
			Marmontians	vc qz arenite	foreset	57/113	45/119	8/206	13/099
	31613 505578	~2585m	top Aroley	pebbly litharen	foreset	36/302	45/292	8/206	12/079
Vallée de Torrent des Glaciers (rive droite)	32312 506227	~1850m	Arguerey	f imp qz arenite	foreset	68/157	60/140	6/189	22/186
	32320 506180	~1820m	Aroley	pebbly litharen	?foreset	52/158	51/148 o/t	30/187	8/010 ?
			Aroley	pebbly litharen	?foreset	48/164	51/148 o/t	30/187	11/002 ?
	32467 506035	~1570m	Aroley	litharenite	foreset	70/120	53/133	14/201	16/118
			Aroley	litharenite	foreset	69/126	53/133	14/201	19/101
			Aroley	litharenite	foreset	64/120	53/133	14/201	14/091
Vallée de Torrent des Glaciers (rive gauche)	32491 506070	~1605m	Aroley	stratified cgl	foreset	60/115	42/123	18/192	18/108
			Aroley	pebbly litharen	scour axis	41/145	42/123	18/192	1/146 ?
	32495 506072	~1620m	high Aroley	thick GS cgl	foreset	63/127	36/143	16/195	27/095
			high Aroley	thick GS cgl	foreset	60/125	36/143	16/195	26/107
			high Aroley	thick GS cgl	foreset	67/114	36/143	16/195	38/100
			high Aroley	thick GS cgl	foreset	57/117	36/143	16/195	26/109
	32497 506073	~1635m	top Aroley	f litharenite	foreset	59/112	40/114	16/194	18/116
			top Aroley	f litharenite	foreset	63/112	40/114	16/194	23/117
High Vallone di Chavannes	33480 506975	~2680m	lower Aroley	pebbly litharen	foreset	9/100	4/345	12/227	12/110
			lower Aroley	pebbly litharen	scour axis	6/120	5/350	15/238	9/118
			lower Aroley	pebbly litharen	scour axis	19/144	3/355	14/225	22/143
C. Planavalle	57215 7277 (s)	~2270m	Aroley	vc litharenite	foreset	28/083	19/135	6/190	21/045

Table 3-2. Palæocurrent data from the Tarentaise Zone. Structurally restored data for the Aroley Formation are plotted in Fig. 3-12.

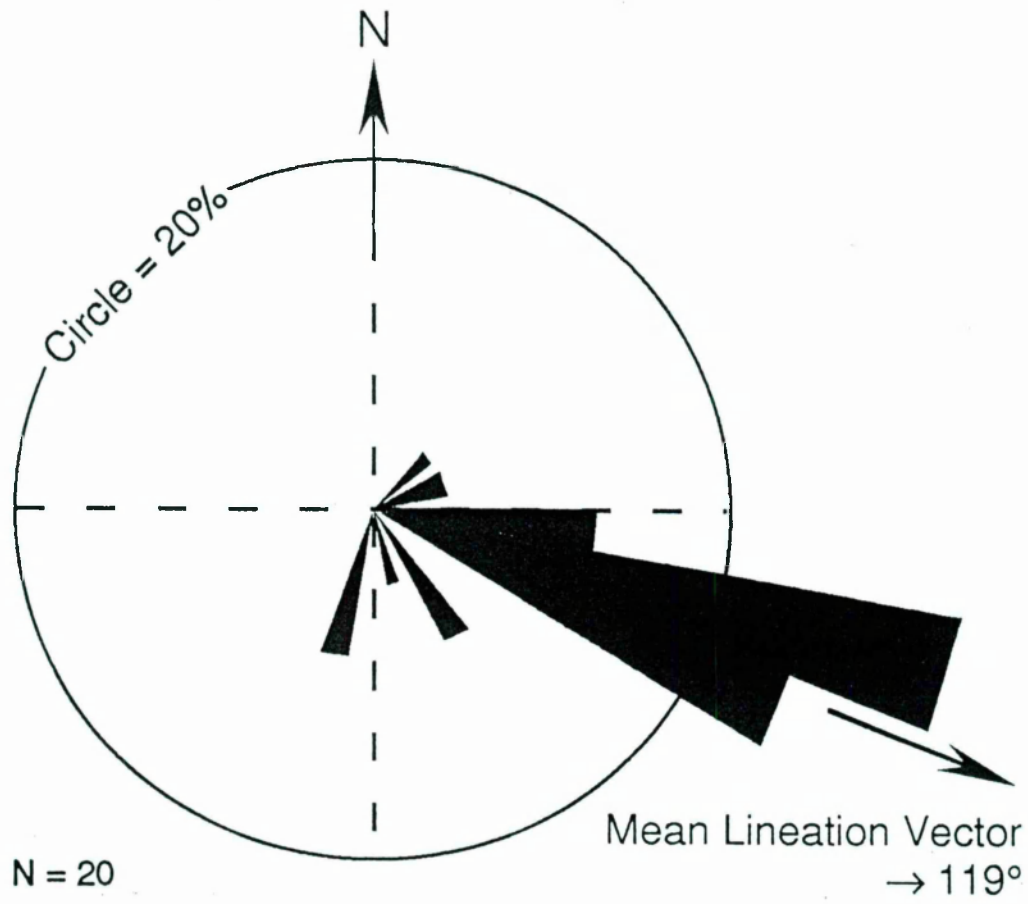

Fig. 3-12. Rose diagram of palæocurrent azimuths from the Aroley Formation, plotted as current–toward lineations corrected for structural dip and plunge. The raw data are tabulated in Table 3-2. This meagre diagram represents the full dataset of reliable palæocurrent indices found in Aroley Formation. Data from the more structurally complex parts of the Tarentaise Zone have been omitted because of the uncertainties involved in removing tectonic rotations.

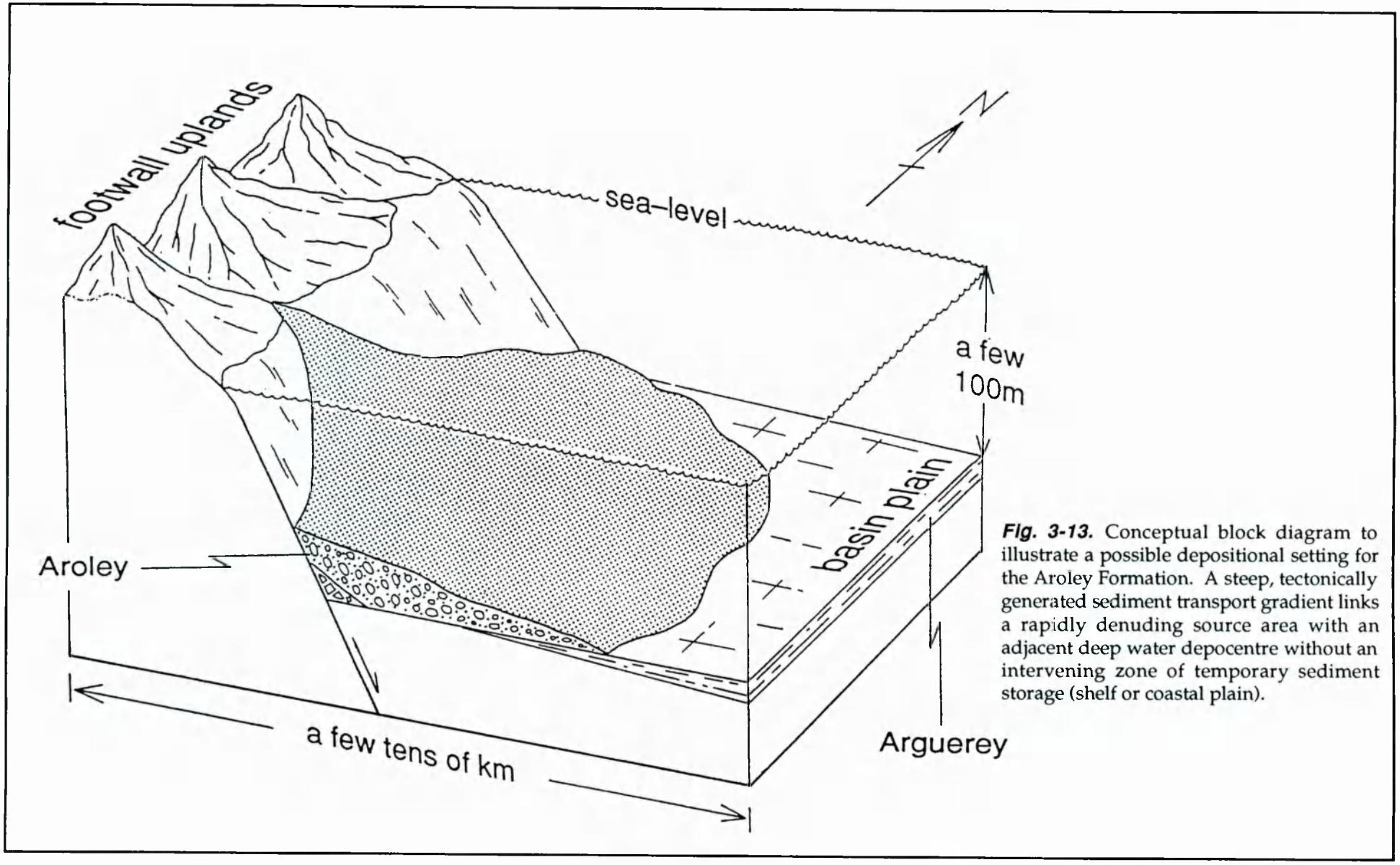

Fig. 3-13. Conceptual block diagram to illustrate a possible depositional setting for the Aroley Formation. A steep, tectonically generated sediment transport gradient links a rapidly denuding source area with an adjacent deep water depocentre without an intervening zone of temporary sediment storage (shelf or coastal plain).

Antoine (1971, 1972) deduced an overall sediment transport direction of SW to NE for the Aroley Formation. Although his conclusion was founded partly on the misinterpretation of tectonic grain-shape lineations as current-induced clast imbrication, this study broadly confirms his general contention that the Aroley Formation was sourced from the cratonward margin of the basin (*i.e.* from the west) rather than the oceanward margin (the east or south-east).

3.3 DISCUSSION OF DEPOSITIONAL SETTING

Tectonic disruption and outcrop limitations preclude any direct reconstruction of the configuration of the Aroley depositional system, but a number of well constrained inferences can be made. The very presence of large quantities of coarse-grained, first-cycle detritus of relatively unresistant lithologies (limestones, dolomites, micaschists *etc.*) is itself suggestive of proximity to a rapidly eroding area of high relief. The occurrence of basement clasts in the earliest beds suggests that the Aroley Formation does not record a progressive stratigraphic unroofing history and that the throw of the initial uplift event was comparable to the thickness of the substratal sedimentary pile veneering the crystalline basement. Palæocurrents and large-scale facies distributions indicate that this uplifted source area lay somewhere to the west of the basin. The relative textural immaturity of all the clastic components and the presence of metre sized megaclasts in many beds make it difficult to envisage a sediment transport path which traversed either a braidplain or broad shelf region. However, the presence of offshore marine faunas (Sodero, 1968) coupled with the absence of any evidence of wave-reworking of arenaceous facies, point to deposition below storm wave base. Thus it may be that alluvial systems conveyed detritus from the upland source area directly into relatively deep water (Fig. 3-13). Similar situations have been intuited for a number of ancient marine conglomerates (*e.g.* Surlyk, 1984; Porebski, 1984; Nemec, 1990; Higgs, 1990, but see Lewis *et al.*, 1991) and the scenario depicted in Figure 3-13 may reflect a relatively common palæoenvironmental arrangement in tectonically active settings. Vertical trends in grain-size, bed thickness and facies demonstrate that the development of the depositional system over time was controlled by declining availability both of coarse sediment and of depositional energy. These conditions can be explained by a variety of combinations of controls, but most easily by progressive depositional reduction of bathymetric slopes, assisted perhaps by decreasing

onshore relief as a result of erosion in the source region. One possible modern analogue for this type of sedimentary response can be found in Holocene fan-deltas building out from the sidewalls of fjords (*e.g.* Prior & Bornhold, 1990). Although in this case the steep marginal slopes are the product of rapid deglaciation rather than extensional faulting, and the scale of the depositional systems is significantly smaller than in the Tarentaise Basin, sedimentation processes are similar and gravitational driving forces may operate in a comparable manner. From detailed studies of the subaqueous morphology of Holocene fjord fan-deltas, Prior & Bornhold (1990) were able to demonstrate a progressive shift towards lower-energy resedimentation processes over a period of about 10 000 years. This appears to have been controlled primarily by the reduction of offshore relief as a result of fan growth.

Thus, a number of good exposures of little deformed rock have permitted detailed sedimentological inroads into an otherwise strongly tectonised basin-fill sequence. Several fundamental points have emerged, summarised below. This study demonstrates the feasibility of sedimentological investigation of highly deformed depositional systems. The relatively well constrained inferences outlined above will help to guide future interpretations in the more deformed parts of the Tarentaise Zone. The regional implications of these findings are discussed in chapter 5.

3.4 SUMMARY

1) The proximal Aroley Formation represents a high-energy depositional system constructed by sediment gravity flows of various types.
2) Sediment was derived from a source area comprising the same lithologies as those forming the floor to the Tarentaise Basin.
3) The range and relative proportions of clast types did not change significantly during the period of accumulation of the Aroley Formation. Clasts of (crystalline) basement lithologies are present throughout the sequence.
4) Sediment entered the basin from its western (cratonward) margin.
5) Textural and grain-size properties testify to a very limited transport history, indicating proximality to a region of coarse sediment production.

6) Availability of coarse sediment diminished with time during the deposition of the Aroley Formation.

7) Up-sequence changes in the dominant facies types imply a tendency towards lower energy depositional events with time.

CHAPTER 4 MAGMATISM

The Alpine mountain belt formed as a result of collision between the continental masses of Europe and Africa-Apulia, facilitated by subduction of the intervening Piémont–Ligurian ocean. Dismembered remnants of this oceanic domain are preserved as major ophiolitic masses within the Piémont nappes of the internal Alps. Smaller ophiolite-like lithostratigraphic assemblages occur elsewhere in the Alps, outside the Piémont Zone, but the palæotectonic significance of these 'ophiolitoids' is unresolved: do they represent small marginal oceanic basins, are they far-travelled Piémont-derived thrust-sheets, or were they formed by intracontinental magmatism? This contribution addresses the problem from an analysis of the stratigraphy and geochemistry of the Versoyen 'ophiolitoid' which occurs on the internal margin of the Tarentaise Zone.

The term 'zone du Versoyen' was coined by Elter & Elter (1957) to distinguish a supposedly 'ophiolitic' assemblage of metabasites, pelites and serpentinites cropping out astride the Franco-Italian border in the upper parts of the Breuil and Versoyen valleys. It equates essentially to the Miravidi thrust sheet discussed in section 2.3 (Fig. 4-1). The Versoyen complex figures significantly in large scale palæogeographic reconstructions of the Western Alps (*e.g.* Trümpy, 1975; Coward & Dietrich, 1989) but its palæotectonic significance has never been satisfactorily elucidated. Field studies by Elter (1954), Loubat (1968, 1975) and Antoine (1971) have furnished a general lithostratigraphic picture of the Versoyen complex. Loubat (1968), Antoine *et al.* (1973) and Loubat & Delaloye (1984) have described the petrography and major element geochemistry of the metabasites. Two important questions remain unresolved by these essentially descriptive studies. First, what are the structural affinities of the Versoyen complex? Does it represent part of the Tarentaise Basin or a palæogeographically unrelated far-travelled thrust sheet? Second, what are the origins of the basaltic magmas? Are they related to oceanic spreading, arc volcanism or continental rifting? The pilot study elaborated in this chapter attempts to address both of these problems: the first using structural and stratigraphic relationships and the second using trace element geochemistry.

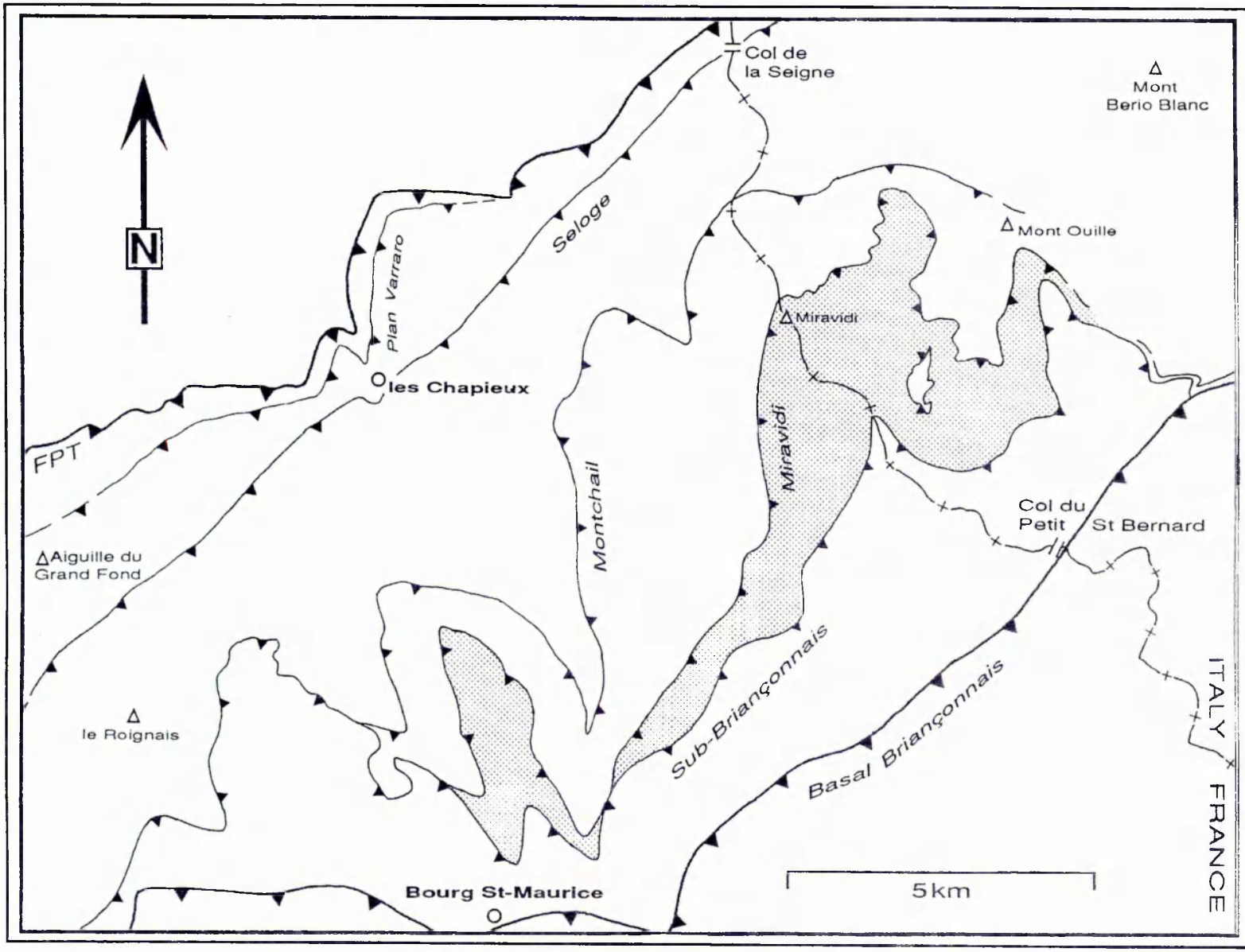

Fig. 4-1. Thrust sheet map of the central Tarentaise Zone showing the outcrop of the Versoyen complex (Miravidi thrust sheet).

4.1 STRATIGRAPHIC SETTING

The stratigraphy of the Versoyen complex contrasts markedly with that of the adjacent zones, consisting essentially of pelites, metabasites, granitic schists and serpentinites. These lithologies have been previously described by Elter (1954), Loubat (1968) and Antoine (1971).

4.1-1 Description of the Lithologies

Pelites in the Versoyen complex are fissile, dark grey rocks comprising quartz + white mica + chlorite ± epidote ± sphene ± rutile (Fig. 4-2a). They are commonly albite-bearing ('adinoles' in the French literature) in the proximity of metabasite bodies and locally graphitic (Fig. 4-2b). A strong penetrative foliation is common with a crenulation cleavage developed locally.

Metabasites (Fig. 4-2c) account for the bulk of the exposed Versoyen complex. They are unpleasant green rocks which are mostly fine- to medium-grained. Minor calcite veining is a ubiquitous feature. Antoine (1971) and Loubat (1975) report vaguely pillow-like structures from several localities. The mineralogy and geochemistry of these nasty green rocks are described further in section 4.3.

Leucogranitic schists crop out in the Breuil valley as one large unit (Punta Rossa, see Fig. 2-19) about 130m thick, and a number of detached smaller bodies. Mineralogically, these granitic rocks ('leptynites' of the French literature) comprise quartz, orthoclase, microcline, albite and muscovite ± chlorite (Fig. 4-2d). A strong undulose schistosity is generally visible.

Serpentinites occur in minor volumes associated with the granitic schists. Typical mineralogies involve ≥80% serpentine, 5-10% iron oxides, and accessory rutile, chlorite, epidote and ?brucite. Rare ghosts or pseudomorphs after (mostly ortho-) pyroxene are discernible in some specimens (Fig. 4-2e). Abundant veins of coarse sparry calcite are common and small talc-magnetite deposits are present locally (*e.g.* at 33333 506264).

4.1-2 Description of the Field Relations

Margins of the granitic schists. In several places (33353 506267, 33379 506289 and especially clearly at 33287 506430) a conglomeratic horizon overlies a highly irregular, fractured top to the schists. These conglomerates (Fig. 4-3) are generally

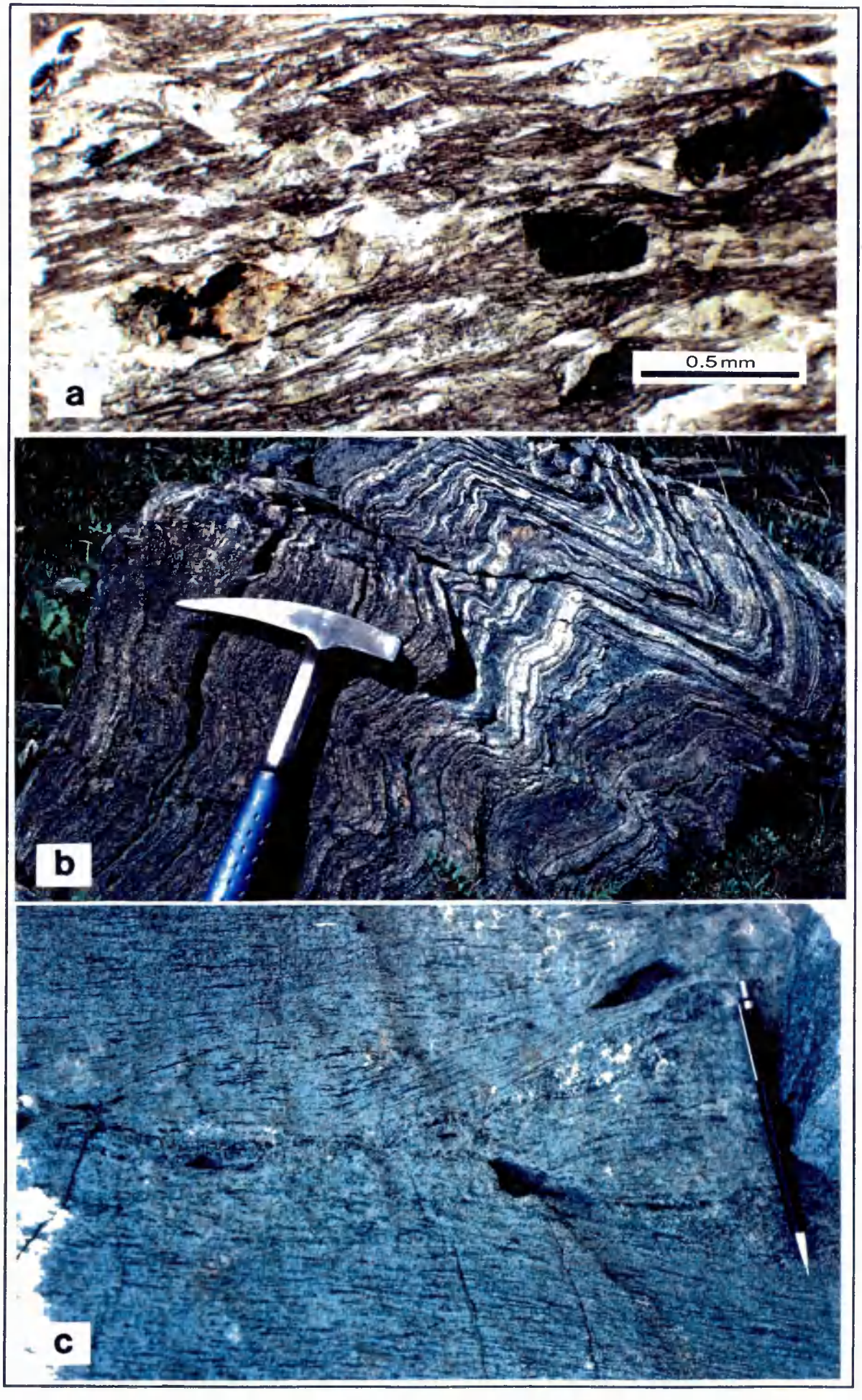
0.5 mm
a
b
c

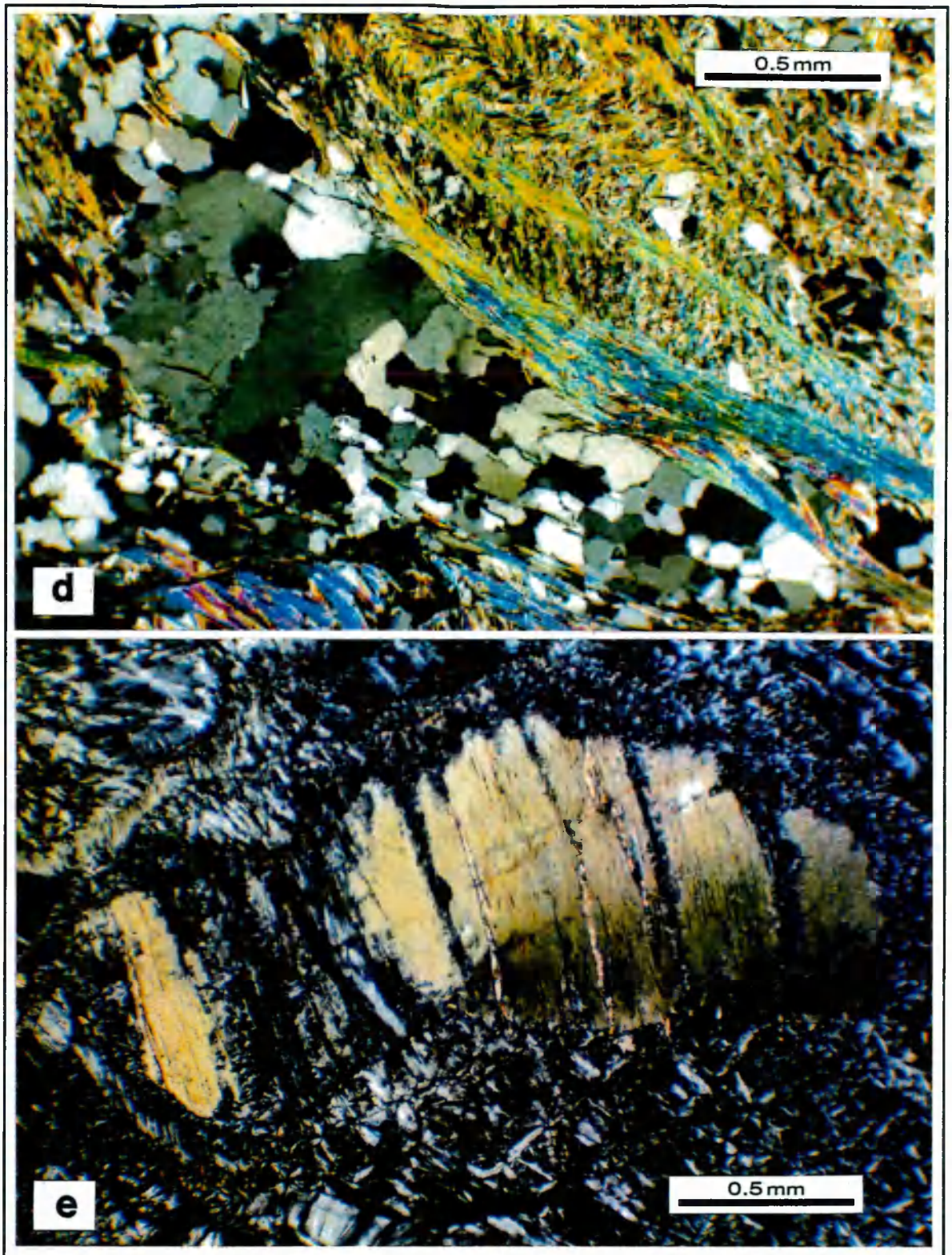

Fig. 4-2. Lithologies of the Versoyen complex (see appendix 1 for specimen details).
a) Photomicrograph of sphene-bearing chloritic pelite (sample FB SH 1), unpolarised light, foliation dips 26→107, left-hand-side=east, right=west. **b**) Folded graphitic pelite (alternating quartzose and graphitic layers), not *in situ* (sample FC 5). **c**) Sheared coarse-grained metabasite from 33308 506330, 400m west of Punta Rossa. The dark green blobs are clots of actinolite + chlorite (±biotite). **d**) Photomicrograph of quartz–muscovite domain in quartz–feldspar–muscovite basement schist, crossed polars. Main foliation dips 45→078, left-hand-side=WSW, right=ENE (sample FB LEPT 1). **e**) Relict (altered) orthopyroxene crystal in serpentinite (sample FC LC 2), crossed polars.

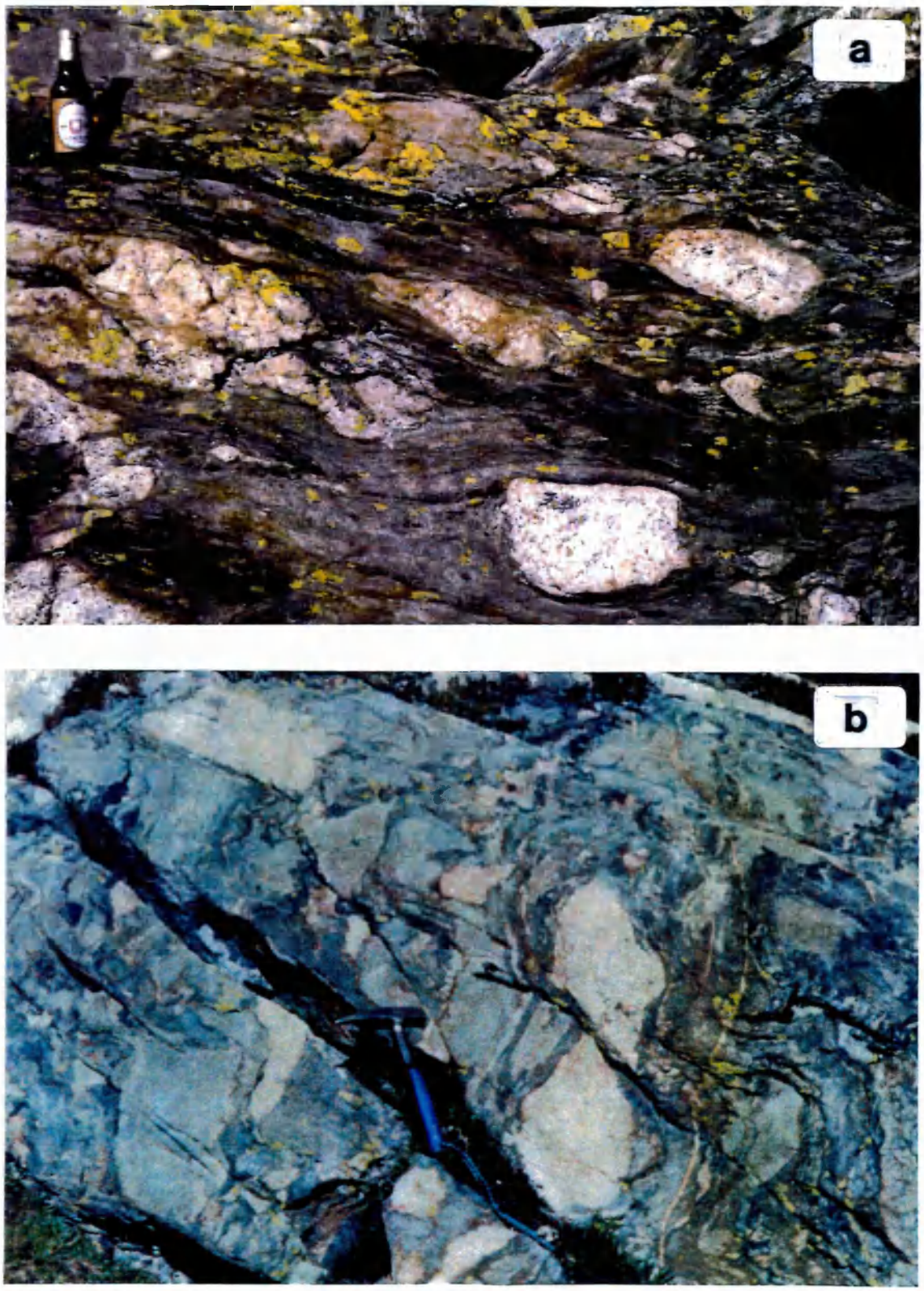

Fig. 4-3. Field photographs of the conglomerates directly overlying the pelite-leucogranite unconformity south of Punta Rossa. **a**) Monomict matrix-supported example from 33377 506285. View looking north at an east-west face, the scale is 18.4cm high. Note that the granitic clasts are unfoliated. **b**) Coarser, polymict rudite from 33354 506267 comprising clasts of leucogranite and quartz-bearing chloritic pelite. View looking east down onto a gently inclined exposure surface.

monomict, being composed entirely of granitic material, but locally also contain clasts of greenish (chloritic) pelite (Fig. 4-3b). The base of the main granitic sheet (Punta Rossa) is an abrupt contact onto pelites (sometimes with intervening serpentinites) marked by a zone of intensified strain.

Serpentinite bodies. The serpentinites are intimately associated with the leucogranitic schists, although Loubat (1968) reports a single stray serpentinite blob apparently isolated within metabasites on a virtually inaccessible spur of the Miravidi massif (~3304 50647?). Contacts with the granitic schists are irregular but sharp (with no evidence of remelting) and often involve thin veins or apophyses of serpentinite invading the granitic host.

Metabasite–pelite contacts. For the most part, metabasaltic bodies occur as sheets 5–50m thick, concordantly interlayered with the pelites (Figs. 4-4 and 4-5). Contacts are variable but often sharp. Adjacent pelites are sometimes bleached for a few centimetres or decimetres away from the contact (Fig. 4-5). In some instances the metabasite margins are marked by intense fracturing and brecciation (Figs. 4-5 and 4-6). On the eastern side of the Comba di Planaval (between 5727 703 and 5735 725) metabasaltic layers are apparently concordant with bedding in the Aroley formation (Fig. 4-7), although reconnaissance mapping in the area failed to discover any exposures of the actual contacts.

4.1-3 Stratigraphic Interpretation

As noted above, the principal lithologies encountered in the Versoyen thrust sheet are pelites, metabasites, granitic schists and serpentinites. Complexities introduced by Alpine deformation mean that the relationships between these stratigraphic elements are often difficult to deduce. It is clear however, that the pelites unconformably overlie the granitic schists and that many of the metabasaltic bodies have intrusive boundaries with the pelites.

Granitic schists form the basement to the Versoyen complex. Since leucogranitic clasts in the overlying rudites (*e.g.* Fig. 4-3) are commonly unfoliated, it is evident that the schistosity is an Alpine one. The schists may represent Hercynian intrusives or possibly rhyolitic tuffs (Antoine, 1971). The schist–pelite contact is demonstrably a sedimentary unconformity where it is veneered by regolith-like breccias and locally derived conglomerates: a cataclastic origin is unlikely in view of the lack of striated and internally fractured grains or other evidence for brittle fragmentation and milling under high confining stresses.

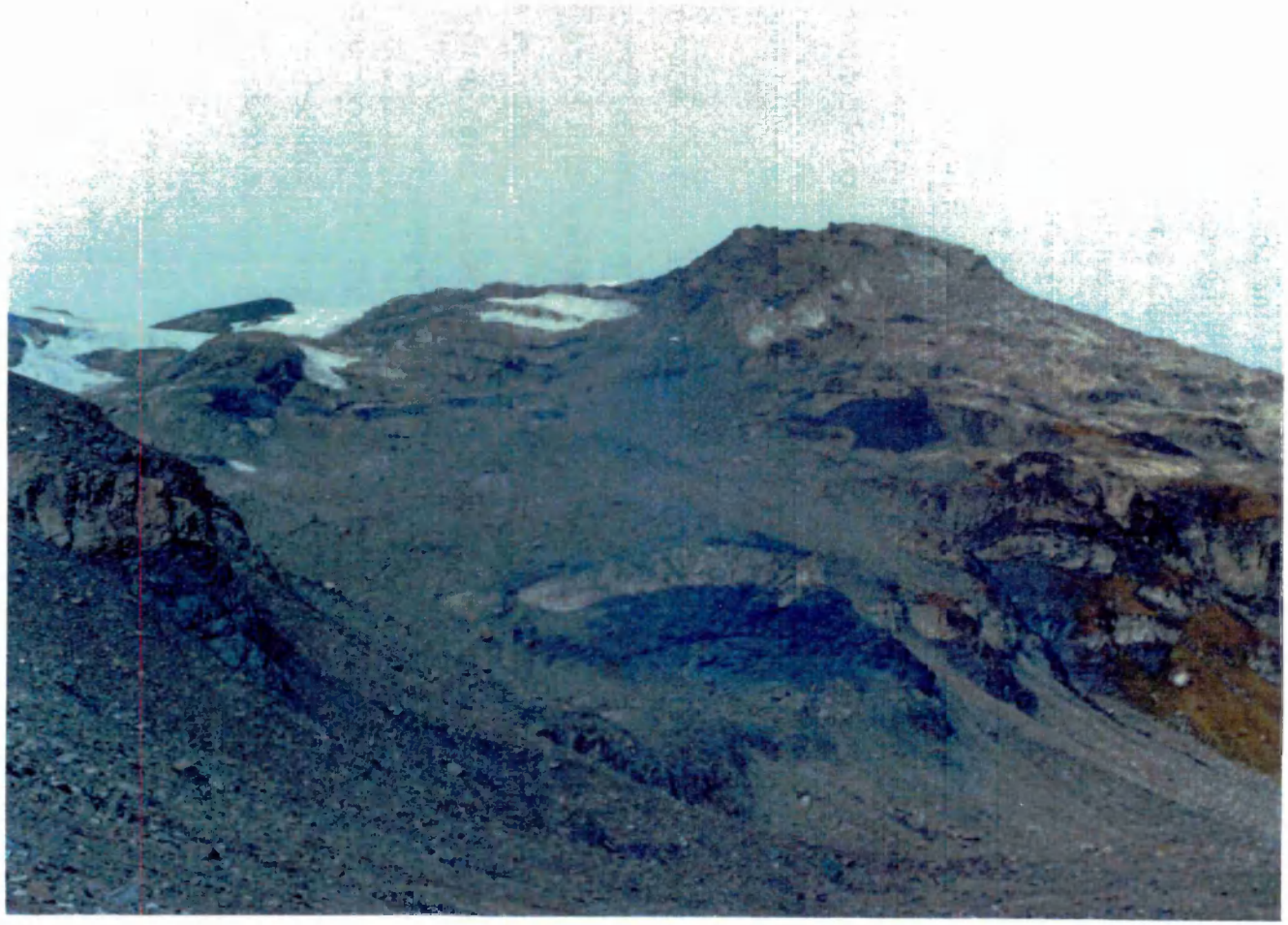

Fig. 4-4. Photograph looking north-west towards Punta dei Ghiacciai (33123 506475) showing metabasite sheets (pale colour) enclosed in dark grey pelites. Total visible vertical relief is approximately 600m.

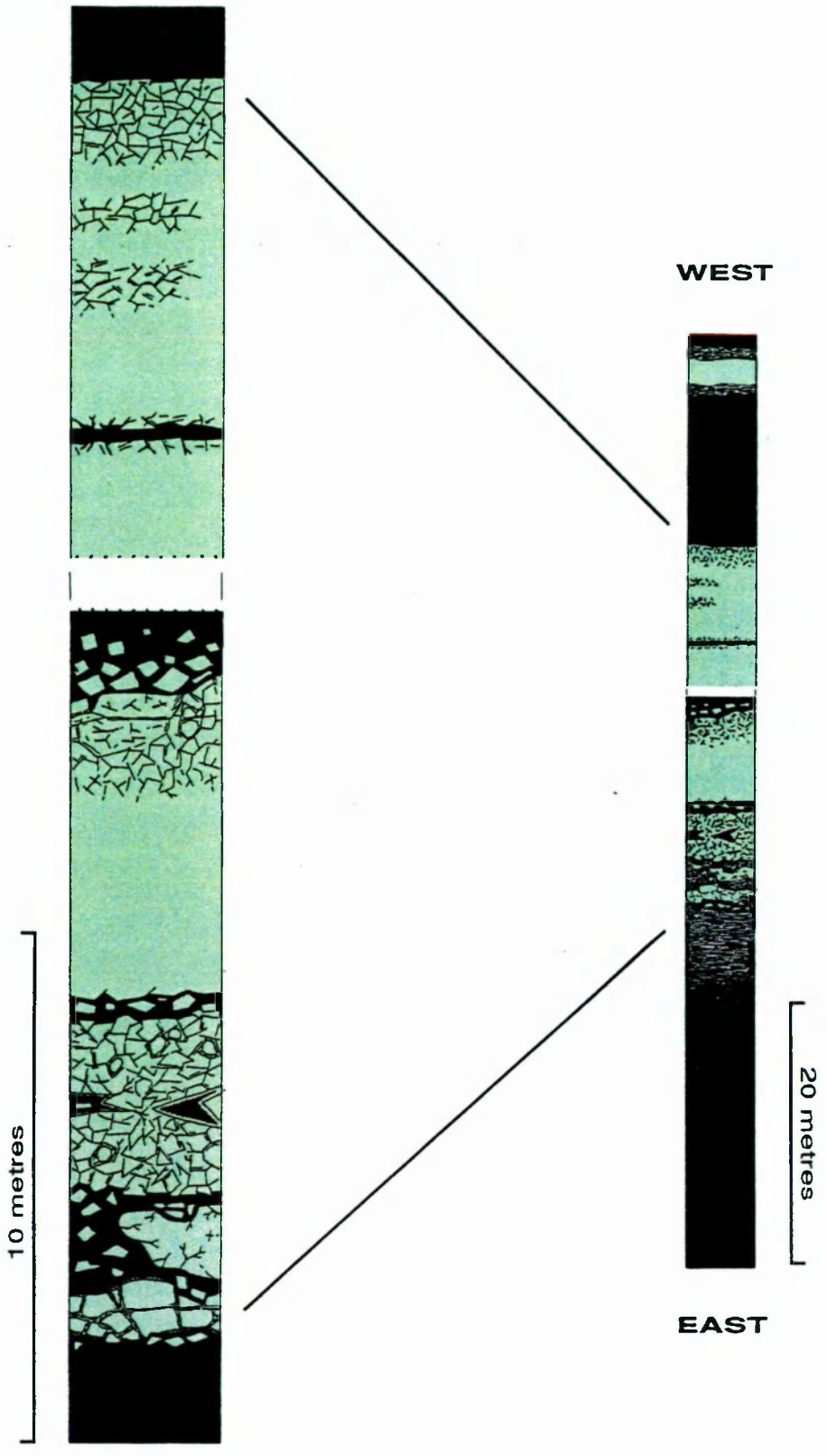

Fig. 4-5. Log through near-continuous subhorizontal exposure of tilted pelites and medium-grained metabasites around 3330 50634, north-west of Punta Rossa.

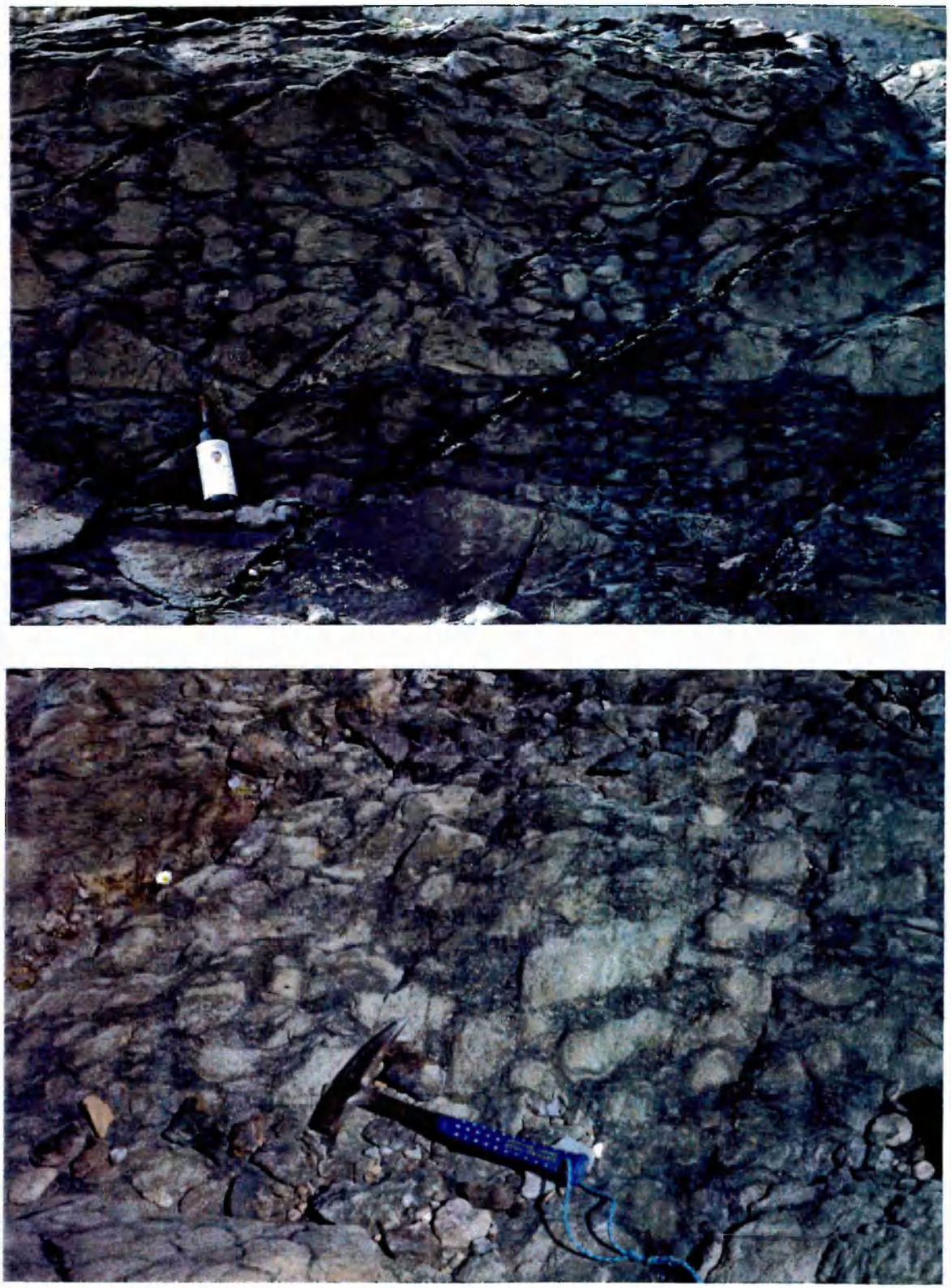

Fig. 4-6. Fragmentation of medium-grained metabasites at the margins of sill-like bodies WNW of Punta Rossa (33302 506338). *Lower*: fractured metabasite in which mixing did not occur between metabasaltic material and host pelites (*i.e.* all the fine-grained material between the blocks is also of metabasaltic composition). The hammer is 35cm long. *Upper*: fracturing associated with partial ingress of pelitic material between metabasite blocks. The scale is 29.3cm high and forms an excellent accompaniment to many pasta and tomato dishes.

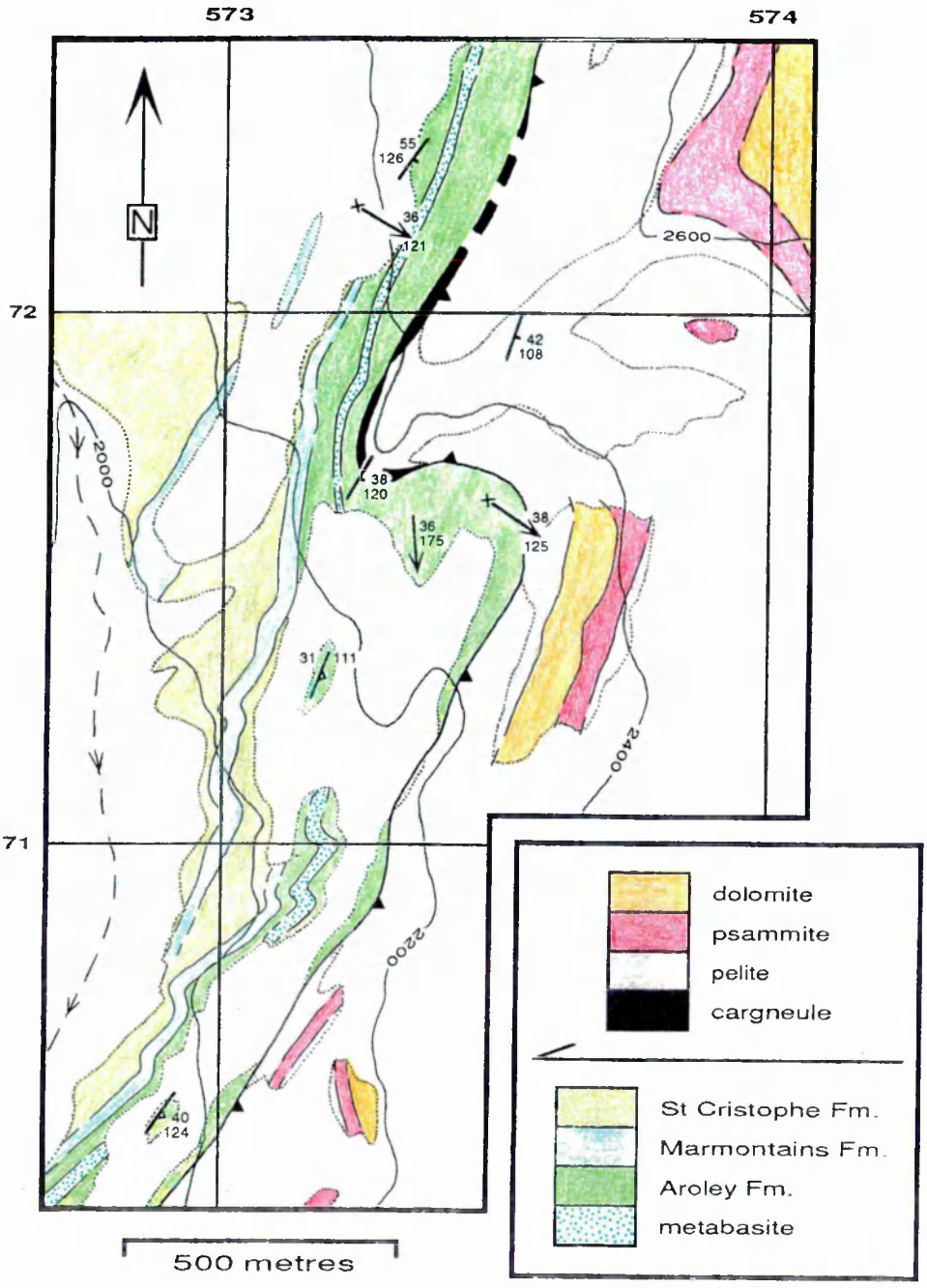

Fig. 4-7. Sketch map of field relations in the eastern Comba di Planaval showing the apparent concordance of a metabasic body with bedding in the enclosing Aroley Formation.

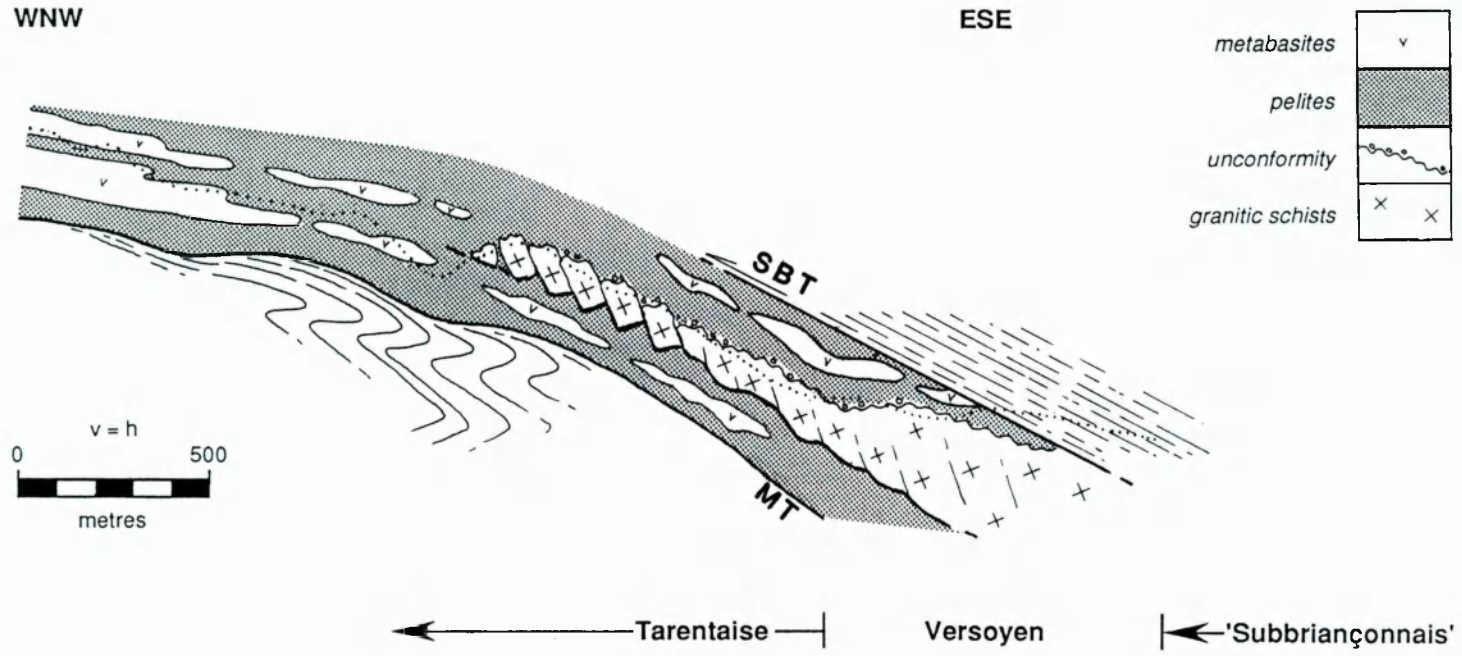

Fig. 4-8. Simplified interpretive cross-section through the Versoyen complex (Miravidi thrust sheet) in the high Breuil valley. Dotted line indicates present erosion level. *MT* = Miravidi Thrust, *SBT* = Sub-Briançonnais Thrust. See Fig. 2-16 for basic structural data and location of section line.

Serpentinites, occurring essentially as part of the basement unit, exhibit sharp, unmelted, invasive contacts with the granitic schists, indicating that they were not emplaced as hot ultramafic intrusives. The serpentinites were presumably squeezed tectonically into fractures within the granitic schists as the most incompetent participant in the Alpine deformation. The absence of residual clinopyroxene may indicate that the primary ultramafic lithology was dunitic (>90% olivine) or harzburgitic (olivine + orthopyroxene) rather than lherzolitic (olivine + clinopyroxene + orthopyroxene), since clinopyroxenes are usually relatively resistant to serpentinisation (Wicks & Whittaker, 1977). This would be atypical relative to the other ultramafic complexes of the Alps, which are predominantly lherzolitic (Nicolas & Jackson, 1972). The crucial question is whether the Versoyen serpentinites are of essentially the same age as the associated granitic rocks (*i.e.* 'basement') or whether they are genetically related to the Versoyen metabasites (*i.e.* part of an 'ophiolite' complex).

Metabasites exhibit a variety of different contacts with the enclosing pelites. The fractured and brecciated margins shown in Fig. 4-6 are suggestive of quench fragmentation processes during intrusion: the sudden juxtaposition of hot magma and cold water or water saturated sediment leading to rapid heat loss from the magma at the interface. Thus, tensile thermal stresses are set up due to the chilling and contraction of the magma, resulting in shattering or fragmentation as a means of pressure release (*e.g.* Cas & Wright 1987). Allied processes may include local explosive brecciation due to boiling of trapped pore waters, and fluidisation of the sediment (Kokelaar, 1982). The metabasite-pelite contact relationships thus indicate that the Versoyen pelites were wet and unconsolidated at the time of intrusion. Moreover, the presence of mixed, brecciated contacts at the base and top of metabasite bodies (Fig. 4-5) indicate that the basalts were emplaced into, rather than extruded onto, the pelites.

Field relations in Comba di Planaval (Fig. 4-7), where metabasites occur enclosed within Aroley Formation litharenites rather than pelites, are potentially critical. Regrettably, exposures of the actual contacts are lacking.

4.2 STRUCTURAL SETTING

The structure of the high Breuil valley has already been described in chapter 2. Figure 4-8 is a summary cross-section through the area which shows the Versoyen

	sample	t-sect nº	grain-size	outcrop	grid ref	locality	characteristics
1	*FB PR 1*	54604	medium	thick sill?	33297 506332	400m WNW of Punta Rossa	*rich in opaques*
2	*FB PR 2*	54601	medium/coarse	thick sill?	33306 506318	450m WSW of Punta Rossa	*has minor biotite*
3	*FB PR 3*	54606	coarse	blob	33308 506325	400m west of Punta Rossa	*~7% zoisite*
4	*– EAE3*	–	coarse	blob	33308 506325	400m west of Punta Rossa	–
5	*FB PR 5*	55294c	medium	sill	33401 506242	1km SE of Punta Rossa	*~70% fine brown groundmass*
6	*FB PR 6*		medium	sill	33407 506243	1km SE of Punta Rossa	*some calcite veining*
7	*– NEL6*	–	medium	sill	33407 506242	1km SE of Punta Rossa	–
8	*FB PR 7*	54605	medium	sill	33410 506245	1km SE of Punta Rossa	*most 'typical' specimen*
9	*FB PR 8*	55295c	fine	sill	33352 506228	1km south of Punta Rossa	*≥70% fine brown groundmass*
10	*– ESR 8*	–	fine	sill	33352 506228	1km south of Punta Rossa	–
11	*FB PR 9*		fine	sill	33395 506255	600m SE of Punta Rossa	*minor calcite veinlets*
12	*FB PR 10*		fine	sill	33361 506272	600m SE of Punta Rossa	*has post-cleavage pyrite*
13	*FB PR 11*		fine	sill	33357 506257	800m SSE of Punta Rossa	*similar to FB PR 9*
14	*– WLB 11*	–	fine	sill	33357 506257	800m SSE of Punta Rossa	–
15	*FB PR 13*	54602	fine	?sill / flow?	57326 7183	Comba di Planaval	*very few opaques*
16	*FB PR 14*		fine	?sill / flow?	57329 7196	Comba di Planaval	*has post-cleavage pyrite*
17	*– WR 14*	–	fine	?sill / flow?	57329 7196	Comba di Planaval	–
18	*FB PR 15*	fb pr 15	fine/medium	?sill / flow?	57320 7169	Comba di Planaval	*some calcite veinlets*
19	*FC LC+6*	54600	medium/coarse	sill/blob	3343 50627	1km ESE of Punta Rossa	*chlorite+actinolite–rich, albite–poor*
20	*– PSP 26*	–	medium/coarse	sill/blob	3343 50627	1km ESE of Punta Rossa	–

Table 4-1. Details of the metabasite sample set analysed in this study. Samples FB PR 5–7 are from different parts of the same sill and samples FB PR 13–15 appear to be from different exposures of the same sheet. A specimen number preceded by '–' is a control (*i.e.* an additional sample collected from the same exposure as that preceding it in the table, but crushed and analysed separately).

complex as a distinct tectonostratigraphic package delimited by the Sub-Briançonnais Thrust above and Miravidi Thrust below. As its boundaries everywhere appear to be tectonic ones, it is difficult to judge whether or not the Versoyen complex has palæogeographic affinities with the Tarentaise Zone. However, the simplest explanation is that the structure depicted in Fig. 4-8 represents the telescoped remnants of three originally contiguous palæogeographic belts. In this respect, the field relations along strike in the Comba di Planaval (Fig. 4-7) are crucial, since they strongly suggest that the Versoyen magmatism involved the Tarentaise Zone stratigraphy.

4.3 METABASITE COMPOSITION

The Versoyen metabasites have been described in detail by Loubat (1968) from a petrographic stand-point and by Antoine *et al.* (1973) and Loubat & Delaloye (1984) in terms of major element chemistry. The appraisal of metabasite composition presented below is intended to summarise and reaffirm, rather than duplicate, these previous studies. The principal objective of this contribution is to demonstrate how trace element geochemistry may help to further constrain the petrogenetic possibilities. This investigation is based primarily on a study of a small sample comprising fourteen metabasites: three from medium- to coarse-grained bodies (FB PR 1–3), eight from medium- to fine-grained sheets interpreted as sills (FB PR 5–11 plus FC LC 6) and three from fine-grained metabasites of unclear field relations from the Comba di Planaval (FB PR 13–15). Samples FB PR 5–7 are from different parts of the same metabasite body (inferred sill). Excruciatingly tedious specimen details are listed in Table 4-1 and repeated as part of Appendix 1.

4.3-1 Modal Composition

Loubat (1968) has reviewed the petrography of various Versoyen lithologies in considerable detail and his descriptions are not challenged by this study. All of the metabasaltic samples analysed in this study display assemblages dominated by albite + chlorite + green amphibole + zoisite + quartz. Calcite is present both as isolated grains and ubiquitous fine (up to ~2mm wide) veinlets. Epidote, biotite, rutile, sphene and opaques (mostly ilmenite?) are common minor constituents. Apart from the rather high abundance of zoisite in some samples,

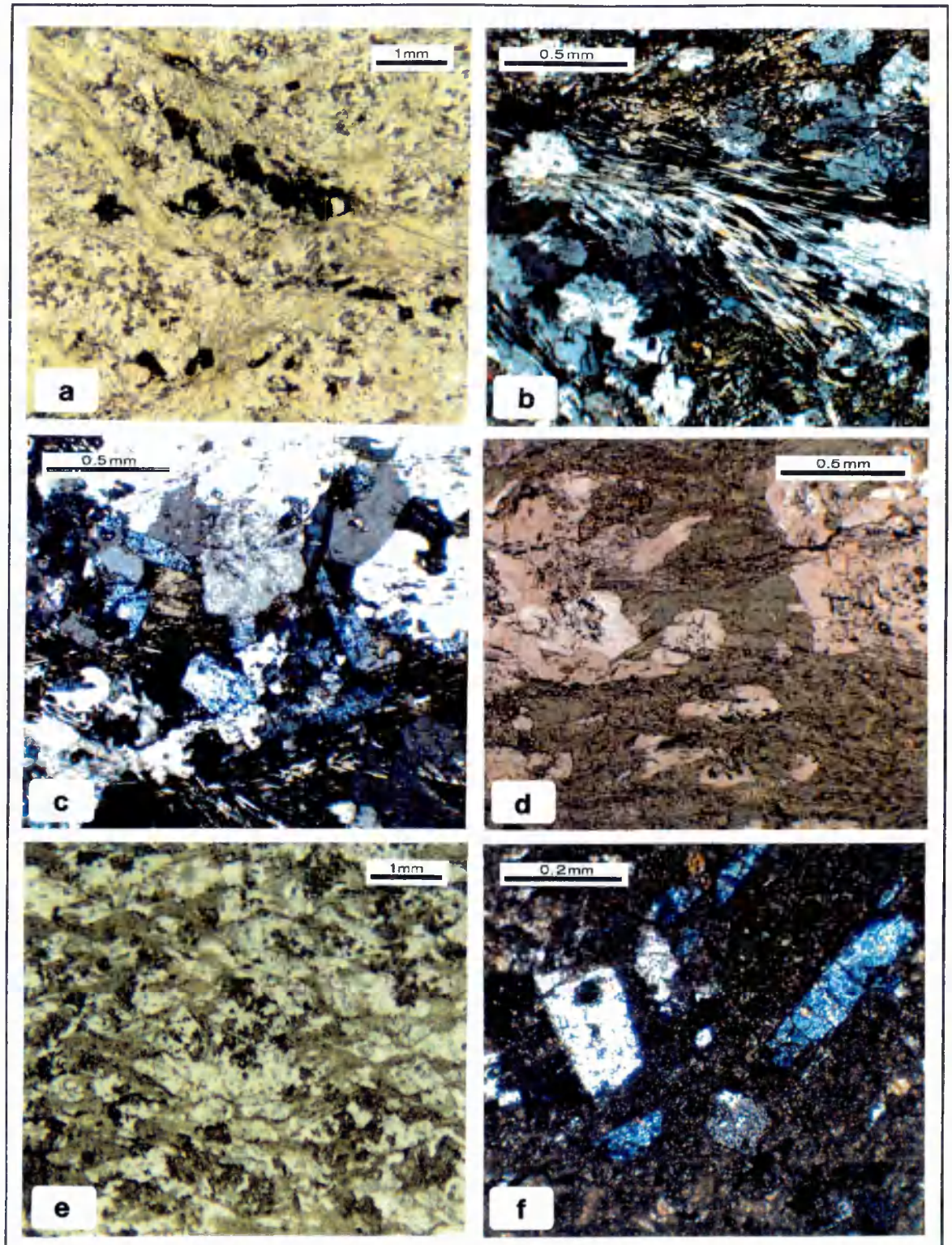

Fig. 4-9. Photomicrographs showing a range of textures from the Versoyen metabasites. See Appendix 1 for specimen details. **a)** Opaque-rich domain (visible assemblage = actinolite + albite + ?ilmenite + chlorite + sphene), sample FB PR 1, unpolarised light. **b)** Deformation fabric picked out by actinolite+chlorite needles, crossing apparently undeformed albites (statically overgrowing the cleavage at a late stage?). Sample FB PR 2, cross-polarised light. **c)** Albite–chlorite–zoisite–epidote domain from sample FB PR 3, cross-polars. **d)** Chlorite–actinolite–albite domain in sample FB PR 13, plane-polarised light. **e)** Two intersecting cleavages (conjugate shears or flattening around rigid albites?) picked out by alignment of actinolite–chlorite domains in FB PR 13, plane-polarised light. **f)** Albite and zoisite crystals (+ minor calcite and epidote) embedded in an anonymous fine-grained murky brown groundmass, sample FB PR 8, crossed polars.

this is a typical greenschist facies metabasaltic paragenesis. A fine-grained murky brown groundmass (seemingly chlorite + actinolite + albite) forms a large volume fraction (typically 20-30%) in many samples and presumably represents devitrified and altered primary glass. This murky brown gunge forms the main component (>70%) of samples FB PR 5 and FB PR 8. Texturally, the metabasites are dominated by complex deformation fabrics; relict igneous textures are scarce. Figure 4-9 shows some of the textures encountered.

4.3-2 Chemical Composition

Chemical composition was assessed by XRF major and trace element analyses on the fourteen samples described in Table 4-1. Analytical procedures are described in Appendix 2. Additional XRF determinations of concentrations of the light rare-earth elements La, Ce and Nd were kindly performed by Tim Brewer at Nottingham University. The results of these analyses are tabulated in Table 4-2 and Table 4-3 summarises the range of values encountered. Overall compositional variation is relatively limited and coarser-grained facies do not differ geochemically from finer-grained rocks, though it should be remembered that the sample sizes are small. The three samples from Comba di Planaval (FB PR 13–15) are essentially identical to the Breuil metabasites in terms of trace element composition, but differ somewhat in respect of major oxides (higher CaO, lower Na_2O and MgO). Two samples from the Breuil valley differ significantly from the rest in terms of chemical composition: FB PR 5 and FB PR 8 both exhibit comparatively low Ti, Y, Zr, Nb and high Mg, Cr, Cu; FB PR 8 also has anomalously high Ni, Sr and low Na. As noted in section 4.3-1, these two samples are also petrographically anomalous, containing a high proportion of highly altered chloritic groundmass.

4.4 BASALT PETROGENESIS

Major element data from the Versoyen metabasites testify to compositions which are essentially those of tholeiitic basalts (Fig. 4-10). This accords with the findings of Antoine *et al.* (1973) and Loubat & Delaloye (1984). However, in view of the likelihood of post-crystallisation alteration of these rocks by metamorph ism or weathering (see section 4.4-2), it is perhaps inappropriate to attempt to discuss their geochemical affinities in terms of potentially mobile major elements.

Table 4-2...

	FB PR 1	FB PR 2	FB PR 3	EAE 3	FB PR 5	FB PR 6	NEL 6	FB PR 7	FB PR 8	FB PR 8r	ESR 8
	M-grained	*M/C-grained*	*C-grained*	*C-grained*	*M-grained*	*M-grained*	*M-grained*	*M-grained*	*F-grained*	*F-grained*	*F-grained*
SiO2	49.30	47.13	50.24	50.12	50.96	47.66	47.75	49.69	48.25	47.90	48.10
TiO2	2.12	2.00	1.63	1.63	1.47	2.11	2.09	1.71	1.25	1.25	1.26
Al2O3	16.57	16.96	18.02	18.02	15.89	14.60	14.61	16.23	16.15	16.04	15.93
Fe2O3	9.46	8.73	7.74	7.73	9.50	11.38	11.37	9.28	10.19	10.21	10.20
MnO	0.21	0.21	0.19	0.19	0.20	0.27	0.27	0.20	0.32	0.32	0.32
MgO	7.01	6.22	6.98	6.85	8.15	7.54	7.52	7.38	9.15	9.30	9.19
CaO	6.30	8.54	6.78	6.80	6.35	5.70	5.75	7.34	7.83	7.90	7.92
Na2O	5.10	5.14	5.22	5.10	4.65	3.85	3.53	4.54	2.13	2.16	2.23
K2O	0.02	0.04	0.04	0.04	0.02	0.03	0.01	0.02	0.00	0.00	0.01
P2O5	0.29	0.27	0.22	0.22	0.13	0.25	0.25	0.19	0.12	0.12	0.12
L.O.I.	3.51	4.82	3.16	3.26	2.95	6.47	6.55	3.64	5.00	4.94	4.99
Total	*99.89*	*100.05*	*100.22*	*99.96*	*100.26*	*99.86*	*99.70*	*100.22*	*100.39*	*100.14*	*100.27*
Sc	35	36	26	29	30	50	47	33	27	35	26
V	262	255	197	201	248	399	394	259	218	200	211
Cr	194	210	268	307	347	280	276	259	327	321	330
Co	42	39	35	37	48	40	47	45	55	55	54
Ni	49	49	77	89	114	51	53	95	168	164	161
Cu	18	18	17	19	62	34	39	51	61	61	58
Zn	88	83	91	99	79	143	148	75	122	122	116
Rb	0	1	0	1	0	0	1	1	0	0	1
Sr	232	384	258	270	209	83	85	287	459	455	452
Y	46	46	36	37	22	37	38	32	29	27	28
Zr	204	182	169	168	74	156	160	128	86	84	84
Nb	6	5	4	5	2	5	6	4	1	2	3
Ba	0	7	1	7	0	0	0	0	2	2	4
Pb	0	1	0	3	2	2	1	6	5	3	2
Th	5	6	5	3	4	4	4	4	5	5	5
U	1	1	2	2	1	1	2	2	1	0	2
Ce	20	21	0	0	0	21	–	25	0	–	26
La	1	0	13	0	0	0	–	4	0	–	0
Nd	24	12	4	1	9	20	–	17	0	–	16
Mg#	74.58	73.83	78.12	77.82	77.26	72.40	72.37	75.90	78.05	78.29	78.11
Zr/Y	4.43	3.96	4.69	4.54	3.36	4.22	4.21	4.00	2.97	3.11	3.00
Zr/Ti	0.016	0.015	0.017	0.017	0.008	0.012	0.013	0.012	0.011	0.011	0.011
Ti/V	48.55	47.06	49.64	48.66	35.56	31.73	31.83	39.61	34.40	37.50	35.83
Cr/Y	4.22	4.57	7.44	8.30	15.77	7.57	7.26	8.09	11.28	11.89	11.79

Table 4-2...

	FB PR 9	FB PR 10	FB PR 11	FB PR 11r	WLB 11	FB P PR 13	FB P PR 14	WR 14	FB P PR 15	FC LC 6	PSP 26mc
	F-grained	*F-grained*	*F-grained*	*F-grained*	*F-grained*	*F-grained*	*F-grained*	*F-grained*	*F/M-grained*	*M/C-grained*	*M/C-grained*
SiO2	49.66	48.28	49.41	49.49	49.36	49.95	48.70	48.82	47.44	48.87	48.50
TiO2	1.92	2.43	2.00	1.98	2.01	1.71	1.73	1.74	1.72	2.11	2.12
Al2O3	15.51	15.30	15.83	15.82	15.74	15.98	15.14	15.14	15.30	15.09	15.12
Fe2O3	10.65	11.55	10.74	10.71	10.77	9.80	8.35	8.41	8.54	11.16	11.16
MnO	0.19	0.22	0.19	0.19	0.18	0.12	0.14	0.14	0.15	0.20	0.19
MgO	7.94	6.27	7.89	7.89	7.81	7.21	6.19	6.12	6.32	7.14	7.19
CaO	6.08	8.66	6.38	6.37	6.39	9.16	11.07	11.18	11.89	8.41	8.43
Na2O	4.58	4.20	4.60	4.61	4.61	3.23	3.16	3.19	3.15	4.07	4.07
K2O	0.01	0.02	0.01	0.01	0.01	0.05	0.05	0.05	0.05	0.01	0.01
P2O5	0.21	0.26	0.21	0.22	0.22	0.10	0.26	0.26	0.25	0.26	0.26
L.O.I.	3.04	2.75	3.04	2.99	2.81	3.04	5.32	5.16	5.73	2.58	2.67
Total	*99.79*	*99.94*	*100.30*	*100.28*	*99.91*	*100.35*	*100.10*	*100.20*	*100.54*	*99.91*	*99.73*
Sc	32	43	28	33	32	34	31	28	24	34	40
V	311	329	309	307	306	233	223	226	220	304	301
Cr	258	229	259	255	257	216	181	187	196	197	196
Co	52	44	49	50	54	44	39	37	42	50	53
Ni	131	84	123	123	125	91	81	81	87	118	117
Cu	47	30	39	40	46	56	36	37	38	42	40
Zn	88	105	87	87	90	74	66	69	71	91	91
Rb	1	0	0	0	0	1	1	1	0	0	1
Sr	177	341	186	187	192	175	224	230	223	228	234
Y	38	51	40	40	41	30	35	37	36	41	42
Zr	156	203	154	155	158	147	157	162	164	172	175
Nb	4	5	4	4	4	7	7	8	7	6	5
Ba	0	0	0	0	0	5	3	5	1	2	0
Pb	1	2	5	3	3	1	2	1	1	5	1
Th	4	4	6	5	5	5	4	3	5	5	5
U	0	0	0	1	1	1	1	1	1	0	1
Ce	27	24	18	–	23	19	14	–	–	–	–
La	0	12	13	–	0	0	0	–	–	–	–
Nd	18	17	13	–	19	16	17	–	–	–	–
Mg#	74.70	68.25	74.42	74.47	74.17	74.45	74.59	74.24	74.56	71.70	71.84
Zr/Y	4.11	3.98	3.85	3.88	3.85	4.90	4.49	4.38	4.56	4.20	4.17
Zr/Ti	0.014	0.014	0.013	0.013	0.013	0.014	0.015	0.016	0.016	0.014	0.014
Ti/V	37.04	44.32	38.83	38.70	39.41	44.03	46.55	46.19	46.91	41.64	42.26
Cr/Y	6.79	4.49	6.48	6.38	6.27	7.20	5.17	5.05	5.44	4.80	4.67

recalculated anhydrous:

	FB PR 1	FB PR 2	FB PR 3	EAE 3	FB PR 5	FB PR 6	NEL 6	FB PR 7	FB PR 8
SiO2	51.15	49.49	51.76	51.83	52.37	51.03	51.26	51.45	50.58
TiO2	2.20	2.10	1.68	1.69	1.51	2.26	2.24	1.77	1.31
Al2O3	17.19	17.81	18.57	18.63	16.33	15.63	15.68	16.80	16.93
Fe2O3	9.82	9.17	7.97	7.99	9.76	12.19	12.21	9.61	10.68
MnO	0.22	0.22	0.20	0.20	0.21	0.29	0.29	0.21	0.34
MgO	7.27	6.53	7.19	7.08	8.38	8.07	8.07	7.64	9.59
CaO	6.54	8.97	6.99	7.03	6.53	6.10	6.17	7.60	8.21
Na2O	5.29	5.40	5.38	5.27	4.78	4.12	3.79	4.70	2.23
K2O	0.02	0.04	0.04	0.04	0.02	0.03	0.01	0.02	0.00
P2O5	0.30	0.28	0.23	0.23	0.13	0.27	0.27	0.20	0.13
Total	*100.00*	*100.01*	*100.00*	*100.00*	*100.01*	*100.00*	*100.00*	*100.00*	*100.00*

	FB PR 9	FB PR 10	FB PR 11	FB PR 11r	WLB 11	FB P PR 13	FB P PR 14	WR 14	FB P PR 15
SiO2	51.33	49.68	50.80	50.87	50.83	51.33	51.38	51.37	50.04
TiO2	1.98	2.50	2.06	2.04	2.07	1.76	1.83	1.83	1.81
Al2O3	16.03	15.74	16.28	16.26	16.21	16.42	15.97	15.93	16.14
Fe2O3	11.01	11.88	11.04	11.01	11.09	10.07	8.81	8.85	9.01
MnO	0.20	0.23	0.20	0.20	0.19	0.12	0.15	0.15	0.16
MgO	8.21	6.45	8.11	8.11	8.04	7.41	6.53	6.44	6.67
CaO	6.28	8.91	6.56	6.55	6.58	9.41	11.68	11.76	12.54
Na2O	4.73	4.32	4.73	4.74	4.75	3.32	3.33	3.36	3.32
K2O	0.01	0.02	0.01	0.01	0.01	0.05	0.05	0.05	0.05
P2O5	0.22	0.27	0.22	0.23	0.23	0.10	0.27	0.27	0.26
Total	*100.00*	*100.00*	*100.00*	*100.00*	*100.00*	*100.00*	*100.01*	*100.01*	*100.00*

Table 4-2. Major and trace element compositional data for the Versoyen metabasite samples described in Table 4-1. Data obtained by XRF analysis on whole rock samples, analytical procedures are detailed in Appendix 2. Selected trace element ratios are indicated. Mg# = 100(Mg/(Mg + Fe^{2+})).

	max	min	mean	st dev	% var
SiO2	50.96	47.13	48.97	1.12	2.3
TiO2	2.43	1.25	1.85	0.31	16.5
Al2O3	18.02	14.60	15.90	0.88	5.5
Fe2O3	11.55	7.73	9.79	1.20	12.3
MnO	0.32	0.12	0.20	0.05	25.0
MgO	9.30	6.12	7.24	0.86	11.8
CaO	11.89	5.70	7.89	1.88	23.8
Na2O	5.22	2.13	4.12	0.91	22.2
K2O	0.05	0.00	0.03	0.02	64.0
P2O5	0.29	0.10	0.22	0.06	28.0
L.O.I.	6.55	2.58	3.93	1.27	32.3
Total	100.54	99.70	100.13	0.23	0.2
Mg#	78.29	68.25	74.49	2.59	3.5
Zr/Y	4.90	2.97	4.12	0.51	12.4
Zr/Ti	0.002	0.008	0.014	0.002	16.3
Ti/V	49.64	31.73	41.85	5.72	13.7
Cr/Y	15.77	4.22	7.09	3.13	44.2

	max	min	mean	st dev	% var
Sc	50	24	33	6.8	20.7
V	399	197	269	55.1	20.5
Cr	347	181	244	50.5	20.7
Co	55	35	45	5.6	12.7
Ni	168	49	94	34.2	36.3
Cu	62	17	39	15.2	38.7
Zn	148	66	90	20.9	23.1
Rb	1	0	0	0.5	139.2
Sr	459	83	248	95.3	38.5
Y	51	22	37	7.6	20.5
Zr	204	74	154	37.3	24.3
Nb	8	1	5	1.8	37.7
Ba	7	0	2	2.2	145.0
Pb	6	0	2	2.0	85.8
Th	6	3	5	0.7	15.4
U	2	0	1	0.7	77.3
Ce	27	0	16	10.1	64.0
La	13	0	4	5.6	156.3
Nd	24	0	14	6.8	48.9

Table 4-3. The compositional range represented by the metabasite analyses tabulated in Table 4-2.

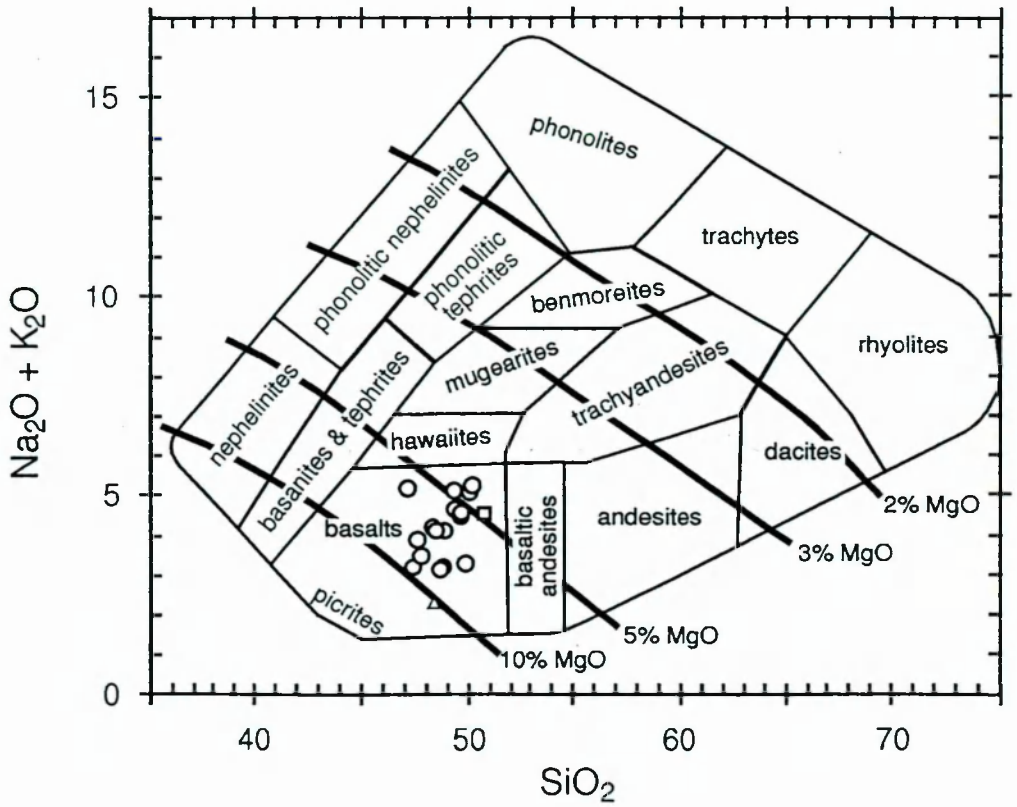

Fig. 4-10. Versoyen metabasite compositions plotted on an alkali-silica diagram with typical igneous variations in MgO indicated by contours. Fields from Cox *et al.* (1979). The petrographically and geochemically anomalous samples FB PR 5 and FB PR 8 are indicated by a box and a triangle respectively.

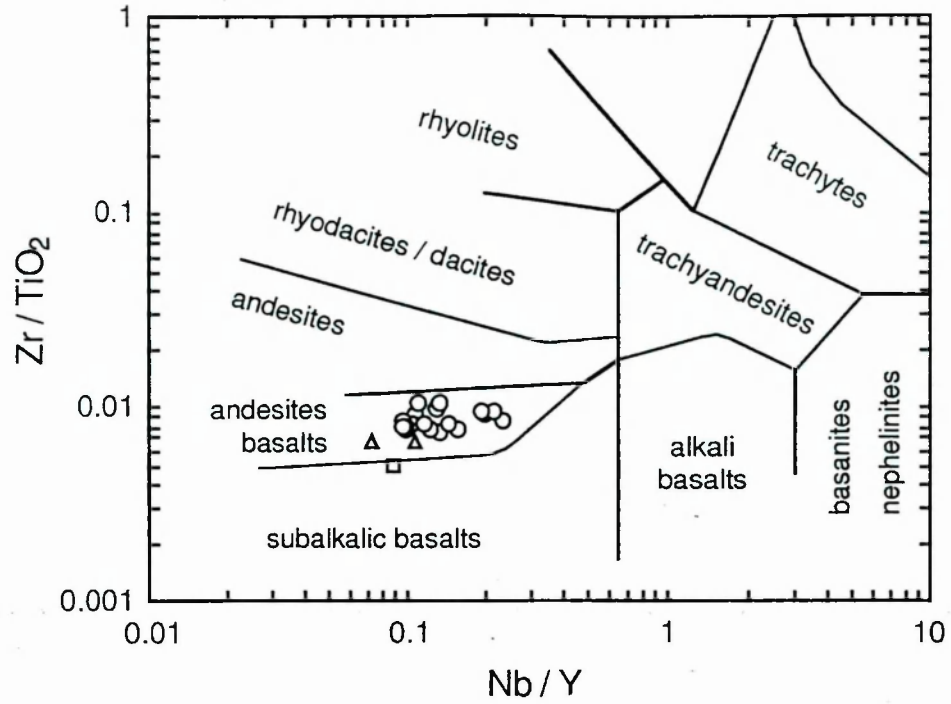

Fig. 4-11. Classification scheme for the non-potassic volcanic rocks according to Zr/Ti – Nb/Y ratios (Winchester & Floyd, 1977). Versoyen samples plot comfortably within the sub-alkalic basalt/andesite field. The anomalous samples FB PR 5 and FB PR 8 are indicated by boxes and triangles respectively.

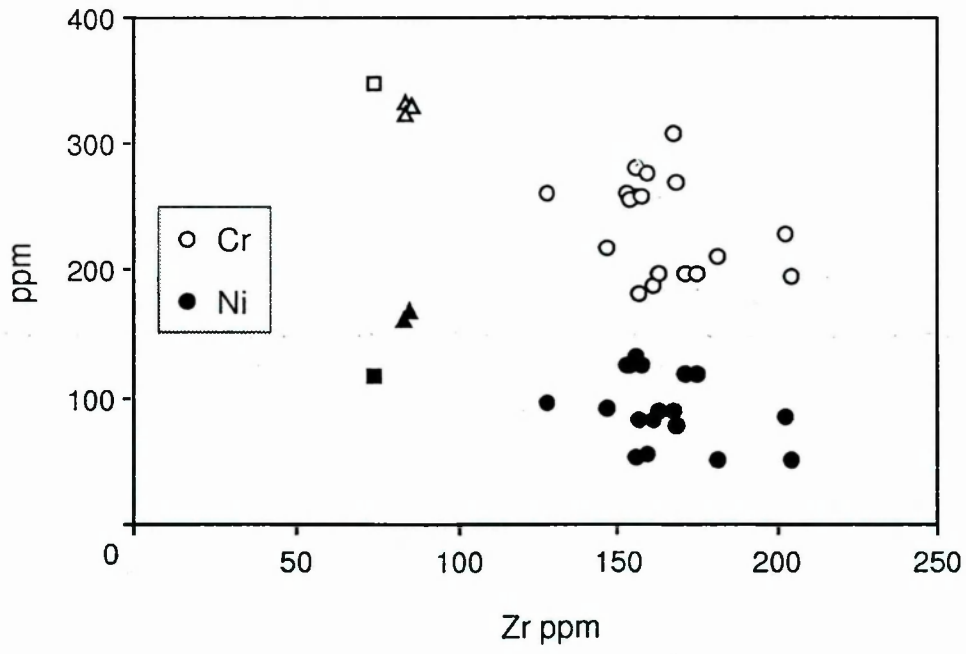

Fig. 4-12. Variations in Ni and Cr with Zr. Zr is highly incompatible with major mantle phases and is therefore generally useful as an index of magmatic differentiation. Ni and Cr are compatible elements: decrease in Ni through a differentiation sequence usually indicates olivine fractionation and decrease in Cr may suggest clinopyroxene or spinel fractionation (*e.g.* Green, 1980). It is clear that the Versoyen samples do not represent a sufficient variation in Zr (or SiO_2 or Mg#) to record a magmatic fractionation trend. The anomalous samples FB PR 5 and FB PR 8 are indicated by boxes and triangles respectively.

A chemical classification of igneous rocks employing immobile minor and trace elements has been suggested by Winchester & Floyd (1977). This scheme uses the ratio of Zr to Ti as a index of fractionation (*i.e.* a surrogate for SiO_2 content or Mg# in fresh rocks) and the ratio of Nb to Y as an measure of alkalinity (as an alternative to Na_2O+K_2O). Plotted on this basis, the Versoyen metabasites classify as non-alkalic basalts or andesites (Fig. 4-11). The samples to do not represent a sufficient range of SiO_2, Mg# or Zr to demonstrate a fractionation trend (*e.g.* Fig. 4-12).

4.4-1 Tectonomagmatic Discrimination

Rationale. Problems of sexual and racial discrimination are gradually being eliminated from the geological community, however, tectonomagmatic discrimination continues to be a widespread source of unhappiness. Since the benchmark paper by Pearce & Cann (1973), a number of studies have attempted to establish geochemical criteria for elucidation of the tectonic setting of ancient basaltic suites (*e.g.* Floyd & Winchester, 1975, 1978; Pearce *et al.*, 1975, 1977; Wood *et al.*, 1979; Shervais, 1982; Pearce, 1982; Mullen, 1983; Meschede, 1986). The rationale underpinning this approach arises from the observation that, for modern volcanic rocks, specific tectonic environments are associated with distinct geochemical characteristics.

In general, major element geochemistry is not a sensitive indicator of tectonic provenance for basaltic rocks: the primary products of upper mantle melting appear to be essentially similar in terms of major element composition (*i.e.* basaltic) regardless of their tectonic setting (Arculus, 1987). Consequently, most geochemical discrimination schemes appeal to subtler variations in terms of trace element or isotopic characteristics. Ideally, the discriminant functions applied should employ elements which show strong discrimination between environments (*i.e.* greater variation between different environments than between different samples from the same environment), and which distinguish as many different environments as possible (Pearce & Cann, 1973). In practice, an overriding consideration is often that of element mobility during weathering or metamorphism. As a result, most tectonomagmatic discrimination schemes use the relative abundances of trace elements such as the high field-strength elements (*e.g.* P, Ti, Y, Zr, Nb, Ta, Hf), the transition metals (*e.g.* Sc, V, Cr, Ni) and the

heavy rare earth elements (REE), which are believed to be essentially immobile (section 4.4-2).

Application. Geochemical discrimination schemes have been applied to various ancient volcanic suites in order to assess their likely petrogenetic settings. One of the earliest applications of the method was to mafic rocks of the Tauern window (Pennine nappes of the Austrian Alps) by Bickle & Nisbet (1972), who were able to demonstrate an oceanic provenance on the basis of Zr-Y-Ti characteristics. Pearce (1975) used similar reasoning to infer an island arc affinity for the Troodos ophiolite in Cyprus. Figure 4-13 shows trace element data from Versoyen metabasites plotted on a veritable gamut of published basalt discrimination diagrams.

One of the most widely applied of all tectonomagmatic discrimination schemes has been the Ti-Zr-Y plot of Pearce & Cann (1973). On this diagram (Fig. 4-13a), the Versoyen metabasites form a tight cluster in the mid-ocean ridge basalt (MORB)–island arc field. However, it has become apparent that this plot cannot distinguish continental tholeiites from MORB or island arc tholeiites (Holm, 1982). On the Ti-Zr-Sr discrimination diagram (Fig. 4-13b), also proposed by Pearce & Cann (1973), the Versoyen data fall mainly within the ocean floor field but exhibit significant variation in terms of Sr content. Strontium is not regarded as a reliable discriminant in rocks which have experienced metamorphism to greenschist facies or higher (Pearce & Cann, 1973) and the degree of scatter evident in Fig. 4-13b suggests that Sr abundances in the Versoyen samples may have been disturbed.

Niobium abundance is a potentially useful discriminant because it shows wide variation between different basalt types, ranging from ~0.2ppm for some depleted (N-type) MORB to >150ppm for typical within-plate basalts (Meschede, 1986). Concentrations of Nb analysed from the Versoyen metabasites are mostly 4-6ppm, which is scarcely above detection limits (~2ppm) and similar to N-MORB values. However, on the Nb-Zr-Y discrimination plot of Meschede (1986), the Versoyen rocks plot unhelpfully across N-MORB, volcanic arc and within-plate tholeiite fields (Fig. 4-13c).

Other trace element ratios also give equivocal results. In terms of Zr-Y abundances, the Versoyen metabasites have unclear affinities, plotting in a

relatively tight cluster on the boundary between ocean island basalt (OIB) and MORB fields of the Pearce & Norry (1979) discrimination diagram (Fig. 4-13d).

Pearce (1982) claims that the relative abundances of Cr and Y provide a useful discriminant between basaltic rocks generated in divergent (MORB) and convergent (volcanic arc) plate margin settings. According to his criteria (*op. cit.*), the Versoyen metabasites have relatively typical MORB characteristics (Fig. 4-13e), although Cr and Y cannot effectively discriminate other tectonomagmatic settings.

Shervais (1982) claims that the ratio of Ti to V gives good discrimination between arc tholeiites, MORB and alkali basalts. Neither Ti nor V are readily transported in the fluid phase and as the two elements show coherent behaviour during alteration, their ratio should remain relatively unaffected by changes in absolute abundances (*op. cit.*). Versoyen metabasites have Ti/V ratios ranging from 31.7 to 49.6, all plotting comfortably in Shervais' MORB field (Fig. 4-13f).

Plotted on the Zr-Ti discrimination diagram of Pearce & Cann (1973), about half of the Versoyen data fall outside the basalt field entirely (Fig. 4-13g), although most lie close to the ocean floor domain. The Versoyen metabasites show more convincing ocean floor affinities on the Cr-Ti plot (Fig. 13h) introduced by Pearce (1975), which purports to distinguish ocean floor (*i.e.* MORB) from island arc (*i.e.* low-K tholeiites) magma types.

Figure 4-14 shows the Versoyen trace element data plotted on a multi-element variation diagram normalised to 'average' N-type MORB, following the approach of Pearce (1983). Whilst this representation of the data cannot readily be used for tectonic discrimination, it does form a convenient basis for comparisons. It is clear that the analysed metabasites have consistent MORB-like characteristics in terms of the relatively immobile trace elements (P, Zr, Ti, Y, Sc, Cr, Ni), but that the more mobile species do not define a sensible trend.

Interpretation. It is apparent from Figs. 4-10–4-14 that the Versoyen metabasites are essentially MORB-similar tholeiites whose geochemical composition has been subsequently modified by non-igneous processes. Trace element discrimination functions do not unequivocally assign the Versoyen suite to any particular tectonomagmatic setting, although most of the data fall within ocean floor or volcanic arc fields. Three main possibilities need to be considered. First, the trace element signals are consistent and the Versoyen rocks represent a change

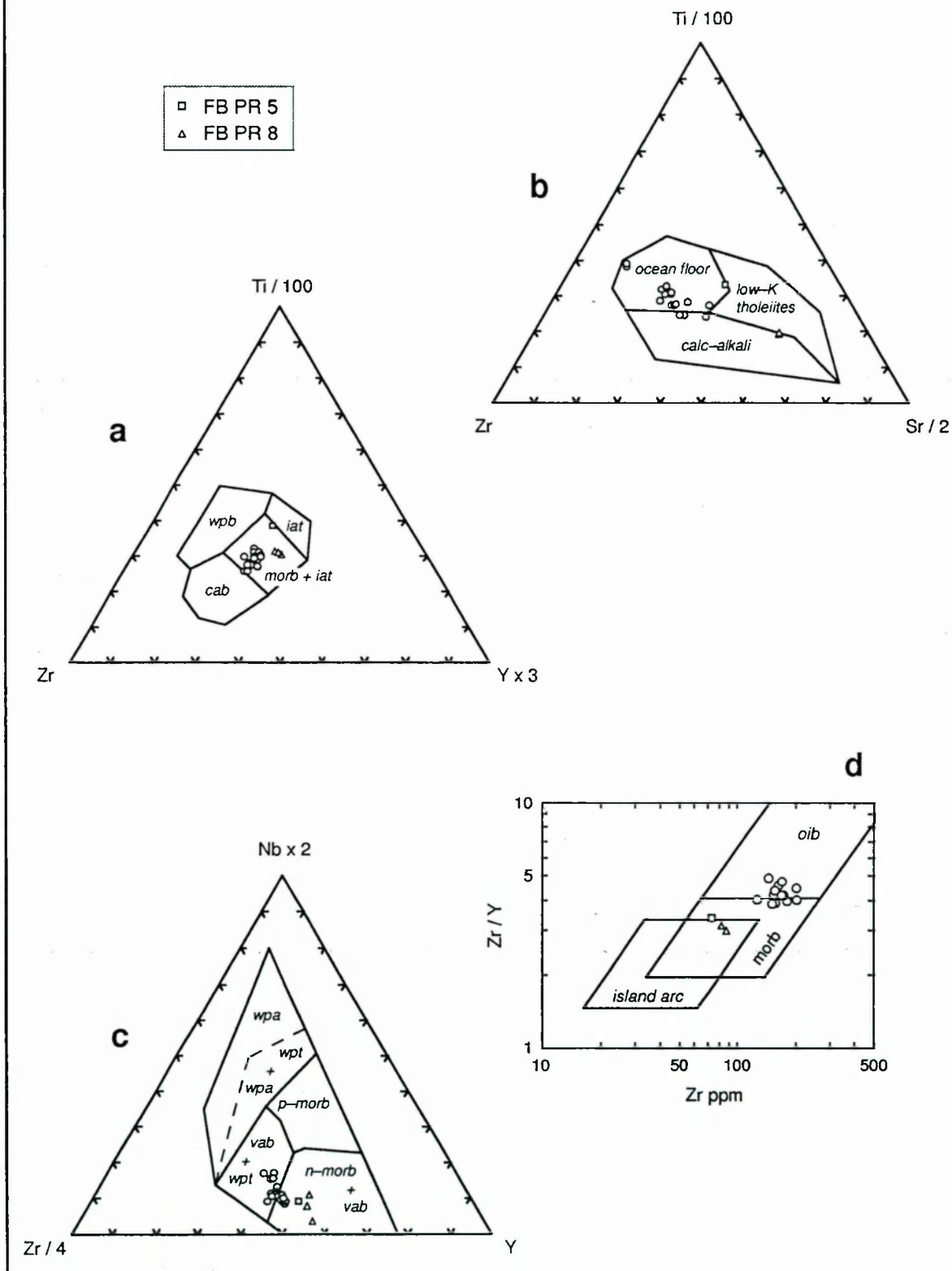
FB PR 5
FB PR 8
a
Ti / 100
Zr
Y x 3
wpb
iat
morb + iat
cab
b
Ti / 100
Zr
Sr / 2
ocean floor
low–K tholeiites
calc–alkali
c
Nb x 2
Zr / 4
Y
wpa
wpt
lwpa
p–morb
vab
wpt
n–morb
vab
d
Zr / Y
Zr ppm
10
5
1
10
50
100
500
oib
morb
island arc

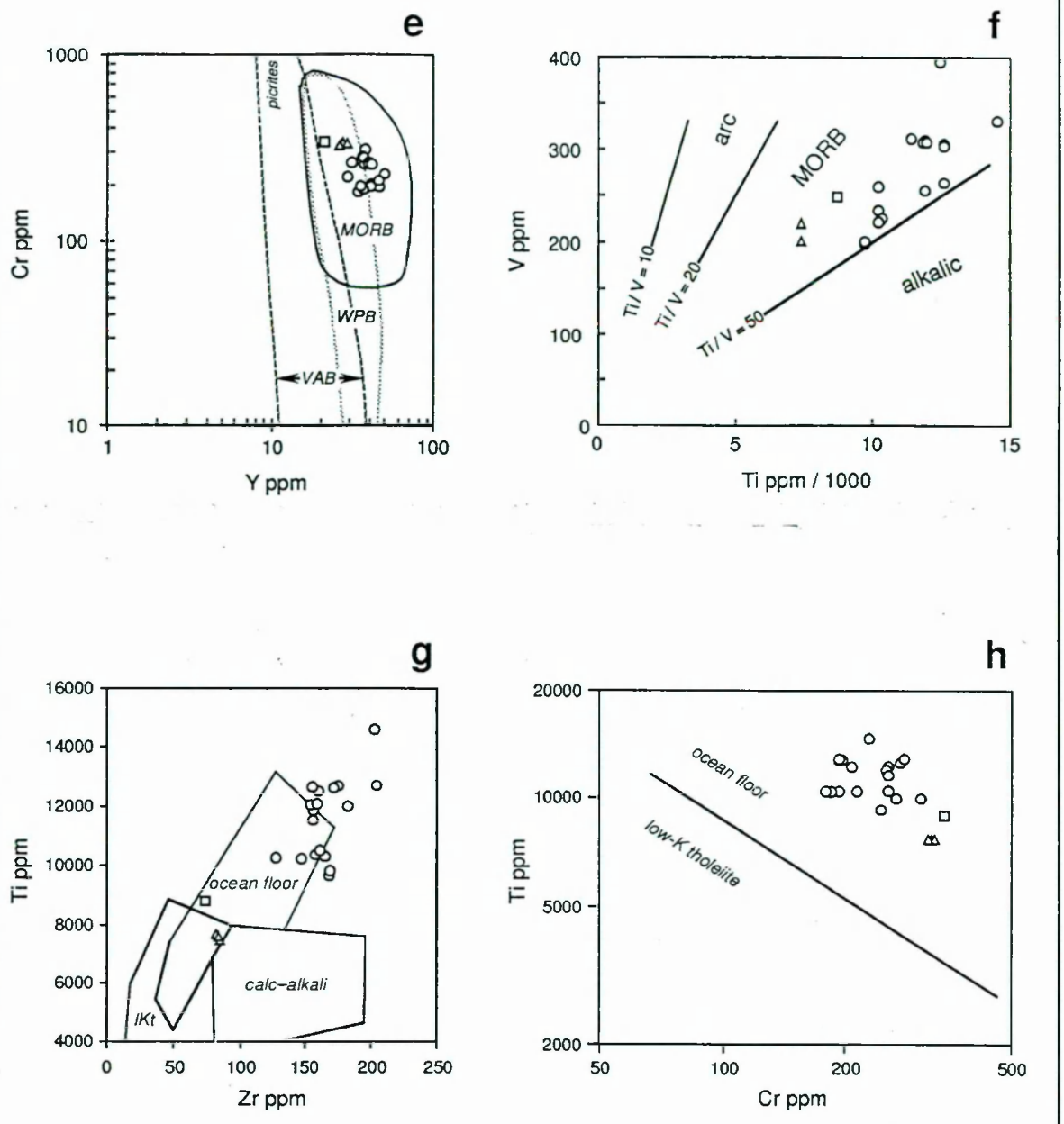

Fig. 4-13. Trace element data for the Versoyen metabasites plotted on various tectono-magmatic discrimination diagrams: **a**) the Ti-Zr-Y plot of Pearce & Cann (1973); **b**) the Ti-Zr-Sr plot of Pearce & Cann (1973); **c**) the Nb-Zr-Y plot of Meschede (1986); **d**) the Zr-Zr/Y plot of Pearce & Norry (1979); **e**) the Y-Cr plot of Pearce (1982); **f**) the Ti-V plot of Shervais (1982); **g**) the Zr-Ti plot of Pearce & Cann (1973); **h**) the Cr-Ti plot of Pearce (1975). Abbreviations: *cab* = calc-alkaline basalt; *iat* = island arc tholeiite; *lKt* = low-potassium tholeiite; *n-morb* = normal-type mid-ocean ridge basalt; *oib* = ocean island basalt; *p-morb* = plume-type (enriched) mid-ocean ridge basalt; *vab* = volcanic arc basalt; *wpa* = within-plate alkalic basalt; *wpb* = within-plate basalt; *wpt* = within-plate tholeiitic basalt.

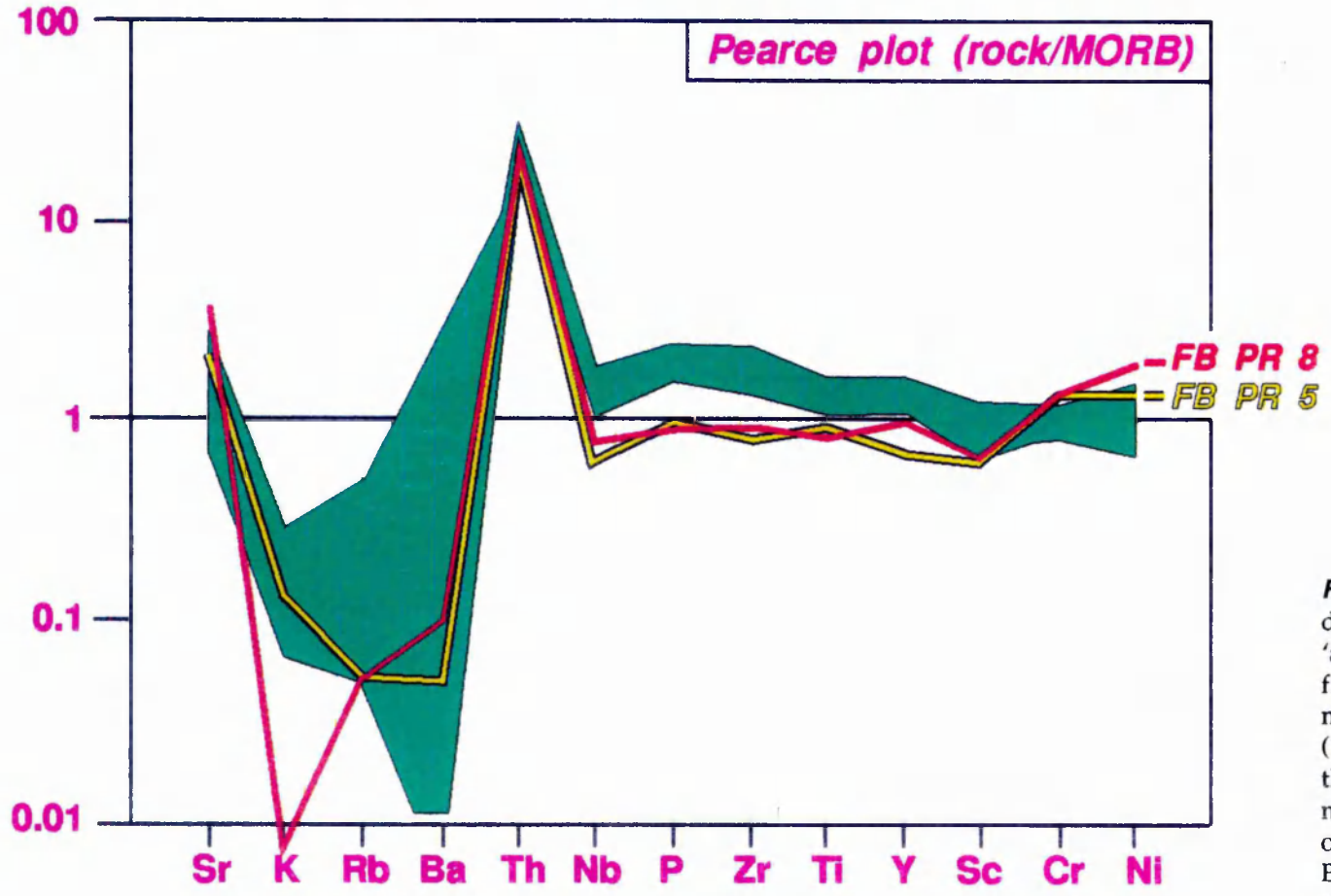

Fig. 4-14. A multi-element variation diagram ('spidergram') normalised to 'average' N-type MORB. showing the field occupied by all 20 Versoyen metabasite samples. Following Pearce (1983), the elements are arranged such that incompatibility (with respect to normal mantle minerals) decreases outward from the centre of the pattern. Elements which are relatively mobile in aqueous fluids (Sr, K, Rb, Ba) plot at the left of the diagram and 'immobile' elements at the right. Normalisation constants from Pearce (1983).

in tectonic environment over time from ocean floor to volcanic arc (or *vice versa*). Second, the primary igneous trace element characteristics gave an ambiguous signal. Third, an originally clear tectonomagmatic signature has been obscured by alteration. There is no stratigraphic evidence to support the first of these options. The second possibility has more credence: widespread application of tectonomagmatic discrimination diagrams over the past fifteen years has revealed a number of examples of discriminant–straddling basaltic suites (Arculus, 1987). For example, many back-arc basalts display trace element characterisitics intermediate between MORB and arc tholeiites (Saunders & Tarney, 1991). The third possibility is also plausible as the Versoyen metabasites show strong evidence of alteration, at least in terms of the large-ion lithophile elements (Fig. 4-14). Clearly, the petrogenetic interpretation of these trace element patterns requires some knowledge of which elements have been mobile since crystallisation. This question is addressed in the following section.

4.4-2 Element Mobility and Inferred Primary Composition

There is general agreement among geochemists that the high field-strength elements (HFSE, *e.g.* P, Ti, Y, Zr, Nb, Hf, Ta), the transition elements (Sc, V, Cr, Co, Ni) and most of the rare earth elements (REE) are essentially immobile during alteration of crystalline rock by water dominated fluids, unless the water/rock ratio is extremely high (Pearce, 1975; Shervais, 1982). However, mobility of Y and some REE has been shown by Sanjuan *et al.* (1988) for hydrothermal systems where carbonate and fluoride complexing has occurred. In contrast, mobility of major elements Si, Na, K, Ca and some trace elements (*e.g.* Rb, Sr, Ba) is well documented (Humphris & Thompson, 1978a, b).

Examination of Table 4-3 reveals fairly large variations in the abundances of most trace elements between the fourteen samples. To what extent is this a product of post-magmatic alteration? Three samples (FB PR 5-7) from the same sill show trace element variations comparable in magnitude to the compositional range represented by the entire sample set. This variation is of particular concern because it highlights significant concentration gradients for several allegedly 'immobile' trace elements including Ti, V, Cr, Y and Zr, casting a certain amount of doubt on the viability of tectonomagmatic discrimination using these elements. Trace element ratios (*e.g.* Ti/V, Zr/Y) are more consistent than individual elemental abundances but nonetheless exhibit appreciable variation (Table 4-3).

The compositional range shown in Table 4-3 is similar to that of a 'pristine' tholeiitic basalt except in terms of some of the alkalis (specifically Na, K, Rb) and alkaline earths (Ca, Sr, Ba). These elements, broadly the large-ion lithophile elements (LILE), are among the most soluble cation species in aqueous fluids. Therefore, it seems probable that the primary geochemical make-up of the Versoyen metabasites has been modified by fluid–rock interaction. How and to what extent has this occurred? This is clearly an important question if geochemical composition is to be used as a basis for an interpretation of magma petrogenesis. Fluid controlled alteration can be envisaged at several stages: during emplacement (direct interaction with sea-water or connate water); during sea-floor weathering or diagenesis ('halmyrolysis'); during extensional 'metamorphism' (hydrothermal processes); during regional metamorphism; and during recent weathering. Possible effects of these alteration processes are considered in turn below.

Syn-emplacement alteration. Chemical interaction between magma and pore-water during intrusion into unconsolidated sediment appears to be an essentially unstudied phenomenon. In view of the limited period of time involved, it seems unlikely that syn-intrusive reactions could significantly modify primary basalt composition outside a very thin contact zone of element redistribution.

Halmyrolysis is a term introduced by Reiche (1950) to encompass a range of 'weathering' processes operative on the sea-floor. It essentially describes chemical interaction between rock and sea-water under oxidative conditions at low temperatures (<70°C) and high water/rock ratios. Analyses of samples dredged from the sea-bed have demonstrated that halmyrolysis of basalts typically involves hydration and alteration of olivine + plagioclase to K-feldspar + smectite clays, oxidation of Fe^{2+} to Fe^{3+} and palagonitisation (*i.e.* hydration and devitrification) of primary glass (Thompson, 1991). Pyroxene generally remains unaltered. Chemically, the rock gains K, Rb, P, U, Th (and perhaps Mn, Fe, U, Zn) and loses Ca, Mg, Si (and possibly Na and Sr, depending on local chemical conditions). Aluminium, Ti, Zr, Nb and the heavy REE are not affected. Drilled basalt samples testify to essentially the same alteration path at shallow depths in the ocean floor, though alteration here proceeds under lower water/rock ratios and less oxidising conditions.

Hydrothermal alteration again involves rock–sea-water interaction, but at the elevated temperatures (100-400°C) associated with fluid convection at an active

spreading system. The supplied heat promotes a number of reactions which serve to lower the Eh and pH of the circulating hydrothermal waters (Bonatti *et al.*, 1975). One important group of reactions involves the removal of Mg^{2+} from sea-water along with OH^- to form clay minerals, leaving an excess of H^+ and hence depressing the pH (Bischoff & Dickson, 1975). Thus, cold, oxygenated, alkaline sea-water is transformed by heating and reaction with the enclosing rock into a reducing, acid hydrothermal solution capable of mobilising various cations. A large number of experimental and empirical studies has resulted in a partly clear picture of the effects of hydrothermal alteration on basalt composition (Seyfried, 1987; Thompson, 1991). Typically, olivine is replaced by chlorite, plagioclase alters to albite + heulandite + chlorite, titanomagnetite is replaced by sphene and pyroxene develops overgrowths (or reactions rims) of actinolite (Thompson, 1991). The end product is effectively a greenschist facies metamorphic assemblage. The associated chemical fluxes involve leaching of K, Si, Ca, Rb (and perhaps Ba, Cu, Zn, U) from the rock and acquisition of Mg and H_2O from sea-water (Mottl, 1983; Thompson, 1991). Aluminium, Ti, P, V, Cr, Y, Zr and Nb appear to be essentially unaffected. Other elements (such as Na, Fe, Sr, Mn, Co, Ni) behave in various ways according to temperature, water/rock ratio and local chemistry (Thompson, 1991). Detailed studies have found these alteration effects to be highly spatially heterogeneous (Alt & Emmerman, 1985): relating presumably to the distribution of fluid pathways. Furthermore, low temperature retrograde reactions may result in the subsequent uptake of alkali metals (*e.g.* Na, K) lost during prograde alteration. Such complexities mean that hydrothermal alteration does not necessarily leave a uniquely recognisable signature in ancient basalts.

Regional metamorphism. The effects of regional metamorphism on the chemistry of the Versoyen basalts are difficult to gauge. There are no *a priori* reasons to suppose that metamorphic changes would have been isochemical. Indeed, the common presence of slightly deformed $CaCO_3$ veinlets testifies to the passage of metamorphic fluids. Hynes (1980) has demonstrated appreciable mobility of Ti, Zr and Y during greenschist facies metamorphism of Ordovician metabasites in Québec. He attributes the mobilisation of these 'immobile' trace elements to high CO_2 levels in the fluid phase during metamorphism. However, the absence of distinctive mineralisation in the Versoyen complex makes the effects of any syn-metamorphic metasomatism difficult to judge.

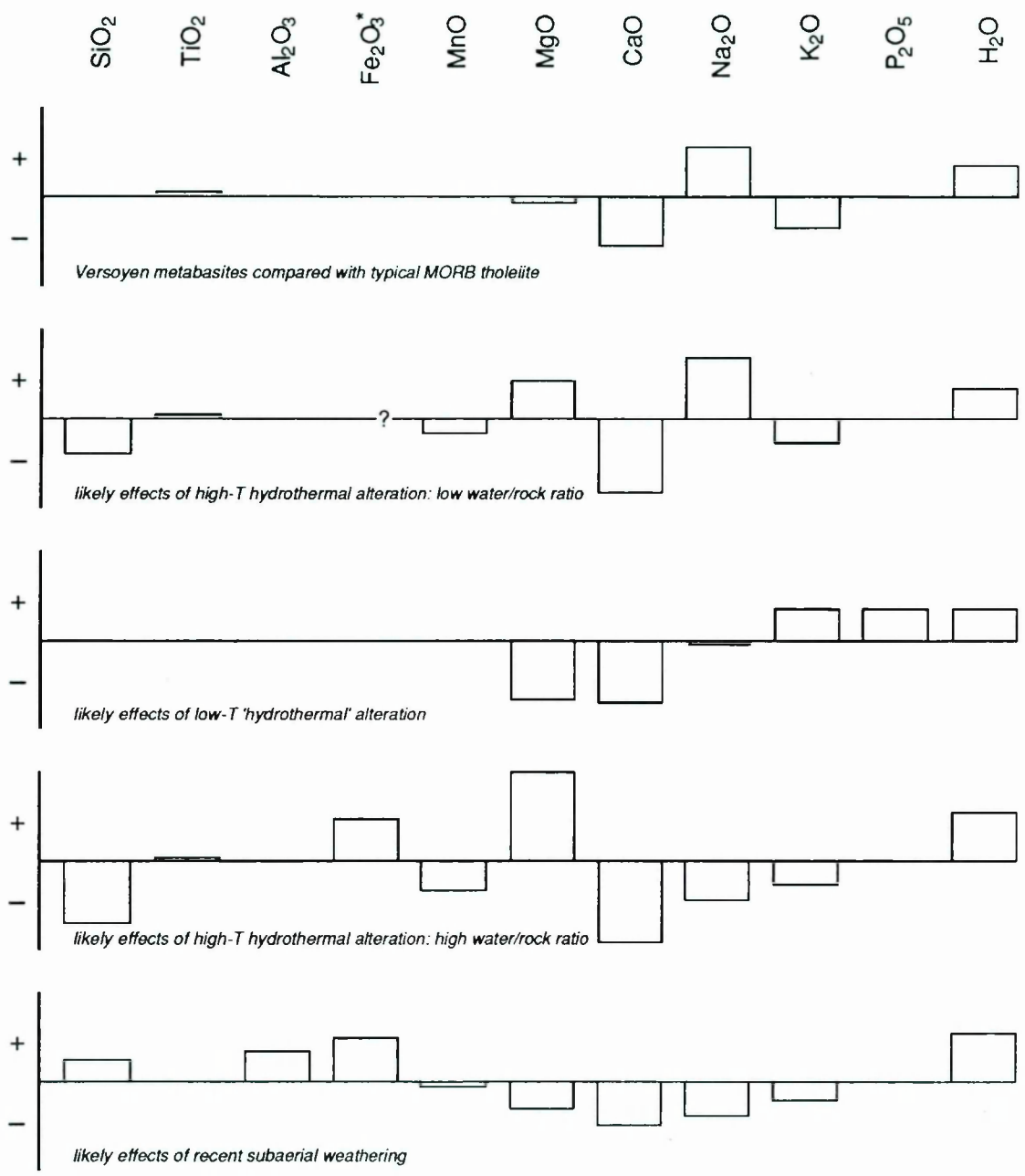

Fig. 4-15. Conceptual diagram to show the likely alteration pathways of a basaltic rock exposed to fluid controlled chemical alteration in different environments. The histograms attempt to depict the *relative* gains and losses experienced by the basalt, hence how an analysis of the altered rock would differ from that of the fresh basalt. Based on data from Alt & Emmermann (1985), Colman (1982), Loughnan (1969), Mottl (1983), Seyfried (1987) and Thompson (1991).

Subaerial weathering. By comparing compositional variations with depth in weathered profiles, several workers have charted the effects of subaerial alteration on basaltic rocks (*e.g.* Keller, 1957; Loughnan, 1969; Colman, 1982; Nesbitt & Wilson, 1992). Results have typically documented that element mobilities occur in the order: Ca≥Na>Mg>Si>Al≥K>Fe>Ti (Smyth, 1913; Reiche, 1950; Colman, 1982), though this is influenced by the precise mineralogy involved – particularly with regard to potassium (Nesbitt & Wilson, 1992). In general, CaO, Na_2O and MgO are removed fairly rapidly by hydrolysis and dissolution, leading to a relative residual increase in the proportion of Al_2O_3, Fe_2O_3 and SiO_2, (these oxides are also leached from the rock, but at much slower rates). TiO_2 and P_2O_5 appear to remain essentially unaffected in absolute terms (Colman, 1982), though their relative abundances increase with the removal of more mobile material.

How then do we account for the observed chemical modification of the Versoyen metabasites? None of the alteration processes discussed above are considerate enough to leave an unambiguous, diagnostic imprint, but a few general trends can be recognised. Figure 4-15 is an attempt to depict the likely effects of weathering and hydrothermal alteration on a fresh basalt. Proceeding from the assumption that the Versoyen metabasites originated as approximately MORB tholeiites (an assumption urged by 'immobile' trace element characteristics), it is clear from Fig. 4-15 that the modification could be accounted for by high-temperature, low water/rock hydrothermal processes subsequently overprinted by lower temperature hydrothermal alteration. In view of the rapid erosion rates operative in the Alps, modern chemical weathering is unlikely to have had time to pervasively modify rock composition (in any case, only the relatively fresh cores of large samples were analysed) but joint controlled infiltration of meteoric waters could lead to localised alteration. Recent weathering could certainly account for the anomalous CaO, Na_2O and MgO of the samples from Comba di Planaval (FB PR 13-15) as Ca, Na and Mg are generally the most mobile species during weathering.

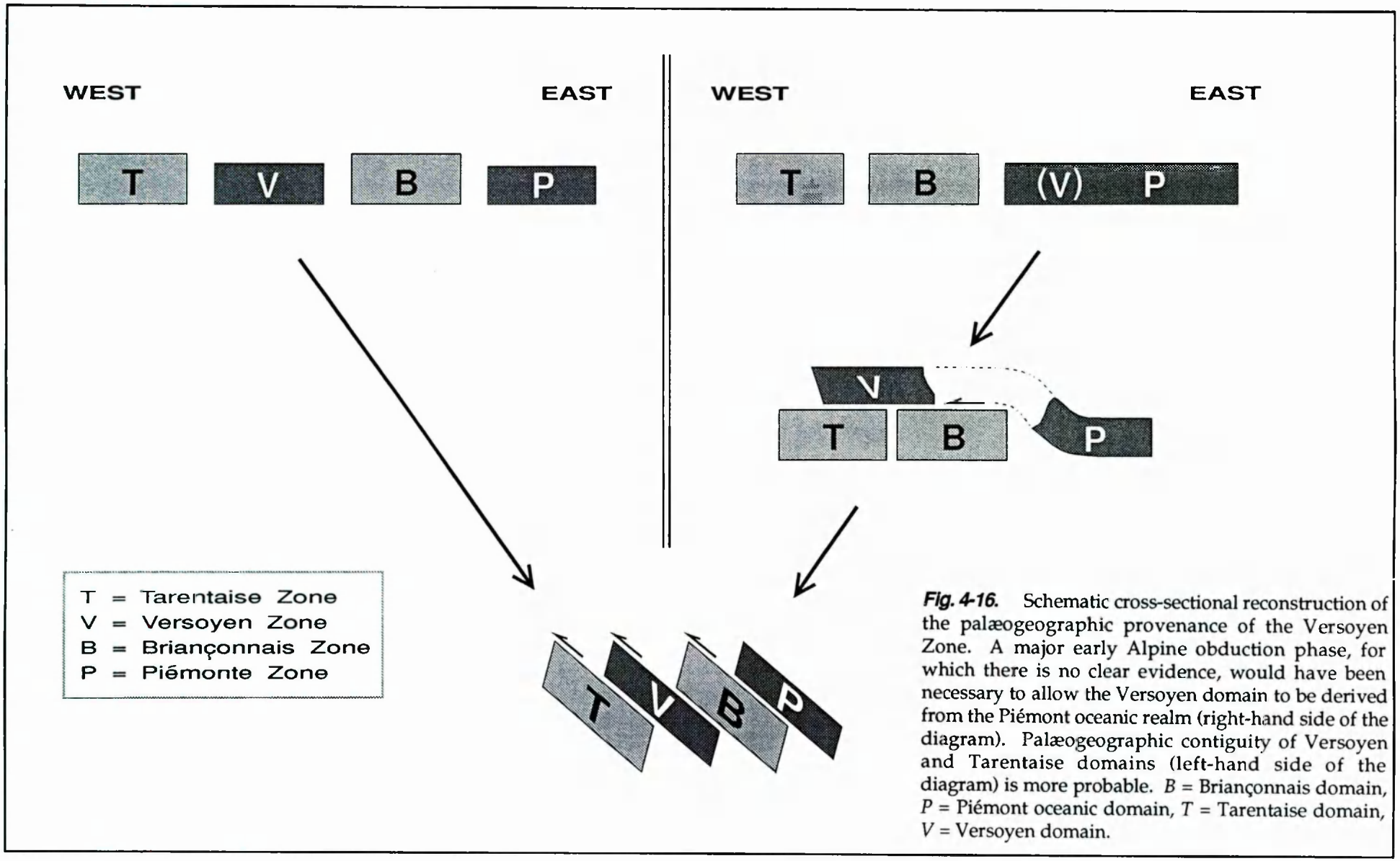

Fig. 4-16. Schematic cross-sectional reconstruction of the palæogeographic provenance of the Versoyen Zone. A major early Alpine obduction phase, for which there is no clear evidence, would have been necessary to allow the Versoyen domain to be derived from the Piémont oceanic realm (right-hand side of the diagram). Palæogeographic contiguity of Versoyen and Tarentaise domains (left-hand side of the diagram) is more probable. *B* = Briançonnais domain, *P* = Piémont oceanic domain, *T* = Tarentaise domain, *V* = Versoyen domain.

4.4-3 Discussion

Returning to the questions posed at the beginning of this chapter:

First, what are the structural affinities of the Versoyen complex? Does it represent part of the Tarentaise Basin or a palæogeographically unrelated far-travelled thrust sheet? The evidence is inconclusive but field relations in Comba di Planaval coupled with the absence of realistic candidates for an intervening palæogeographic belt permit the belief that the Versoyen complex essentially constituted the outboard portion of the Tarentaise Basin prior to Alpine collision. This is also the most reasonable explanation from a structural point of view since derivation of the Versoyen complex from the Piémont domain would require tectonic contortions for which there is little evidence (Fig. 4-16). Thus, Antoine's (1971, 1972) belief in stratigraphic continuity between the Versoyen pelites and the Arguerey/Peula Formation does seem to be the most likely explanation. Acceptance of this correlation dates the age of the igneous activity as late Cretaceous since the intrusions have been shown to be broadly syn-sedimentary (section 4.1-3) and the Arguerey contains Santonian–Maastrichtian microfossils (section 1.4-3).

Second, what are the origins of the basaltic magmas? Are they related to oceanic spreading, arc volcanism or continental rifting? Again, the available evidence does not compel a particular interpretation, but the trace element geochemistry is difficult to reconcile with arc volcanism and is most consistent with a MORB-like provenance. True mid-ocean ridge basalts are thought to be produced by relatively large degrees (10-20%) of partial melting of the upper mantle (*e.g.* Klein & Langmuir, 1987). The impetus for this melting is provided by regional lithospheric stretching which induces passive upwelling (and hence adiabatic decompression) of the asthenosphere (*e.g.* Foucher *et al.*, 1982). Alternatively, voluminous tholeiitic magmatism with MORB-similar characteristics can also be produced as a result of the influence of mantle thermal plumes. Since plume-related asthenospheric temperature anomalies have a typical diameter in excess of 2000km at the base of the lithosphere (Griffiths & Campbell, 1990), volcanism is generally induced over a wide area, and preferentially at sites of previous lithospheric stretching (Thompson & Gibson, 1991). An absence of late Cretaceous tholeiitic magmatism from the Tethyan belt negates the possibility of a plume origin for the Versoyen basalts and makes it necessary to infer an extension-driven genesis. Theoretical and empirical findings indicate that significant rift-related volcanism can be produced at stretching factors as low as

β=2 (where β = the ratio of final to initial surface area of the stretched region), but that such volcanism is almost inevitably alkaline; tholeiitic magmas appear to require β>3 (Le Pichon & Sibuet, 1981; McKenzie & Bickle, 1988). Thus the Versoyen complex probably represents a zone of intense (if perhaps localised) extension.

An analogy has been drawn by Loubat (1975, 1984) and Kelts (1981) between the lower Penninic 'ophiolitoids' (including the Versoyen complex) and the Pliocene to Holocene situation in the Gulf of California, where incipient sea-floor spreading occurs in an area of rapid active sedimentation, resulting in young, upwardly mobile basaltic melts intruding water-rich sediments (Einsele *et al.*, 1980). The analogy is indeed striking, to the extent that trace element characteristics reported from the Gulf of California basalts (Saunders *et al.*, 1982) are very similar to those obtained here from the Versoyen metabasites. Drilling in the central and northern Gulf of California encountered only tholeiitic sills and intercalated sediments with no unequivocal extrusives (Saunders *et al.*, 1982). Einsele *et al.* (1980) have demonstrated that sill injection was accompanied by expulsion of sediment porewaters which served both to provide space for the intrusions and to set up a localised hydrothermal circulation. One effect of this hydrothermal activity could be an alteration path similar to that envisaged for the Versoyen metabasites (section 4.4-2). Thus the central Gulf of California analogue may well be worth pursuing as part of future research into the Versoyen complex.

4.5 SUMMARY

1) The Versoyen complex comprises a stratigraphically distinct thrust-bounded package derived from the internal margin of the Tarentaise Zone.

2) Stratigraphically, the Versoyen units involve metabasaltic sills intruded into a thick pelitic succession which in turn unconformably overlies leucogranitic basement (*i.e.* fairly convincing continental crust).

3) Contact relationships in the high Breuil valley indicate that the basaltic sills were emplaced into wet, unconsolidated sediment.

4) In the Comba di Planaval, Versoyen metabasite sheets are enclosed in Aroley Formation metasediments.

5) The metabasites resemble MORB tholeiites in terms of trace element geochemistry, although compositions have been modified by post-magmatic fluid interaction.

6) The style of chemical alteration of the basalts is suggestive of the operation of high-temperature hydrothermal processes.

7) The Versoyen tholeiites testify to intense lithospheric stretching adjacent to a zone experiencing rapid vertical tectonic movements, suggesting a possible genetic link between the Versoyen magmatism and opening of the Tarentaise Basin.

CHAPTER 5 BASIN FORMATION

It is accepted that the Alps formed as a result of continental collision between the European and Apulian plates during the late Cretaceous and early Tertiary. The ocean consumed by this convergence, the Piémont-Ligurian Tethys, is thought to be the product of early Jurassic lithospheric stretching. Thus, the elevation of the Alpine mountain chain involved the orogenic re-stacking of the opposing continental margins of this Mesozoic oceanic domain. Attempts to understand the subsidence histories of these continental margins have spawned a number of models which have proven influential among Alpine workers (*e.g.* Winterer & Bosellini, 1981; Lemoine *et al.*, 1986). However, geological studies in the crucial internal zones are severely hampered by an inconsiderate tectono-metamorphic overprint and consequently these models have not been adequately tested for the zone of presumed maximum Mesozoic extension. The late Cretaceous sediments of the Tarentaise Zone may allow a partial test of some of these ideas. This chapter examines the formation of the Tarentaise Basin in the context of the Tethyan continental margin system and discusses the implications of active late Cretaceous subsidence for the passive margin model.

5.1 THE TETHYAN CONTINENTAL MARGINS

Stratigraphic differences between lithotectonic units exposed in the Alps point to the existence of several distinct palæogeographic domains during the Mesozoic. Recognition that, palinspastically, these domains crudely define a contemporaneous transition between shallow water sediments overlying continental basement and pelagic facies apparently deposited on oceanic crust (section 1.3) has allowed the wholesale interpretation of these palæogeographic domains as a continental margin system bordering the Mesozoic Tethys. Numerous analogies have been drawn between the evolution of Tethyan stratigraphies and the development of parts of the Atlantic continental margins (*e.g.* Bernoulli, 1972; Graciansky *et al.*, 1979; Lemoine *et al.*, 1986). A basic implication of the passive margin interpretation is that the formation of the Alpine palæomargins was a result of regional extension. Hence the prevailing

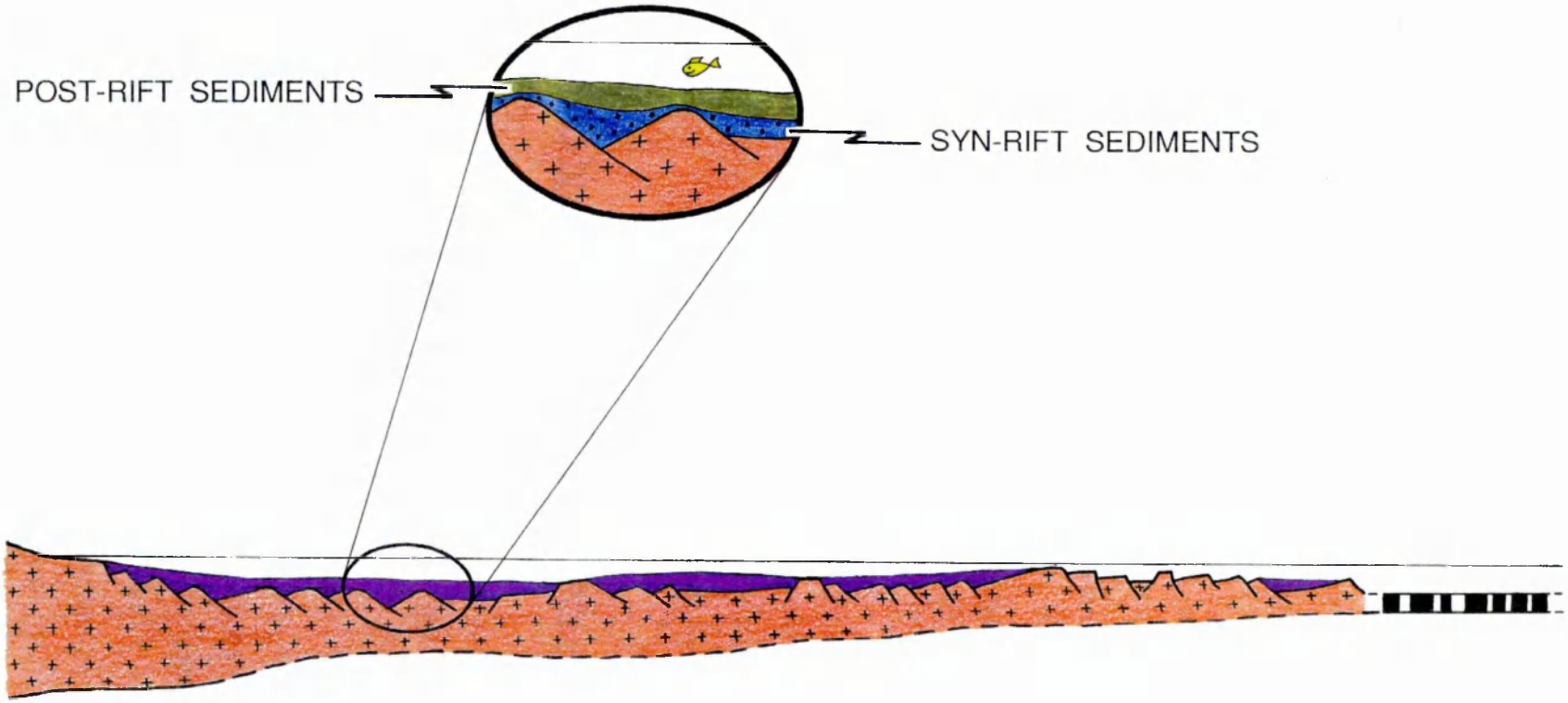

Fig. 5-1. Cross sectional view of a hypothetical mature passive margin formed essentially by bulk pure shear extension of the crust (crosses) and sub-continental lithosphere. The relative thickness of syn-rift versus post-break-up deposits is a function of sediment availability: if sediment input remains roughly constant, the thermal subsidence package may be somewhat thicker than than the syn-rift.

belief that their subsidence should be explicable in terms of theoretical models of lithospheric stretching (*e.g.* Ménard *et al.*, 1991; Wooler *et al.*, 1992).

5.1-1 Stretching Models

It is generally accepted that passive margin subsidence is a direct consequence of lithospheric thinning during regional extension (Barr, 1992). Simple lithospheric stretching models which have evolved from the ideas of McKenzie (1978) appear to account adequately for the observed stratigraphies of rifted continental margins (Sclater & Christie, 1980; Le Pichon & Sibuet, 1981; Sawyer *et al.*, 1982; Barton & Wood, 1984; White, 1990; Bott, 1992). Such models predict a two-stage subsidence history for extending continental crust: an initial fault-controlled rift stage being followed by a longer phase of gradual subsidence related to the decay of the initial thermal perturbation. Subsidence is driven primarily by isostatic effects throughout. Thus, during rifting, continental crust is stretched, thinned and effectively replaced by passively upwelling denser asthenospheric material (elevated above the initial depth to the base of the lithosphere). The need for isostatic compensation mandates crustal subsidence. Since the thermal recovery time of the lithosphere is long (60-100Ma) compared with the duration of active rifting (typically 10-30Ma), vertical separation between isotherms decreases and the young basin experiences high heat flow (McKenzie, 1978; Jarvis & McKenzie, 1980). Following rifting, this compressed geothermal gradient gradually decays by conductive heat loss, promoting further post-rift subsidence as a result of thermal contraction and lithosphere re-thickening (Sleep, 1971). The magnitude of extension-produced subsidence is amplified by loading due to sediment accumulation on the continental margin. As the lithosphere cools, its flexural rigidity increases, distributing this load effect over a broader area and promoting progressive cratonward onlap of successively younger sediments (Watts, 1982; Karner & Watts, 1982), resulting in a so-called 'steer's head' profile (Dewey, 1982). Typically, sediments deposited during the post-rift stage are comparable in thickness to, or somewhat thicker than, those deposited during stretching (Le Pichon & Sibuet, 1981; Bott, 1992). In passive margin settings (Fig. 5-1), the onset of the post-rift phase is approximately synchronous with continental break-up and the initiation of sea-floor spreading (*e.g.* Brice *et al.*, 1983). The transition from stretched continental to accreted oceanic lithosphere is seen as being controlled by the production of a threshold volume of partial melting in the

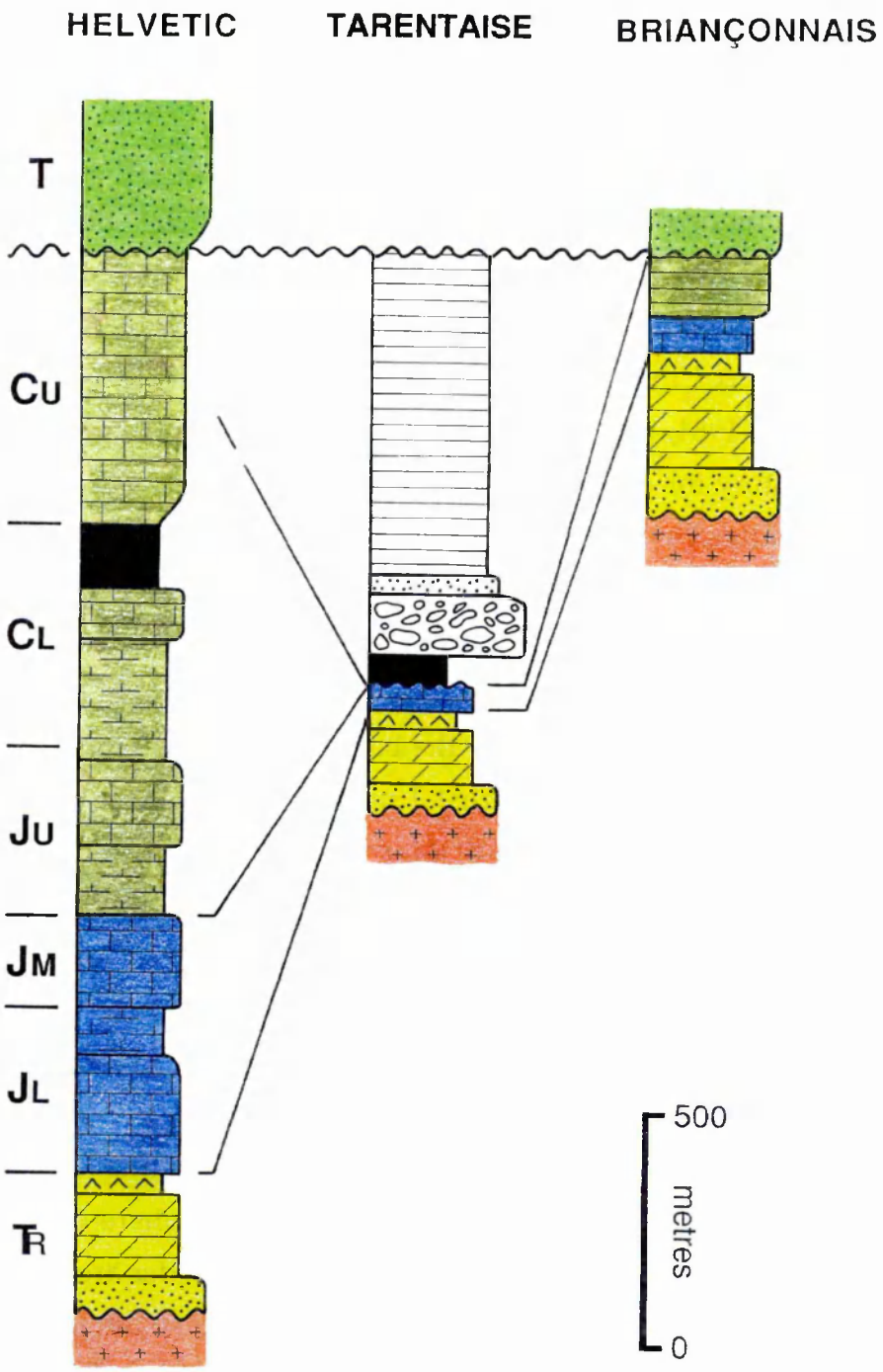

Fig. 5-2. Simplified stratigraphic profiles for three of the principal palæogeographic domains in the Western Alps, showing (perhaps) syn-rift in blue, post-break-up in that rather nasty olive green and syn-orogenic 'flysch' in brighter green. The fill of the Tarentaise Basin, which is difficult to pigeonhole into any of these classes, is unshaded. Based on Debelmas & Kerckhove (1980) and Lemoine *et al.*, (1986). Abbreviations: *CL–U* = Lower–Upper Cretaceous; *JL–M–U* = Lower–Middle–Upper Jurassic; *T* = Tertiary; *TR* = Triassic.

uppermost asthenosphere (Foucher *et al.*, 1982). For the uniform stretching model of McKenzie (1978), this appears to require regional stretching of $\beta > 3$ for mantle of normal temperature (Foucher *et al.*, 1982). Figure 5-1 depicts a profile through a hypothetical, thermally mature (*i.e.* late post-rift subsidence stage) passive continental margin developed as a result of simple lithospheric stretching.

5.1-2 Application of Stretching Models to Alpine Stratigraphy

On the basis of stratigraphic studies in the Western Alps, it has become widely accepted that simple lithospheric stretching models can account for the Mesozoic development of the North Tethyan continental margin (section 1.3-1). Superficially, the gross stratigraphy of the Alpine remnants of this margin (Fig. 5-2) accords well with an early Jurassic 'rift' phase followed by 'thermal' subsidence into the Cretaceous; stratigraphic thicknesses diminishing oceanwards as a function of increasing water depths (Winterer & Bosellini, 1981; Lemoine *et al.*, 1986; Ménard *et al.*, 1991). Recent work by Wooler *et al.* (1992) marks the first significant attempt to apply quantitative concepts of lithospheric stretching to analysis of the Tethyan palæomargins. Wooler *et al.* (1992) derive subsidence curves for Mesozoic stratigraphic sections from both the northern and southern passive margins in an attempt to quantify the magnitude and duration of the stretching episode (Fig. 5-3). Their results are interesting for two reasons: first, they suggest that rifting commenced somewhat earlier than previously believed (*i.e.* early/mid Triassic rather than late Triassic); and second, the inferred stretching factor is generally small ($\beta = 1.1$-1.3). The analysis includes eight sections from the Western Alps: two from the Dauphinois Zone, one from the Sub-Briançonnais Zone and five from the Briançonnais. For the latter, a low stretching factor ($\beta \approx 1.1$) is unsurprising since Jurassic sequences are condensed or absent in the Briançonnais and this domain is thought to have acted as an anomalously high-standing block through much of the Mesozoic (*e.g.* Trümpy, 1982; Lemoine *et al.*, 1986). The stretching factors deduced by Wooler *et al.* (1992) for the Dauphinois Zone are slightly higher ($\beta \approx 1.3$) but are still relatively low for the margin to a spreading ocean (β ranges up to 2 in the North Sea and $\beta \geq 3$ is thought to be required for the formation of oceanic lithosphere). Both of the stratigraphic sections used in this case were taken from Jurassic platform areas rather than the main Dauphinois depocentre (the Vocontian Trough). Wooler *et*

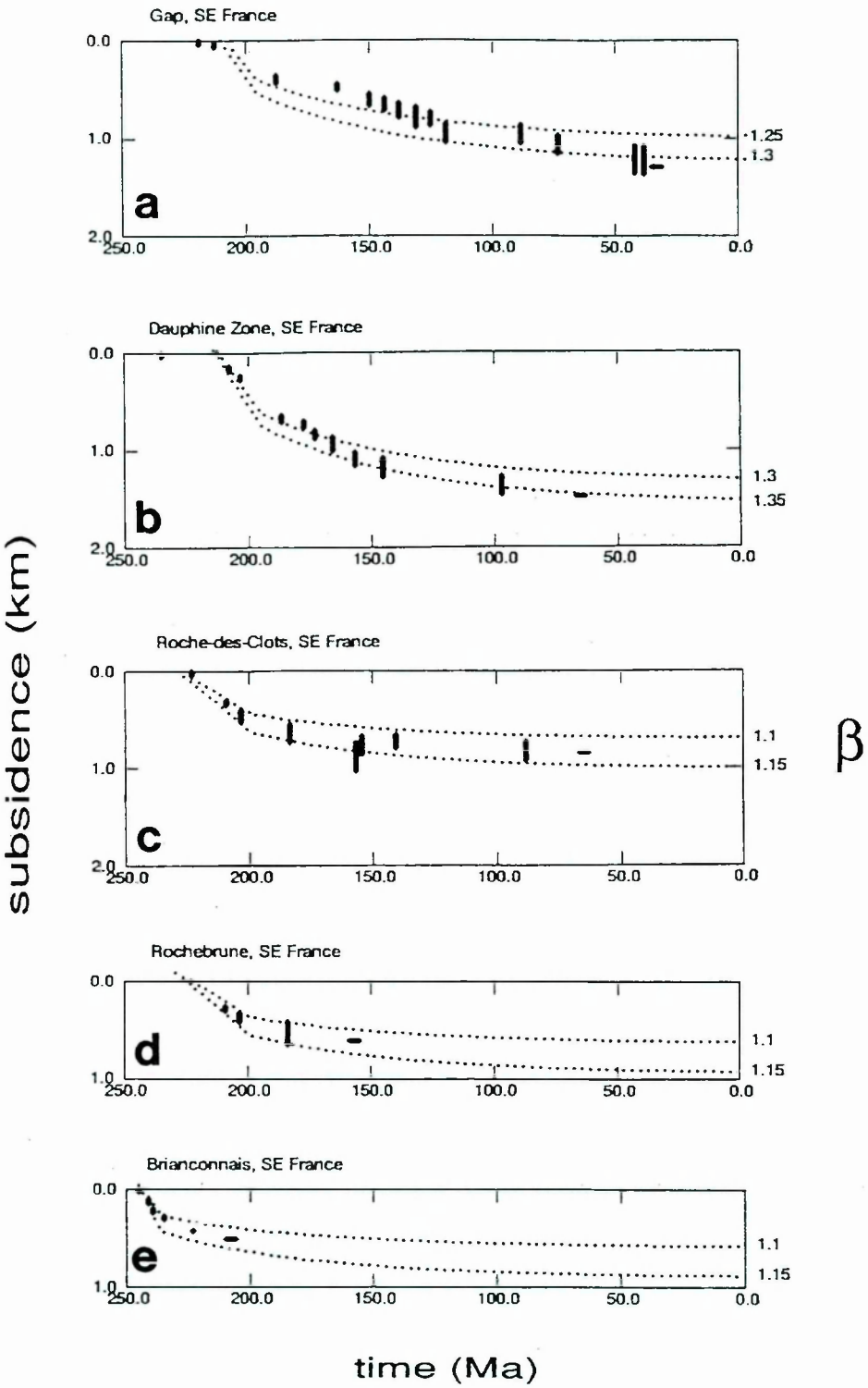

Fig. 5-3. Subsidence curves determined by Wooler *et al.*, (1992) for stratigraphic sections from the Western Alps. **a** and **b** are from the Dauphinois Zone and display stretching factors of 1.3 with an apparent onset of rifting at ~210Ma. **c**, **d** and **e** are seemingly from the Briançonnais Zone: the inferred stretching factor is 1.1 in each case, assuming that rifting began at 220-245Ma.

al. (1992) did not attempt to analyse any sections from the Ultra-Briançonnais or Piémont Zones. The former existence of a spreading ocean implies that extension would have attained $\beta \geq 3$ at the outboard edge of the European continental margin. Consequently, the results of Wooler *et al.* (1992) appear to indicate that most of the associated continental extension was concentrated in the Piémont domain.

The onset of rifting is usually dated as latest Triassic to early Jurassic from stratigraphic evidence for increased subsidence rates and the development of widespread block faulting (*e.g.* Bernoulli & Jenkyns, 1974; Barfety *et al.*, 1979; Grand *et al.*, 1987). In contrast, the subsidence curves of Wooler *et al.* (1992) place the start of stretching in the early to mid Triassic (typically 245-230Ma), which would significantly shift the pre-rift/syn-rift distinction on Fig. 5-2. The notion of early Triassic rifting is not, however, supported by evidence of extensional faulting or widespread volcanism at this time, which casts some doubt on the hypothesis. Early to mid Triassic sequences are very thick (several hundreds of metres) in parts of the Alps and the origins of the subsidence which accommodated these deposits require clarification. However, a genetic link between this early subsidence and the subsequent (late Triassic to early Jurassic) Tethyan rifting is unsubstantiated. Thus, the ages of earliest rifting proposed by Wooler *et al.*, (1992) appear to have been assigned rather arbitrarily.

Although some uncertainty surrounds the details, acceptance that Alpine Mesozoic stratigraphy records syn-rift and post-break up phases of subsidence is borne out by detailed qualitative analyses (*e.g.* Lemoine *et al.*, 1986) and preliminary quantitative studies (Wooler *et al.*, 1992). Hence it seems reasonable to redraw Fig. 5-1 specifically for the Western Alps (Fig. 5-4). This then constitutes an ostensibly plausible prediction for the state of the North Tethyan continental margin in the mid to late Cretaceous prior to the onset of plate convergence: highly attenuated and therefore deeply submerged.

5.2 THE TARENTAISE BASIN

The younger stratigraphy of the Tarentaise Zone represents a basin developed on the southern continental margin of Europe sometime in the late Cretaceous which became closed and dismembered during the Tertiary by the Alpine orogeny. Basic inferences concerning the early infilling of the Tarentaise Basin, as deduced

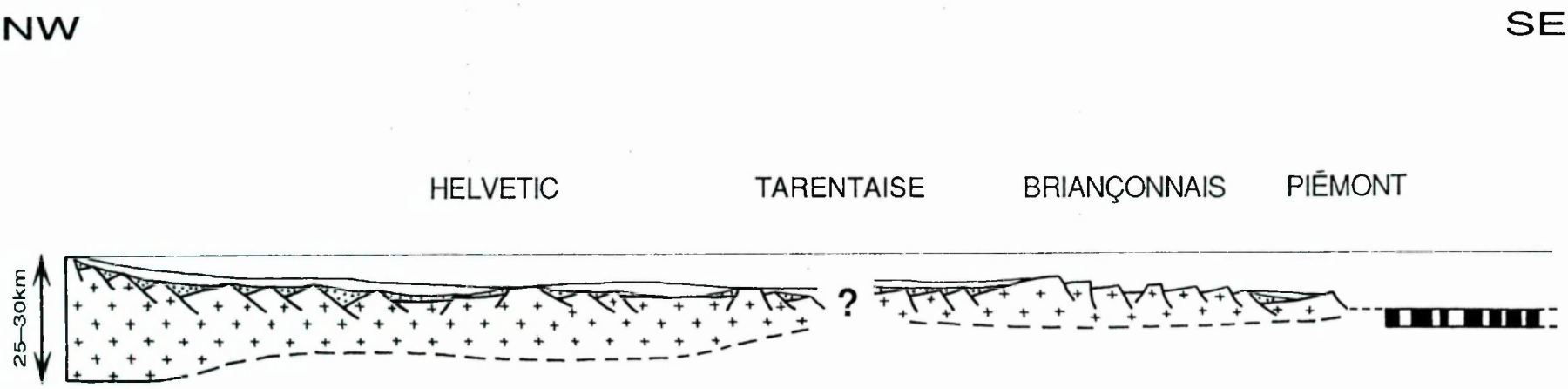

Fig. 5-4. The general mature passive margin model of Fig. 5-1 redrawn specifically for the palæogeographic domains represented in the Western Alps. This constitutes the predicted situation for the north Tethyan continental margin in the mid to late Cretaceous (prior to the onset of plate convergence and about 100 Ma after the onset of rifting): highly attenuated and deeply submerged. Implied vertical scale is shown, horizontal scale uncertain. Modified after Lemoine *et al.* (1986).

from the sedimentology of the Aroley Formation, are detailed in chapter three. This evidence is strongly suggestive of active (*i.e.* fault controlled) subsidence. This section considers additional stratigraphic data which provide critical constraints on models of basin formation.

5.2-1 The Basal Unconformity

The sequence boundary marking the onset of late Cretaceous subsidence (Fig. 5-5) is a major truncation surface of regional extent (*i.e.* across the whole of the Tarentaise Zone). The timing of subsidence is constrained only by Antoine's (1965) discovery of *Globotruncana lapparenti* at the top of the Arguerey Formation, which indicates an age of late Santonian to early Maastrichtian (*i.e.* approximately 85-70 Ma). Cretaceous units rest upon all of the substratal formations including crystalline basement (at 3079 50421). An angular discordance of bedding dip across the unconformity is usually evident (Fig. 5-6), indicating the involvement of tectonic uplift in its formation. Unequivocal evidence of subaerial exposure is lacking but submarine processes are only considered to be capable of deeply eroding lithified bedrock locally within canyons (Shanmugam, 1988) and a subaerial origin for the unconformity seems clear. Possible palæosols are represented by an Fe^{3+}-encrusted surface at 31967 506130 (*cf.* Antoine *et al.*, 1972b; Fudral, 1973), a nodular clay-rich horizon at 31965 505875 and a regolith-like veneer at 32312 506227. Since the subaerially-formed unconformity is directly overlain by deep-sea sediments (shales and turbidites which have yielded off-shelf planktonic foraminifera), without any intervening shallow marine deposits, subsidence must have been very rapid relative to sedimentation. A significant time lag may have elapsed between initial subsidence and the onset of sedimentation but this is unconstrained.

5.2-2 Cretaceous Stratigraphy

The various elements of the Cretaceous stratigraphy (Fig. 1-8) form a sequence which is continuous from the Arguerey Formation up to at least the lower parts of the St. Cristophe Formation, a thickness of 400-800m. Above this, low bulk competence and high anisotropy have spawned a degree of structural complexity which has so far defied stratigraphic analysis. Boundaries between the four formations are essentially gradational, except for the base of the Aroley, which is locally erosive into the shale-rich Arguerey Formation. The Aroley, Marmontains

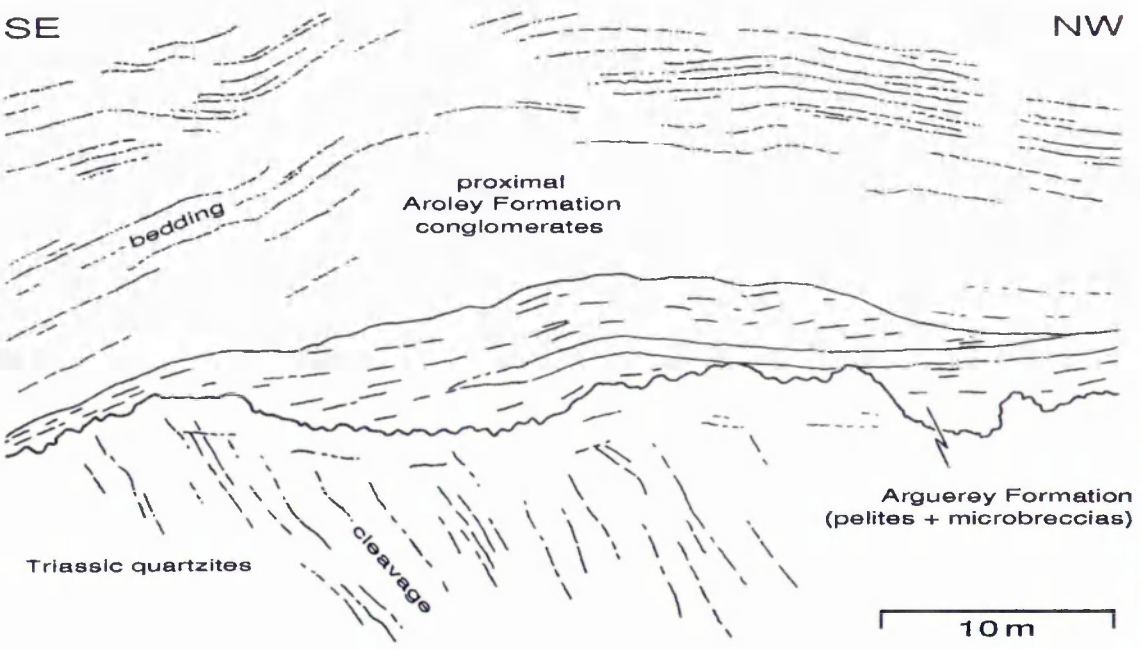

Fig. 5-5. The unconformity at the base of the Cretaceous Tarentaise Basin-fill in the Seloge thrust sheet. View looking south-west towards 32860 505918 showing an irregular top to massive Triassic quartzites (bedding not discernible) blanketed by a thin interval of fine-grained deposits (Arguerey Formation).

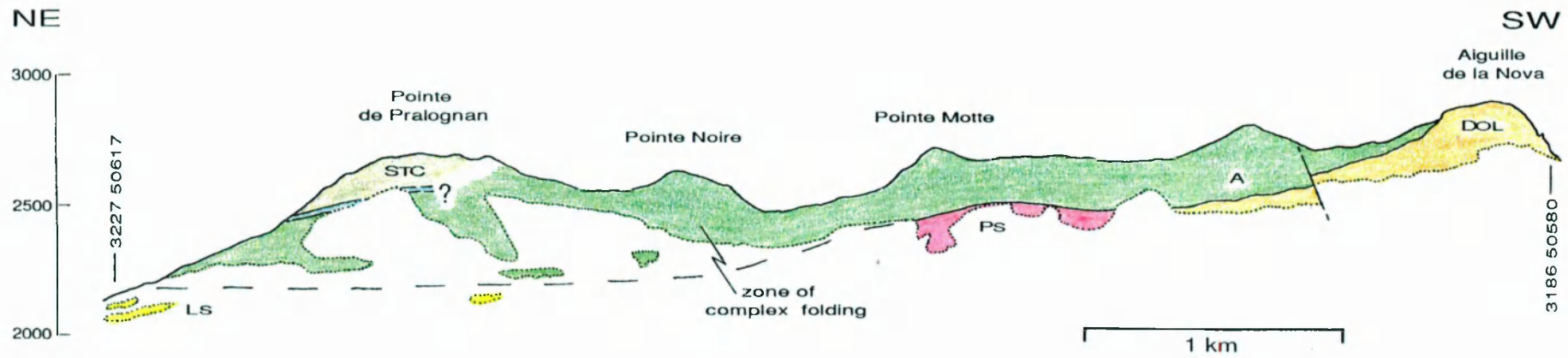

Fig 5-6. **a)** Exposure of the unconformity in the cliffs forming the south-east edge of the Combe de la Neuva, showing the Aroley Formation resting on progressively older substratal units from north-east to south-west. The Arguerey Formation is very thin or absent here. Section line lies almost normal to the thrust transport direction (the Seloge Thrust crops out 100-300m below the unconformity). Dotted line indicates lower limit of exposure (*i.e.* top of scree). Abbreviations: *A* = Aroley Formation; *DOL* = Triassic dolomites; *LS* = Liassic limestones; *PS* = Triassic psammites; *STC* = St. Cristophe Formation.

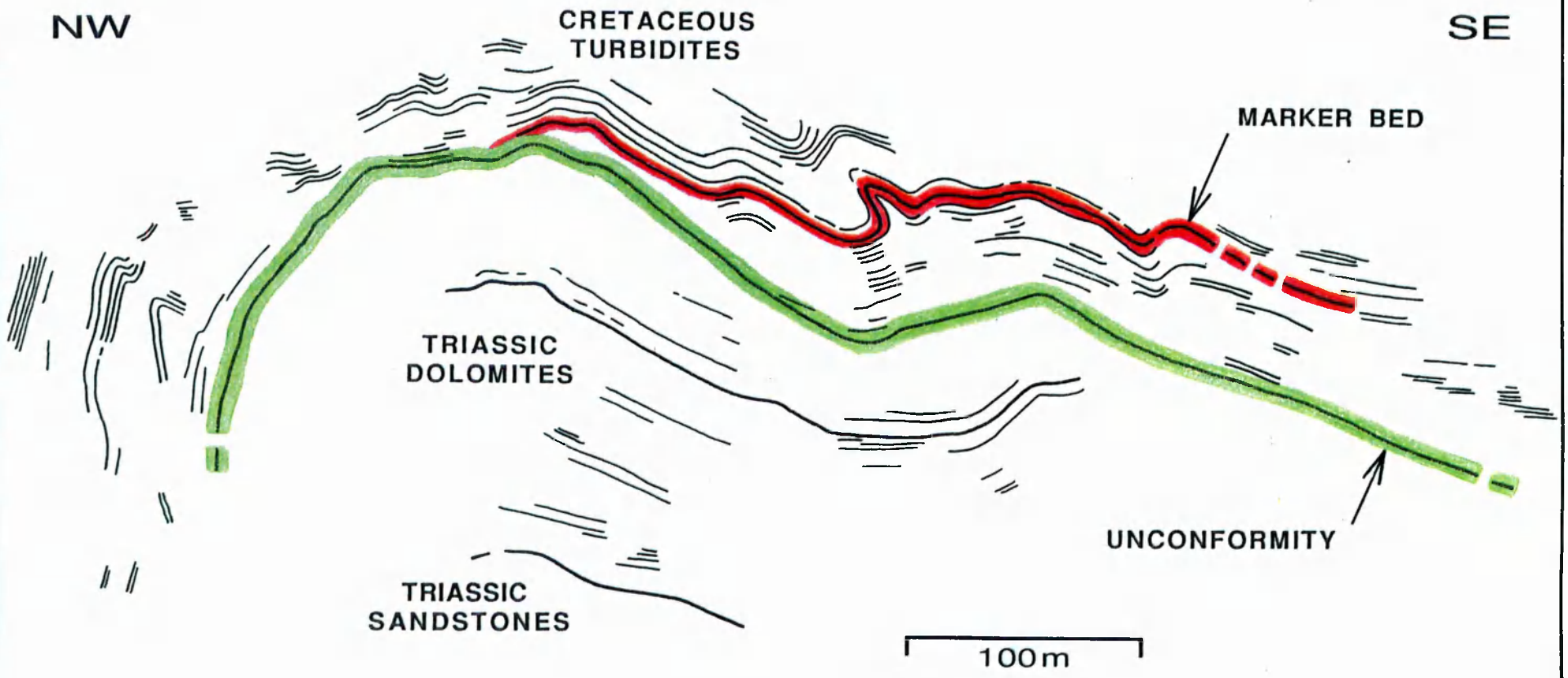

Fig. 5-6. **b)** Angular discordance across the unconformity at 3245 50614 in the Vallée des Chapieux showing truncation of bedding in dolomites and apparent onlap of Aroley Formation turbidites onto the unconformity. Section normal to fold axis and approximately parallel to thrust displacement direction. (Note that this is a different view of the structure shown in Fig. 2-30.)

and basal St. Cristophe together form a progression of upwardly decreasing grain-sizes and bed thicknesses. This progression is not a smooth, monotonic transition (*e.g.* Fig. 3-2) but it is nonetheless a definite and consistent trend of basin-wide extent (*cf.* Antoine, 1971; Fudral, 1973; Collart, 1973; Jeanbourquin & Burri, 1991). The modal composition of the coarser-grained facies remains approximately similar throughout this vertical sequence: gritty litharenites in the lower St. Cristophe Formation contain dolomite, limestone, sandstone and 'basement' fragments in roughly the same proportions (typically 60:10:20:10) as the coarse conglomerates of the Aroley Formation. The Marmontains Formation represents a brief compositional excursion away from a carbonate-dominated provenence (section 1.4-2) but litharenites in this formation nevertheless contain clasts of dolomite (typically 35-45%), limestone (~5%) and crystalline feldspathic material (~10%) in addition to the main quartzose component.

The observations outlined above are indicative of relatively progressive denudation of a single source terrain, sediment supply to the basin waning over time. This is most easily explained by a model in which uplift (and subsidence) rates were initially high but diminished rapidly, forming a steep basin margin relief which was more gradually degraded by processes of erosion and deposition. The influence of sea-level fluctuations on sediment supply is difficult to resolve from the stratigraphic data. In principle, it would be possible to 'backstrip' the Tarentaise stratigraphic column to obtain a detailed curve of subsidence against time using the method described by Watts & Ryan (1976). In practice, this would be fruitless since age constraint is currently virtually non-existent and palæobathymetries are unknown.

5.2-3 Sediment Derivation

One of the most prominent map scale sedimentological attributes of the early Tarentaise basin-fill is the south-eastward diminution of grain-sizes and bed thicknesses (*e.g.* Antoine, 1971, 1972), which occurs in a down-current direction relative to the available palæocurrent data (Figs. 2-48 and 3-12). This primary observation remains valid when tectonic complexities are considered (section 2.4-3). The obvious conclusion is that sediment entered the basin from its western or north-western edge (see section 3.2-4). Grain-sizes and grain shapes are suggestive of short-range sediment derivation. Clasts types evident in the Aroley Formation (Fig. 3–10) are all similar to the lithologies observed in the substratum

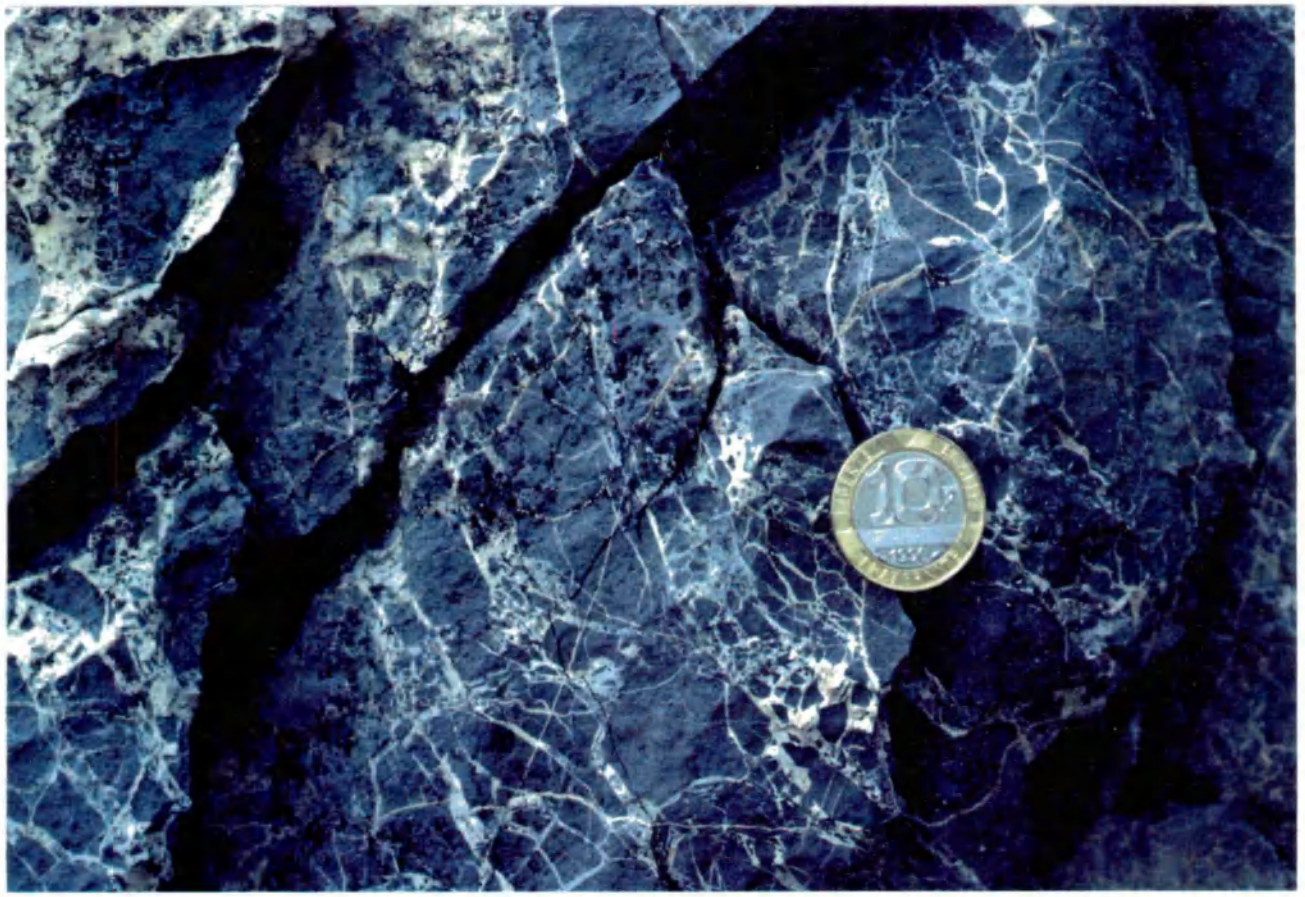

Fig. 5-7. Small scale example of *in situ* fragmentation of massive limestone in the Triassic carbonate sequence at 32050 506133, Plan Varraro thrust sheet. The fractures are filled by a mixture of finely comminuted limestone and calcite cement. The coin is 22mm across.

and do not indicate significant input from an exotic source (section 3.2-4). This conclusion is supported by data from Wildi (1985), whose synthesis of heavy mineral suites in Alpine 'flysch' includes nine samples from the Cretaceous rocks of the Tarentaise Zone. The dense mineral fractions in these samples are dominated by zircon, tourmaline, apatite and rutile; consistent with derivation from an essentially non-metamorphic continental terrain. In contrast, the heavy mineral assemblages of the 'true' Alpine flysch units (*e.g.* the North Penninic flysch of the Prealps) generally contain garnet ±staurolite, indicative of a relatively high-grade metamorphic source component (*op. cit.*). For the Tarentaise Basin then, sediment supply from a local uplifted source area adjacent to the western basin margin is implicated (perhaps the 'cordillera tarine' envisaged by Barbier (1948) or the 'Hautecour cordillera' of Antoine, 1971: see section 1.4-2).

5.2-4 A Fault Controlled Basin Margin?

All the available data indicate that early fill of Tarentaise Basin was sourced from its western or north-western edge. What was the nature of this basin margin? In chapter 3 it was proposed that the Aroley Formation represents an immature sediment body deposited proximally to a rapidly eroding source area and that the sediment transport gradient linking source to basin is most likely to have been tectonically generated. The structurally lowest, most external portions of the Tarentaise Zone (see section 2.3-5) expose a number of sedimentological features which indirectly corroborate this interpretation, pointing towards the presence of an extensional fault system along the western basin margin.

***In situ* brecciation of the 'substratum'** is a common feature of the most external parts of the Tarentaise Zone (primarily the Plan Varraro thrust sheet) which is not evident in the rest of the Zone. Partial brecciation of the Liassic limestones of the Piramidi Calcaree (331 5070) was noted in passing by Antoine (1971) but otherwise the feature has apparently not previously been reported from the Tarentaise.

Description. The brecciation is observed chiefly in the massive carbonate lithologies of the Lias and Trias. A variety of different styles is apparent but most typically, a random fracture network defines a mosaic of coarse (2–200mm), angular to subangular carbonate fragments separated by a matrix of comminuted carbonate grains and calcite cement (Fig. 5-7). All of the breccias are monomict

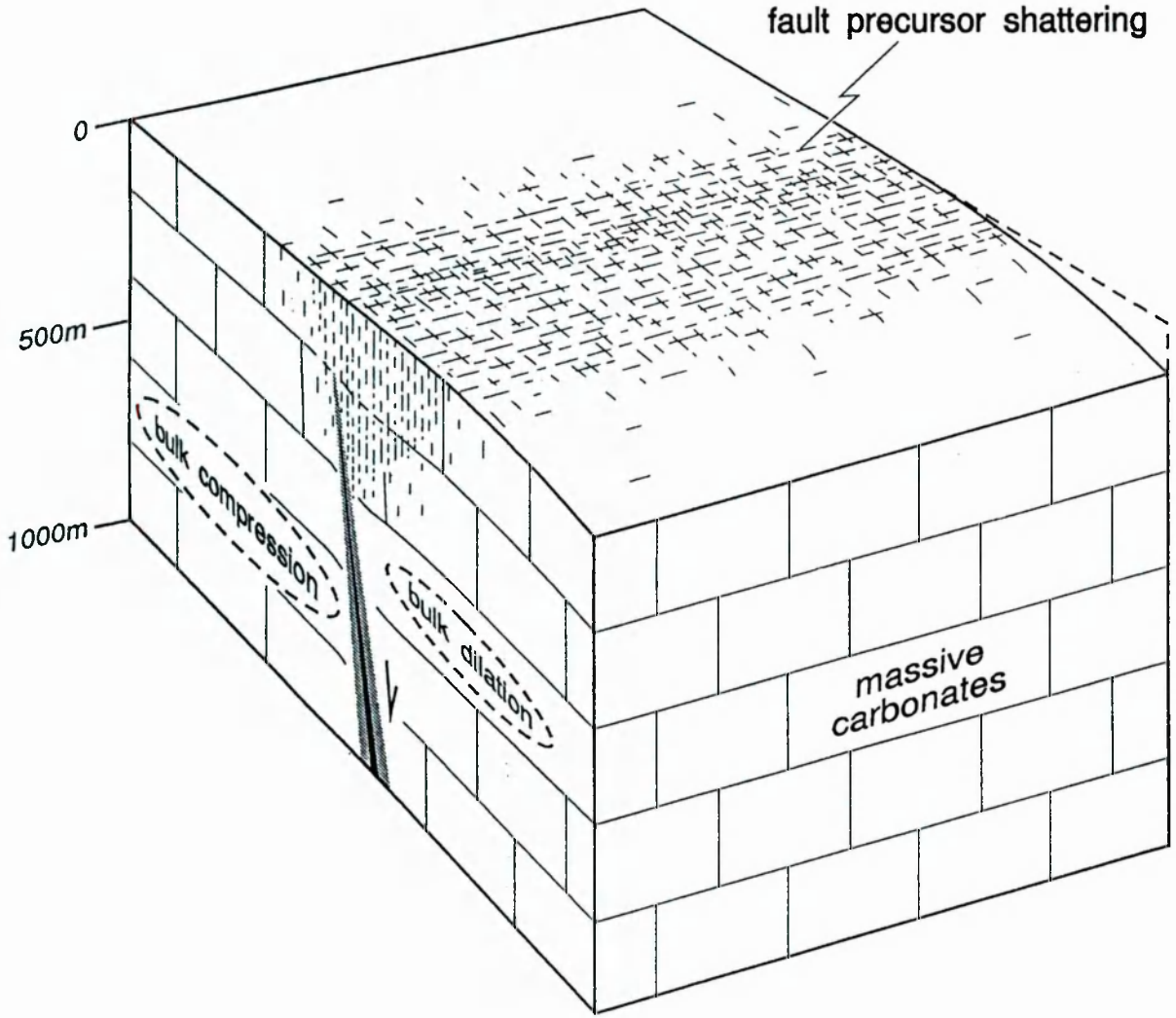

Fig. 5-8. Model for the formation of fragmentites such as those shown in Fig. 5-7 by near-surface shattering of massive carbonates above an upward-propagating fault tip. Adapted from Stewart & Hancock (1990).

and fabrics are generally chaotic. Some exposures show a gradual transition to unfractured rock of identical composition. In these cases, the fracture 'front' is observed to cross-cut bedding at a high angle.

Interpretation. This fragmentation is readily explicable as fault precursor shattering. Sibson (1986) has discussed the distributed microfracturing which may occur around a propagating fault when movement is impeded on the main slip plane. Stewart & Hancock (1988, 1990) describe partial brecciation of carbonate lithologies from zones around active normal faults in the Aegean region which may be formed in this way. The genetic model proposed by Stewart & Hancock (1990) accounts for the brecciation in terms of distributed brittle deformation ahead of an upwardly propagating fault tip (Fig. 5-8). The phenomenon is thought to be restricted to very shallow crustal levels (<500m), where confining pressures are low, and to the immediate vicinity of active propagating faults (Sibson, 1986; Stewart & Hancock, 1990). In view of the metamorphic grade and the lack of spatial correlation with observed contractional structures, the shattering presumably relates to pre-orogenic faulting.

The Brèches du Grand Fond (see section 1.4-2) separate the Aroley Formation from its pre-Cretaceous substratum in the external (structurally lower, western) part of the Tarentaise Zone. As with the fracturing described above, these breccias are a feature of the Plan Varraro thrust sheet and are not significantly developed elsewhere.

Description. These rudites form a very coarse, unsorted, clast-supported, polymict debris pile as described in section 1.4-2. Clast angularity is generally high and some blocks show internal fracturing similar to that outlined above. The uppermost breccias are matrix-rich and crudely sorted. Facies which may be transitional between these matrix-supported Grand Fond–type breccias and facies CD of the Aroley Formation, which is interpreted as the product of cohesionless debris flow processes (section 3.2-2), are exposed in the external part of the Seloge thrust sheet (Fig. 5-9).

Interpretation. The presence of these breccias in the Plan Varraro thrust sheet requires a steep, actively eroding sediment source towards the western edge of the early basin. The highly fractured, eminently erodible material described above (Figs. 1-9c and 5-7) would provide an obvious source. The bulk of the

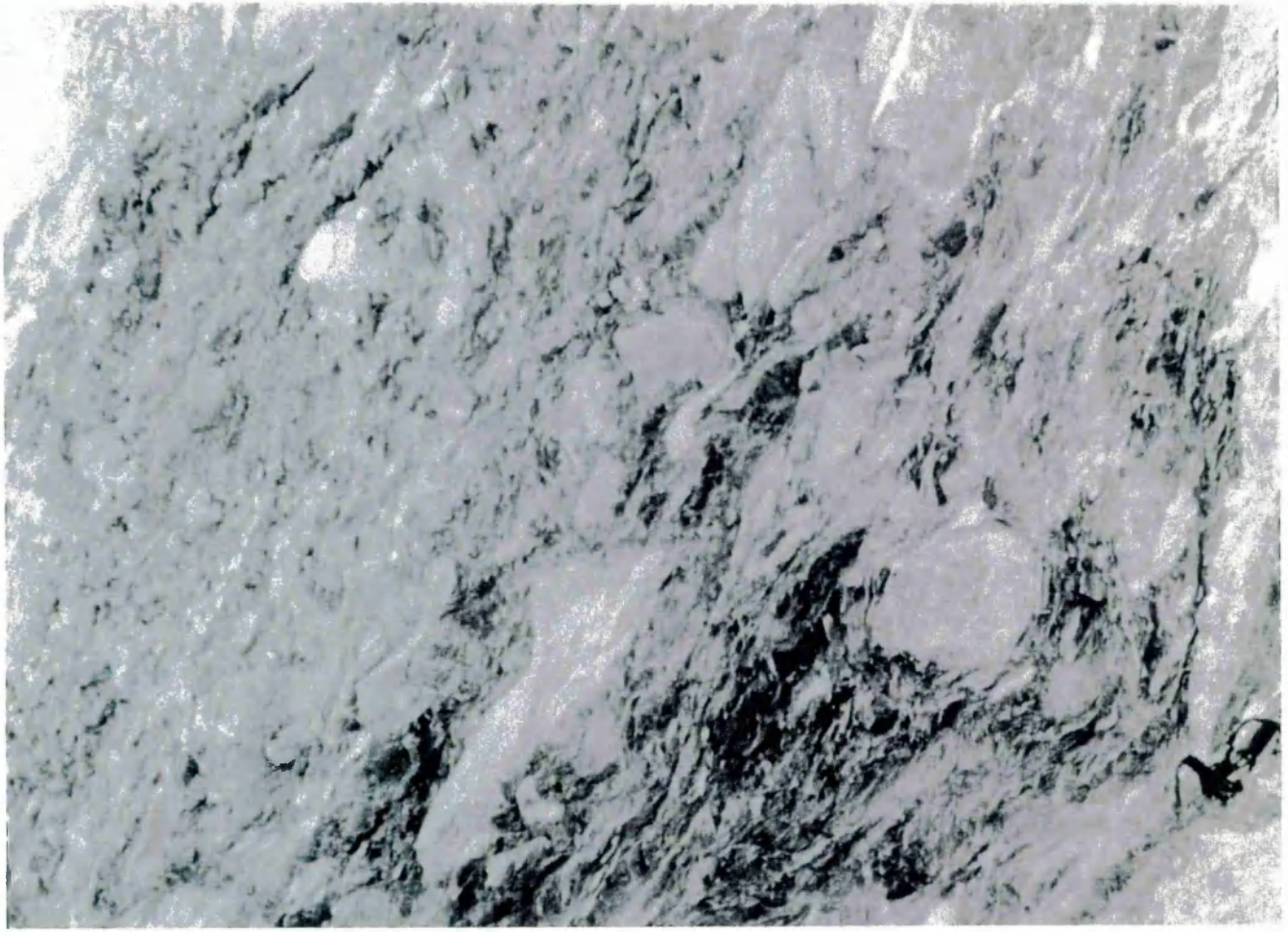

Fig. 5-9. Very coarse composite matrix-supported breccio-conglomerate unit which represents a transition between the Brèches du Grand Fond and facies CD of the Aroley Formation (see section 3.1). View looking SSW at an inverted SE-dipping bed, ~14m thick, at 32328 506187 in the Seloge thrust sheet. Rucksac (70cm) in the bottom right corner for scale.

Grand Fond rudites, which are structureless and clast-supported, is readily interpreted as scarp talus, emplaced essentially by gravity-fall processes adjacent to a rocky headwall. A subaqueous setting is likely as the preservation potential of subaerial talus is extremely low. Debris-fall avalanching involves the downslope movement of granular dispersions in which each component is driven essentially by its own momentum (*cf.* Laznicka, 1988; Nemec, 1990). The upper, matrix-rich, parts of the breccia sequence probably represent a transition to more highly concentrated debris avalanches in which enhanced particle interference led to the development of dispersive pressures, suppressing the tendency for clast segregation and promoting a relatively coherent mass-flow rheology. Since the Brèches du Grand Fond constitute the oldest sediments in this part of the basin, their parent scarp is likely to be directly related to the basin-forming event. Thus, the breccias record the degradation of a steep, fault-related slope initially close to, or delimiting, the western margin of the Tarentaise Basin.

5.2-5 The Versoyen Complex

As discussed in chapter 4, the MORB-like metabasites of the Versoyen Zone are most easily interpreted as the products of extension-driven partial melting of the asthenosphere. The metabasites are interleaved with Aroley Formation turbidites (Fig. 4-7) and with Arguerey Formation pelites which were unconsolidated at the time of intrusion (section 4.1-3). Thus the Versoyen volcanism occurred concomitantly with opening of the Tarentaise Basin. Theoretical considerations (Le Pichon & Sibuet, 1981; Foucher *et al.*, 1982; McKenzie & Bickle, 1988) suggest that large stretching factors ($\beta > 3$) are required to produce significant tholeiitic magmas outside regions affected by mantle plumes. The possibility of a plume origin can be dismissed for the Versoyen basalts (see section 4.4-3) and it is therefore necessary to embrace the notion of volcanism induced by regional extension, again implying the involvement of active tectonism in the formation of the Tarentaise Basin.

5.2-6 Evaluation of Basin Models

It is clear that the late Cretaceous sedimentation represented in the Tarentaise Zone does not fit comfortably into the passive margin subsidence phase of the Piémont-Ligurian realm, which resulted essentially from late Triassic–early Jurassic extension. On the grounds of its age, the Tarentaise Basin has been

regarded by many Alpine workers as an early orogenic 'flysch' basin, receiving debris shed from the emerging thrust sheets (*e.g.* Homewood & Caron, 1982). This interpretation is unsatisfactory for three main reasons: **i)** the Tarentaise Basin formed by rapid active subsidence (indicated by the palæoenvironmental jump across the basal sequence boundary and by the development of contemporaneous basaltic volcanics in the eastern part of the basin) rather than the passive infilling of inherited bathymetry; **ii)** all sediment was derived from the west (*i.e.* the foreland, not an encroaching orogen) and does not include any 'exotic' clasts; **iii)** the basin-wide fining-upward *motif* of the late Cretaceous fill is the reverse of what would be expected for a young foreland basin, sourced from a rising, advancing thrust stack. Thus, the subsidence episode represented by the Aroley, Marmontains and basal St Cristophe Formations, strongly suggestive of active rifting, is not consistent with the 'flysch' model. The possibility that a major sequence boundary exists within the St. Cristophe Formation and that the upper part of this formation represents such a flysch cannot be ruled out but is not required by the available data.

Thus the subsidence and infilling of the Tarentaise Basin belongs neither to the extensional episode which formed the Tethyan passive margins nor to the early orogenic phase of flysch sedimentation. The Cretaceous stratigraphy of the Tarentaise Zone bears witness to relatively rapid subsidence from subaerial to moderately deep marine, with infill by mass-flow events which decreased in competence and (probably) volume over time. This evolution is most economically explained by a single phase of combined extension and uplift in the late Cretaceous, followed by rapid denudation of the uplands and essentially passive infilling of the adjacent accommodation space. The upward fining and thinning trend suggests that the initial uplift was not renewed and thus the basin history can be viewed as a single tectonic impulse–relaxation event. If, as seems highly plausible, the Versoyen metabasites are the magmatic products of the initial basin-forming event, then stretching factors must have been locally high. The Tarentaise sediment source may therefore be the product of 'rift-flank' uplift related to this stretching. Relatively localised uplift can be a necessary isostatic consequence of either homogeneous or inhomogeneous regional stretching, particularly where upper crustal extension is accommodated on by shallow rooted, steep, widely spaced faults (*e.g.* Jackson & McKenzie, 1983; Coward, 1986; Barr, 1987).

5.3 IMPLICATIONS FOR THE DEVELOPMENT OF THE NORTH TETHYAN MARGIN

What then of the starting hypothesis of a thinned, deeply submerged late Cretaceous continental margin (section 5.1-2)? The assumption of greatly attenuated crust (*e.g.* Lemoine *et al.*, 1986; Ménard *et al.*, 1991) carries with it the implication that the depositional surface would be submerged beneath relatively deep water. This in turn implies that marginal uplift associated with any subsequent extensional episode would be unlikely to generate arealy extensive sediment sources. Such a prediction of 'crustal impotence' is starkly irreconcilable both with the large volumes of coarse clastic sediment manifestly derived into the Tarentaise Basin in the Santonian/Maastrichtian, and also with the post–early Jurassic subaerial erosion surface which floors the basin. Nor can the Tarentaise Basin be readily dismissed as a 'flysch' basin in a proto-foredeep setting. Thus, the Tarentaise case, although specific to a single segment of the North Tethyan continental margin, makes it necessary to reconsider some widely held beliefs about the extensional precursors to the Alpine orogen.

5.3-1 Implications for Quantitative Models

Wooler *et al.* (1992) have recently demonstrated that stretching factors on the cratonward parts of the passive margins were generally low ($\beta = 1.1–1.3$), but their analysis does not extend significantly into the internal zones, which presumably represent the belt of greatest Mesozoic crustal thinning. In contrast, Ménard *et al.* (1991) used subsidence data to argue that crustal thicknesses in the aftermath of the stretching phase were very low across the entire south European margin. That the Tarentaise domain was strongly uplifted and rifted in the late Cretaceous implies that it was not greatly thinned and submerged as a result of the earlier extensional phase. This supports the contention (*e.g.* of Wooler *et al.*, 1992) that formation of the North Tethyan passive margin did not involve a broad zone of crustal attenuation. This may in turn indicate that most of the continental extension associated with the birth of the Piémont-Ligurian ocean was concentrated in the Piémont domain.

5.3-2 Implications for Alpine Palæogeography

At least part of the North Tethyan continental margin was not greatly thinned by the early Mesozoic extensional phase. If most of the passive margin was not

dramatically stretched during its Mesozoic extensional history, then the observed oceanward transition towards predominantly pelagic deposition (section 1.2) is potentially explicable simply in terms of increasing distance from continental sediment sources rather than increasing water depths, as generally assumed.

The large magnitude stretching implied by the Versoyen tholeiites and by the coarse fill of the Tarentaise Basin indicates a major extensional episode in the late Cretaceous. Is contemporaneous extension recorded elsewhere in the Alps? Deville (1990) has described a localised occurrence of Upper Cretaceous basaltic tuffs in the Vanoise (Briançonnais zone) which may testify to rift-related volcanism, but other evidence for rifting of this age is sparse. Although late Cretaceous sedimentation was widespread across the former passive margin, most of this is attributed to the 'flysch' stage of compression-related sediment dispersal. The subsidence histories of many of the so-called flysch basins have not been analysed in detail and it may be that some of these sediment packages accumulated in areas of active extension. If regional extension affected areas which were already under fairly deep water, major sediment sources might not be generated and this extension would therefore not be clearly recorded. Alternatively, if the Tarentaise rifting was restricted palæogeographically to the Tarentaise domain, then a zone of transtension may best account for the localisation of stretching. The activation of major strike-slip faults during the early stages of plate convergence is generally likely unless plate motions are nearly orthogonal (Woodcock, 1986) and the relative trajectories of Europe and Africa are known to have been markedly oblique at this time (Dewey *et al.*, 1989).

5.3-3 Implications for Alpine Crustal Budgets

Did the Tarentaise crustal region become 'rafted off' during the Jurassic (together with the Briançonnais domain) as an anomalously strong, relatively unrifted block whilst adjacent belts (both cratonwards and oceanwards) underwent much greater thinning and stretching? Alternatively, was the entire margin only slightly thinned, as the findings of Wooler *et al.* (1992) appear to suggest? Such details are important because the thickness and geometry of the passive margin have crucial implications with mass balance considerations for models of the development of the Alpine orogen. Large scale restorations of structural geometries suggest that orogenic contraction involved horizontal shortening of the order of 400km in the Western Alps (Butler, 1986) which ostensibly implies

either immense vertical thickening or underthrusing of continental crust into the mantle beneath northern Italy (Fig. 1-7b). Helwig (1976) pointed out that intense crustal shortening could be achieved without vastly increased crustal thickening if the continental margins involved had been greatly thinned prior to compression. Similarly, Ménard *et al.* (1991) inferred that much of the south European crust was thinned to about 10-15km during Jurassic extension and hence that orogenic restacking need not have resulted in excessive vertical thickening or significant subduction of continental crust (Fig. 1-7c). Assuming that European continental crust was initially of 'normal' thickness (25–35km), then Jurassic stretching factors would have to have been of the order of $\beta \geq 2.5$ on a regional scale to accomplish the degree of crustal attenuation required by the Ménard *et al.* model. This hypothesis is seemingly refuted by a growing body of stratigraphic evidence (Wooler *et al.*, 1992; this study) which supports the view that crustal thicknesses were not greatly reduced as result of passive margin formation.

5.4 SUMMARY

1) The regional sequence boundary defining the base of the Cretaceous Tarentaise basin-fill is a subaerial erosion surface which records a phase of post-early Jurassic, pre- late Cretaceous uplift.

2) The presence of relatively deep marine sediments directly overlying this subaerial truncation surface indicates that subsidence of the Tarentaise Basin occurred rapidly relative to deposition.

3) Basin-wide upward-fining and vertical consistency of sediment composition are suggestive of the progressive denudation of a single detrital source area.

4) Breccias and untransported fragmentites in the Plan Varraro thrust sheet support the notion of a fault controlled western margin to the basin.

5) Active, presumably fault controlled, crustal extension is implied by the inferred rapid subsidence (point **2** above) and by the apparent contiguity of a belt of extension-related basaltic intrusions.

6) The evolution of the Tarentaise Basin does not accord with the 'flysch' basin model since its stratigraphy implies active subsidence, cratonward sediment derivation and progressive retreat of the sediment source.

7) That the Tarentaise domain was capable of being elevated above sea-level in post-early Jurassic times indicates that it was not greatly thinned and submerged as a result of the main Tethyan extensional phase.

8) The formation of the Piémont–Ligurian Tethys probably did not involve a broad zone of severe crustal thinning.

9) The Cretaceous metasediments of the Tarentaise Zone represent an important phase of pre-orogenic extension which has not been generally recognised in the Alpine vestiges of the North Tethyan passive continental margin.

CHAPTER 6 CONCLUSIONS

The purpose of this brief chapter is simply to list some of the principal findings to emerge from this research and to suggest a number of potentially fruitful avenues of future investigation.

6.1 CONCLUSIONS

6.1-1 Structural Conclusions

1) The Tarentaise Zone represents a stratigraphically distinct package bounded on its external margin by the Frontal Pennine Thrust and on its internal margin by the Miravidi and 'Sub-Briançonnais' Thrusts. The Frontal Pennine Thrust is apparently unfolded in this area whereas the Miravidi thrust has been gently folded by subsequent deformation. Emplacement of the Versoyen Complex on the Miravidi Thrust was probably kinematically linked with the formation of tight to isoclinal SSE-plunging F1 folds in its footwall. The Sub-Briançonnais Thrust breaches structures in the underlying Versoyen and Tarentaise Zones and appears to be a late, out-of-sequence structure.

2) Internally, the Tarentaise Zone is dissected by other minor (ductile) thrusts with a top-to-the-WNW movement direction. Décollement along mechanically weak stratigraphic units (Carboniferous pelites, Triassic evaporites, Arguerey Formation) seems to have been important in the localisation of some of these thrusts. All of the thrust sheets exhibit regionally consistent WNW-vergent open folding but fragmentary exposure means that mesoscale structural geometries are poorly constrained. Many of the observed deformation features are explicable in terms of rheological contrasts between adjacent stratigraphic units.

3) Strike-parallel (NNE-SSW) stretching lineations are abundant throughout the Tarentaise Zone. Spencer (1992) regarded this as evidence for major along-strike extension. A more plausible interpretation explains the lineations as localised zones of prolate (constrictional) strain developed in the F2 fold hinges when amplification became mechanically inhibited.

6.1-2 Sedimentological Conclusions (Aroley Formation)

1) The proximal Aroley Formation represents a high-energy depositional system constructed by sediment gravity flows of various types. The more distal correlatives are likely to be turbidites but sedimentological studies are hampered by a complex and pervasive deformation state.

2) Sediment was derived from a source area comprising the same lithologies as those forming the floor to the Tarentaise Basin. The range and relative proportions of clast types did not change significantly during the period of accumulation of the Aroley Formation and clasts of (crystalline) basement lithologies are present throughout the sequence. From this it may be inferred that detritus was probably supplied from a single source terrain but that this terrain had already become deeply dissected by the time of the earliest coarse sediment pulses into the Tarentaise Basin: the Aroley Formation does not record a progressive stratigraphic unroofing history.

3) Textural and grain-size properties testify to a very limited transport history, indicating proximality to a region of coarse sediment production. Since relatively deep-water (more than a few tens of metres) is implied by the associated faunas (*e.g.* Sodero, 1968), the depositional system is likely to have been some form of deep-water fan-delta. The suggestion by Antoine (1971) that sediment entered the basin from its cratonward margin is confirmed. Palæocurrent indicators are scarce but consistent and define a unimodal ESE-directed sediment transport path for the proximal Aroley Formation. Antoine's (1971) proposal that the Marmontains Formation was supplied from a separate source area (from the north-east) is not substantiated by this study.

4) A well defined basin-wide vertical fining and thinning trend is apparent, indicating that availability of coarse sediment diminished with time during the deposition of the Aroley Formation. Up-sequence changes in the dominant facies types imply a tendency towards lower energy depositional events with time. In conjunction, these observations are consistent with an impulse-relaxation model of basin development in which the topographic relief created by an initial tectonic perturbation (uplift + adjacent rapid subsidence) was progressively reduced by 'sedimentary' processes (denudation and deposition).

6.1-3 The Versoyen Complex

1) The Versoyen complex comprises a stratigraphically distinct thrust-bounded package on the internal margin of the Tarentaise Zone. Stratigraphically, the Versoyen units generally involve metabasaltic sills intruded into a thick pelitic succession which in turn unconformably overlies leucogranitic basement (*i.e.* fairly convincing continental crust). Contact relationships in the high Breuil valley indicate that the basaltic sills were emplaced into wet, unconsolidated sediment. The pelites may correlate laterally with the Arguerey/Peula Formation of the Tarentaise Zone, as suggested by Antoine (1971, 1972).

2) In the Comba di Planaval, Versoyen metabasite sheets are enclosed in Aroley Formation metasediments, although the contacts appear to be unexposed. These relationships support the idea of palæogeographic contiguity between Versoyen and Tarentaise domains in the late Cretaceous. If the metabasite/Aroley boundaries are stratigraphic rather than tectonic, then the age of volcanism is constrained to be Santonian or younger.

3) The metabasites resemble MORB tholeiites in terms of trace element geochemistry, although compositions have been modified heterogeneously by post-magmatic fluid interaction. The style of chemical alteration of the basalts is suggestive of the operation of high-temperature hydrothermal processes.

4) The Versoyen tholeiites testify to intense lithospheric stretching. The analogy drawn by Loubat (1975, 1984) with sill intrusion (related to incipient ocean spreading) in the Gulf of California appears to be appropriate also in terms of immobile trace element characteristics. Since the Versoyen complex probably has palæogeographic affinities with the Tarentaise domain, a genetic link between the Versoyen magmatism and opening of the Tarentaise Basin is likely.

6.1-4 Stratigraphic Conclusions

1) The regional sequence boundary defining the base of the Cretaceous Tarentaise basin-fill is a subaerial erosion surface which records a phase of post-early Jurassic, pre- late Cretaceous uplift. The presence of relatively deep marine sediments directly overlying this subaerial truncation surface indicates that subsidence of the Tarentaise Basin occurred rapidly relative to deposition.

2) Active, presumably fault controlled, crustal extension is implied by the inferred rapid subsidence (point 1, above) and by the apparent contiguity of a belt of extension-related basaltic intrusions. Breccias and untransported fragmentites in the Plan Varraro thrust sheet support the notion of a fault controlled western margin to the basin. Although contemporaneous with the early phase of compression-related sedimentation, the evolution of the Tarentaise Basin does not accord with the 'flysch' basin model since its stratigraphy implies active subsidence, cratonward sediment derivation and progressive retreat of the sediment source.

3) That the Tarentaise domain was capable of being elevated above sea-level in post-early Jurassic times indicates that it was not greatly thinned and submerged as a result of the main Tethyan extensional phase. This is consistent with other studies (*e.g.* Wooler *et al.*, 1992) which suggest that the formation of the Piémont–Ligurian Tethys probably did not involve a broad zone of severe crustal thinning.

6.1-5 General Conclusion

The late Cretaceous metasediments of the Tarentaise Zone record an important phase of pre-orogenic extension which has not been generally recognised in the Alpine vestiges of the North Tethyan passive continental margin.

6.2 RECOMMENDATIONS FOR FUTURE WORK

1) ***Biostratigraphy.*** In common with large tracts of the internal Alps, age information on the Tarentaise sequence is very poor; at present, the age of subsidence is dated essentially by a single fossil (section 1.4-3). Adequate understanding of the Cretaceous extension in the context of Tethyan evolution requires much tighter constraints on rates and timing of subsidence. Similarly, improved fossil constraint on age and bathymetries would allow far more detailed analysis of the Tarentaise subsidence through backstripping of stratigraphic sections. Consequently, a carefully targeted micropalæontological examination of biostratigraphically promising strata (*e.g.* pelites and originally fine-grained calcareous beds which have recrystallised to coarser grain-sizes) could be extremely profitable.

2) ***Structure.*** Although hillside scale exposures portray relatively simple fold-thrust geometries, the Alpine structure of the Tarentaise Zone has proved extremely difficult to explain by recourse to convenient conventional concepts of compressional deformation. Existing interpretative cross sections (Antoine, 1971; Fudral, 1973, 1980; Butler, 1989a; Spencer, 1990; this study) are inadequate simplifications of a complex and poorly understood situation. In part, this deficiency may be the result of the rather fragmentary exposure and a general shortage of stratigraphic markers. Nevertheless, good control on three dimensional geometries and deformation history is a necessary prerequisite of any comprehensive reconstruction of the Tarentaise Basin. Very detailed structural analysis of key areas is needed to establish tight kinematic and geometric constraints on the character of deformation.

3) ***Parallelism between stretching lineations and fold axes.*** A consistent alignment of stretching lineations at right-angles to the inferred thrust slip direction is a relatively common feature of the strongly sheared internal zones of orogenic terrains which has not satisfactorily been explained (*e.g.* Ridley, 1986). Are all instances of this parallelism explicable by a single mechanism (*e.g.* superimposed strains or fold hinge lock-up) or is each example different? This is a well defined problem which has received surprisingly little direct attention and which forms an obvious avenue for future research, both via field-based case studies and through theoretical/analogue modeling.

4) ***Versoyen complex.*** A late Cretaceous age for the Versoyen igneous activity seems probable from stratigraphic considerations. This hypothesis needs to be tested geochronologically. Whole rock K-Ar or Rb-Sr techniques (rapid and straightforward) *might* yield an approximate emplacement age for the basalts although U-Pb systematics on zircon separates (extremely difficult and time-consuming) would be necessary to obtain robust magmatic crystallisation ages. The palæogeographic relationships between the Versoyen and Tarentaise domains also require clarification. In this respect, the Comba di Planaval exposures (where metabasite sheets are concordantly interlayered with Aroley Formation calc-schists) are crucial and merit detailed examination.

5) ***Marmontains Formation.*** If the intervening Marmontains unit is disregarded, the litharenites and conglomerates of the upper Aroley and lower St. Cristophe Formations form a relatively smooth progression of upwardly decreasing grain-sizes and bed thicknesses involving a particular suite of clastic constituents in

roughly constant proportions. The more quartzose psammites and non-calcareous pelites of the Marmontains Formation thus represent a somewhat anomalous punctuation of the sedimentary sequence in terms of both grain-size and composition. Clearly there are some significant implications for basin evolution here. In several areas, the Marmontains Formation is well exposed and little deformed. Sedimentary structures are locally preserved and the dark grey pelites are potentially (slightly) fossiliferous. Hence the Marmontains Formation is potentially amenable to the type of sedimentological analysis applied in this study to the Aroley Formation.

6) ***South-western termination of the Tarentaise Zone.*** The outcrop of the Tarentaise Zone is amputated by the intersection of the Sub-Briançonnais and Frontal Pennine Thrusts near the town of Moûtiers. It is generally assumed that this termination approximately corresponds to the primary edge of the Tarentaise Basin since comparable Cretaceous units are not known from areas to the south or west (Antoine, 1972; Antoine & Barbier, 1978; Spencer, 1992). The coincidence of the Tarentaise termination with the outcrop of a small ($<10km^2$) enigmatic Eocene mélange (the Niélard Zone) of uncertain affinities (Tarentaise, Sub-Briançonnais or neither?) is curious. Martinez-Reyes (1980) has provided useful stratigraphic and structural descriptions of the mélange but more detailed sedimentological and stratigraphic studies are needed to clarify its palæogeographic significance.

7) ***Tethyan margin subsidence.*** Preliminary backstripping of Mesozoic stratigraphic columns from the Tethan belt (Wooler *et al.*, 1992) has demonstrated the feasibility of establishing quantitative subsidence histories for the passive continental margin system which became the Alps. Although the curves produced by Wooler *et al.* (1992) are severely devalued by a number of rather arbitrary assumptions and a failure to incorporate other geological evidence, the method itself appears to hold a great deal of promise. A carefully designed programme integrating refined backstripping techniques with well constrained palæoenvironmental and palæogeographic inferences, and targeting the internal Alps in particular, would have considerable potential for clarifying the pre-orogenic evolution of the Alpine chain.

6.3 CONCLUDING STATEMENT

The work outlined in this thesis highlights the importance of adopting an integrated approach when attempting to analyse either the formation or the deformation of an orogenically crumpled sedimentary basin. Depositional architecture, palæogeography and basin evolution cannot be unravelled in detail unless the tectonic overprint is clearly resolved but equally, orogenic deformation should not be considered in isolation from basin architecture since the inherited disposition of rheological heterogeneities may have exerted a major control on the development of compressional structures.

APPENDIX 1
SAMPLE CATALOGUE

Details of all the rock specimens collected and curated in the course of this research project, including those not otherwise mentioned in this thesis.
Abbreviations: *DP* = double-polished thin section; *LF* = large format thin section; *M* = analysed for major elements; *NT* = ordinary thin section; *P* = polished thin section; *R* = analysed for Ce, La, Nd; *T* = analysed for trace element abundances.

	Sample Code	Lectn Number	Lithology	Stratigraphic Unit	Features	Orientation	Grid Ref	Locality Description	Date Collected	Thin Section	XRF Analyses
1	FA M1	54304	limestone mylonite	Arolay??	no clear stretching lineation	44/149 on top	32098 506237	Cornet de Rossland, France	Oct-88	NT,LF	
2	FB LT1	53143	qzose calc-schist	Arolay?	strong lithology-|| foliation	41/156 on 'top' (o/f)	56175 6345	old La Thuile roadcut, Italy	Sep-88	NT	
3	FB LT2	53144	qzose calc-schist	Arolay?	" " "	41/161 on 'base' (o/f)	56175 6345	old La Thuile roadcut, Italy	Sep-88	NT	
4	FB LT3	53145	qzose calc-schist	Arolay/Mammonts ns?	" " "	48/155 on 'base' (o/f)	56175 6345	old La Thuile roadcut, Italy	Sep-88	NT	
5	FB LT4	53146	qzose calc-schist	Mammontains	" " "	~51/178 on 'base' (o/f)	56175 6345	old La Thuile roadcut, Italy	Sep-88	NT	
6	FB LT5	53147	qzose calc-schist	Mammontains	" " "	48/173 on 'base' (o/f)	56175 6345	old La Thuile roadcut, Italy	Sep-88	NT	
7	FB LT6	53148	qzose calc-schist	Mammontains	" " "	45/161 on 'base' (o/f)	56175 6345	old La Thuile roadcut, Italy	Sep-88	NT	
8	FB LT7	53149	qzose calc-schist	Mammontains/St Chist?	" " "	38/163 on 'top' (o/f)	56176 6345	old La Thuile roadcut, Italy	Sep-88	NT	
9	FB LT8	53150	qzose calc-schist	St. Cristophe?	" " "	none	56175 6345	old La Thuile roadcut, Italy	Sep-88	NT	
10	FB LT9	53151	qzose calc-schist	St. Cristophe	" " "	43/151 on 'base' (o/f)	56176 6345	old La Thuile roadcut, Italy	Sep-88	NT	
11	FB LT 9b	53159	qzose calc-schist	St. Cristophe	" " "	SSE on 'top' (o/f)	56176 6345	old La Thuile roadcut, Italy	Sep-88	DP	
12	FB SH1	53152	pelite	Arguerey/Versoyen	sphene-bearing	26/107 on 'top'	33378 506242	900m SSE of Punta Rossa, Italy	Sep-88	NT	M,T
13	FB WM 1	54451	qz-bpx-mica schist	cryst basement	marbly white rock	51/048 on irregular top surf.	33318 506270	600m SW of Punta Rossa, Italy	Sep-88	NT	
14	FB SERP 1		serpentinite	(Versoyen basement)		none	33313 506264	750m SW of Punta Rossa, Italy	Aug-88	NT	
15	FB LEPT1	53154	granitic schist	cryst basement	foliated leucogranite	45/078 on top	~33353 506270	south of Punta Rossa, Italy	Sep-88	DP	
16	FB H1	53156	schist	cryst basement		49/126 and 58/118 on 'top'	-3062 50418	south of Hautecour, France	Aug-88	DP	
17	FB CH1	54603	pelitic schist	Mammontains?	minor smeared-out fold	44/084 on top (foliation)	57682 8202	south of Monte Taillere, Switzerland	Aug-88	NT	
18	FB HSA 1	53160	qzose calc-schist	Arolay	tectonite	8/256 on 'top'	33286 506448	NW of Tormotta, Italy	Sep-88	DP	M,T,R
19	FB A1	53161	lithanite	Arolay		10/005 on base (bedding)	33480 506975	high Vallone di Chavannes, Italy	Sep-88	DP	M,T,R
20	FB MM1	53162	qzose calc-schist	Mammontains?		80/119 on east ('top') (o/f)	32427 506166	mid Vallée des Chapieux, France	Sep-88	DP	M,T,R
21	FB PR 1	54604	metabasite	Versoyen	rich in opaques	bed	33297 506332	400m WNW of Punta Rossa, Italy	Sep-88	P,NT	M,T,R
22	FB PR 2	54601	metabasite	Versoyen	minor biotite	61/119 on west surf. (base)	33306 506318	450m WSW of Punta Rossa, Italy	Sep-88	P,NT	M,T,R
23	FB PR 3	54606	metabasite	Versoyen	coarse-grained	none	33308 506325	400m west of Punta Rossa, Italy	Sep-88	NT	M,T,R
24	FB PR 5	55294c	metabasite	Versoyen	rich in gunky brown groundmass	none	33401 506242	1km SE of Punta Rossa, Italy	Sep-88	NT	M,T,R
25	FB PR 6		metabasite	Versoyen	minor calcite veining	none	33407 506243	1km SE of Punta Rossa, Italy	Sep-88		M,T,R
26	FB PR 7	54605	metabasite	Versoyen		none	33410 506245	1km SE of Punta Rossa, Italy	Sep-88	P,NT	M,T,R
27	FB PR 8	55295c	metabasite	Versoyen	rich in gunky brown groundmass	none	33352 506228	1km south of Punta Rossa, Italy	Sep-88	NT	M,T,R
28	FB PR 9		metabasite	Versoyen	minor calcite veinlets	none	33395 506255	600m SE of Punta Rossa, Italy	Sep-88		M,T,R
29	FB PR 10		metabasite	Versoyen	post-foliation pyrite	none	33361 506272	600m SE of Punta Rossa, Italy	Sep-88		M,T,R
30	FB PR 11		metabasite	Versoyen		none	33357 506257	600m SSE of Punta Rossa, Italy	Sep-88		M,T,R
31	FB PR 13	54602	metabasite	Versoyen'	conspicuously opaque-poor	37/111 on base (joint plane)	57326 7183	Combe di Planaval, Italy	Sep-88	NT	M,T,R
32	FB PR 14		metabasite	Versoyen'	post-foliation pyrite	none	57329 7196	Combe di Planaval, Italy	Sep-88		M,T,R
33	FB PR 15		metabasite	Versoyen'	minor calcite veinlets	none	57320 7189	Combe di Planaval, Italy	Sep-90	P	M,T
34	FC 1		dolomite/limestone	Triassic	horizontal burrow-like traces	boulder	32051 506132	150m NE of Dent d'Arpire, France	Jul-90		
35	FC 2	54451	dolomite	Triassic	has disrupted laminae	boulder (local bed ~30/130)	~3193 50588	Combe de la Neuva, France	Aug-90	LF	
36	FC 3	53157	psammite	Triassic	chloritic, shows minor fold hinge	scree	32035 505662	Combe de la Neuva, France	Aug-90	NT,DP	
37	FC 3b	54304	psammite	Triassic	(cut parallel to fold hinge)	"	"	"	Aug-90	NT	
38	FC 4		purple pelite	Lias?	(Mesozoic) weathering product?	none	31355 506270	Crête de la Raisse, France	Aug-90		
39	FC 5	53155	graphitic pelite	Arguerey/Versoyen	has minor fold hinge	scree	3342 50638	east slope of Punta Rossa, Italy	Aug-90	NT	
40	FC 6		calcite vein	serp basement	v. coarse, sparry brown carbonate	none	33300 506342	500m NW of Punta Rossa, Italy	Aug-90	NT	
41	FC 7		ironstone	within Arolay	chamosite + ?dolerite?	none	33304 506352	450m NW of Punta Rossa, Italy	Aug-90	NT	M,T
42	FC 8a		conglomerate	?? (Versoyen)	carbonate clast	boulder	33312 506335	350m WNW of Punta Rossa, Italy	Sep-90	NT	
43	FC 8b		conglomerate	"	coarse matrix	"	"	"	Sep-90	NT	
44	FC 8c		conglomerate	"	fine matrix	"	"	"	Sep-90	NT	
45	FC 9		baloic pelite	Arguerey	30cm unit between metabasites	none	33302 506338	420m WNW of Punta Rossa, Italy	Sep-90		M,T
46	FC 10a		v. indurated pelite	Arguerey	80cm below metabasite sheet	none	33303 506341	400m WNW of Punta Rossa, Italy	Sep-90		M,T
47	FC 10b		"	"	"	"	"	"	Sep-90	NT	M,T
48	FC 11		lasite pelite	Arguerey	crenulated foliation	none	33303 506341	400m WNW of Punta Rossa, Italy	Sep-90		M,T
49	FC LC a,b	53153	c. qzose arenite	Mammontains	dolomite-rich, angular clasts	none	31580 505530	Rulsseau de Jerbois, France	Sep-90	NT	
50	FC LC-1		chloritic pelite	basement	irregular veneer on unconformity	foliation dips 43/240	33292 506430	450m NW of Tormotta, Italy	Sep-90	NT	M,T
51	FC LC-2	54385	serpentinite	(Versoyen basement)	abundant pyroxene ghosts	none	~3329 50641	450m west of Tormotta, Italy	Sep-90	NT	
52	FC LC-3	53154	calc-schist	Arolay	has qzose & carbonate domains	none	33310 506365	NW of Punta Rossa, Italy	Sep-90	NT	
53	FC LC-4	54452	qz-carb tectonite	Arolay	strong lineation	none	(fol ~ 20/300, lin ~ 100/15)	Vallone del Breuil, Italy	Sep-90	P,NT	
54	FC LC-5a,b		serpentinite	(Versoyen basement)		none	33331 50635	500m south of Punta Rossa, Italy	Sep-90	NT	
55	FC LC-6	54600	metabasite	Versoyen	medium/coarse-grained	none	33335 506275	500m south of Punta Rossa, Italy	Sep-90	NT	M,T
56	FD 1	54303	lithanite	St. Cristophe	tectonite with multiple fabrics	boulder	3343 50627	1km ESE of Punta Rossa, Italy	Sep-90	NT	
							3285 50650	Plan de Fordaz, France	Aug-91	LF	

APPENDIX 2
XRF ANALYTICAL DETAILS

XRF analyses were conducted at Leeds University on whole rock samples ruthlessly crushed to powder at the Open University.

CRUSHING

Samples weighing 1–3kg were initially trimmed to remove weathered surfaces then split using a hydraulic splitter. The fresh chunks were ground by two passes through a steel jaw crusher to produce chips of 1–2mm diameter. Quartered portions of these chips were then powdered by 12–20 minutes of agitation in an agate-barrel Tema mill. Jaw crusher and Tema barrel were meticulously cleaned between each sample. Periodically, a relatively pure natural quartzite was pulverized using the same procedure. Test analysis of the resulting crushate (Table A-1) suggests that trace contamination of Al and Zr could potentially be conferred via the crushing equipment. Silica might also be contributed by the Tema barrel.

	weight %		*ppm*
SiO_2	98.48	Sc	(1)
TiO_2	0.05	V	7
Al_2O_3	0.95	Cr	18
Fe_2O_3	0.06	Co	(0)
MnO	(0.00)	Ni	(0)
MgO	0.09	Cu	(2)
CaO	(0.02)	Zn	8
Na_2O	(0.05)	Rb	4
K_2O	0.27	Sr	7
P_2O_5	(0.02)	Y	1
LOI	0.33	Zr	77
Total	*100.34*	Nb	(1)
		Ba	14
		Pb	7
		Th	5
		U	(1)

Table A-1. XRF analyses of the quartzite used in the rock crushing room at the Open University. Values in brackets lie below effective detection limits for the elements concerned.

Element	Line	Collimator	Detector	Crystal	2-theta	Offsets +	Offsets −	Time (sec)	kV	mA
Na	K α	Coarse	Flow	PX 1	28.60	1.2	1.2	160	40	60
Mg	K α	Coarse	Flow	PX 1	23.67	1.6	1.6	80	40	60
Al	K α	Coarse	Flow	PET	144.90	2.0	–	40	40	60
Si	K α	Coarse	Flow	InSb	144.56	2.2	–	20	40	60
P	K α	Coarse	Flow	Ge	141.03	2.0	–	20	40	60
K	K α	Fine	Flow	LiF 200	136.69	5.0	–	20	40	60
Ca	K α	Fine	Flow	LiF 200	113.09	–	–	20	40	60
Ti	K α	Fine	Flow	LiF 200	86.14	3.0	–	20	40	60
Mn	K α	Fine	Flow	LiF 200	62.97	1.6	–	20	40	60
Fe	K α	Fine	Flow	LiF 200	57.52	–	1.5	16	40	60
Sc	K α	Fine	Flow	LiF 200	97.75	0.6	0.6	80	50	50
V	K α	Fine	Flow	LiF 200	76.96	0.8	0.8	80	50	50
Cr	K α	Fine	Flow	LiF 200	69.38	1.0	1.0	80	50	50
Co	K α	Fine	Flow	LiF 220	77.89	0.5	–	80	80	30
Ni	K α	Fine	Flow	LiF 200	48.67	1.0	–	80	80	30
Cu	K α	Fine	Flow	LiF 200	45.03	0.6	1.0	80	80	30
Zn	K α	Fine	Scintillation	LiF 200	41.76	1.0	–	80	80	30
Rb	K α	Fine	Scintillation	LiF 200	26.62	0.5	0.8	80	80	30
Sr	K α	Fine	Scintillation	LiF 200	25.15	0.6	0.6	80	80	30
Y	K α	Fine	Scintillation	LiF 200	23.80	0.8	0.8	80	80	30
Zr	K α	Fine	Scintillation	LiF 200	22.55	0.4	0.8	80	80	30
Nb	K α	Fine	Scintillation	LiF 220	30.39	0.6	0.6	80	80	30
Ba	K α	Fine	Scintillation	LiF 220	15.54	0.5	0.3	80	80	30
Pb	L β	Fine	Scintillation	LiF 200	28.26	0.5	1.0	80	80	30
Th	L α	Fine	Scintillation	LiF 220	39.24	0.9	0.5	200	80	30
U	L α	Fine	Scintillation	LiF 200	26.15	1.0	0.4	200	80	30

Table A-2. Operating conditions for the Philips PW1400 wavelength-dispersive X-ray spectrometer in the Earth Sciences Department at Leeds.

MAJOR ELEMENT ANALYSES

Major element concentrations were measured on 40mm diameter glass fusion discs. Powders were dried overnight at 105°C then, when cool, mixed with a lithium metaborate:tetraborate flux (Johnson Matthey Spectroflux 110) in a ratio of 1:10 (0.400g powder to 4.000g flux). The mixture was fused in a muffle furnace at 1000°C for 40 minutes in a covered 5%Au-95%Pt crucible. The cooled crucible was re-weighed and flux added to return the flux weight to 4.00g (in compensation for water loss during fusion). This mixture was re-melted over a four-jet Bunsen burner for 10–20 minutes, rolled and swirled to ensure good mixing, and cast into a copper ring held at ~180°C on a stainless steel platten. The disc was cooled for about 30 minutes on the platten, then trimmed, labelled and sealed in a plastic bag to avoid hydration of the surface of the glass. Volatile content of the sample was determined from the weight loss ('loss on ignition,' LOI) of 1g of oven-dried powder heated in a porcelain crucible at 1000°C for 80 minutes.

TRACE ELEMENT ANALYSES

Trace element analyses were conducted on 40mm diameter pressed powder pellets. The pellets were manufactured from approximately 15g of rock powder bound with 1.4ml of PVA (polyvinyl alcohol) glue. Powder and binding agent were thoroughly mixed using state-of-the-art procedures involving a disposable plastic cup and a wooden lolly stick. The mixture was next transferred to a polished steel pellet-mould lined with disposable polythene discs and pressed in a hydraulic press at a pressure of 10 tons per square inch (154MPa). All parts of the mould were rigorously cleaned between each sample. The pressed pellets were dried at 105°C for 18–24 hours before analysis.

INSTRUMENTATION

Analyses were carried out on the Philips PW1400 wavelength-dispersive X-ray spectrometer in the Earth Sciences Department at Leeds. Operating conditions are detailed in Table A-2. The lower limits of detection for metabasaltic rocks under these conditions were: 1ppm for Y, Zr; 2ppm for Rb, Sr, Nb, Th, U; 4ppm for V, Cr, Ni, Zn; 5ppm for Sc, Co, Pb, and approximately 8–9ppm for Cu, Ba. Effective detection limits for major elements were better than 0.1wt% (oxide equivalent) in all cases.

Machine drift is checked daily against internal laboratory standards and periodic re-calibration is undertaken with reference to the following international standards: US Geol. Surv. *G-2, GSP-1, AGV-1, BCR-1, PCC-1;* Canadian Cer. Ref. Mat. Proj. *SY-2, MRG-1;* Brit. Chem. Stds. *BCS269, BCS309, BCS315, BCS364, BCS375, BCS376;* SA Nat. Inst. Metallurgy *NIM-G, NIMK-S, NIM-N, NIM-D.*

REPRODUCIBILITY

Analytical consistency was assessed by repeat analyses of two metabasite samples: FBPR8 and FBPR11. For major element analyses, which are strongly

	Max	Min	Mean	σ	% error
SiO_2	49.48	49.30	49.41	0.057	0.12
TiO_2	2.01	1.99	2.01	0.007	0.33
Al_2O_3	15.81	15.69	15.76	0.039	0.25
Fe_2O_3	10.82	10.76	10.79	0.020	0.19
MnO	0.19	0.18	0.19	0.003	1.59
MgO	7.87	7.78	7.84	0.029	0.37
CaO	6.41	6.36	6.39	0.016	0.24
Na_2O	4.71	4.65	4.68	0.016	0.35
K_2O	(0.02)	(0.01)	(0.02)	(0.005)	(33.33)
P_2O_5	0.23	0.21	0.22	0.006	2.75
[LOI]	[3.09]	[3.09]	[3.09]	–	–
Total	*100.50*	*100.25*	*100.39*	*0.097*	*0.10*

Table A-3. Analytical consistency for major elements based on ten analyses of a single glass fusion disc (sample FB PR 11). The term σ refers to the standard deviation of the distribution and '% error' is σ expressed as a percentage of the mean. All values for K_2O lie below effective detection limits.

	Max	Min	Mean	σ	% error
SiO_2	49.70	49.40	49.52	0.099	0.20
TiO_2	2.02	1.98	2.00	0.014	0.72
Al_2O_3	15.89	15.79	15.83	0.037	0.23
Fe_2O_3	10.86	10.71	10.77	0.046	0.43
MnO	0.19	0.18	0.19	0.005	2.53
MgO	7.94	7.77	7.87	0.049	0.62
CaO	6.45	6.34	6.41	0.036	0.56
Na_2O	4.72	4.57	4.62	0.038	0.81
K_2O	(0.02)	(0.01)	(0.01)	(0.004)	(31.94)
P_2O_5	0.23	0.21	0.22	0.007	3.44
LOI	3.13	2.81	3.00	0.117	3.90
Total	*100.65*	*100.22*	*100.43*	*0.141*	*0.13*

Table A-4. Overall major element reproducibility determined from repeat analyses of sample FB PR 11. Three analyses were made on each of five separate fusion discs prepared from the same powder. All values for K_2O lie below effective detection limits.

affected by weighing accuracy and glass homogeneity, reproducibility is largely preparation dependent (Table A-3 *cf.* Table A-4). The test detailed in Table A-4 indicates that all the major oxide abundances were reproducible to a standard deviation (σ) of less than 0.06wt% and relative errors of less than 0.1% for all the major species except MnO, K_2O and P_2O_5, which are present only in minor proportions (sic). The least reproducible value was that for loss on ignition (LOI) which varied between 2.81% and 3.13% (*i.e.* $\sigma = 0.12$, relative error = 3.9%) for sample FB PR 11. Reproducibility of trace element abundances (Table A-5) is primarily a function of machine counting errors and is relatively insensitive to preparation factors. For those trace elements consistently present above detection limits, concentrations were reproducibile to within σ<7.5ppm (Table A-5).

	Max	Min	Mean	σ	% error
Sc	35	26	30	3.1	10
V	218	200	208	5.1	2
Cr	335	321	328	4.2	1
Co	55	50	53	1.6	3
Ni	168	161	164	2.2	1
Cu	62	58	61	1.3	2
Zn	125	116	121	2.6	2
Rb	(1)	(0)	(0)	(0.5)	(115)
Sr	471	452	461	7.3	2
Y	29	27	29	0.7	3
Zr	86	84	85	0.9	1
Nb	3	(1)	(2)	(0.6)	(34)
Ba	(8)	(0)	(2)	(2.7)	(119)
Pb	5	(2)	(3)	(1.2)	(40)
Th	5	4	5	0.5	10
U	2	(0)	(1)	(0.7)	(127)

Table A-5. Reproducibility of trace element concentrations (parts per million) determined from repeated analysis of sample FB PR 8. Three analyses were made on each of three separate pressed pellets prepared from the same powder. Brackets denote values which lie below meaningful detection limits for the element concerned.

REFERENCES

ACKERMANN, T., BURRI, M., JEANBOURQUIN, P. & MANCKTELOW, N. (1991) La zone Sion-Courmayeur en Haut-Valais et comparaison avec flyschs valaisans dans les Alpes occidentales. *Eclogae Geol. Helv.*, **84** pp255–263.

AHRENDT, H. (1980) Die Bedeutung der Insubrischen Linie für den tektonischen Bau der Alpen. *Neues Jahr. Geol. Pal. Abhandlungen*, **160** pp336–62.

ALT, J.C. & EMMERMANN, R. (1985) Geochemistry of hydrothermally altered basalts: DSDP hole 504B, leg 83. In: Anderson, R.N., Honnorez, J., Becker, K. *et al., Init. Repts. DSDP 83, US Govt. Printing Office, Washington*, pp249–262.

AMIEUX, P. & JEANBOURQUIN, P. (1989) Cathodoluminescence et origine diagénétique tardive des cargneules du massif des Aiguilles Rouges (Valais, Suisse). *Bull. Soc. Géol. France*, **8 V** pp123–132.

ANTOINE, P. (1965) Sur l'existence de crétacé supérieur daté dans le nappe des brèches de Tarentaise au Nord des Chapieux (Savoie). *C.R. Acad. Sci. Paris*, **261** pp3640–3642.

ANTOINE, P. (1968) Sur la position structurale de la "zone du Versoyen" (Nappe des Brèches de Tarentaise sur les confines franco-italiennes). *Géol. Alpine*, **44** pp6–26.

ANTOINE, P. (1970) Une nouvelle subdivision dans le domaine valaisan, en Tarentaise et dans le haut Val d'Aoste. *C.R. Acad. Sci. Paris*, **270** pp1548–1551.

ANTOINE, P. (1971) La zone des Brèches de Tarentaise entre Bourg-Saint-Maurice (vallée de l'Isère) et la frontière italo-suisse. *Mém. Lab. Géol. Grenoble*, **9** 367pp.

ANTOINE, P. (1972) Le domaine pennique externe entre Bourg-Saint-Maurice (Savoie) et la frontière italo-suisse. *Géol. Alpine*, **48** pp5–40.

ANTOINE, P. & BARBIER, R. (1978) La terminaison méridionale de la zone des Brèches de Tarentaise au sud de Moûtiers (Savoie). *C.R. Acad. Sci. Paris (série D)*, **286** pp1849–1851.

ANTOINE, P., BARBIER, R. & COLLART, J. (1972a) Sur la présence de faciès volcano-sédimentaires à la base des schistes de la Bagnaz (zone des Brèches de Tarentaise, Savoie). *Géol. Alpine*, **48** pp41–47.

ANTOINE, P., BARBIER, R. & COLLART, J. (1973a) Mise en évidence d'un pli couché kilometrique (6km) dans la zone des Brèches de Tarentaise au Nord-Ouest d'Aime (Savoie) et ses conséquences structurales. *Géol. Alpine*, **49** pp13–19.

ANTOINE, P., BARBIER, R., DEBELMAS, J. & FUDRAL, S. (1972b) Précisions chronologiques et paléogéographiques sur les Brèches du massif du Grand Fond (zone des Brèches de Tarentaise, Savoie). *Céol. Alpine*, **48** pp49–59.

ANTOINE, P., LOUBAT, H. & VATIN-PÉRIGNON, N. (1973b) Hypothèses nouvelles sur l'origine et la signification des "Ophiolites" du domaine pennique externe (Savoie-Valais). *Géol. Alpine*, **49** pp21-39.

ANTOINE, P., PAIRIS, J-L. & PAIRIS, B. (1975) Quelques observations nouvelles sur la structure de la couverture sédimentaire interne du massif du Mont Blanc, entre le col Ferret (frontière italo-suisse) et la Tête des Fours (Savoie, France). *Géol. Alpine*, **51** pp5–23.

ARCULUS, R.J. (1987) The significance of source versus process in the tectonic controls of magma genesis. *J. Volcanol. Geotherm. Res.*, **32** pp1–12.

ARGAND, E. (1916) Sur l'arc des Alpes occidentales. *Eclogae Geol. Helv.*, **14** pp145–191.

ARGAND, E. (1924) La tectonique de l'Asie. *Proc. Congrés Géol. International XIII*, **13** pp171–372.

AVIGAD, D. (1992) Exhumation of coesite-bearing rocks in the Dora Maira massif (western Alps, Italy). *Geology*, **20** pp947–950.

BARBIER, R. (1948) Les zones ultradauphinoise et subbriançonnais entre l'Arc et l'Isère. *Mém. Serv. Carte Géol. France*, 291pp.

BARBIER, R. (1951) Sur la découverte de fossiles aux 'Pyramides calcaires' (Haut Val d'Aoste) et aux 'Etroits du Siaix' (Tarentaise) et sur ses conséquences. *C.R. Acad. Sci. Paris*, **332** pp748.

BARFETY, J.C., GIDON, M., LEMOINE, M. & MOUTERDE, P. (1979) Tectonique synsédimentaire liassique dans les massifs cristallins de la zone externe des Alpes Occidentales françaises: la faille de Col d'Ornon. *C.R. Acad. Sci. Paris (série D)*, **289** pp1207–1210.

BARNICOAT, A.C. & FRY, N. (1986) High-pressure metamorphism of the Zermatt-Saas Fee ophiolite zone, Switzerland. *J. Geol. Soc. Lond.*, **143** pp607–18.

BARR, D. (1987) Lithospheric stretching, detached normal faulting and footwall uplift. In: Coward, M.P., Dewey, J.F. & Hancock, P.L. (eds.) Continental Extensional Tectonics. *Geol. Soc. Lond. Spec. Pub.*, **28** pp75–94.

BARR, D. (1992) Passive continental margin subsidence. *J. Geol. Soc. Lond.*, **149** pp803–804.

BARTON, P. & WOOD, R. (1984) Tectonic evolution of the North Sea basin: crustal stretching and subsidence. *Geophys. J. Roy. Astronom. Soc.*, **79** pp987–1022.

BAYER, R. *ET AL.* (22 OTHERS) (1987) Premiers resultats de la traversée des Alpes occidentales par sismique reflexion verticale (Programme ECORS-CROP). *C.R. Acad. Sci. Paris (série II)*, **305** pp1461–1470.

BEARTH, P. & STERN, W. (1979) Zur Geochemie von metapillows der region Zermatt-Saas. *Schweiz. Min. Pet. Mitt.*, **59** pp349–373.

BECCALUVA, L., DAL PIAZ, G.V. & MACCIOTTA, G. (1984) Transitional to MORB affinities in ophiolitic metabasites from the Zermatt-Saas, Combin and Antrona units, Western Alps: implications for the paleogeographic evolution of the Western Tethyan Basin. *Geol. Mijn.*, **63** pp165–177.

BERNOULLI, D. (1972) North Atlantic and Mediterranean Mesozoic facies: a comparison. In: Hollister, C.D., Ewing, J.I. et al. *Init. Repts. DSDP 11, US Govt. Printing Office, Washington*, pp801–871.

BERNOULLI, D. & JENKYNS, H.C. (1974) Alpine, Mediterranean, and central Atlantic Mesozoic facies in relation to the early evolution of the Tethys. *SEPM Spec. Pub.*, **19** pp129–160.

BERTHÉ, D., CHOUKROUNE, P. & GAPAIS, D. (1979) Orientations préfèrentielles du quartz et orthogneissification progressive en régime cisaillant: l'exemple du cisaillement sud-armoricain. *Bulletin de Minéralogie*, **102** pp265–272.

BERTRAND, J. & DELALOYE, M. (1976) Datation par la méthode K–Ar de diverses ophiolites du flysch des Gets (Haute–Savoie, France). *Eclogae Geol. Helv.*, **69** pp335–341.

BICKLE, M.J. & NISBET, E. (1972) The oceanic affinities of some alpine mafic rocks based on their Ti–Zr–Y contents. *J. Geol. Soc. Lond.*, **128** pp267–271.

BIJU-DUVAL, B., DERCOURT, J. & LE PICHON, X. (1977) From the Tethys Ocean to the Mediterranean seas: a plate tectonic model of the evolution of the Western Alpine system. In: Biju-Duval, B. & Montadert, L. (eds.) International Symposium on the Structural History of the Mediterranean Basins. *Editions Technip, Paris*, pp143–164.

BISCHOFF, J.L. & DICKSON, F.W. (1975) Seawater–basalt interaction at 200°C and 500 Bars: implications for origin of sea–floor heavy–metal deposits and regulation of seawater chemistry. *Earth Planet. Sci. Lett.*, **25** pp385–397.

BLUMENFELD, P. & BOUCHEZ, J.L. (1988) Shear criteria in granite and migmatite deformed in the magmatic and solid states. *J. Struct. Geol.*, **10** pp361–372.

BONATTI, E., HONNOREZ, J., KIRST, P. & RADICATI, F. (1975) Metagabbros from the mid–Atlantic ridge at 06°N: contact–hydrothermal–dynamic metamorphism beneath the axial valley. *J. Geol.*, **83** pp61–78.

BOTT, M.H.P. (1992) Passive margins and their subsidence. *J. Geol. Soc. Lond.*, **149** pp805–812.

BOYER, S.E. & ELLIOTT, D. (1982) Thrust systems. *Am. Assoc. Petrol. Geol. Bull.*, **66** pp1196–1230.

BRICE, S.E., COCHRAN, M.D., PARDO, G. & EDWARDS, A.D. (1983) Tectonics and sedimentation of the South Atlantic rift sequence: Cabinda, Angola. In: Watkins, J.S. & Drake, C.L. (eds.) Studies in Continental Margin Geology. *Am. Assoc. Petrol. Geol. Mem.*, **34** pp5–18.

BROSTER, B.E. & HICOCK, S.R. (1985) Multiple flow and support mechanisms and the development of inverse grading in a subaquatic glacigenic debris flow. *Sedimentology*, **32** pp645–657.

BUTLER, R.W.H. (1983) Balanced cross-sections and their implications for the deep structure of the northwest Alps. *J. Struct. Geol.*, **5** pp125–137.

BUTLER, R.W.H. (1985) The restoration of thrust systems and displacement continuity around the Mont Blanc massif, NW external Alpine thrust belt. *J. Struct. Geol.*, **7** pp569–582.

BUTLER, R.W.H. (1986) Thrust tectonics, deep structure and crustal subduction in the Alps and Himalayas. *J. Geol. Soc. Lond.*, **143** pp857–873.

BUTLER, R.W.H. (1987) Thrust sequences. *J. Geol. Soc. Lond.*, **144** pp619–634.

BUTLER, R.W.H. (1989a) The influence of pre-existing basin structure on thrust system evolution in the Western Alps. In: Cooper, M.A. & Williams,

G.D. (eds.) Inversion Tectonics. *Geol. Soc. Lond. Spec. Pub.*, **44** pp105–122.

BUTLER, R.W.H. (1989b) The geometry of crustal shortening in the Western Alps. In: Sengor, A.M.C. (ed.) Tectonic Evolution of the Tethyan Region. *Kluwer Academic Publishers*, pp43–76.

BUTLER, R.W.H., MATTHEWS, S.J. & PARISH, M. (1986) The NW external Alpine thrust belt and its implications for the geometry of the Western Alpine Orogen. In: Coward, M.P. & Ries, A.C. (eds.) Collision Tectonics. *Geol. Soc. Lond. Spec. Pub.*, **19** pp245–260.

CARON, C., HOMEWOOD, P. & WILDI, W. (1989) The original Swiss flysch: a reappraisal of the type deposits in the Swiss Prealps. *Earth-Sci. Rev.*, **26** pp1–45.

CARON, M. (1989) Chapter 4: Cretaceous Planktic foraminifera. In: Bolli, H.M., Saunders, J.B. & Perch-Nielson, K. (eds.) Plankton Stratigraphy (vol 1). *Cambridge University Press*, pp17–86.

CARTER, R.M. (1975) A discussion and classification of subaqueous mass-transport with particular application to grain-flow, slurry-flow and fluxoturbidites. *Earth-Sci. Rev.*, **11** pp145–177.

CAS, R.A.F. & WRIGHT, J.V. (1987) Volcanic Successions, Modern and Ancient. *Allen & Unwin, London*, 528pp.

CASTELLARIN, A., LUCCHINI, F., ROSSI, P.L., SIMBOLI, G., BOSELLINI, A. & SOMMAVILLA, E. (1980) Middle Triassic magmatism in the Southern Alps II: a geodynamical model. *Rivista Ital. Pal. Strat.*, **85** pp1111–1124.

CHOPIN, C. (1984) Coesite and pure pyrope in high-grade blueschists of the Western Alps - a first record and some consequences. *Contrib. Min. Pet.*, **86** pp107–118.

CHOPIN, C. (1987) Very-high-pressure metamorphism in the Western Alps - implications for subduction of continental crust. *Phil. Trans. R. Soc. Lond.*, **A321** pp183–197.

CHOPIN, C & MONIÉ, P. (1984) A unique magnesiochloritoid–bearing, high–pressure assemblage from the Monte Rosa, Western Alps: petrologic and ^{40}Ar–^{39}Ar radiometric study. *Contrib. Min. Pet.*, **87** pp388–398.

CHOUKROUNE, P., BELLEVRE, M., COBBOLD, P., GAUTIER, Y., MERLE, O. & VUICHARD, J-P. (1986) Deformation and motion in the Western Alpine arc. *Tectonics*, **5** pp215–226.

COBBOLD, P.R. & WATKINSON, A.J. (1981) Bending anisotropy: a mechanical constraint on the orientation of fold axes in an anisotropic medium. *Tectonophysics*, **72** ppT1–T10.

COLMAN (1982) Chemical weathering of basalts and andesites: evidence from weathering rinds. *Geol. Surv. Prof. Pap.*, **1246** 51pp.

COLLART, J. (1973) La zone des Brèches de Tarentaise entre Montgirod et le vallon du Cormet d'Arêches (au nord de Moûtiers), Savoie. *Thèse 3ème cycle, l'Université de Grenoble (unpublished)*, 99pp.

COLLET, L.W. (1927) The Structure of the Alps. *Edward Arnold, London*, 289pp.

COMPAGNONI, R., DAL PIAZ, G.V., HUNZIKER, J.C., GOSSO, G., LOMBARDO, B. & WILLIAMS, P.F. (1977) The Sezia-Lanzo Zone, a slice of continental crust with Alpine high pressure-low temperature assemblages in the Western Alps. *Rendiconti Soc. Ital. Min. Pet.*, **33** pp281–334.

COWARD, M.P. (1986) Heterogeneous stretching and basin development. *Earth Planet. Sci. Lett.*, **80** pp325–336.

COWARD, M.P. & DIETRICH, D. (1989) Alpine tectonics - an overview. In: Coward, M.P., Dietrich, D. & Park, R.G. (eds.) Alpine Tectonics. *Geol. Soc. Lond. Spec. Pub.*, **45** pp1–29.

COWARD, M.P., GILLCRIST, R. & TRUDGILL, B. (1991) Extensional structures and their tectonic inversion in the Western Alps. In: Roberts, A.M., Yielding, G. & Freeman, B. (eds.) The Geometry of Normal Faults. *Geol. Soc. Lond. Spec. Pub.*, **56** pp93–112.

COX, K.G. BELL, J.D. & PANKHURST, R.J. (1979) The Interpretation of Igneous Rocks. *George Allen & Unwin, London*, 450pp.

DARDEAU, D. (1987) Inversion du style tectonique et permanence des unités structurales dans l'histoire mésozoïque et alpine du bassin des Alpes maritimes, partie de l'ancienne marge passive de la Tethys. *C.R. Acad. Sci. Paris (série II)*, **305** pp483–486.

DEBELMAS, J. (1957) Quelques rémarques sur la conception actuelle du terme de "cordillère" dans les Alpes internes françaises. *Bull. Soc. Géol. France*, **6 VIII** pp463–474.

DEBELMAS, J. (1976) Deux coupes transversales des Alpes franco-italiennes. *Schweiz. Min. Pet. Mitt.*, **56** pp561–565.

DEBELMAS, J. (1989) Some key features of the evolution of the Western Alps. In: Sengor, A.M.C. (ed.) Tectonic Evolution of the Tethyan Region. *Kluwer Academic Publishers*, pp23–42.

DEBELMAS, J. & KERCKHOVE, C. (1980) Les Alpes franco-italiennes. *Géol. Alpine*, **56** pp21–58.

DEBELMAS, J. & LEMOINE, M. (1970) The Western Alps: palaeogeography and structure. *Earth-Sci. Rev.*, **6** pp221–256.

DECANDIA, F.A. & ELTER, P. (1972) La zona ofiolifera del Bracco nel settore compreso fra Levanto e la Val Gaveglia (Apennino Ligure). *Mem. Soc. Geol. Italiana*, **11** pp503–530.

DERCOURT, J. *ET AL.* (18 OTHERS) (1986) Geological evolution of the Tethys belt from the Atlantic to the Pamirs since the Lias. *Tectonophysics*, **123** pp241–315.

DEVILLE, E. (1990) Within-plate type meta-volcaniclastic deposits of Maastrichtian-Paleogene age in the Grande Motte unit (French Alps, Vanoise): a first record and some implications. *Geodinamica Acta (Paris)*, **4** pp199–210.

DEVILLE, E., FUDRAL, S., LAGABRIELLE, Y., MARTHALER, M. & SARTORI, M. (1992) From oceanic closure to continental collision: a synthesis of the 'schistes lustrés' metamorphic complex of the Western Alps. *Geol. Soc. Am. Bull.*, **104** pp127–139.

DEWEY, J.F. (1982) Plate tectonics and the evolution of the British Isles. *J. Geol. Soc. Lond.*, **139** pp371–412.

DEWEY, J.F., HELMAN, M.L., TURCO, E., HUTTON, D.H.W. & KNOTT, S.D. (1989) Kinematics of the western Mediterranean. In: Coward, M.P., Dietrich, D. & Park, R.G. (eds.) Alpine Tectonics. *Geol. Soc. Lond. Spec. Pub.*, **45** pp265–283.

DEWEY, J.F., PITMAN, W.C., RYAN, W.B.F. & BONIN, J. (1973) Plate tectonics and the evolution of the Alpine system. *Geol. Soc. Am. Bull.*, **84** pp3137–3180.

DIETRICH, D. (1976) La geologia della Catena Costiera Calabra tra Cetraro e Guardia Piemontese. *Mem. Soc. Geol. Italiana*, **17** pp61–121.

DUMONT, T. (1988) Late Triassic–early Jurassic evolution of the western Alps and of their European foreland; initiation of the Tethyan rifting. *Bull. Soc. Géol. France*, **8 IV** pp601–611.

DZULYNSKI, S. & SANDERS, J.E. (1962) Current marks on firm mud bottom. *Trans. Conn. Acad. Arts Sci.*, **42** pp57–96.

EINSELE, G. *ET AL.* (18 OTHERS) (1980) Intrusion of basaltic sills into highly porous sediments, and resulting hydrothermal activity. *Nature*, **283** pp441–445.

ELLENBERGER, F. (1958) Etude Géologique du Pays de Vanoise. *Mem. Explic. Carte Géol. France*, **50** 561pp.

ELLIOTT, D. (1976) The motion of thrust sheets. *J. Geophys. Res.*, **81** pp949–963.

ELLIOTT, D. (1976) The energy balance and deformation mechanisms of thrust sheets. *Phil. Trans. R. Soc. Lond.*, **A273** pp289–312.

ELLIS, A.C., BARNICOAT, A.C. & FRY, N. (1989) Structural and metamorphic constraints on the tectonic evolution of the upper Pennine Alps. In: Coward, M.P., Dietrich, D. & Park, R.G. (eds.) Alpine Tectonics. *Geol. Soc. Lond. Spec. Pub.*, **45** pp173–188.

ELTCHANINOFF-LANCELOT, C., TRIBOULET, S., DOUDOUX, B., FUDRAL, S., RAMPNOUX, J–P. & TARDY, M. (1982) Stratigraphie et tectonique des unités delphino–helvitiques comprises entre Mont–Blanc et Belledonne (Savoie – Alpes occidentales). Implications régionales. *Bull. Soc. Géol. France*, **XXIV** pp817–830.

ELTER, P. (1954) Etudes géologiques dans le Val Veni et le vallon du Breuil (Petit-Saint-Bernard). *Publ. Lab. Géol. de l'Université de Genève*, **66** 39pp.

ELTER, P. & ELTER, G. (1957) Sull' existenza, nei dintorni del Piccolo San Bernardo, di un elemento tettonico riferibile al ricoprimento del Pas du Roc. *Rend. dell'Acad. Naz. dei Lincei*, **8 XXII** pp181–187.

ELTER, G. & ELTER, P. (1965) Carta geologica della regione del Piccolo San Bernardo (versante italiano). *Mem. Istit. Geol. Min. Univ. Padova*, **XXXV** 53pp.

ENGLAND, P. & MOLNAR, P. (1990) Surface uplift, uplift of rocks, and exhumation of rocks. *Geology*, **18** pp1173–1177.

ENOS, P. (1977) Flow regimes in debris flow. *Sedimentology*, **24** pp133–142.

ESCHER, A. & WATTERSON, J. (1974) Stretching fabrics, folds and crustal shortening. *Tectonophysics*, **22** pp223–231.

FABRE, J. (1961) Contribution à l'étude de la zone houillère, en Maurienne et Tarentaise (Alpes de Savoie). *Mem. Bur. Rech. Géol. Min.*, **2** 315pp.

FLOYD, P.A. & WINCHESTER, J.A. (1975) Magma type and tectonic setting discrimination using immobile elements. *Earth Planet. Sci. Lett.*, **27** pp211–218.

FLOYD, P.A. & WINCHESTER, J.A. (1978) Identification and discrimination of altered and metamorphosed volcanic rocks using immobile elements. *Chem. Geol.*, **21** pp291–306.

FOUCHER, J.P., LE PICHON, X. & SIBUET, J.C. (1982) The ocean-continent transition in the uniform stretching model; role of partial melting in the mantle. *Phil. Trans. R. Soc. Lond.*, **A305** pp27–43.

FREEMAN, B. & LISLE, R.J. (1987) The relationship between tectonic strain and the three-dimensional shape fabrics of pebbles in deformed conglomerates. *J. Geol. Soc. Lond.*, **144** pp635–639.

FRY, N. (1989a) Southwestward thrusting and tectonics of the western Alps. In: Coward, M.P., Dietrich, D. & Park, R.G. (eds.) Alpine Tectonics. *Geol. Soc. Lond. Spec. Pub.*, **45** pp83–109.

FRY, N. (1989b) Kinematics of the Alpine arc. *J. Geol. Soc. Lond.*, **146** pp891–892.

FUDRAL, S. (1973) Contribution à l'étude de l'unité de Moûtiers (Zone des Brèches de Tarentaise) entre le vallon du Cormet d'Arêches et le hameau des Chapieux (Savoie). *Thèse 3ème cycle, l'Université de Grenoble (unpublished)*, 129pp.

FUDRAL, S. (1980) Une nouvelle interprétation de l'unité ed Salins (zone des Brèches de Tarentaise) au nord-ouest de Bourg-St-Maurice (Savoie). Conséquences structurales. *C.R. Acad. Sci. Paris (série D)*, **290** pp1333–1336.

GILLCRIST, R., COWARD, M. & MUGNIER, J-L. (1987) Structural inversion and its controls: examples from the Alpine foreland and the French Alps. *Geodinamica Acta*, **1** pp5–34.

GOFFÉ, B. (1977) Succession de subfacies métamorphiques en Vanoise méridionale (Savoie). *Contrib. Min. Pet.*, **62** pp23–42.

GOGUEL, J. (1963) L'interpretation de l'arc des Alpes occidentales. *Bull. Soc. Géol. France*, **5** pp20–33.

GOSSO, G., DAL PIAZ, G.V., PIOVANO, V. & POLINO, R. (1979) High pressure emplacement of early-Alpine nappes, post-nappe deformations and structural levels. *Mem. Istit. Geol. Min. Univ. Padova*, **32** pp5–15.

GRAND, T., DUMONT, T. & PINTO-BULL, F. (1987) Distensions liées au rifting téthysien et paléochamps de contrainte associés dans le bassin liasique de Bourg d'Oisans (Alpes occidentales). *Bull. Soc. Géol. France*, **8 III** pp699–704.

GRACIANSKY, P-C. DE, BOURBON, M., CHARPAL, O. DE, CHENET, P.Y. & LEMOINE, M. (1979) Genèse et évolution comparées de deux marge continentales passives: marge ibérique de l'océan Atlantique et marge européenne de la Téthys dans les Alpes occidentales. *Bull. Soc. Géol. France*, **21** pp663–674.

GRACIANSKY, P-C. DE, DARDEAU, G., LEMOINE, M. & TRICART, P. (1988) De la distension à la compression: l'inversion structurale dans les Alpes. *Bull. Soc. Géol. France*, **8 IV** pp779–785.

GREEN, T.H. (1980) Island arc and continent-building magmatism: a review of petrogenetic models based on experimental petrology and geochemistry. *Tectonophysics*, **63** pp367–385.

GRIFFITHS, R.W. & CAMPBELL, I.H. (1990) Stirring and structure in mantle starting plumes. *Earth Planet. Sci. Lett.*, **99** pp66–78.

GÜNZLER-SEIFFERT, H. (1942) Persistente Brüche im Jura der Wildhorn-Decke des Berner Oberlandes. *Eclogae Geol. Helv.*, **34** pp164–172.

HAMPTON, M.A. (1975) Competence of fine-grained debris flows. *J. Sed. Petrol.*, **49** pp834–844.

HANMER, S. & PASSCHIER, C.W. (1991) Shear-sense indicators: a review. *Geol. Surv. Can. Pap.*, **90–17** 72pp.

HEIN, F.J. (1982) Depositional mechanisms of deep-sea coarse clastic sediments, Cap Enragé Formation, Quebec. *Can. J. Earth Sci.*, **19** pp267–287.

HEIN, F.J. & WALKER, R.G. (1982) The Cambro-Ordovician Cap Enragé Formation, Québec, Canada: conglomeratic deposits of a braided submarine channel with terraces. *Sedimentology*, **29** pp309–329.

HELWIG, J. (1976) Shortening of continental crust in orogenic belts and plate tectonics. *Nature*, **266** pp768–770.

HENDRY, H.E. (1972) Breccias deposited by mass flow in the Breccia nappe of the French Pre-Alps. *Sedimentology*, **18** pp277–292.

HIGGS, R. (1990) Sedimentology and tectonic implications of Cretaceous fan-delta conglomerates, Queen Charlotte Islands, Canada. *Sedimentology*, **37** pp83–103.

HOLLIGER, K. (1990) A composite, depth-migrated deep seismic reflection section along the Alpine segment of the EGT derived from the NFP20 eastern and southern traverses. In: Freeman, R., Giese, P. & Mueller, St. (eds.) The European Geotraverse: Integrative Studies. *European Science Foundation, Strasbourg*, pp245–253.

HOLM, P.E. (1982) Non-recognition of continental tholeiites using the Ti–Y–Zr diagram. *Contrib. Min. Pet.*, **79** pp308–310.

HOMEWOOD, P., ACKERMANN, T., ANTOINE, P. & BARBIER, R. (1984) Sur l'origine de la nappe du Niesen et la limite entre les zones ultrahelvétique et valaisanne. *C.R. Acad. Sci. Paris (série II)*, **299** pp1055–1059.

HOMEWOOD, P., ALLEN, P.A. & WILLIAMS, G.D. (1986) Dynamics of the Molasse Basin of western Switzerland. In: Allen, P.A. & Homewood, P. (eds.) Foreland Basins. *Spec. Pub. Int. Ass. Sediment.*, **8** pp199-217.

HOMEWOOD, P. & CARON, C. (1982) Flysch of the Western Alps. In: Hsü, K.J. (ed.) Mountain Building Processes. *Academic Press, London*, pp157–168.

HOMEWOOD, P., GOSSO, G., ESCHER, A. & MILNES, A. (1980) Cretaceous and Tertiary evolution along the Besançon–Biella traverse (Western Alps). *Eclogae Geol. Helv.*, **73** pp635–649.

HOMEWOOD, P. & LATELTIN, O. (1988) Classic Swiss clastics (flysch & molasse): the Alpine connection. *Geodinamica Acta*, **2** pp1–11.

HSÜ, K.J. (1989) Time and place in Alpine orogenesis - the Fermor Lecture. In: Coward, M.P., Dietrich, D. & Park, R.G. (eds.) Alpine Tectonics. *Geol. Soc. Lond. Spec. Pub.*, **45** pp421–443.

HSÜ, K.J. (1991) Exhumation of high-pressure metamorphic rocks. *Geology*, **19** pp107–110.

HUBBARD, M. & MANCKTELOW, N.S. (1992) Lateral displacement during Neogene convergence in the western and central Alps. *Geology*, **20** pp943–946.

HUMPHRIS, S.E. & THOMPSON, G. (1978a) Hydrothermal alteration of oceanic basalt by sea water. *Geochim. Cosmochim. Acta*, **42** pp107–125.

HUMPHRIS, S.E. & THOMPSON, G. (1978b) Trace element mobility during hydrothermal alteration of oceanic basalts. *Geochim. Cosmochim. Acta*, **42** pp127–136.

HUNZIKER, J.C. (1970) Polymetamorphism in the Monte Rosa, western Alps. *Eclogae Geol. Helv.*, **63** pp151–161.

HUNZIKER, J.C. (1974) Rb-Sr and K-Ar age determination and the Alpine tectonic history of the western Alps. *Mem. Istit. Geol. Min. Univ. Padova*, **31** 54pp.

HUNZIKER, J.C., DESMONS, J. & MARTINOTTI, G. (1989) Alpine thermal evolution in the central and the western Alps. In: Coward, M.P., Dietrich, D. & Park, R.G. (eds.) Alpine Tectonics. *Geol. Soc. Lond. Spec. Pub.*, **45** pp353–367.

HURFORD, A.J., FLISCH, M. & JÄGER, E. (1989) Unravelling the thermo-tectonic evolution of the Alps: a contribution from fission track analysis and mica dating. In: Coward, M.P., Dietrich, D. & Park, R.G. (eds.) Alpine Tectonics. *Geol. Soc. Lond. Spec. Pub.*, **45** pp369–398.

HYNES, A (1980) Carbonatization and mobility of Ti, Y, and Zr in Ascot Formation metabasalts, SE Quebec. *Contrib. Min. Pet.*, **75** pp79–87.

ISHIWATARI, A. (1985) Alpine ophiolites: product of low-degree mantle melting in a Mesozoic transcurrent rift zone. *Earth Planet. Sci. Lett.*, **76** pp93–108.

JACKSON, J. & McKENZIE, D. (1983) The geometrical evolution of normal fault systems. *J. Struct. Geol.*, **5** pp471–482.

JARVIS, G.T. & McKENZIE, D.P. (1980) Sedimentary basin formation with finite extension rates. *Earth Planet. Sci. Lett.*, **48** pp42–52.

JEANBOURQUIN, P. (1985) Les cornieules du versant sud de l'Argentera: Fracturation hydraulique et phénomènes associés. *Eclogae Geol. Helv.*, **78** pp517–535.

JEANBOURQUIN, P. (1988) Nouvelles observations sur les cornieules en Suisse occidentale. *Eclogae Geol. Helv.*, **81** pp511–538.

JEANBOURQUIN, P. & BURRI, M. (1991) Les métasédiments du Pennique inférieur dans la région de Brigue–Simplon. Lithostratigraphie, structure et contexte géodynamic dans le bassin Valaisan. *Eclogae Geol. Helv.*, **84** pp463–481.

JOHNSON, A.M. (1970) Physical Processes in Geology. *Freeman, San Francisco*, 571pp.

KARNER, G.D. & WATTS, A.B. (1982) On isostasy at Atlantic-type continental margins. *J. Geophys. Res.*, **87** pp2923–2948.

KARNER, G.D. & WATTS, A.B. (1983) Gravity anomalies and flexure of the lithosphere at mountain ranges. *J. Geophys. Res.*, **88** pp10449–10477.

KELLER, W.D. (1957) The Principles of Chemical Weathering. *Lucas, Columbia (Missouri).*

KELLING, G. & HOLROYD, J. (1978) Clast size, shape and composition in some ancient and modern fan gravels. In: Stanley, D.J. & Kelling, G. (eds.) Sedimentation in Submarine Canyons, Fans and Trenches. *Dowden, Hutchinson & Ross, Stroudsburg, PA*, pp138–159.

KELTS, K. (1981) A comparison of some aspects of sedimentation and translational tectonics from the Gulf of California and the Mesozoic Tethys, North Penninic Margin. *Eclogae Geol. Helv.*, **74** pp317–338.

KILIAN, W. & REVEL, J. (1893) Une excursion géologique en Tarentaise (la brèche nummulitique et son extension au Nord de Moûtiers). *Bull. Soc. Hist. Nat. Savoie*, **VII** pp28–40.

KILIAN, W. & REVEL, J. (1916) Sur les brèches (conglomérats) de Tarentaise. *C.R. Acad. Sci. Paris*, **163** pp552–555.

KLEIN, E. M. & LANGMUIR, C.H. (1987) Global correlations of ocean ridge basalt chemistry with axial depth and crustal thickness. *J. Geophys. Res.*, **92** pp8089–8115.

KOKELAAR, B.P. (1982) Fluidization of wet sediments during the emplacement and cooling of various igneous bodies. *J. Geol. Soc. Lond.*, **139** pp21–33.

LACASSIN, R. (1989) Plate-scale kinematics and compatibility of crustal shear zones in the Alps. In: Coward, M.P., Dietrich, D. & Park, R.G. (eds.) Alpine Tectonics. *Geol. Soc. Lond. Spec. Pub.*, **45** pp339–352.

LAUBSCHER, H.P. (1971) The large-scale kinematics of the western Alps and the northern Apennines and its palinspastic implications. *Am. J. Sci.*, **271** pp193–226.

LAUBSCHER, H.P. (1978) Foreland folding. *Tectonophysics*, **47** pp325–337.

LAUBSCHER, H.P. (1988a) Material balance in Alpine orogeny. *Geol. Soc. Am. Bull.*, **100** pp1313–1328.

LAUBSCHER, H.P. (1988b) Décollement in the Alpine system: an overview. *Geol. Rundschau*, **77** pp1–9.

LAUBSCHER, H.P. & BERNOULLI, D. (1977) Mediterranean and Tethys. In: Biju-Duval, B. & Montadert, L. (eds.) International Symposium on the Structural History of the Mediterranean Basins. *Editions Technip, Paris*, pp129–132.

LAUBSCHER, H.P. & BERNOULLI, D. (1982) History and deformation of the Alps. In: Hsü, K.J. (ed.) Mountain Building Processes. *Academic Press, London*, pp169–180.

LAZNICKA, P. (1988) Breccias and Coarse Fragmentites: petrology, environments, associations, ores. *Elsevier, Amsterdam*, 832pp.

LEMOINE, M. (1980) Serpentinites, gabbros and ophicalcites in the Piémont-Ligurian domain of the Western Alps: possible indicators of oceanic fracture zones and of associated serpentinite protrusions in the Jurassic-Cretaceous Tethys. *Archives des Sciences (Genève)*, **33** pp103–115.

LEMOINE, M. (1984) Mesozoic evolution of the Western Alps. *Annales Geophysicae*, **2** pp171–172.

LEMOINE, M., GIDON, M. & BARFETY, J.C. (1981) Les massifs externes cristallins des Alpes occidentales: d'anciens blocs basculés nés au Lias du rifting téthysien. *C.R. Acad. Sci. Paris*, **292** pp917–920.

LEMOINE, M., TRICART, P. & BOILLOT, G. (1987) Ultramafic and gabbroic ocean floor of the Ligurian Tethys (Alps, Corsica, Apennines): in search of a genetic model. *Geology*, **15** pp622–625.

LEMOINE, M. & TRÜMPY, R. (1987) Pre-oceanic rifting in the Alps. *Tectonophysics*, **133** pp305–320.

LEMOINE, M. *ET AL.* (10 OTHERS) (1986) The continental margin of the Mesozoic-Tethys in the Western Alps. *Mar. & Petrol. Geol.*, **3** pp178–199.

LE PICHON, X. & SIBUET, J.C. (1981) Passive margins: a model of formation. *J. Geophys. Res.*, **86** pp3708–3720.

LEWIS, P.D., THOMPSON, R.I., HAGGART, J.W. & HICKSON, C.J. (1991) Sedimentology and tectonic implications of Cretaceous fan-delta conglomerates, Queen Charlotte Islands, Canada: Discussion. *Sedimentology*, **38** pp1173–1182.

LISTER, G.S. & SNOKE, A.W. (1984) S-C mylonites. *J. Struct. Geol.*, **6** pp617–638.

LISTER, G.S. & WILLIAMS, P.F. (1979) Fabric development in shear zones: theoretical controls and observed phenomena. *J. Struct. Geol.*, **1** pp283–297.

LISTER, G.S. & WILLIAMS, P.F. (1983) The partitioning of deformation in flowing rock masses. *Tectonophysics*, **92** pp1–33.

LIVERMORE, R.A. & SMITH, A.G. (1985) Some boundary conditions for the evolution of the Mediterranean region. In: Stanley, D.J. & Wezel, F.C. (eds.) Geological Evolution of the Mediterranean Basin. *Springer-Verlag, New York*, pp83–98.

LOUBAT, H. (1968) Etude pétrographique des ophiolites de la zone du Versoyen, Savoie (France), Province d'Aoste (Italie). *Archives des Sciences (Genève)*, **21** pp265–457.

LOUBAT, H. (1975) La zone du Versoyen, témoin possible d'une intersection entre dorsale volcanique océanique et marge continentale. *Archives des Sciences (Genève)*, **28** pp101–116.

LOUBAT, H. (1984) Considérations préliminaires sur la configuration horizontale de l'édifice subvolcanique du Versoyen (Alpes franco-italiennes) analogue aux bassins en distension du type Golfe de Californie. *Géol. Alpine*, **60** pp37–44.

LOUBAT, H. & DELALOYE, M. (1984) La zone du Versoyen (Alpes franco-italiennes): le témoin d'une océanisation mésozoïque circonscrite constituant un milieu hybride, subvolcano-sédimentaire avec mobilisats et adinoles. *Géol. Alpine*, **60** pp45–76.

LOUGHNAN, F.C. (1969) Chemical Weathering of Silicate Minerals. *Elsevier, London*, 155pp.

LOWE, D.R. (1976) Grain flow and grain flow deposits. *J. Sed. Petrol.*, **46** pp188–199.

LOWE, D.R. (1982) Sediment gravity flows: II. Depositional models with special reference to the deposits of high-density turbidity currents. *J. Sed. Petrol.*, **52** pp279–297.

MALAVIEILLE, J., LACASSIN, R. & MATTAUER, M. (1984) Signification tectonique des linéations d'allongement dans les Alpes occidentales. *Bull. Soc. Géol. France*, **7 XXVI** pp895–906.

MARTINEZ-REYES, J. (1980) Contribution à l'étude géologique des Alpes occidentales entre Arc et Isère, région du Mont Niélard et du Cheval-Noir (Savoie): le problème des unités à flysch. *Thèse de Docteur-Ingénieur, l'Université Pierre et Marie Curie, Paris (unpublished)*, 144pp.

MASSARI, F. (1984) Resedimented conglomerates of a Miocene fan-delta complex, Southern Alps, Italy. In: Koster, E.H. & Steel, R.J. (eds.) Sedimentology

of Gravels & Conglomerates. *Can. Soc. Petrol. Geol. Memoir,* **10** pp259–278.

McCLAY, K.R. (1987) The mapping of Geological Structures. *Geological Society of London Handbook, Open University Press, Milton Keynes,* 161pp.

McKENZIE, D. (1978) Some remarks on the development of sedimentary basins. *Earth Planet. Sci. Lett.,* **40** pp25–32.

McKENZIE, D. & BICKLE, M.J. (1988) The volume and composition of melt generated by extension of the lithosphere. *J. Petrol.,* **29** pp625–679.

MÉNARD, G., MOLNAR, P. & PLATT, J.P. (1991) Budget of crustal shortening and subduction of continental crust in the Alps. *Tectonics,* **10** pp231–244.

MESCHEDE, M. (1986) A method of discriminating between different types of mid-ocean ridge basalts and and continental tholeiites with the Nb-Zr-Y diagram. *Chem. Geol.,* **56** pp207–218.

MIDDLETON, G.V. (1967) Experiments on density and turbidity currents III. Deposition of sediment. *Can. J. Earth Sci.,* **4** pp475–505.

MIDDLETON, G.V. & SOUTHARD, J.B. (1978) Mechanics of Sediment Movement. *SEPM short course notes,* **3** 242pp.

MILLS, H.H. (1979) Downstream rounding of pebbles - a quantitative review. *J. Sed. Petrol.,* **49** pp295–302.

MONIÉ, P. (1985) La méthode ^{39}Ar–^{40}Ar appliquée au métamorphisme alpin dans le massif du Mont-Rose (Alpes Occidentales). Chronologie détaillée depuis 110 Ma. *Eclogae Geol. Helv.,* **78** pp487–517.

MOTTL, M.J. (1983) Metabasalts, axial hot springs, and the structure of hydrothermal systems at mid–ocean ridges. *Geol. Soc. Am. Bull.,* **94** pp161–180.

MUELLER, ST. (1982) Deep structure and recent dynamics in the Alps. In: Hsü, K.J. (ed.) Mountain Building Processes. *Academic Press, London,* pp181–199.

MUELLER, ST. (1989) Deep-reaching geodynamic processes in the Alps. In: Coward, M.P., Dietrich, D. & Park, R.G. (eds.) Alpine Tectonics. *Geol. Soc. Lond. Spec. Pub.,* **45** pp303–328.

MUGNIER, J-L., GUELLEC, S., MÉNARD, G., ROURE, F., TARDY, M. & VIALON, P. (1990) A crustal scale balanced cross-section through the external Alps deduced from the ECORS profile. *Mém. Soc. Géol. France,* **156** pp203–216.

MULLEN, E.D. (1983) $MnO/TiO_2/P_2O_5$: a minor element discriminant for basaltic rocks of oceanic environments and its implications for petrogenesis. *Earth. Planet. Sci. Lett.,* **62** pp53–62.

NAYLOR, M.A. (1980) The origin of inverse grading in muddy debris flow deposits-a review. *J. Sed. Petrol.,* **50** pp1111–1116.

NEMEC, W. (1990) Apsects of sediment movement on steep delta slopes. In: Colella, A. & Prior, D.B. (eds.) Coarse-Grained Deltas. *Spec. Pub. Int. Ass. Sedimentol.,* **10** pp29–73.

NEMEC, W. & STEEL, R.J. (1984) Alluvial and coastal conglomerates: their significant features and some comments on gravelly mass-flow deposits. In: Koster, E.H. & Steel, R.J. (eds.) Sedimentology of Gravels and Conglomerates. *Can. Soc. Petrol. Geol. Memoir,* **10** pp1–31.

NEMEC, W., STEEL, R.J., POREBSKI, S.J. & SPINNANGR, A. (1984) Domba conglomerate, Devonian, Norway: process and lateral variability in a mass-flow dominated, lacustrine fan-delta. In: Koster, E.H. & Steel, R.J. (eds.) Sedimentology of Gravels & Conglomerates. *Can. Soc. Petrol. Geol. Memoir,* **10** pp295–320.

NESBITT, H.W. & WILSON, R.E. (1992) Recent weathering of basalts. *Am. J. Sci.,* **292** pp740–777.

NEUMAYR, M. (1883) Klimatische zonen während der Jura und Kreidezeit. *Denkschrift der Kaiserlichen Akademie der Wissenschaften Wien,* **47** pp1–34.

NICOLAS, A. & JACKSON, E.D. (1972) Répartition en deux provinces des péridotites des chaînes alpines longeant la Mediterranée: implications géotectoniques. *Schweiz. Min. Pet. Mitt.,* **52** pp479–495.

OBERHÄNSLI, R., HUNZIKER, J.C., MARTINOTTI, G. & STERN, W.B. (1985) Geochemistry, geochronology and petrology of Monte Mucrone - an example of eo-Alpine eclogitization of Permian granitoids in the Sesia-Lanzo zone, Western Alps, Italy. *Chem. Geol.,* **52** pp165–184.

OHNENSTETTER, M., OHNENSTETTER, D., VIDAL, P., CORNICHET, J., HERMITTE, D. & MACE, J. (1981) Crystallisation and age of zircon from Corsican ophiolitic albitites: consequences for oceanic expansion in Jurassic times. *Earth. Planet. Sci. Lett.,* **54** pp397–408.

PANTIC, N. & ISLER, A. (1978) Palynologische Untersuchungen in Bündnerschiefern (II). *Eclogae Geol. Helv.,* **71** pp447–465.

PASSCHIER, C.W. & SIMPSON, C. (1986) Porphyroclast systems as kinematic indicators. *J. Struct. Geol.,* **8** pp831–844.

PEARCE, J.A. (1975) Basalt geochemistry used to investigate past tectonic environments on Cyprus. *Tectonophysics,* **25** pp41–67.

PEARCE, J.A. (1982) Trace element characteristics of lavas from destructive plate boundaries. In: Thorpe, R.S. (ed.) Andesites. *John Wiley & Sons, New York,* pp525–548.

PEARCE, J.A. (1983) The role of sub-continental lithosphere in magma genesis at destructive plate margins. In: Hawkesworth, C.J. & Norry, M.J. (eds.) Continental Basalts and Mantle Xenoliths. *Shiva, Nantwich,* pp230–249.

PEARCE, J.A. & CANN, J.B. (1973) Tectonic setting of basic volcanic rocks determined using trace element analyses. *Earth Planet. Sci. Lett.,* **19** pp290–300.

PEARCE, J.A. & NORRY, M.J. (1979) Petrogenetic implications of Ti, Zr, Y, and Nb variations in volcanic rocks. *Contrib. Min. Petrol.,* **69** pp33–47.

PEARCE, J.A., GORMAN, B.E. & BIRKETT, T.C. (1975) The TiO_2–K_2O–P_2O_5 diagram: a method of discriminating between oceanic and non-oceanic basalts. *Earth Planet. Sci. Lett.,* **24** pp419–426.

PEARCE, J.A., GORMAN, B.E. & BIRKETT, T.C. (1977) The relationship between major element chemistry and tectonic environment of basic and intermediate volcanic rocks. *Earth Planet. Sci. Lett.,* **36** pp121–132.

PERRIER, R. & QUIBLIER, J. (1974) Thickness changes in sedimentary layers during compaction history; methods for quantitative evaluation. *Am. Assoc. Petrol. Geol. Bull.,* **58** pp507–20.

PICKERING, K.T., HISCOTT, R.N. & HEIN, F.J. (1989) Deep Marine Environments: Clastic Sedimentation and Tectonics. *Unwin Hyman, London,* 416pp.

PICKERING, K.T., STOW, D.A.V., WATSON, M.P. & HISCOTT, R.N. (1986) Deep-water facies, processes and models: a review and classification scheme for modern and ancient sediments. *Earth-Sci. Rev.,* **23** pp75–174.

PLATT, J.P. (1986) Dynamics of orogenic wedges and the uplift of high-pressure metamorphic rocks. *Geol. Soc. Am. Bull.,* **97** pp1037–1053.

PLATT, J.P. (1987) The uplift of high-pressure–low-temperature metamorphic rocks. *Phil. Trans. R. Soc. Lond.,* **A321** pp87–103.

PLATT, J.P., BEHRMANN, J.H., CUNNINGHAM, P.C., DEWEY, J.F., HELMAN, PARISH, M., SHEPLEY, M.G., WALLIS, S. & WESTON, P.J. (1989a) Kinematics of the Alpine arc and the motion history of Adria. *Nature,* **337** pp158–161.

PLATT, J.P. & HSÜ, K.J. (1992) Comment and reply on "Exhumation of high-pressure metamorphic rocks". *Geology,* **20** pp186–187.

PLATT, J.P. LISTER, G.S., CUNNINGHAM, P., WESTON, P., PEEL, F., BAUDIN, T. & DONDEY, H. (1989b) Thrusting and backthrusting in the Briançonnais domain of the western Alps. In: Coward, M.P., Dietrich, D. & Park, R.G. (eds.) Alpine Tectonics. *Geol. Soc. Lond. Spec. Pub.,* **45** pp135–152.

PLATT, J.P. & VISSERS, R.L.M. (1980) Extensional structures in anisotropic rocks. *J. Struct. Geol.,* **2** pp397–410.

POREBSKI, S.J. (1984) Clast-size and bed thickness trends in resedimented conglomerates: example from a Devonian fan-delta succession, southwest Poland. In: Koster, E.H. & Steel, R.J. (eds.) Sedimentology of Gravels & Conglomerates. *Can. Soc. Petrol. Geol. Memoir,* **10** pp399–411.

POSTMA, G., NEMEC, W. & KLEINSPEHN, K.L. (1988) Large floating clasts in turbidites: a mechanism for their emplacement. *Sediment. Geol.,* **58** pp47–61.

POWERS, M.C. (1953) A new roundness scale for sedimentary particles. *J. Sed. Petrol.,* **23** pp117–119.

PRICE, N.J. & COSGROVE, J.W. (1990) Analysis of Geological Structures. *Cambridge University Press,* 502pp.

PRIOR, D.B. & BORNHOLD, B.D. (1990) The underwater development of Holocene fan deltas. In: Colella, A. & Prior, D.B. (eds.) Coarse-Grained Deltas. *Spec. Pub. Int. Ass. Sediment.,* **10** pp75–90.

RAMSAY, J.G. (1962) Interference patterns produced by the superposition of folds of similar types. *J. Geol.,* **70** pp466–481.

RAMSAY, J.G. (1963) Stratigraphy, structure and metamorphism in the western Alps. *Proc. Geol. Assoc.,* **74** pp357–391.

RAMSAY, J.G. (1967) Folding and Fracturing of Rocks. *McGraw-Hill, New York,* 568pp.

RAMSAY, J.G. (1980) Shear zone geometry: a review. *J. Struct. Geol.,* **2** pp83–89.

RAMSAY, J.G. (1982) Rock ductility and its influence on the development of tectonic structures in mountain belts. In: Hsü, K.J. (ed.) Mountain Building Processes. *Academic Press, London,* pp111–127.

RAMSAY, J.G. & HUBER, M.I. (1983) The Techniques of Modern Structural Geology. Volume 1: Strain Analysis. *Academic Press, London,* 307pp.

RATSBACHER, L., FRISCH, W. & LINZER, H-G. (1991) Lateral extrusion in the eastern Alps, Part 2: Structural analysis. *Tectonics,* **10** pp257–271.

REICHE, P. (1950) A survey of weathering processes and products. *University of New Mexico Press, Alberquerque,* 95pp.

RICCI LUCCHI, F. (1975) Depositional cycles in two turbidite formations of northern Apennines (Italy). *J. Sed. Petrol.,* **45** pp3–43.

RICOU, L.E. (1984) Les Alpes occidentales: chaîne de décrochement. *Bull. Soc. Géol. France,* **26** pp861–874.

RICOU, L.E. & SIDDANS, A.W.B. (1986) Collision tectonics in the Western Alps. In: Coward, M.P. & Ries, A.C. (eds.) Collision Tectonics. *Geol. Soc. Lond. Spec. Pub.,* **19** pp229–244.

RIDLEY (1986) Parallel stretching lineations and fold axes oblique to a shear displacement direction–a model and observations. *J. Struct. Geol.,* **8** pp647–653.

ROCHELEAU, M. & LAJOIE, J. (1974) Sedimentary structures in resedimented conglomerate of the Cambrian flysch, L'Islet, Quebec Appalachians. *J. Sed. Petrol.,* **44** pp826–836.

RUBIE, D.C. (1984) A thermal-tectonic model for high-pressure metamorphism and deformation in the Sesia zone, western Alps. *J. Geol.,* **92** pp21–36.

SADLER, P.M. (1982) Bed-thickness and grain size of turbidites. *Sedimentology,* **29** pp37–51.

SANDERS, J.E. (1965) Primary sedimentary structures formed by turbidity currents and related resedimentation mechanisms. In: Middleton, G.V. (ed.) Primary Sedimentary Structures and their Hydrodynamic Interpretation. *SEPM Spec. Pub.,* **12** pp192–219.

SANJUAN, B., MICHARD, A. & MICHARD, G. (1988) Influence of the temperature of CO_2-rich springs on their aluminium and rare earth element contents. *Chem. Geol.,* **68** pp57–67.

SAUNDERS, A.D., FORNARI, D.J. & MORRISON, M.A. (1982) The composition and emplacement of basaltic magmas produced during the development of continental-margin basins: the Gulf of California, Mexico. *J. Geol. Soc. Lond.,* **139** pp335–346.

SAUNDERS, A.D. & TARNEY, J (1991) Back-arc Basins. In: Floyd, P.A. (ed.) Oceanic Basalts. *Blackie, Glasgow,* pp219–263.

SAVOSTIN, L.A., SIBUET, J.-C., ZONENSHAIN, L.P., LE PICHON, X. & ROULET, M.-J. (1986) Kinematic evolution of the Tethys belt from the Atlantic Ocean to the Pamirs since the triassic. *Tectonophysics,* **123** pp1–35.

SAWYER, D.S., SWIFT, B.A., SCLATER, J.G. & TOKSÖZ, M.N. (1982) Extensional model for the subsidence of the northern United States Atlantic continental margin. *Geology,* **10** pp134–140.

SCHMID, S.M., AEBLI, H.R., HELLER, F. & ZINGG, A. (1989) The role of the Periadriatic Line in the tectonic evolution of the Alps. In: Coward, M.P., Dietrich, D. & Park, R.G. (eds.) Alpine Tectonics. *Geol. Soc. Lond. Spec. Pub.,* **45** pp153–171.

SCHOELLER, H. (1929) La nappe de l'Embrunais au Nord de l'Isère. *Bull. Carte Géol. France,* **XXXIII (175)** 422pp.

SCLATER, J.G. & CHRISTIE, P.A.F. (1980) Continental stretching: an explanation of the post–mid–Cretaceous subsidence of the central North Sea basin. *J. Geophys. Res.*, **85** pp3711–3739.

SEYFRIED, W.E. JR. (1987) Experimental and theoretical constraints on hydrothermal alteration processes at mid–ocean ridges. *Ann. Rev. Earth Planet. Sci.*, **15** pp317–335.

SHACKLETON, R.M. & RIES, A.C. (1984) The relation between regionally consistent stretching lineations and plate motions. *J. Struct. Geol.*, **6** pp111–117.

SHANMUGAM, G. (1980) Rhythms in deep sea fine-grained turbidite and debris flow sequences, Middle Ordovician, eastern Tennessee. *Sedimentology*, **27** pp419–432.

SHANMUGAM, G. (1988) Origin, recognition and importance of erosional unconformities in sedimentary basins. In: Kleinspehn, K.L. & Paola, C. (eds.) New Perspectives in Basin Analysis. *Springer-Verlag, New York*, pp83–108.

SHERVAIS, J.W. (1982) Ti–V plots and the petrogenesis of modern and ophiolitic lavas. *Earth Planet. Sci. Lett.*, **59** pp101–118.

SIBSON, R.H. (1986) Brecciation processes in fault zones: inferences from earthquake rupturing. *Pure Appl. Geophys.*, **124** pp156–175.

SIMPSON, C. & SCHMID, S.M. (1983) An evaluation of the criteria used to deduce the sense of movement in rocks. *Geol. Soc. Am. Bull.*, **94** pp1281–1288.

SINCLAIR, H.D., COAKLEY, B.J., ALLEN, P.A. & WATTS, A.B. (1991) Simulation of foreland basin stratigraphy using a diffusion model of mountain belt uplift and erosion: an example from the central Alps, Switzerland. *Tectonics*, **10** pp599–620.

SLEEP, N.H. (1971) Thermal effects of the formation of the Atlantic continental margins by continental break up. *Geophys. J. Roy. Astron. Soc.*, **24** pp325–350.

SLOMAN, L.E. (1989) Triassic shoshonites from the Dolomites, northern Italy; alkaline arc rocks in a strike-slip setting. *J. Geophys. Res.*, **94** pp4655–4666.

SMITH, A.G. (1971) Alpine deformation and the oceanic areas of Tethys, Mediterranean and Atlantic. *Geol. Soc. Am. Bull.*, **82** pp2039–2070.

SMITH, A.G. & WOODCOCK, N.H. (1982) Tectonic syntheses of the Alpine-Mediterranean region: a review. In: Berckhemer, H. & Hsü, K.J. (eds.) Alpine–Mediterranean Geodynamics. *American Geophysical Union, Geodynamic Series*, **7** pp15–38.

SMITH, G.A. (1986) Coarse-grained nonmarine volcaniclastic sediment: terminology and depositional process. *Geol. Soc. Am. Bull.*, **97** pp1–10.

SMYTH, C.H. JR. (1913) The relative solubilities of the chemical constituents of rocks. *J. Geol.*, **XXI** pp105–120.

SNEED, E.D. & FOLK, R.L. (1958) Pebbles in the lower Colorado River, Texas: a study in particle morphogenesis. *J. Geol.*, **66** pp114–150.

SODERO, D. (1968) Sull'età Barremiana-Aptiana delle formazioni basali del "Flysch" della Zona delle Brecce di Tarantasia in Valle D'Aosta. *Boll. Soc. Geol. Italia*, **87** pp223–231.

SPENCER, S. (1990) The Nature of the North Pennine Front: French Alps. *PhD thesis, Imperial College, University of London (unpublished)*, 256pp.

SPENCER, S. (1992) A kinematic analysis incorporating incremental strain data for the Frontal Pennine Zones of the western French Alps. *Tectonophysics*, **206** pp285–305.

STALDER, P.J. (1979) Organic and inorganic metamorphism in the Taveyannaz sandstone of the Swiss Alps and equivalent sandstones in France and Italy. *J. Sed. Petrol.*, **49** pp463–82.

STAMPFLI, G.M. & MARTHALER, M. (1990) Divergent and convergent margins in the North-Western Alps confrontation to actualistic models. *Geodinamica Acta*, **4** pp159–184.

STEWART, I.S. & HANCOCK, P.L. (1988) Normal fault zone evolution and and fault scarp degradation in the Aegean region. *Basin Research*, **1** pp137–153.

STEWART, I.S. & HANCOCK, P.L. (1990) Brecciation and fracturing within neotectonic normal fault zones in the Aegean region. In: Knipe, R.J. & Rutter, E.H. (eds.) Deformation Mechanisms, Rheology and Tectonics. *Geol. Soc. Lond. Spec. Pub.*, **54** pp105–112.

SUESS, E. (1893) Are great ocean depths permanent? *Natural Sciences*, **2** pp180–187.

SURLYK, F. (1984) Fan-delta to submarine fan conglomerates of the Volgian-Valanginian Wollaston Forland Group, East Greenland. In: Koster, E.H. & Steel, R.J. (eds.) Sedimentology of Gravels & Conglomerates. *Can. Soc. Petrol. Geol. Memoir*, **10** pp359–382.

THOMPSON, G. (1991) Metamorphic and hydrothermal process: basalt–seawater interactions. In: Floyd, P.A. (ed.) Oceanic basalts. *Blackie, Glasgow*, pp148–173.

THOMPSON, R.N. & GIBSON, S.A. (1991) Subcontinental mantle plumes, hotspots and pre-existing thinspots. *J. Geol. Soc. Lond.*, **148** pp973–977.

TOZER, E.T. (1989) Tethys, Thetis, Thethys, or Thetys? What, where, and when was it? *Geology*, **17** pp882–884.

TRICART, P. (1984) From passive margin to continental collision: a tectonic scenario for the western Alps. *Am. J. Sci.*, **284** pp97–120.

TRICART, P. & LEMOINE, M (1983) Serpentinitic oceanic bottom in South Queyras ophiolites (French Western Alps): Record of the incipient oceanic opening of the Mesozoic Ligurian Tethys. *Eclogae Geol. Helv.*, **76** pp611–629.

TRICART, P. & LEMOINE, M (1986) From faulted blocks to megamullions and megaboudins: Tethyan heritage in the structure of the Western Alps. *Tectonics*, **5** pp95–118.

TRÜMPY, R. (1951) Sur les racines helvétiques et les "Schistes lustrés" entre le Rhône et la Vallée de Bagnes (région de la Pierre Avoi). *Eclogae Geol. Helv.*, **44** pp338–347.

TRÜMPY, R. (1954) La zone de Sion-Courmayeur dans le haut Val Ferret valaisan. *Eclogae Geol. Helv.*, **47** pp315–359.

TRÜMPY, R. (1955) Remarques sur la corrélation des unités Penniques externes entre la Savoie et le Valais et sur l'origine des nappes préalpines. *Bull. Soc. Géol. France*, **6** pp217–231.

TRÜMPY, R. (1960) Palaotectonic evolution of the Central and Western Alps. *Geol. Soc. Am. Bull.*, **71** pp843–908.

TRÜMPY, R. (1973) Timing of orogenic events in the Central Alps. In: Jong, K.A. de & Scholten, R. (eds.) Gravity and Tectonics. *John Wiley & Sons, New York*, pp229–251.

TRÜMPY, R. (1975) Penninic-Austoalpine boundary in the Swiss Alps: a presumed former continental margin and its problems. *A. J. Sci.*, **275** pp209–238.

TRÜMPY, R. (1982) Alpine paleogeography: a reappraisal. In: Hsü, K.J. (ed.) Mountain Building Processes. *Academic Press, London*, pp149–156.

TRÜMPY, R. (1988) A possible Jurassic-Cretaceous transform system in the Alps and the Carpathians. In: Clark, S.P., Burchfiel, B.J. & Suppe, J. (eds.) Processes in Continental Lithospheric Deformation. *Geol. Soc. Am. Spec. Pap.*, **218** pp93–109.

VANDENBERG, J. (1979a) Reconstructions of the western Mediterranean area for the Mesozoic and Tertiary timespan. *Geol. Mijn.*, **58** pp161–174.

VANDENBERG, J. (1979b) Palaeomagnetic data from the western Mediterranean: a review. *Geol. Mijn.*, **58** pp161–174.

WALKER, R.G. (1975) Generalised facies models for resedimented conglomerates of turbidite association. *Geol. Soc. Am. Bull.*, **86** pp737–748.

WALKER, R.G. (1978) Deep water sandstone facies and ancient submarine fans: models for exploration for stratigraphic traps. *Am. Assoc. Petrol. Geol. Bull.*, **62** pp932–966.

WALKER, R.G. & MUTTI, E. (1973) Turbidite facies and facies associations. In: Middleton, G.V. & Bouma, A.H. (eds.) Turbidites and Deep-Sea Sedimentation. *SEPM Pacific Section, short course notes*, pp119–157.

WARRAK, M. (1974) The petrography and origin of dedolomitised, veined or brecciated carbonate rocks, the 'cornieules', in the Fréjus region, French Alps. *J. Geol. Soc. Lond.*, **130** pp229–247.

WATKINSON, A.J. (1975) Multilayer folds initiated in bulk plane strain, with the axis of no change perpendicular to the layering. *Tectonophysics*, **28** ppT7–T11.

WATTS, A.B. (1982) Tectonic subsidence, flexure and global changes of sea-level. *Nature*, **297** pp469–474.

WATTS, A.B. & RYAN, W.B.F. (1976) Flexure of the lithosphere and continental margin basins. *Tectonophysics*, **36** pp25–44.

WEISSERT, H.J. & BERNOULLI, D. (1985) A transform margin in the Mesozoic Tethys: evidence from the Swiss Alps. *Géol. Rundschau*, **74** pp665–679.

WELBON, A. (1988) The influence of intrabasinal faults on the development of a linked thrust system. *Geol. Rundschau*, **77** pp76–10.

WESTCOTT, W.A. & ETHRIDGE, F.G. (1990) Fan deltas – alluvial fans in coastal settings. In: Rachocki, A.H. & Church, M. (eds.) Alluvial Fans: A Field Approach. *Wiley, Chichester*, pp195–211.

WHEELER, J. (1987) The determination of true shear senses from the deflection of passive markers in shear zones. *J. Geol. Soc. Lond.*, **144** pp73–77.

WHEELER, J. (1991) Structural evolution of a subducted continental sliver: the northern Dora Maira massif, Italian Alps. *J. Geol. Soc. Lond.*, **148** pp1101–1113.

WHITE, N (1990) Does the uniform stretching model work in the North Sea? In: Blundell, D.J. & Gibbs, A.D. (eds.) Tectonic Evolution of the North Sea Rifts. *Clarendon Press, Oxford,* pp217–235.

WHITE, R.S. (1992a) Crustal structure and magmatism of North Atlantic continental margins. *J. Geol. Soc. Lond.*, **149** pp841–854.

WHITE, R.S. (1992b) Magmatism during and after continental break-up. In: Storey, A.B., Alabaster, T. & Pankhurst, R.J. (eds.) Magmatism and the Causes of Continental Break-up. *Geol. Soc. Lond. Spec. Pub.*, **68** pp1–16.

WHITE, S.H., BRETAN, P.G. & RUTTER, E.H. (1986) Fault-zone reactivation: kinematics and mechanisms. *Phil. Trans. R. Soc. Lond.*, **A317** pp81–97.

WICKS, F.J. & WHITTAKER, E.J.W. (1977) Serpentine textures and serpentinization. *Canadian Mineralogist,* **15** pp459–488.

WILDI, W. (1985) Heavy mineral distribution and dispersal pattern in penninic and ligurian flysch basins (Alps, northern Apennines). *Giornale di Geologia,* **47** pp77-99.

WILSON, G. & COSGROVE, J.W. (1982) Introduction to Small-Scale Geological Structures. *George Allen & Unwin, London,* 128pp.

WINCHESTER, J.A. & FLOYD, P.A. (1977) Geochemical discrimination of different magma series and their differentiation products using immobile elements. *Chem. Geol.*, **20** pp325–343.

WINKLER, W. & BERNOULLI, D. (1986) Detrital high pressure/low temperature minerals in a late Turonian flysch sequence of the eastern Alps (western Austria): Implications for early Alpine tectonics. *Geology,* **14** pp596–601.

WINN, R.D. JR. & DOTT, R.H. JR. (1977) Large-scale traction-produced structures in deep-water fan-channel conglomerates in southern Chile. *Geology,* **5** pp41–44.

WINTERER, E.L. & BOSELLINI, A. (1981) Subsidence and sedimentation on Jurassic passive continental margin, Southern Alps, Italy. *Am. Assoc. Petrol. Geol. Bull.* **65** pp394–421.

WOOD, D.A., JORON, J–L. (1979) Re–appraisal of the use of trace elements to classify and discriminate between magma series erupted in different tectonic settings. *Earth Planet. Sci. Lett.*, **45** pp326–336.

WOODCOCK, N.H. (1986) The role of strike-slip faults at plate boundaries. *Phil. Trans. R. Soc. Lond.*, **A317** pp13–29.

WOOLER, D.A., SMITH, A.G. & WHITE, N. (1992) Measuring lithospheric stretching on Tethyan passive margins. *J. Geol. Soc. Lond.*, **149** pp517–532.

YE, S. & ANSORGE, J. (1990) A crustal section through the Alps derived from the EGT seismic refraction data. In: Freeman, R., Giese, P. & Mueller, St. (eds.) The European Geotraverse: Integrative Studies. *European Science Foundation, Strasbourg,* pp221–236.

ZÜLAUF, R. (1964) Zür geologie der penninischen Zonen nördlich der Dora Baltea im oberen Val d'Aosta (Italien). *Thesis, Zurich,* 150pp.

typical Alpine exposure

SUBBRIAN-ÇONNAIS

CS — *calc-schists (L. Jurassic?)*

VERSOYEN

MB — *metabasites*

PEL — *pelites (Arguerey Formation)*

SRP — *serpentinites*

GT — *granitic schists*

TARENTAISE

STC — *St. Cristophe Formation*

M — *Marmontains Formation*

A — *Aroley Formation*

GF — *Grand Fond Formation*

PEL — *pelites (Arguerey / Peula Fm)*

LS — *limestones (L. Jurassic)*

GY \ CG — *gypsum \ cargneule*

DOL — *dolomites (Triassic)*

PS — *psammites (Trias + ?Permian)*

SH — *pelites (Carboniferous)*

ULTRA-HELVETIC

MPS — *marly / pelitic schists (Jurassic)*

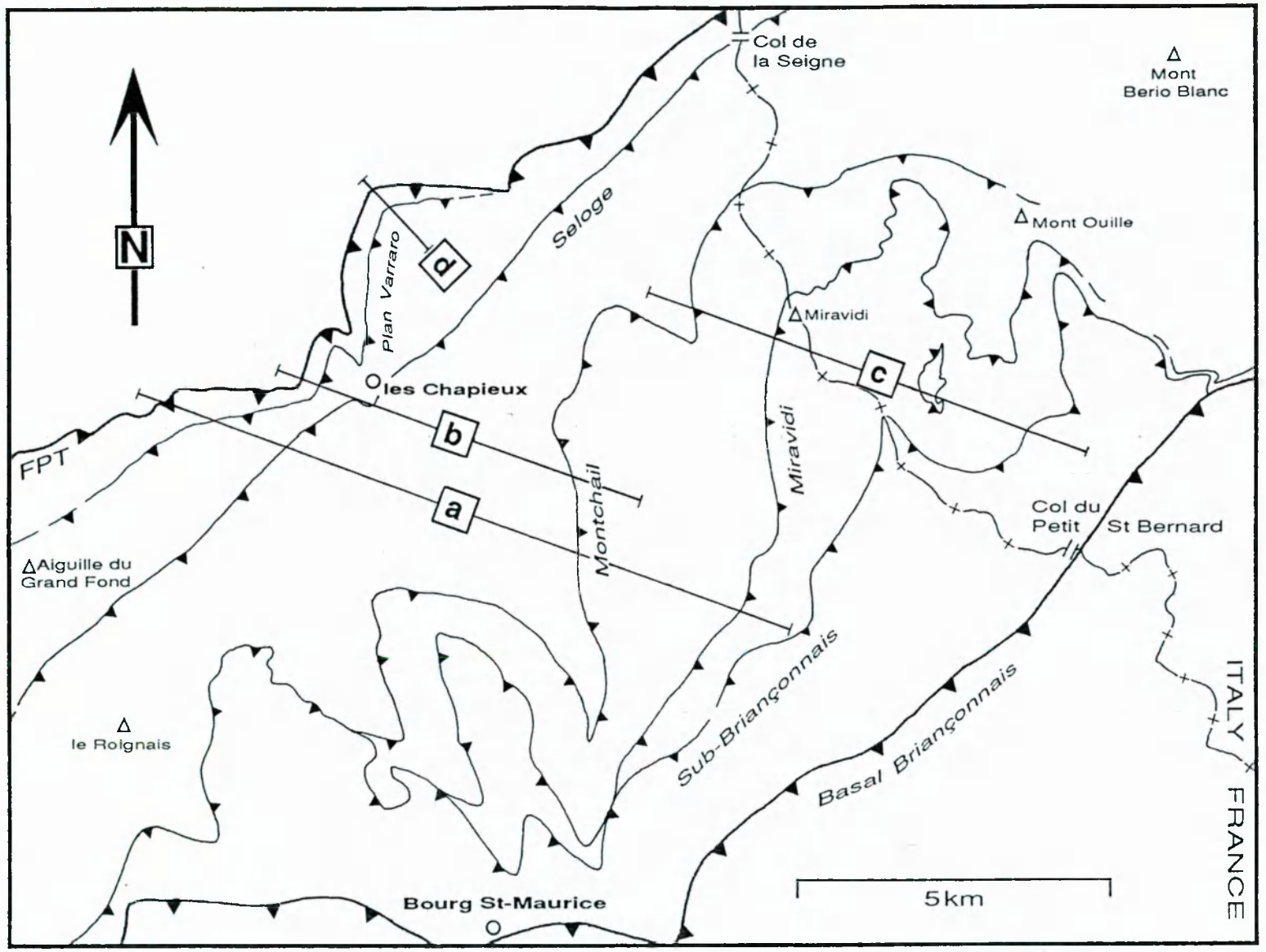

observed and inferred geological boundaries

dip of bedding

S — *dip of tectonic fabrics*
Sx = high strain fabric where lithology and foliation are parallel

direction of younging

vergence of minor folds: F1, F2

Key to Cross Sections: Map shows location of section lines relative to the outcrop of the thrusts which bound and compartmentalise the Tarentaise Zone: line **a** is Fig. 2-14, line **b** is Fig. 2-15, line **c** is Fig. 2-16 and line **d** is Fig. 2-35.

Key to Cross Sections

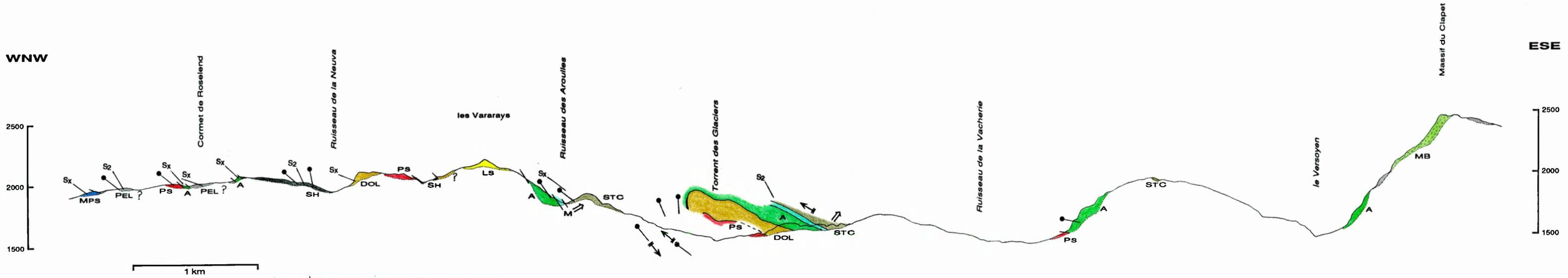

Fig. 2-14. Cross-section line a between 31947 506273 and 33048 505880 showing lithologies and representative structural data. Discontinuous dotted line below topographic level indicates vertical extent of exposure within 200m (horizontally) of the section line. Geological information is projected from up to 500m (horizontally) of the line of section. See accompanying key for explanation of symbols and abbreviations.

Enclosure **a** *(Fig. 2-14)*

Enclosure **b** *(Fig. 2-15)*

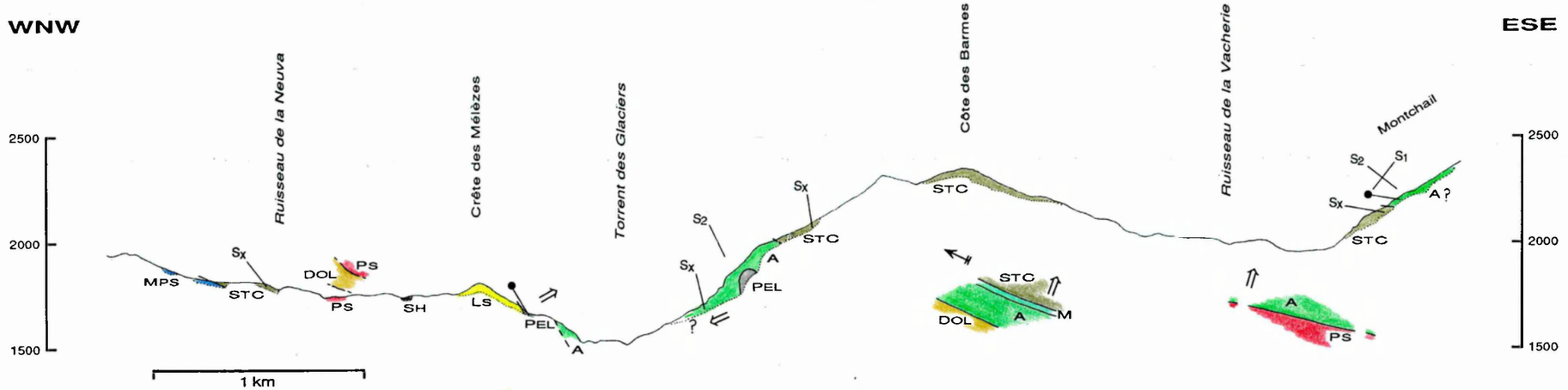

Fig. 2-15. Cross-section line **b** across the Vallée des Chapieux between 32152 506307 and 32763 506087, showing lithologies and representative structural data. Discontinuous dotted line below topographic level indicates vertical extent of exposure within 200m (horizontally) of the section line. Geological information is projected from up to 500m (horizontally) of the line of section. See accompanying key for explanation of symbols and abbreviations.

Enclosure **c** *(Fig. 2-16)*

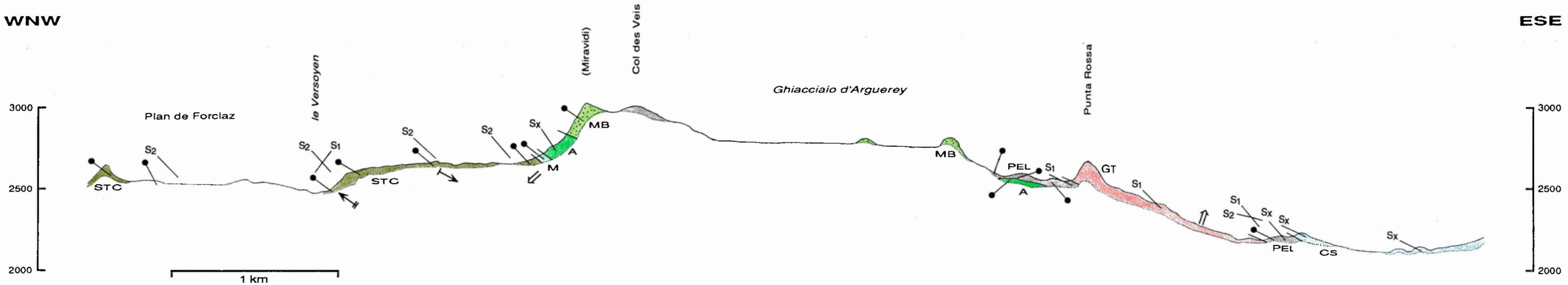

Fig. 2-16. Cross-section line **c** through the upper Breuil and Versoyen valleys between 32763 506532 and 33563 506242, showing lithologies and representative structural data. Discontinuous dotted line below topographic level indicates vertical extent of exposure within 200m (horizontally) of the section line. Geological information is projected from up to 500m (horizontally) of the line of section. See accompanying key for explanation of symbols and abbreviations.

Enclosure **d** *(Fig. 2-41)*

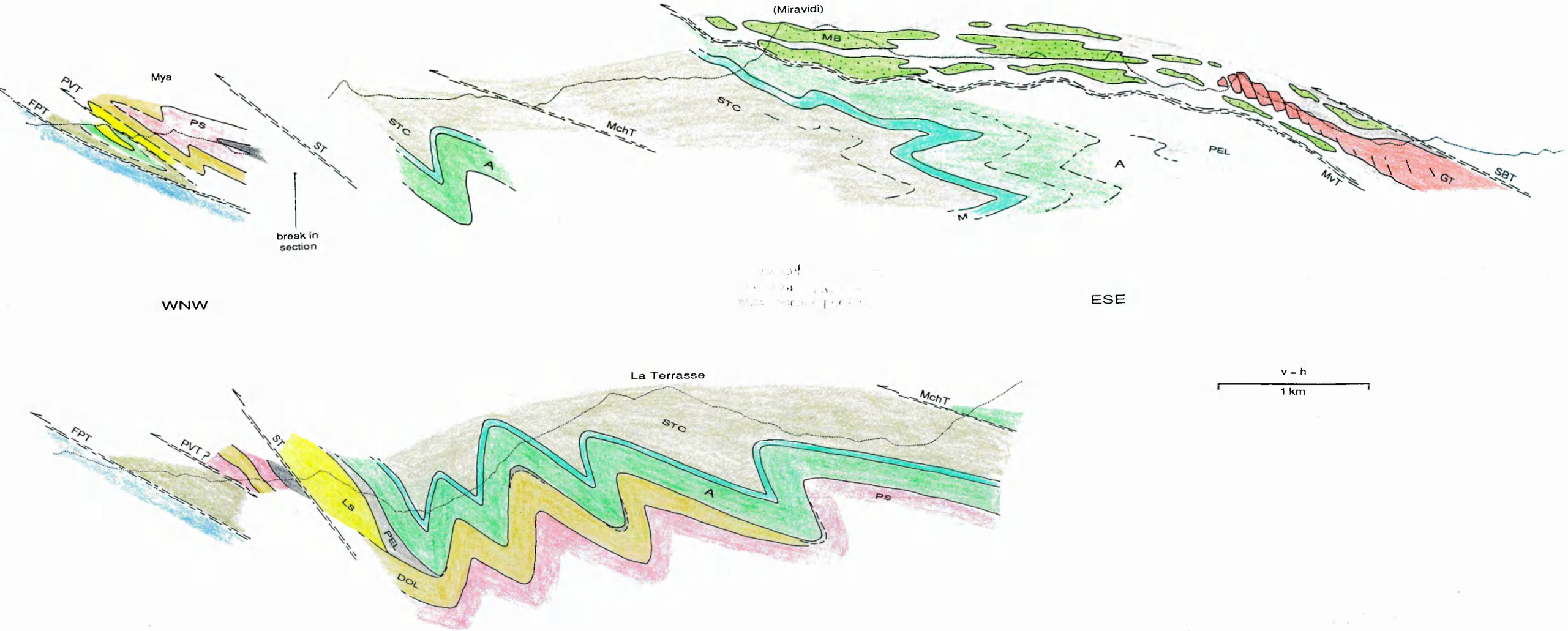

Fig. 2-41. Sketch sections showing preliminary interpretations of: ***upper*** - section lines **d** (Fig. 2-35) and **c** (Fig. 2-16); ***lower*** - section line **b** (Fig. 2-15). Thickness of thrusts somewhat exaggerated. Dotted line indicates present erosion level. *Abbreviations: FPT* = Frontal Pennine Thrust; *MchT* = Montchail Thrust; *MvT* = Miravidi Thrust; *PVT* = Plan Varraro Thrust; *SBT* = Sub-Briançonnais Thrust; *ST* = Seloge Thrust. See accompanying key for explanation of lithostratigraphic scheme.